



Technical University of Crete
School of Electrical and Computer Engineering, Chania

**Modeling and Optimization of a Hydroelectric Power Plant
for a National Grid Power System Supply.
Case Study: Stratos Hydroelectric Dam**
| Diploma Thesis |

Panagiotis Margonis

Presentation Date: 24 March 2017
Supervisor: Prof. George Stavrakakis

Committee members
Prof. George Stavrakakis
Prof. Kostas Kalaitzakis
Dr. Eleftheria Sergaki

Preface

This diploma thesis has been carried out at the Department of Electrical & Computer engineering at the Technical University of Crete (TUC) during the fall of 2016.

I would like to thank my two supervisors Professor George Stavrakakis and Doctor Eleftheria Sergaki, for their guidance and readiness to help, whenever it was needed, despite always being busy with their heavy schedule, and doing so with good spirits.

I would also like to thank the member of the selection committee, Professor Kostas Kalaitzakis for the precious knowledge he has given me all the years of my studies at the Technical University of Crete.

The extent of the thesis would not be possible without an accurate numerical model, and great thanks are expressed towards Mr. George Lappas who did not only provide with data and knowledge about the Kastraki dam and the Stratos I dam, but has taken the time to answer questions and help with his understanding of some results.

A special thanks goes out to Mr. Dimitrios Papakammenos manager (PPC S.A) of Achelous dams for allowing a very interesting and educational visit to the Kastraki & Stratos I Hydroelectric Plants.

Still, I always thank my parents for their confidence in me over the years and to support me in my effort to give courage and strength to go on.

Writing this thesis has yielded much factual knowledge, but also experience in prioritizing. It has been rewarding to study an actual problem, which may be of interest beyond the academic.

Panagiotis Margonis
Chania, March 10, 2017

Abstract

Renewable Energy Sources (RES) are defined as energy sources, which are in abundance in the natural environment and are practically inexhaustible. More specific Hydroelectricity (HE) is an important component of world renewable energy supply and hydropower remains a major source of electricity generation due to its environmental friendly nature. In Greece the total installed capacity exceeds 3 GW. In this diploma thesis I am focusing in the Modeling and the Optimization of a Hydroelectric Power Plant. As numerical models I use the Kastraki HPP (320 MW) and Stratos I HPP (150 MW) because I had my internship in those two stations during the summer of 2015 and I had access to special parameters of the units after communication with the supervisor engineers of my internship. Modeling is the analysis of the non-linear models that can represent the basic components of a HPP (governor, turbine, servomotor). This thesis studies accurate and detailed hydro turbine and governor models, and the implementation of these models in Matlab/Simulink combined with the Simscape Power Systems (SPS). The way of their implementation and the construction of the two stations in Matlab/Simulink is explained analytically using basic function blocks or modifications of them. For the purpose of the Optimization I tried the heuristic Ziegler–Nichols tuning method in order to specify the coefficients of governor (PID-PI) under different percentages of electricity production of the unit. Also Matlab/Simulink gave me the opportunity to record and compare the figures of the two station with PID & PI controllers through simulation tests in the most common cases (three-phase fault, load demand change, change in the production level of each unit) with a view of studying the efficiency and the stability of these two generating stations.

Contents

Chapter 1	1
Introduction	1
1.1 Electric current & Electric power	1
1.2 Electric Power Systems (EPS)	1
1.3 Renewable Energy Sources (RES)	3
1.3.1 Types of Renewable Energy Sources	4
1.3.2 Advantages of RES	6
1.3.3 The situation of RES in Greece	6
1.4 Hydrologic Cycle	7
1.5 Hydropower	9
1.6 Classification of hydropower plants	10
1.7 Hydropower in Greece	11
1.8 Thesis objectives	13
Chapter 2	15
Achelous river: Kastraki Dam and Stratos I Dam	15
2.1 Achelous River	15
2.1.1 The Achelous estuary and its ecological importance	15
2.1.2 The river Achelous water resource system	16
2.2 Kastraki HPP	20
2.2.1 Main features of Kastraki project	21
2.2.2 Useful figures Kastraki HPP	24
2.3 Stratos I HPP	26
2.3.1 Power House-Stratos I HES	27
2.3.2 Main features of Stratos I project	27
2.3.3 Useful figures Stratos I HPP	28
Chapter 3	31
Theory	31
3.1 Hydraulic Energy	31
3.2 Water balance Description	32
3.3 General Description of Hydroelectric Plants	34
3.4 Flow Rate	36
3.5 Capacity Factor	36
3.6 Penstocks	36
3.6.1 Water Hammer	37

3.7	Reservoirs, Wicket Gate.....	38
3.8	Generators	38
3.9	Synchronous generators	39
3.9.1	Generator Control	43
3.10	Hydroturbines	43
3.10.1	Francis Turbine (Reaction Turbine).....	45
3.10.2	Spiral casing.....	47
3.10.3	Stay Vanes and Wicket Gates	47
3.10.4	Runner.....	47
3.10.5	Power and Efficiency Expressions.....	47
3.10.6	Self governing	48
3.10.7	Draft Tube	49
3.10.8	Turbine Losses	49
3.11	Turbine-Generator relationship	50
3.12	Power System and Grid	51
3.12.1	Frequency.....	52
3.12.2	Load distribution and permanent Speed Droop	52
3.13	Per Unit System	53
Chapter 4.....		55
Modeling of a Hydroelectric Power Plant.....		55
4.1	Introduction	55
4.2	Hydroelectric Power Plant components	55
4.3	Non-Linear Mathematical Modeling.....	56
4.4	Model of Hydropower plant	56
4.5	Synchronous machine model.....	57
4.6	Hydro Turbine and Governor	58
4.6.1	Hydro Turbine Model	59
4.6.2	Hydraulic Turbine Governor Systems	62
4.7	Stability and PID coefficients limits	65
4.7.1	Routh's Test.....	66
4.8	Model of Excitation.....	67
Chapter 5.....		69
Software Implementation		69
5.1	Dymola software	69
5.2	TOPSYS software	70
5.3	Labview Transient, Lvtrans.....	70

5.4	Simpow software	71
5.5	Simsen software	71
5.6	PowerSim	72
5.7	Matlab/Simulink Simscape PowerSystems Implementation.....	73
5.7.1	Simulink.....	73
5.7.2	Simscape PowerSystems.....	74
5.7.3	Hydropower Plant in Simscape Power Systems	74
5.7.4	Hydraulic Turbine and Governor Simulation	74
5.7.5	Synchronous Machine pu Standard block.....	78
5.7.6	Excitation System	82
Chapter 6.....		87
Kastraki and Stratos I model in Simulink/Matlab.....		87
6.1	Parallel Operation.....	87
6.2	Kastraki HPP Simscape Power Systems Model.....	87
6.3	Stratos I HPP Simscape Power Systems Model.....	93
6.4	Summary	97
Chapter 7.....		99
Tuning PI and PID coefficients in governor		99
7.1	PI and PID controllers	99
7.2	Ziegler-Nichols Tuning method table	100
Chapter 8.....		103
Simulation of the HPP with PI and PID controller		103
8.1	Simulation Results under normal conditions in Kastraki HPP.....	103
8.1.1	PSS implementation in Kastraki HPP model.....	106
8.2	Simulation Results under normal conditions in Stratos I HPP.....	110
8.2.1	PSS implementation in Stratos I HPP model.....	114
8.3	Conclusions about normal responses and PSS.....	117
8.4	No controller in the HPPs.....	118
8.4.1	Kastraki HPP with no controller	118
8.4.2	Stratos I HPP with no controller	120
8.4.3	Conclusions.....	121
8.5	Transient Stability Analysis and Simulations Tests.....	121
8.6	Three Phase Fault	123
8.6.1	Kastraki HPP in Three Phase Fault case	123
8.6.2	Stratos I HPP in Three Phase Fault case	129
8.6.3	Conclusions for Three Phae Fault Simulation Tests.....	136

8.7	Load Demand Increase	137
8.7.1	Kastraki HPP in Load Demand increase case	137
8.7.2	Stratos I HPP in Load Demand increase case	143
8.8	Load Demand Decrease.....	150
8.8.1	Conclusions for Load Demand Increase/Decrease Simulation Tests	150
8.9	Power Load Change	152
8.9.1	Katraki HPP in Power Load changes case	152
8.9.2	Stratos I HPP in Power Load changes case.....	157
8.9.3	Conclusions for Power Load Change Simulation Tests.....	161
Chapter 9	163
Conclusion and Future work	163
9.1	Conclusion.....	163
9.2	Future work	163

Chapter 1

Introduction

1.1 Electric current & Electric power

An electric current is the electrical charge flow rate from one area to another. The SI unit for measuring an electric current is the ampere, which is the flow of electric charge across a surface at the rate of one coulomb per second. The energy that carries the electric current (the kinetic energy of the moving electron) is called electricity. Electric power is the rate, per unit time, at which electrical energy is transferred by an electric circuit. The SI unit of power is the watt, one joule per second.

1.2 Electric Power Systems (EPS)

The electricity produced by converting another form of energy firstly to mechanical using the drive engine (e.g. turbine) and then into electricity through the generator.

Electric Power System (EPS) is the set of facilities and instruments used to provide electricity in performing areas of consumption. The electric power systems of scale argument can be divided into National systems, Regional Systems and Private Systems as long as respective cover an entire country, an entire geographical area or individual private complex needs. Basic good operating prerequisites of a power system are to provide electricity anywhere there is a demand with 1) minimum cost and minimum environmental impact, 2) ensuring a constant frequency, 3) constant voltage and 5) high supply reliability.

Despite differences in size, mainly of electric power systems, there are some common features between them. Specifically, the majority of the EPS is three-phase AC and the frequency is 50 or 60 Hz (for the Greek and European general 50 Hz), in exceptional cases, however, it is possible to use direct current to carry. The voltage of the bus bar system is constant in normal operation, the transmission lines and the medium-voltage distribution lines having three phase conductors, and low-voltage lines have additional neutral conductor (although there are single-phase low voltage two-conductor lines).

In an EPS are 3 separate functions aimed at the consumer supply: production, transport and distribution of electricity. The production of electricity is made in power plants, which produce electricity and transferred to a high voltage through the step-up substation. The production of electricity is mainly the conversion of thermal energy of (carbon fossil fuels, oil, gas), of water power engineering and waterfalls and of nuclear energy from nuclear fission (uranium, thorium, plutonium) into electricity. In recent years it is also becoming more intense the electricity production from

renewable energy plants such as wind (wind), sea waves, solar energy, geothermal energy and biomass. From thermal power stations the steam-power and nuclear power stations use steam as a mean of mechanical energy production through steam-turbines (external combustion). In contrast, oil plants use internal combustion engines, which are either gas turbines or reciprocating diesel generators. The transfer of power is in large quantities from the production plants to the consumption areas through high and extra-high voltage lines that carry electricity to the respective substations of lowered voltage to medium voltage supplying the distribution networks. The distribution networks distribute electricity to consumers through the distribution channels and through the low voltage lines 400 / 230 V (Europe). It is noted that the transfer of power takes place at high voltages, because it means lower electrical losses and thus more economical operation. In cases where it is not possible to link the network is called to work autonomously. Such systems are commonly found in Greek islands, where there is no connectivity to the National grid. Autonomous systems are more prone to sudden load changes and their specific provisions must respond effectively to these. Also, there is the possibility of sharing the load encountered in the interconnected system, and thus, each system must be able to self-treat any service supply difficulties.

It is worth mentioning that the global electricity production in 2004 amounted to 17531 TWh and came at 65.8% from fossil fuel combustion, 16.5% from hydro, 15.6% from nuclear energy and only 2.1% from renewable. In 2009, total consumption in Greek Interconnected System came to 52.8 TWh. Of these, 4.4 TWh came from imports, while domestic production was covered at 62.9% (30.5 TWh) lignite, 3.5% (1.7 TWh) of oil, 19.4% (9.4 TWh) of natural gas, 10.3% (5 TWh) by hydropower production and 3.9% (1.9 TWh) from renewable sources, mainly wind.

Briefly power system should be designed and operated properly, while it should meet the following requirements:

- It should provide electricity to all areas of consumption that serves.
- It should be able to meet the ever-changing demand for electricity.
- It should provide good quality of electricity, which means that should ensure stable frequency, stable voltage and high supply reliability.
- It should to provide electricity at the lowest possible economic cost and minimum impact on the environment.

The structure of a power system consists of the following four main parts:

- Electric Power generation.
- Electricity transmission.
- Electricity distribution.
- Load.

1.3 Renewable Energy Sources (RES)

Renewable Energy Sources (RES) are defined as energy sources, which are in abundance in the natural environment and are practically inexhaustible. Usually the for the exploitation of them is not required a highly active intervention (e.g. mining, pumping, burning) as the already used energy sources, but merely exploitation of the existing energy flow in nature. Their use does not pollute the environment and their uptake is only the development of reliable and economically acceptable technologies that will bind their potential. "Renewable sources" are generally considered alternative to traditional power sources (e.g., oil or coal), as solar and wind energy. RES based essentially on solar radiation, with the exception of the geothermal energy, which is energy flow from the interior of the earth's crust, and the energy from tides from gravity. Those based on solar mild radiation forms of energy is renewable, since it is not exhausted as long as the sun exists, i.e. for a few more billion years. Essentially it is about solar energy "packed" in one way or another, the biomass is solar energy bound in the tissues of plants through photosynthesis and precipitating, wind energy exploits winds caused from heating the air while they water-based sources of energy operating the evaporation-condensation cycle of water and its release. Geothermal energy is not renewable, and geothermal fields sometime exhausted. RES in the modern era used either directly (mainly for heating) or indirectly converted into other forms of energy (mainly electricity or mechanical energy). It is estimated that the technically exploitable energy potential from mild forms energy is multiple times the world's total energy consumption.

Although the high price until recently, of new energy applications, technical problems implementation as well as political and economic considerations that have to do with keeping the current status quo in the energy sector prevented the operation even and part of this potential. In Greece, where the topography and climate suitable for new energy applications, the exploitation of this energy potential is promising energy independence of the country. The interest in renewable energy sources actually first appeared in the early 1970, caused mainly by the successive oil crises of the era, but also the degradation of the environment and quality of life by the use of classical sources energy. Particularly expensive in the beginning, started as a pilot program. However, today RES taken into account in the official plans of developed countries energy and, although are a very small percentage of their energy production, preparing steps for further exploitation. The cost of the mild forms of energy progressively reduced over the past years. So especially wind, hydropower, and biomass, can now compete on equal terms the traditional energy sources such as coal and nuclear energy. Indicatively, in USA 6% of energy from renewable sources, while in the European Union the primary production of renewable energy (mainly hydro and biomass) within the EU-28 in 2017 was 196 million tones — a 25.4 % share of total primary energy production from all sources. The quantity of renewable energy produced within the EU-28 increased overall by 73.1 % between 2004 and 2017, equivalent to an average increase of 5.6 % per year (mainly hydro and biomass).

1.3.1 Types of Renewable Energy Sources

- **Wind energy:** Wind energy is utilized by the wind-turbines, which convert the kinetic energy of wind into electrical. Formerly used to pump water from wells and for mechanical applications (grinding windmills). It has begun widely used for power.
- **Solar energy:** Solar Energy is used either through photovoltaic generators, which convert directly solar energy into electricity, or the concentration of solar rays through solar panels to achieve high temperatures and finally the generation of electricity. Finally, widespread use of solar energy is to heat water or spaces. Used more for heating applications (solar water heaters and ovens) and its use for production electricity is beginning to gain ground, with the help of promotion policy of Renewable Energy Sources from the Greek state and the European Union.
- **Hydropower:** It is mainly used for peak power plants. It is exploited both in small and large scale. Their installation and operation touches upon serious social and environmental problems, as well as causing significant disruption of natural energy resources. In contrast, small hydro projects in rivers and streams do not have similar problems and grow successfully throughout the world. The electricity produced by them is proportional to the amount of water passing through the turbine and the stack covered by the water on its way to the turbine through a pressure pipe. Thus, the same power can be detached, in case of a large amount of water that falls from a small height, and in case of a small amount of water that falls from a great height. In the first case, however, the dimensions of individual units of the small hydroelectric power plant will be much larger than those of the second, with obvious implications for siting issues and conduct studies, environmental impacts of installations. The comparative advantages of small hydroelectric power plants, compared with some RES is the direct connection / disconnection to the network or its autonomous operation, reliable uninterrupted and without fluctuations in energy conversion, long service life, the little time amortization of necessary investments, low maintenance costs, zero emissions (during the operational phase), satisfaction and other water needs (water supply, irrigation), etc.
- **Biomass:** Biomass is the production of thermal or chemical energy by processing biofuels, using residual forest holdings and the exploitation industrial agricultural (plant and animal) and municipal waste. The derivatives such as bioethanol and biogas are compared with traditional fuels, and they are more ecofriendly.
- **Geothermal energy** (geothermal energy high and low enthalpy): It comes from the heat generated from the nuclear precession on rocks of the earth. It is usable where the heat is coming up naturally to the surface, e.g. the geysers or hot springs. It can be used either directly for thermal applications or for power production.
- **Energy from tides:** Exploiting the phenomena caused by gravity of the Sun and the Moon, raising the water level. The water is stored as it rises, and to downloaded again forced to pass through a turbine, producing electricity.

- **Energy from waves:** Exploiting the kinetic energy of waves of sea, usually by using special floats.
- **Energy from the Oceans:** It exploits the temperature difference between the layers of the ocean, using thermal cycling. Is being on intensive research stage.

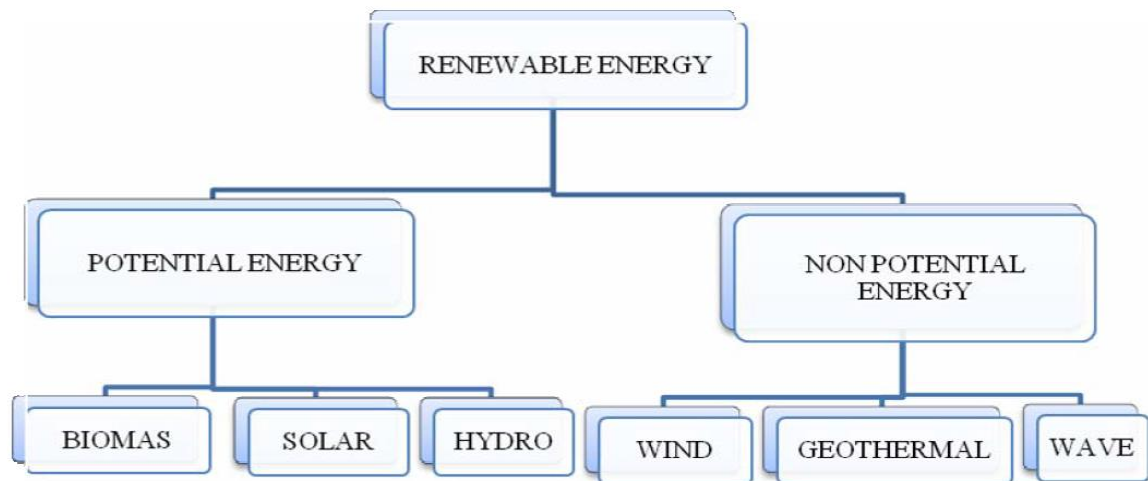


Figure 1.1: General renewable energy sources [1]

Figure 1.1 and Figure 1.2 show the forms of renewable energy separated in Potential Energy and Non Potential Energy and the forms of the Potential Energy in Greece respectively. In Greece the forms of Potential Energy Are Biomass, Hydro and Solar renewable sources.

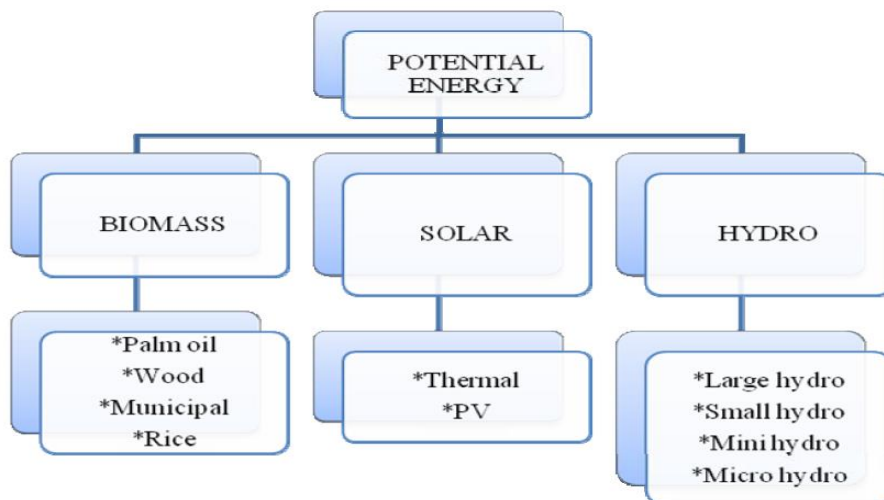


Figure 1.2: Potential energy in Greece [1]

1.3.2 Advantages of RES

- They are very friendly to the environment and man, having essentially zero residues and waste.
- They are practically inexhaustible sources of energy and help to reduce the dependence on finite conventional energy sources.
- They usually have low operating costs, which in addition is not affected by fluctuations in the international economy and especially of contract prices of fuels.
- The equipment is simple in construction and the maintenance and has a long life span.
- The exploitation of RES facilities is available in small sizes and have small construction duration, allowing rapid response to bid energy demand, with repetitive systems in many cases.
- They are domestic energy sources and contribute in enhancing energy independence and security of energy supply at the national level. So, they can help the energy self-sufficiency of small and developing countries, and to be the alternative solution to the economy.
- They can be in many cases core of revival of economically and socially deprived areas and pole for the local development, promoting investments based on the contribution of renewable energy (e.g. greenhouses with geothermal energy).
- They are geographically dispersed and leading to decentralized energy system, enabling to meet the energy needs of local and regional level, relieving infrastructure systems and reducing the transmission losses. In this sense it is an effective answer to problem of energy independence the islands.
- They are subsidized by most governments.
- The RES investments are labor intensive, creating many places of employment particularly at local level.

1.3.3 The situation of RES in Greece

The total contribution of RES consistently recording an upward trend in recent years, as a result of massive private investments carried out in the context of policies have been taken, as part of the financial support measures, and the RES utilization perspective. More specifically, in the context of an integrated EU policy on climate change and where energy released at EU level, the targets for reducing greenhouse gas emissions, the penetration of RES and saving primary energy (also known as 20-20-20 targets), adopted by the Member States a wide legislative " packet". There including the

Directive 2009/28 / EC on the promotion of the use of energy from renewable sources, setting the legally binding target of 20% participation of renewable energy in the EU final energy consumption-27 by 2020, while in Greece the corresponding target determined at 18%.

According to this directive:

- There is a legally binding European target of 20% share of RES in final energy consumption by 2020, including a 10% participation in the transport sector.
- It is scheduled for a first time the exploitation of RES in all energy uses (electricity, cooling / heating, transport / biofuels).
- The specialization in national targets based on GDP (gross domestic product) with starting point the share of renewable energy in every member state in 2005, with this figure for Greece to be determined at 18%.

The Greek Government by Law 3851/2010 has increased its national share of RES target in final energy consumption to 20%, which specializes in 40% contribution of RES to electricity production, 20% in heating and cooling needs and 10% in transport. Furthermore, within the scope of Directive 2009/28 / EC, is prepared and submitted to the European Commission the National Action Plan for Renewable Energy, who is now the prime energy planning tool by 2020.

According to the Office for RES, the total power from RES stations in our country increased by 290 MW in 2010, summing a total installed capacity of 1736 MW, over 1446 MW in the end of 2009. Champions in developing new capacity was the year that the solar panels, which almost quadrupled their penetration in our energy system, starting from 53 MW at the end of 2009 and ending at 198 MW at the end of 2010. The new wind power added in 2010 stands at 131 MW, resulting in a total of 1298 MW, while a small but significant is the increase of small hydropower from 182.6 MW at the end of 2009, to 196.3 at the end of 2010. Concerning the wind energy, according to the Ministerial Decree 19 598 / 01.10.2010, for the desired ratio of installed capacity by 2020 between various RES technologies, determine the desired installed capacity of wind projects with first allocation period 2014 to 4000 MW and with a time horizon of 2020 to 7.500 MW. Our national targets for 2020, in line with the results of energy models, is expected to meet to hand power to develop approximately 13300 MW RES (about 4000 MW today), bringing together all the technologies projecting wind parks 7500 MW, 3000 MW of hydropower and solar with about 2500 MW, while heating and cooling with the development of heat pumps, solar thermal systems and biomass applications.

1.4 Hydrologic Cycle

Solar energy has the property to cause the evaporation of water from the seas, rivers and lakes. As Figure 1.3 shows the water in the form of rain, snow etc. condenses and returns to the Earth's surface. The water resulting in mountains and streams and acquires a potential energy, which is proportional to altitude which is located. By making use of the potential energy because of the altitude the water through of streams and rivers, ends to sea to continue again the same circular path - Hydrologic Cycle.

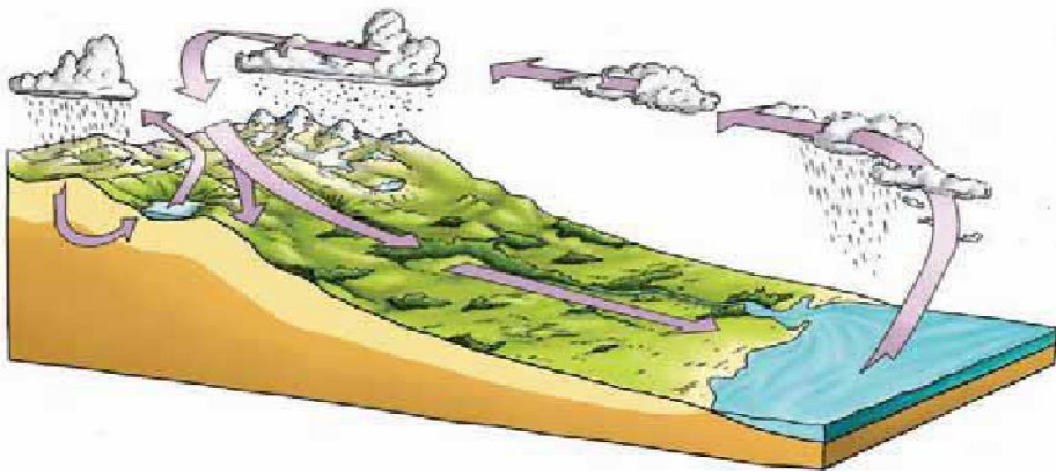


Figure 1.3: Hydrologic Cycle [2]

The potential energy acquired by the water before reaching the sea is usable and can be converted to electricity through hydroelectric power station. The exploitation and the conversion of potential energy water into electricity, has started from the old times and continues to today. This conversion has secured the planet huge amounts energy, which exceed 25% of the total consumption of the planet [2]. Despite the already installed hydroelectric potential, yet there are many margins increasing exploitation of the potential energy of the water, as according to estimations, only 15% of the available hydro potential has developed and there are many margins of further growth. The biggest hydroelectric projects in the world is the Three Gorges in China (built in 2011) with installed capacity of about 20 GW, and the Itaipu in Brazil and Paraguay (build 2003), with an installed capacity of 14 GW. The Three Gorges Dam is the world's largest power station until today in terms of installed capacity (22.500 MW). In 2014 the dam generated 98.8 TWh of electricity, setting a new world record by 0.17 TWh previously held by the Itaipu Dam on the Brazil/Paraguay border in 2013 of 98.63. But in 2015, the Itaipu power plant resumed the lead in annual worldwide production, producing 89.5 TWh, while production of Three Gorges was 87 TWh [63] [64].

The exploitation of the potential energy of water to produce energy has appeared many years ago in mankind as mentioned in many references and textbooks. The presence of water mills and water wheels described by many writers and water power is referred to as the "White coal", which helps the man to the path of development. Significant stop the exploitation of hydropower was the development of applications electricity (20th century), which enable the transport energy from the output position in place for consumption by relatively easy way. Then, this exploitation is called "Hydroelectric" wherein potential energy of the water is converted into mechanical, via the impact water with the hydraulic turbine, then is converted into electrical energy, transferred via cables to positions for consumption. It should be noted that hydropower is the largest and most mature renewable source energy.

1.5 Hydropower

Electricity production by exploiting the power of water called hydroelectricity (HE). Water located at high altitudes is dynamic energy which is converted into kinetic by the flow at lower altitudes. Then, with the use of water turbines produced mechanical energy that eventually converted into electricity via generator. All works and equipment through which is the conversion of hydraulic energy into electricity is called Hydroelectric Project (HEP). The capture and storage of water quantities in natural or artificial lakes, for a Hydroelectric Station, practically is equivalent to saving hydropower. The scheduled release of these amounts of water and their expansion in turbines lead to controlled electricity production. Given that the adequate water resources and their supply with the necessary rainfalls, Hydroelectricity becomes a significant alternative source of renewable energy. The use of hydrodynamic of a country is definitely a national target since it is a renewable energy source with significant advantages over other renewable energies. Some of these advantages are the low environmental impact, the high specific power (power per weight equipment) and the possibility of combining with other water uses. Furthermore, in contrast with fossil fuels, water is not wasted by not producing electricity energy and can be used for other purposes. Figure 1.4, presents the key elements of a hydro power plant with reservoir.

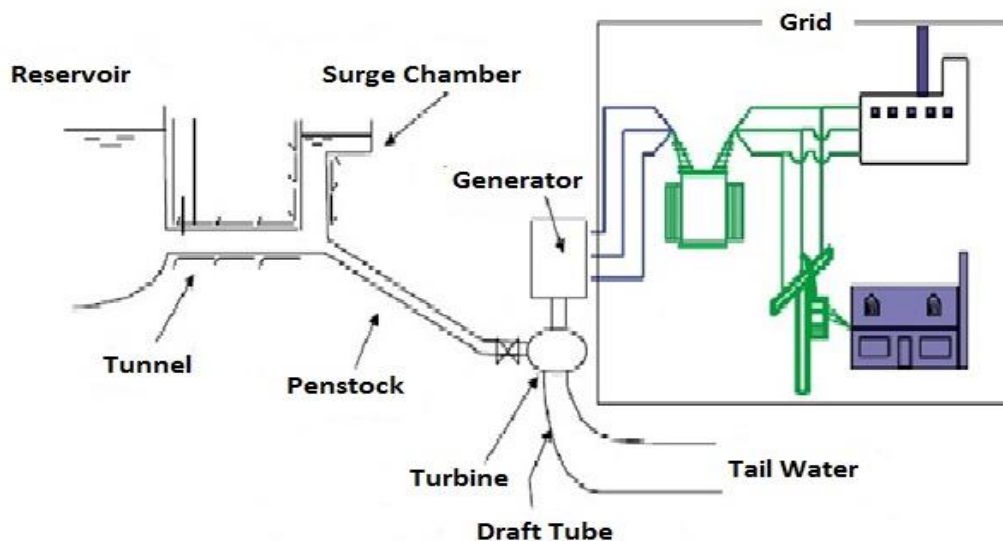


Figure 1.4: Principal sketch of a hydropower system [3]

A hydropower system consists of various components interlinked by fluid conduits. A change in load demand in the electric power grid, will necessitate a regulation of the turbine, as well as the attached generator. This will result in a change of flow velocity at one point in the system. This, in turn, results in a change in pressure that will propagate throughout the system via the conduits (penstocks in Figure 1.4). These fluctuations will influence upstream components, and when the pressure wave reflects and returns, the behavior of the turbine-generator assemblies themselves. These fluctuations are a disturbance in the system, originating from variations in the power grid. Europe's energy production is experiencing a shift towards larger volumes of renewable energy. This development, although it is

beneficial, poses several challenges. One of them being the lack of regulation, as the energy is available when nature permits from grid to reservoir were implemented.

1.6 Classification of hydropower plants

A hydroelectric project is a "small" or "large" according to the characteristics that has, which is not only quantitative but also quality. A hydroelectric project called "small" when the rated power less than 10 MW, without this value to be a generally accepted limit. In some countries, the discrimination value is set to 5 MW. The little one hydroelectric mentioned briefly as SHP (Small Hydroelectric Station) and in large hydropower, the term "large" is omitted and referred to as HES (Hydroelectric Power Station). The nominal capacity of large hydroelectric plants is greater than 10MW to produce enough electricity to supply large cities through extensive electrical networks. Small hydropower plants supply national grids with capacity below 10 MW, but greater than 1 MW. Next, come the mini-hydropower plants covering a small power range: from 100 kW to 1 MW, followed by micro-hydropower plants with rated powers of less than 100 kW. A subset of micro-hydropower plants are the pico-hydro power plants with a power output of less than 5 kW. Smaller hydroelectric power stations belonging to the last three categories are not connected to the main national network, but usually installed in remote and isolated rural areas to power small communities or crafts. The Greek Legislation (N.1559 / 85 N.2244 / 95) defines small stations with a capacity of less than 10 MW, with the proviso that only the installed power projects up to 2 MW can be freely active.

Large hydropower projects are accompanied by large dams and reservoirs, and there are not among the exploitation systems of Renewable Energy Sources (RES).

Generally, it is believed that the large dams affect the ecosystem, as installed in natural areas currents and reduce the amount of oxygen in the area. The table below shows a classification, which classifies HPPs under their strength.

Water can be harnessed on a large or a small scale. The categories which are commonly used to define the power output form hydropower are outlined as follows:

- i.** Large-hydro: more than 100 MW and usually feeding into a large grid.
- ii.** Medium-hydro: 15 - 100 MW and usually feeding a grid.
- iii.** Small-hydro: 1 - 15 MW and usually feeding into a grid.
- iv.** Mini-hydro: between 100 kW and 1 MW; either standalone schemes or more often feeding into the grid.
- v.** Micro-hydro: ranging from a few hundred watts for battery charging or food processing applications up to 100 kW, providing power for a small community or rural industry in remote areas away from the grid.

Another distinction of HPP refers to the size of the available hydraulic failure, whose value expresses the mass per unit hydraulically energy of water, wherein the following three categories are distinguished.

Table 1.1 Classification based on Drop Height [4]

Hydroelectric Dams	Drop height
Small Height	< 20 Meters
Medium Height	20 – 150 Meters
Large Height	> 150 Meters

1.7 Hydropower in Greece

In Greece, the total installed capacity exceeds 3 GW, which provide approximately 4.000 - 5.000 GWh to national grid annually. The average contribution to the network is 8-10%, while it is remarkable that the energy from Hydroelectric Station (HES), covering electrical loads peak and ensure the stability of the national grid. The larger HEPs operating in Greece is in Kremasta (437MW), in Thisavros (384 MW) and in Polyfyto (385 MW). The hydrodynamic available in Greece is quite large, especially in western and northern Greece, where precipitations are intense and the existence of large mountain ensures drainage basins with large height differences [65].



Figure 1.5: The Hydroelectric Stations of PPC S.A.(Greece) [5]

Table 1.2 The Hydroelectric Stations of PPC S.A today (2017)

Acheloos complex (Kremasta, Kastraki Stratos I & II, Giona, Glaucus)	Total 925.6 MW
Aliakmonas complex (Polyfyto, Sfikia, Asomata, Ag. Barbara Makrochori, Vermio, Agra, Edessaïos)	Total 880.2 MW
Arachthos complex (S. Aouu, Pournari I & II, Louros)	Total 553.9 MW
Nestos complex (Thisavros, Platanovrissi)	Total 500 MW
HEP N. Plastiras	129.9 MW
HEP Ladonas	70 MW
Other Small HPP	1.3 MW
Total in Greece	<u>3.061 MW</u>

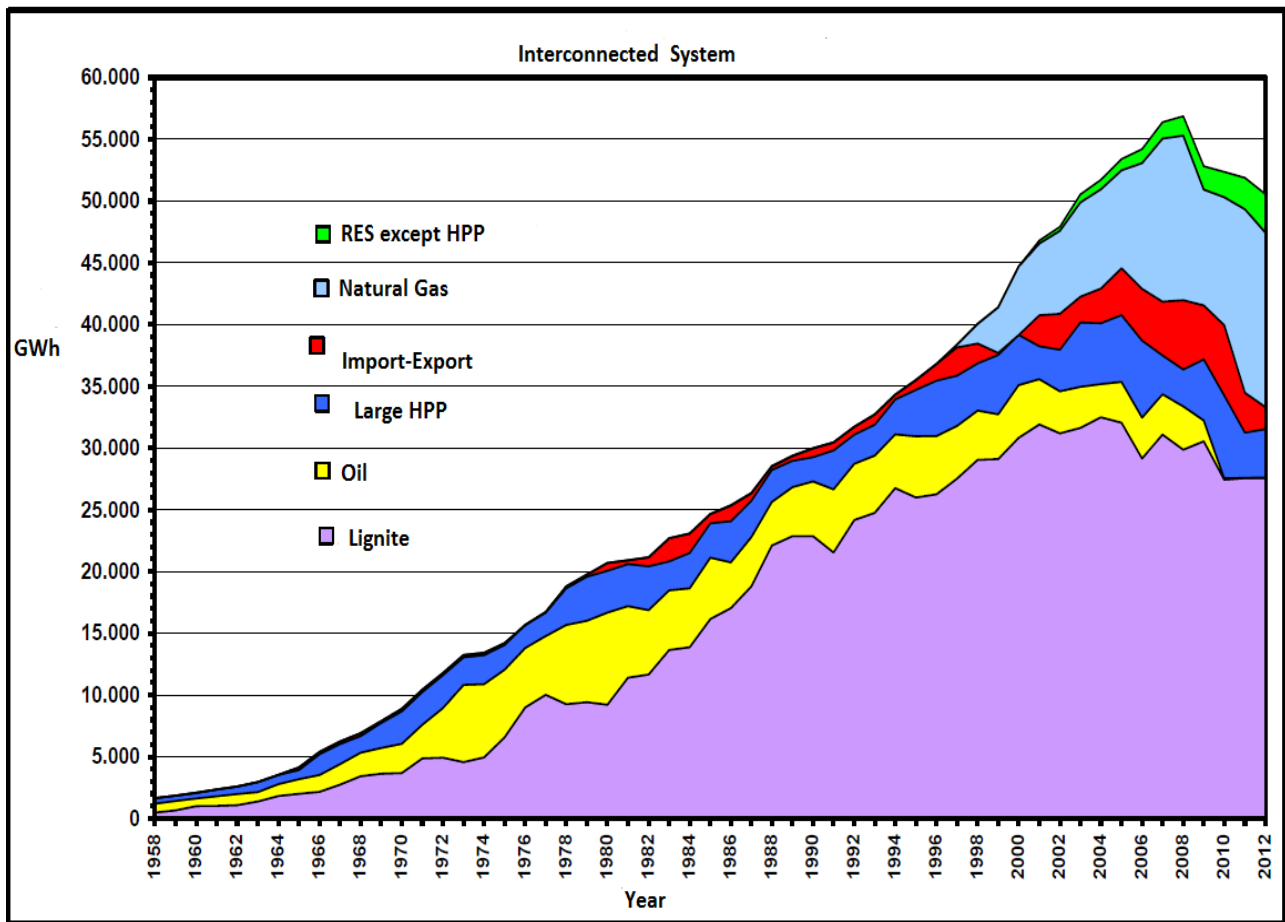


Figure 1.6: Production of electric energy 1958-2012 Greece [6]

Table 1.3 Hydroelectric Power Plants of PPC S.A [13]

16 Large HPP			11 Small HPP	
Location	Year	Reservoir (hm ³)	Location	Year
LOYROS	1954	0.035	GLAYCUS	1927
AGRAS	1954	3.8	VERMIO	1929
LADONAS	1955	46.2	AGIA CRETE	1929
PLASTIRAS	1960	300	ALMIROS CRETE	1931
KREMASTA	1966	2805	AG.IOANNIS SERRON	1931
KASTRAKI	1969	53	GKIONA	1988
EDESSAIOS	1969	0.46	STRATOS II	1988
POLYFYTO	1974	1020	MAKROCHORI	1992
POYRNARI	1981	303	AG.VARVARA ALIAKMONA	2008
ASOMATA	1985	10	SMOKOVO	2008
SFIKIA	1985	16	PAPADIA	2010
STRATOS	1989	11		
S.AOOY	1990	145		
THISAVROS	1997	570		
POYRNARI II	1999	3.6		
PLATANOVRISSE	1999	12		

1.8 Thesis objectives

This diploma thesis briefly, has the following main achievements:

- Modeling of the Hydroelectric Power Plants (HPP) in Kastraki & Stratos I Dams of PPC S.A. -Chapter 6
- Study of the dynamic stability in a unit (turbine & generator) of a HPP. -Chapter 4
- Choosing an appropriate software (Simulink/Matlab) to become feasible the mathematical modeling in a computer and the construction of models in the two stations that I study. -Chapter 5
- Verification of the correctness of the operation of the two stations in steady state. -Chapter 8
- Tuning of the PID-PI coefficients. -Chapter 7
- Simulation of the models and recording of the figures of the models with PID & PI controllers in the most common cases (three-phase fault, load demand change, change in the production level of each unit). -Chapter 8

Also this thesis can be useful as:

- A presentation of the theoretical background of a hydroelectric power station. -Chapter 3
- A description of the characteristics of the Kastraki & Stratos I Hydroelectric Stations and the Achelous water resource system. -Chapter 2
- A literature search of the available software which serve in any optimization of a real HPP - Chapter 5

Chapter 2

Achelous river: Kastraki Dam and Stratos I Dam

We are focusing on Achelous river and the Hydroelectric power plants in Kastraki and Stratos I, because these two were the stations where I had my internship with PPC S.A.

2.1 Achelous River

The Achelous River is located in Central Western Greece, and is the largest river of the country in terms of flow and the second one in terms of length (~220 km). Its river basin, covers an area of 5027 km². The mean annual precipitation reaches 1350 mm and the mean annual (naturalized) discharge at the estuary is estimated to be 136.9 m³/s, which corresponds to an equivalent depth of more than 850 mm and a runoff coefficient of 63%. In the mountainous areas, due to the domination of low permeability formations (flysch), the mean annual runoff exceeds 1000 mm and the runoff coefficient is around 70% – an outstanding percentage for Mediterranean catchments.

2.1.1 The Achelous estuary and its ecological importance

The environmental value of the entire river basin of Achelous is indisputable. For instance, the riverine ecosystems in the upper and middle course have been identified as important habitats for many threatened species of fresh water fish and birds. Fortunately, this part of the basin is only slightly influenced by human interventions. Yet, the most important and sensitive ecosystems are hosted in the estuary, extended areas of which belong to the NATURA 2000 sites, while the Achelous Delta is protected by the Ramsar Convention (Varveris et al, 2010).

The geomorphological and hydrodynamic conditions of the estuary (e.g. distribution of brackish and fresh water) favoured the development of important wetlands, such as lagoons, coastal salt lacustrine and freshwater marshes, with remarkable biological diversity (Fourniotis,2012). In particular, in the lower course and the estuary, three main types of riparian forests grow, i.e. riparian forests with *Salix alba* and *Populus nigra* as dominant species, a forest of *Fraxinus angustifolia*, and clusters with *Tamarix parviflora* and *Vitex agnus-castus*. Regarding fish fauna, 41 species have been identified, including Endangered Sturgeon (*Acipenser Sturio*), *Barbus Albanicus*, *Barbus Peloponnesius*, *Trichonovelonitsa* (*Cobitis Trichonica*), Greek Dromitsa (*Rutilus Ylikiensis*), as well as the unique European species of *Silurus Aristotelis*. Birds are the largest group of vertebrates, recording 259 species (*Fulica Atra*, *Larus Genei*, *Egretta Alba*, *Phalacrocorax Carbo*, *Aythya ferina*, *Anas Penelope*, etc.). For this reason, the Achelous Delta has also been included in the Special Bird Areas list. Finally, there exist at least 20 species of reptiles and amphibians that are protected at international level.

2.1.2 The river Achelous water resource system

From the early 1960s, the Public Power Corporation (PPC) constructed four major dams and interconnected hydropower stations in the middle and lower course of the river. Their characteristics are summarized in Table 2.1. The system hosts 43% of the installed hydropower capacity of the country, i.e. 1302 out of 3060 MW, and today produces 42% of the annual hydroelectric energy, i.e. 1880 out of 4500 GWh (official data by the PCC; Argirakis 2009). As is shown in Figure 2.1 the oldest dam (Plastiras) is located on a tributary of Achelous (Tavropos), and diverts the entire runoff of its upstream basin (161 km²) to the adjacent plain of Thessaly for irrigation and water supply, also taking advantage of an exceptional hydraulic head, ranging from 561 to 577 m. The other three dams (Kremasta, Kastraki, Stratos) form a cascade along the main river course. The hydroelectric development of Achelous and its tributaries (Inachos, Agrafiotis, Tavropos etc.) included in the first stage projects of Tavropos (130 MW), Kremasta (437 MW) and Katsraki (320 MW) which were built during the 1955-69 period. The second stage of Achelous river development proceeded with regard to Stratos HPP (156 KW) on the lower Achelous. In course of construction are Messochora HPP (160 MW) and Sykia HPP (60 MW), considering partial deviation of Achelous river) located on upper Achelous and scheduled for commissioning by the year 1994.

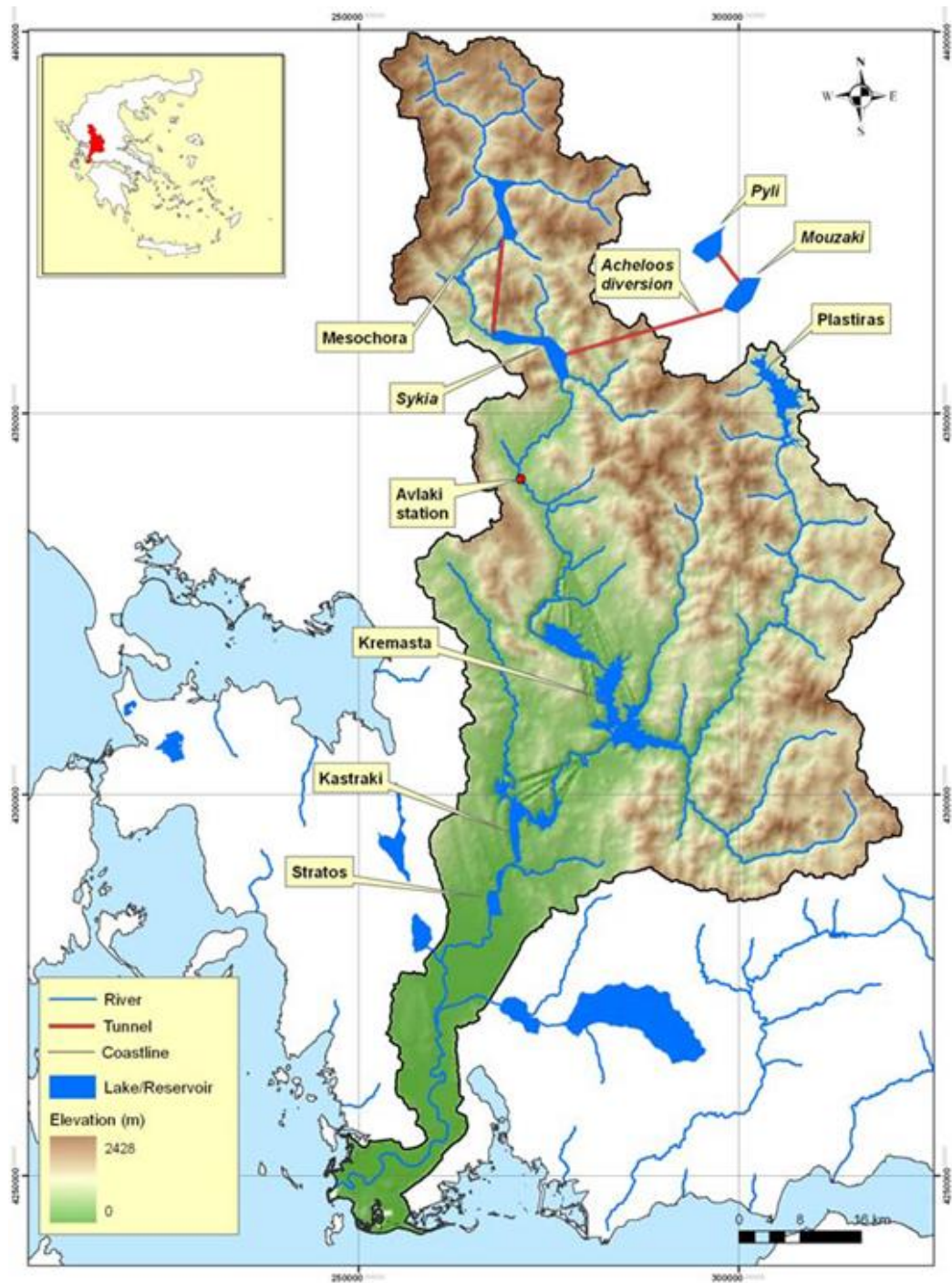


Figure 2.1: The Achelous river basin and its reservoir system (map by A.Koukouvinos) [7]

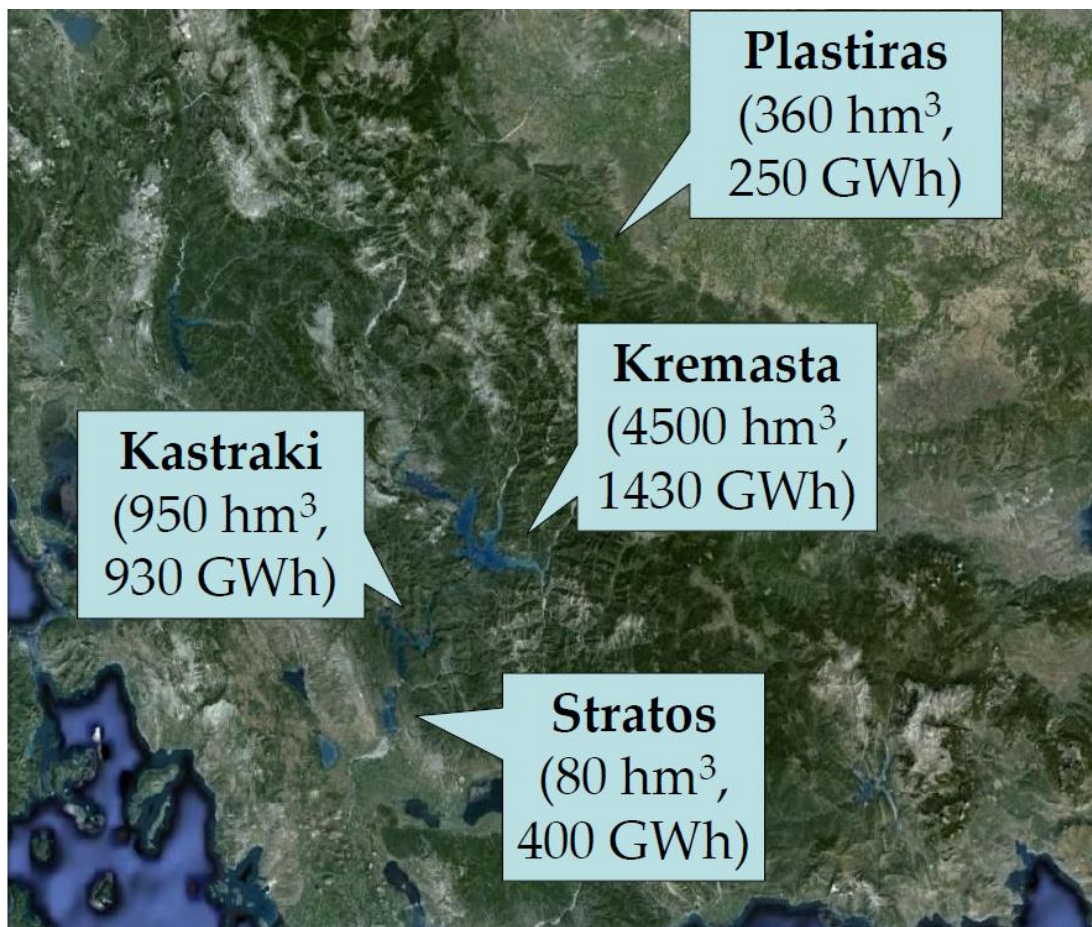


Figure 2.2: Our study area are the two hydroelectric dams (Katsraki, Stratos), operated by the Public Power Corporation (PPC S.A.) [8]

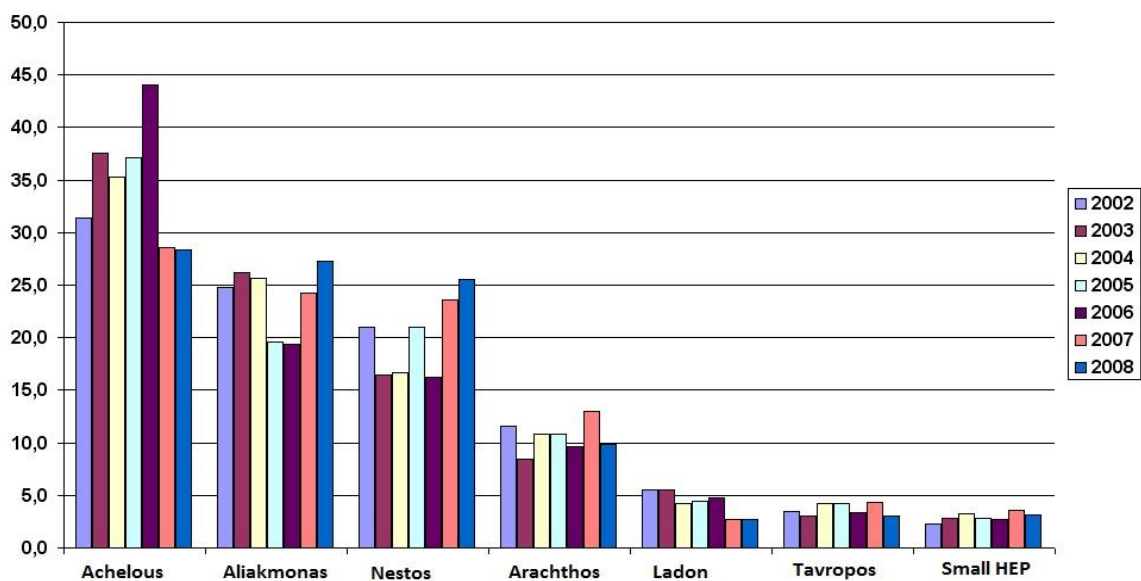


Figure 2.3: Percentage of contribution of each river (Greece) in total production (%) [9]

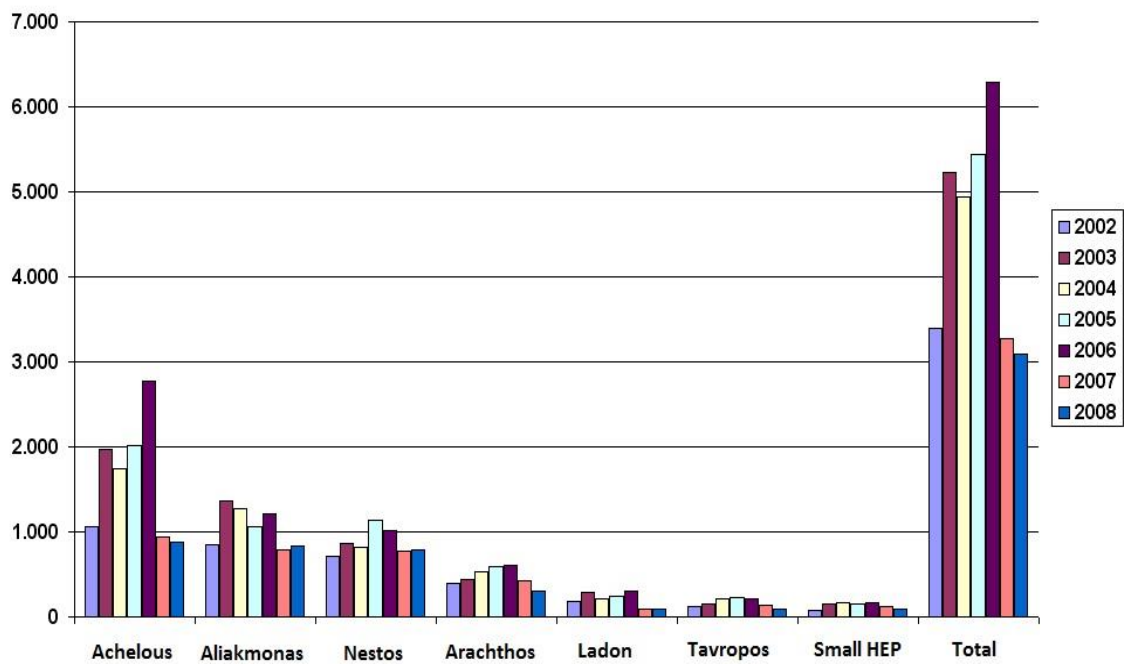


Figure 2.4: Annual Hydroelectric production per river [9]

Table 2.1 Hydroelectric complex of Achelous in Aetolia-Acarmania [5]

<i>Achelous</i>	<i>Height m</i>	<i>Reserv. mi M3</i>	<i>Capacity MW</i>
<i>Kremasta HPP</i>	165	3300	437.2
<i>Kastraki HPP</i>	96	53	320
<i>Stratos HPP I</i>	26	11	150
<i>Small Stratos HPP II</i>	-	-	6.2

2.2 Kastraki HPP



Figure 2.5: Kastraki HPP [5]

The hydropower station in Kastraki is located 20 km north of Agrinio and is approximately 300 km far from Athens. Has been constructed 35 km downstream to Kremasta. The project has three purposes energy production, water supply and irrigation of wider areas. The Kastraki Dam is an earth-fill embankment dam on the Achelous River near the village of Kastraki in Aitoloakarnania, Greece. It was completed in 1969 for the purposes of hydroelectric power generator, flood control and irrigation. The dam's power station houses four 80 MW Francis turbine generators for an installed capacity of 320 MW. It receives the outflows of Kremasta and the runoff of the intermediate sub-basin, which covers an area of 548 km². Since no abstractions exist in the river course between the two dams, and in order to estimate the naturalized flows at Kastraki we add the daily runoff of the aforesaid sub-basin to the naturalized flows at Kremasta.

General information [10]

Location: Aetolia-Acarnania prefecture

Dam type: earthfill (TE)

Dam height: 96 m

Crest length: 547 m

Dam Volume: 5.2×10^6 m³

Reservoir capacity: $785 \times 10^6 \text{ m}^3$
Reservoir surface: $24 \times 10^6 \text{ m}^2$
Use: HIS (Hydropower, Water Supply, Irrigation)
Power: 320 MW
Energy: 598 GWh/yr
Owner: Public Power Corporation (PPC)
Year of operation: 1969

2.2.1 Main features of Kastraki project

Source [10]

Production Units: 4x80 MW

Turbines: Vertical shaft-Francis

- Manufacturer: Baldwin-Lima-Hamilton
- Rated Speed: 166.5 rpm

Net design head: 72.40 m

Generators: Synchronous vertical shaft, umbrella type

- Manufacturer: Hitachi
- Pole Pairs: 18 (36 pole stators)
- Rated Output: 89 MVA
- P.F: 0.90
- Rated voltage-frequency: 15.75 KV-50 Hz

Power Transformers: Three phase with forced cooling

- Manufacturer: Hitachi
- Number: 4
- Rated output: 90 MVA
- Rated voltage: 161.25 KV/15.75 KV

Dam

- Type: Earth fill with central clay core and river sand and gravels
- Crest length: 547 m
- Elev.(nom): 154 m
- Width (min): 8 m
- Max. height: 95.7 m

Intakes

- Type: Vertical
- Dimensions at the power tunnel mouth: 5.80 m x 5 m

Spillways

- Type: open, side length without gates
- Crest elev: 144.2 m
- Crest length: 120 m
- Charging: $3700 \text{ m}^3/\text{sec}$
- Power tunnels (four)

- Max.Diameter: 5.80 m
- Min.Diameter: 4.93 m
- Length of num.1: 254.2 m
- Length of num.2: 246.8 m
- Length of num.3: 238.6 m
- Length of num.4: 230.6m
- Max. supply 116 m³/sec

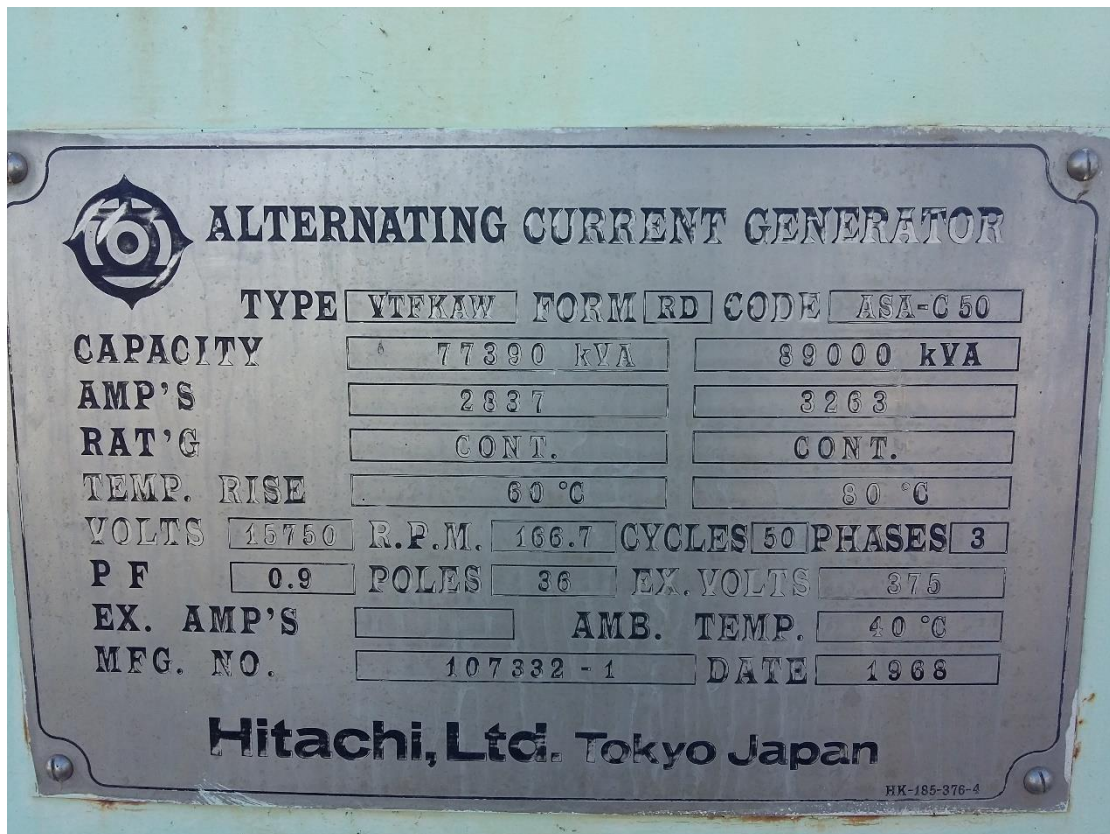


Figure 2.6: Kastraki HPP Generator characteristics (personal archive)



Figure 2.7: Kastraki HPP Power Transformer (personal archive)



Figure 2.8: Kastraki HPP Unit 2 (personal archive)

2.2.2 Useful figures Kastraki HPP

The data are from period 2013-2016, we used Matlab to create the Figures.

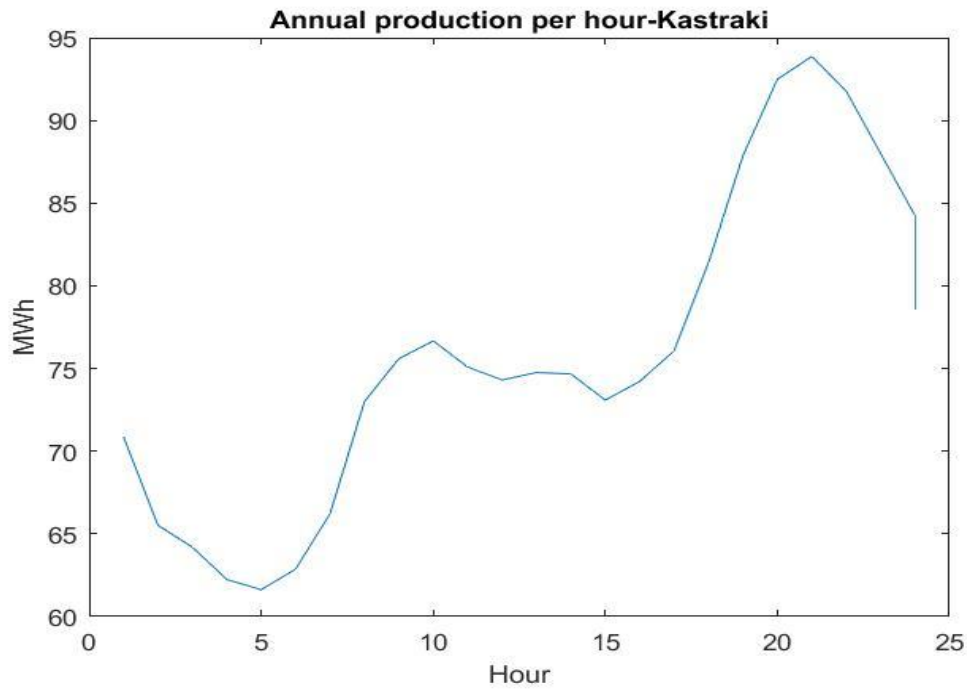


Figure 2.9: Annual average production per hour (personal calculations from Data [2013-2016]in [12])

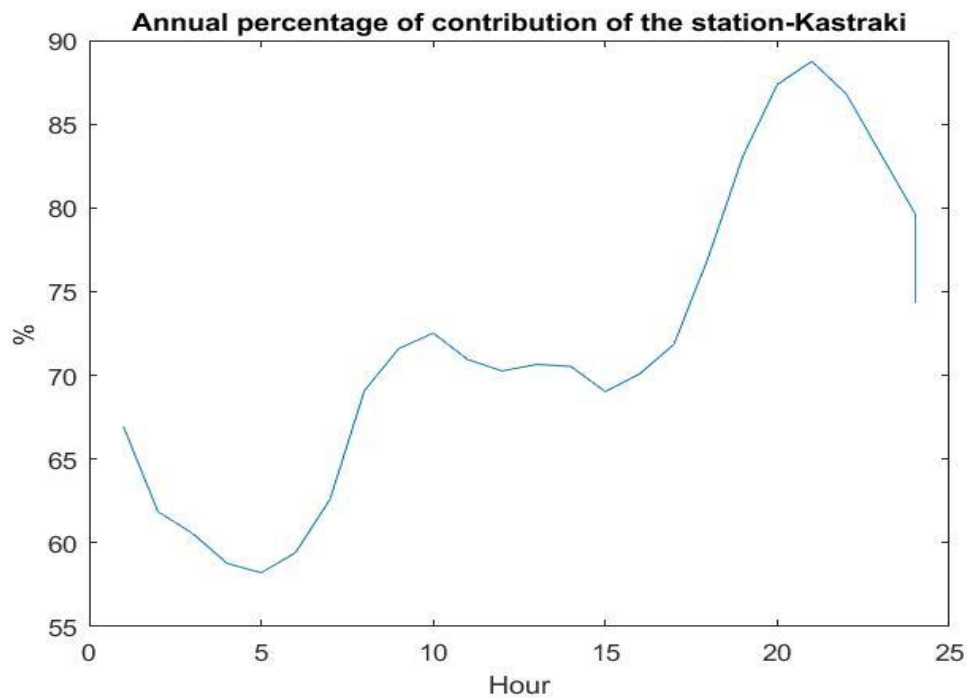


Figure 2.10: Annual percentage of contribution of the station per hour (personal calculations from Data [2013-2016]in [12])

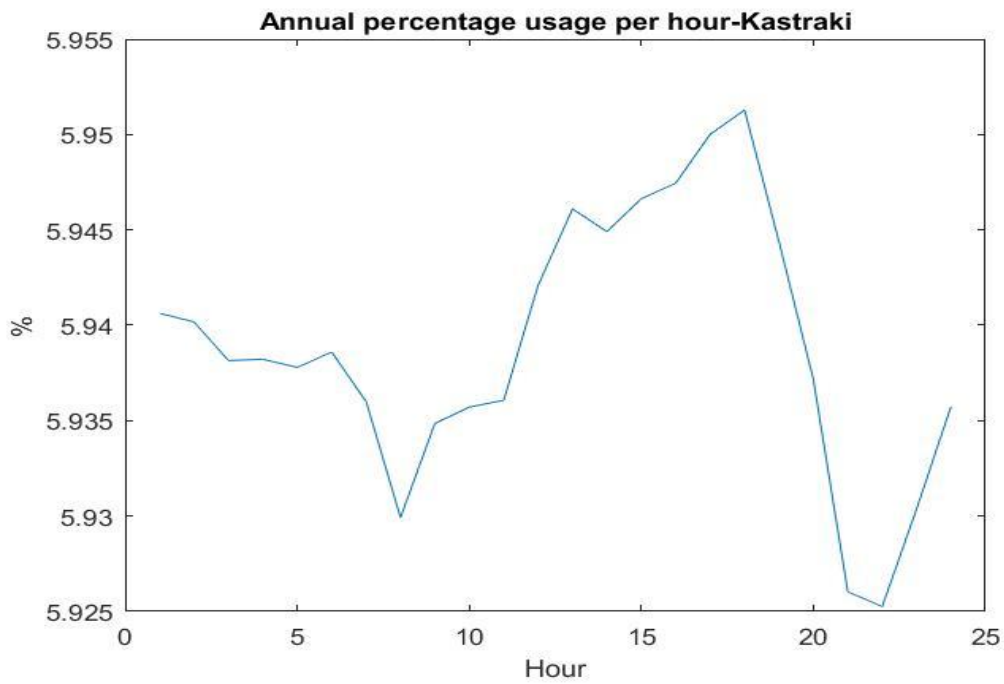


Figure 2.11: Annual percentage of usage of the station per hour (personal calculations from Data [2013-2016]in [12])

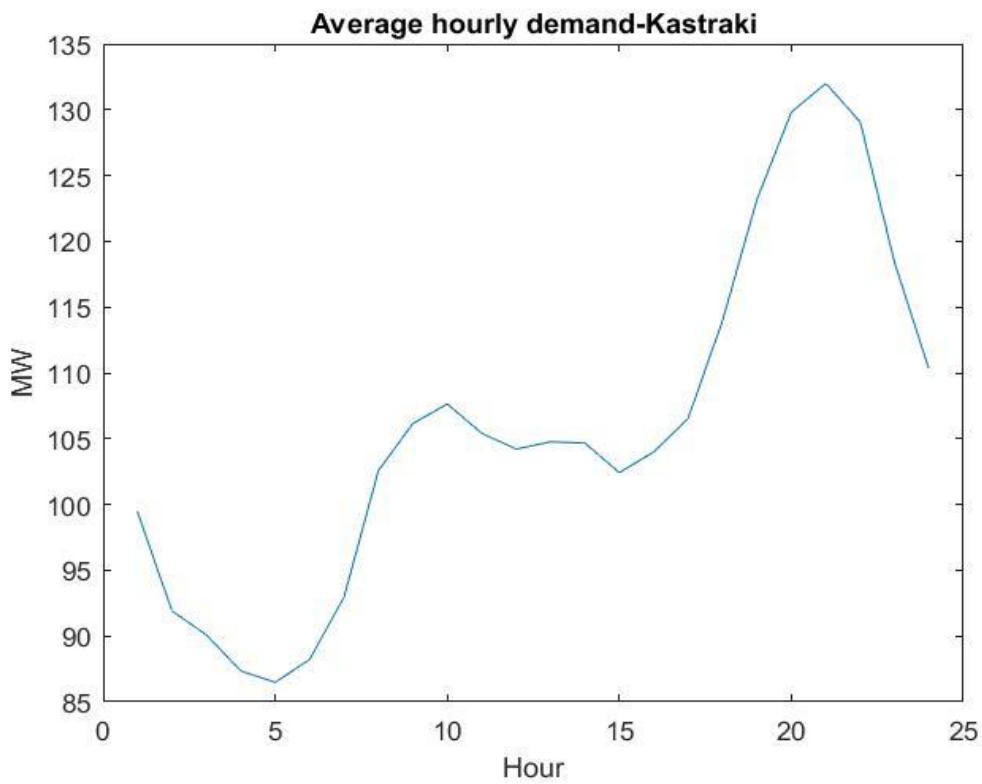


Figure 2.12: Average hourly demand per year (personal calculations from Data [2013-2016]in [12])

2.3 Stratos I HPP



Figure 2.13: Stratos I HPP [5]

As we see from Figure 2.13 the Stratos I HPP is located 8 km downstream of Kastraki HPP and about 0.8 km upstream of the Achelous irrigation dam. The distance from Athens is 285 km and 9 km west of Agrinio to the right abutment of the dam and the Trailrace Tunnels outlet, there can be observed significant sections of the ruins of the wall fortifications of the ancient city of Stratos I flourishing during the fourth century B.C. The project's dual objective is energy production and irrigation.

The reservoir has a capacity of 80 mi m³ for max P.P level at el. 68.6 m. The project consists of an earthfill Dam with crest elevation at 73 m (a.s.l) the underground Power House in the right (west) abutment of the dam and the relevant waterways, the Tailrace Canal, the Spillway and the small outdoor Powerhouse connected with the Spillway, at the left abutment. The underground P.H has two vertical units Francis type rated at 75 MW each with total annual generating capacity 400 GWh approx. The small P.H has two axial-S type units, rated at 3,35 MW each with total annual generating capacity 16 GWh.

General information [11]

Location: Aetolia-Acarmania prefecture

Dam type: earthfill (TE)
Dam height: 26 m
Crest length: 1900 m
Dam Volume: $2.8 \times 10^6 \text{ m}^3$
Reservoir capacity: $11 \times 10^6 \text{ m}^3$
Reservoir surface: $8.4 \times 10^6 \text{ m}^2$
Use: HIS (Hydropower, Water Supply, Irrigation)
Irrigated area: 400.000 m
Power: 150 MW
Energy: 598 GWh/yr
Owner: Public Power Corporation (PPC)
Year of operation: 1989

2.3.1 Power House-Stratos I HES

The underground P.H (Power House) is located into the right abutment. Downstream are provided two draft tubes, a gate chamber equipped with stop logs and an overhead crane, two tailrace tunnels and the tailrace canal, 7km long. The underground P.H is 71.90 m long and 21.10 m wide. Arrangement has been made for the housing of the units, the erection and maintenance for the E./M(Electric/Mechanical) equipment bay and auxiliary space. The spacing of the units (axis) is 21.30 m. The P.H basically comprises two floors at el. 39.80 m (generators floor) and 34.20 m (turbine floor). The turbine distributor centerline setting is at el. 29.0 m. Two gantry cranes are available with a total combined lifting capability of 360 t.

2.3.2 Main features of Stratos I project

Source [11]

Production Units: 2x75 MW

Turbines: Vertical shaft-Francis

- Rated Output: 102.000 HP (75 MW)
- Rated Speed: 107 rpm
- Pole Pairs: 28 (56 pole stators)

Net design head: 36.60 m

Generators: Synchronous vertical shaft, umbrella type

- Rated Output: 84 MVA
- P.F: 0.90
- Overload capability at max. head: 81 MVA
- Rated voltage-frequency: 15.75 KV-50 Hz

Power Transformers: Three phase with forced cooling

- Number: 2
- Rated output: 84 MVA
- Rated voltage: 150 KV/15.75 KV

Dam

- Type: Earth fill with central clay core and river sand and gravels
- Crest length: 1900 m
- Elev.(nom): 73 m
- Width (min): 9 m
- Max. height: 26 m

Intakes

- Type: inclined with trash racks
- Dimensions at the power tunnel mouth: 5.90 m x 11.30 m
- Means for closure: slide gates and stop logs

Spillways

- Type: gated with chute and stilling basin
- Gates: 5 radial 14.5 m x 9.44 m with lifting mechanisms
- Crest elev: 60 m
- Design flood discharge: 4000 m³/sec

Power tunnels (two)

- Diameter, circular cross section: 7.30 m
- Length: 74.45 m
- Tunnel axis elev. at intake: 58.00 m
- Tunnel axis elev. at P.H: 29.00 m
- Lining: concrete and steel liner

2.3.3 Useful figures Stratos I HPP

The data are from period 2013-2016, we used Matlab to create the Figures.

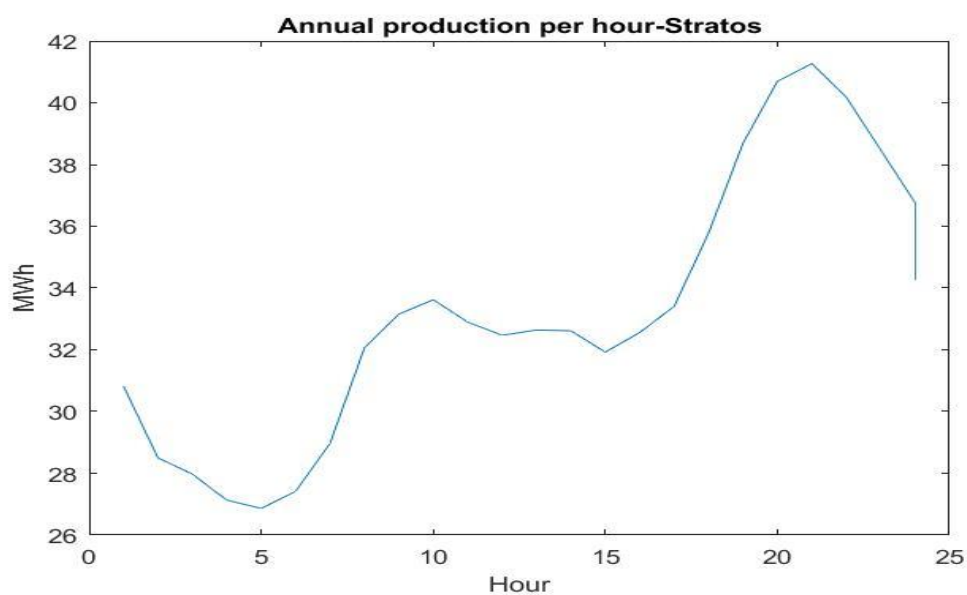


Figure 2.14: Annual average production per hour (personal calculations from Data [2013-2016]in [12])

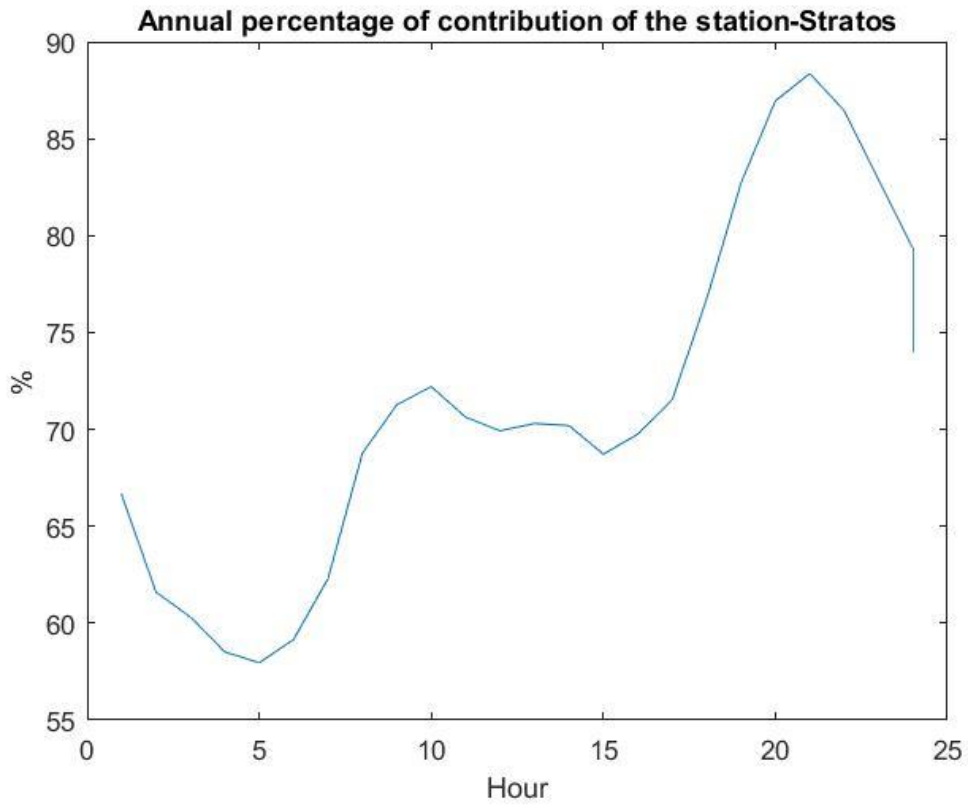


Figure 2.15: Annual percentage of contribution of the station per hour (personal calculations from Data [2013-2016]in [12])

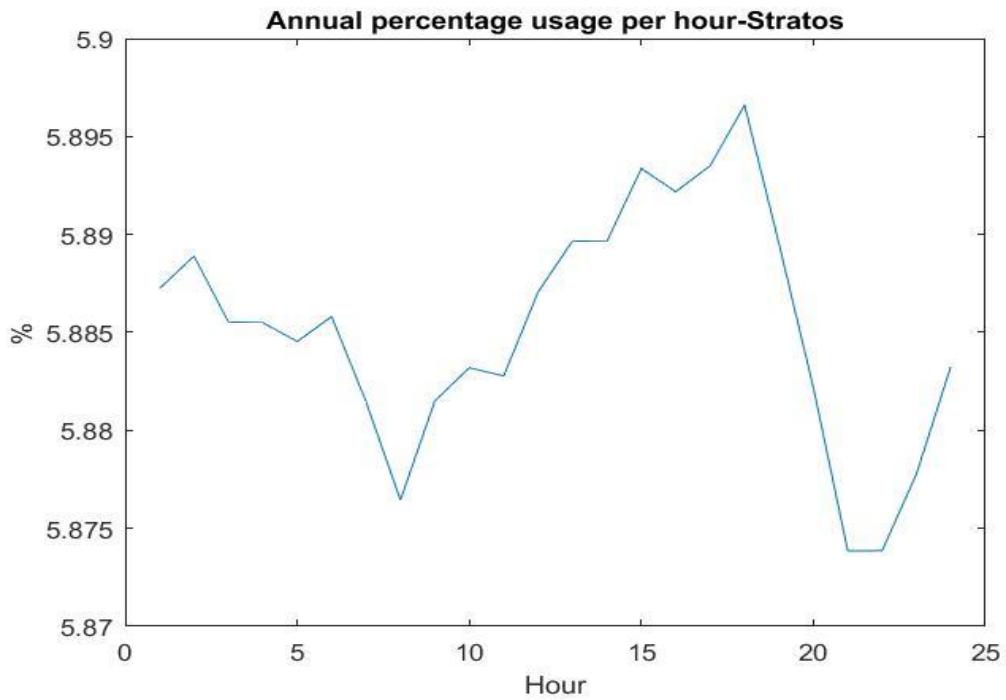


Figure 2.16: Annual percentage of usage of the station per hour (personal calculations from Data [2013-2016]in [12])

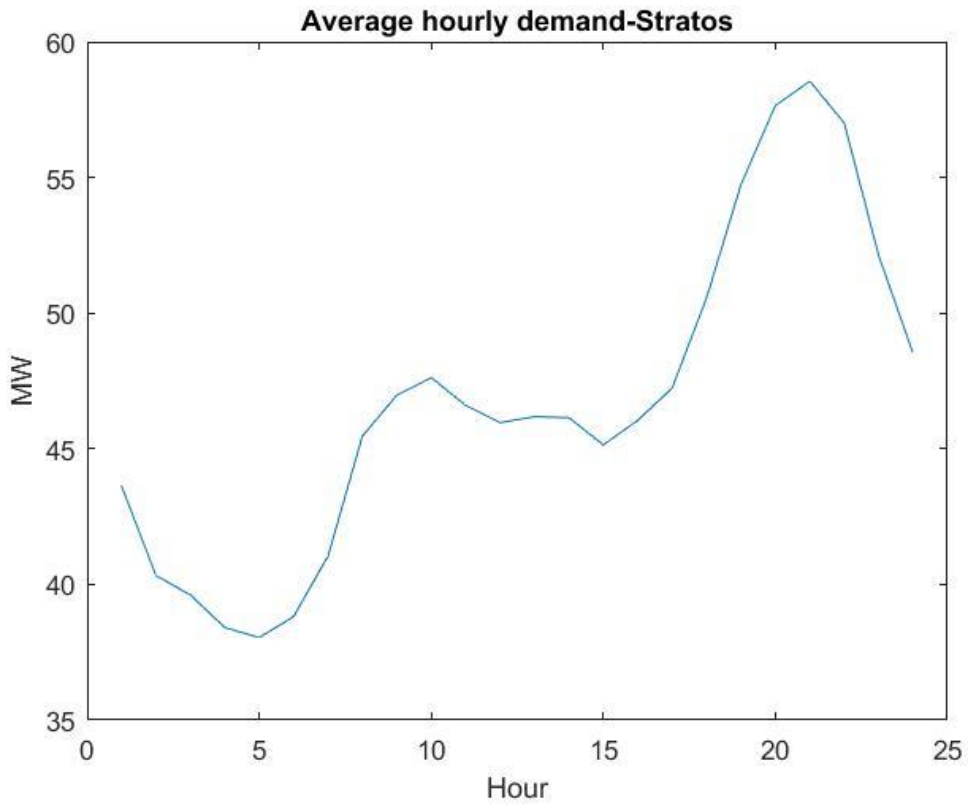


Figure 2.17: Average hourly demand per year (personal calculations from Data [2013-2016]in [12])

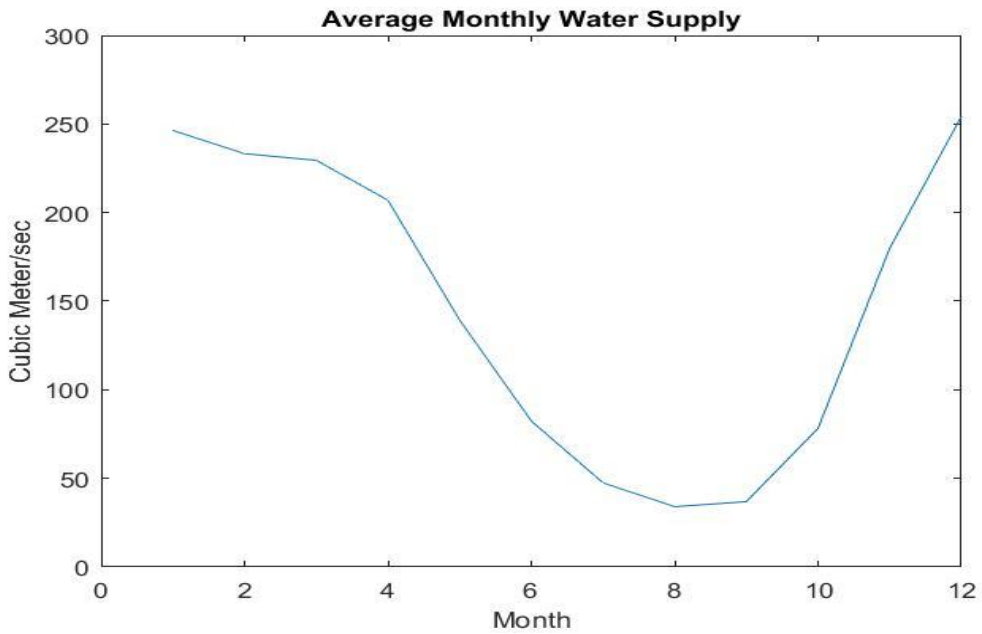


Figure 2.18: Average monthly discharge per month in Kastraki and in Stratos I 1937-1976 (personal calculations from Data [2013-2016]in [12])

Chapter 3

Theory

The purpose of this chapter is to provide the reader with a brief overview as to how hydropower systems operate, in order to supply users connected to the power grid with stable reliable power when demand dictates. An introduction to the properties of fluid conduits, hydropower system components water balance, hydroelectric generation, generators, turbines and their interaction will be given.

3.1 Hydraulic Energy

If water is a natural flow collected at a higher level Z_E , led to a lower level Z_A after passing through a turbine it becomes possible to convert the energy per unit mass.

$$g(Z_E - Z_A) \quad (3.1)$$

of the transit provider to mechanical energy, minus any kind losses. Because the generated mechanical energy, i.e. the torque on the rotatable shaft, cannot be transferred satisfactorily to the place of consumption is converted into electricity by the generator directly coupled to the shaft of the turbine. For this reason, all the works and equipment through which the hydraulic energy is converted into mechanical and then into electricity is called hydroelectric project.

The Hydroelectric project (HEP) is a complex project that includes major civil engineering projects and major electromechanical equipment. The main parts of the works of civil engineering of a hydroelectric plant are: dam, water abstraction, the inlet and exhaust systems of water and hydroelectric power plant (HPP). By electromechanical equipment of HPP meant turbines, power generators, transformers, the lifting equipment (cranes), the compressed air and oil system and automation included in the accessories. Each generator is directly coupled to the turbine on the same shaft, apart from some small units in which interposed gear transmission. The purpose of the transformer is to raise the voltage produced by the generator to the high voltage grid to transfer energy to become smaller losses.

The selection of the station's position depends mainly on the type of hydraulic energy and the type of installation (river flow, waterfall, etc.). In the usual case of pond construction requires proper selection of the dam site and the hydropower plant. Creating artificial lake should be based on hydrological studies and statistical data of collection water in the basin from various sources (streams, snow, etc.). Soil impermeability of the basin under full load conditions is a basic fact of the problem and must be supported by appropriate soil and rock mechanics studies. Where the HEP combined with other projects such as irrigation, water supply etc. The position of the block affected by these

projects. Finally, small HPP (power less than 10 MW) does not require the construction of a dam and large pond.

3.2 Water balance Description

The report of the water balance is in the reservoir level. By this it is meant the basic inventory description relationship and resulting from the application of continuity equation (mass balance):

$$\frac{dS}{dt} = I(t) - O(t) \quad (3.2)$$

Where:

- $S(t)$: storage of reservoir at each time step, t.
- $\frac{dS}{dt}$: the storage rate of change.
- $I(t)$: total inflows to the reservoir.
- $O(t)$: total reservoir outflows.

As is shown in Figure 3.1 the inflows and outflows in this balance expressed in discharge units, like the storage change rate.

The inflows consist of:

- i. Runoff upstream basin I , the components of which can be surface (streams, rivers) and underground (aquifers). The upstream basin refers in this reservoir.
- ii. Precipitation P in the reservoir surface (rainfall, snowfall).

The outflows consist of:

- i. The evaporation E from the water surface of the reservoir.
- ii. Possible underground leaks G , which largely depend on the form the geological formations of the area (aquifer with large hydraulic conductivity and excellent water permeability).
- iii. Downstream runoff: the reservoir overflows Y , withdrawals from the reservoir R .

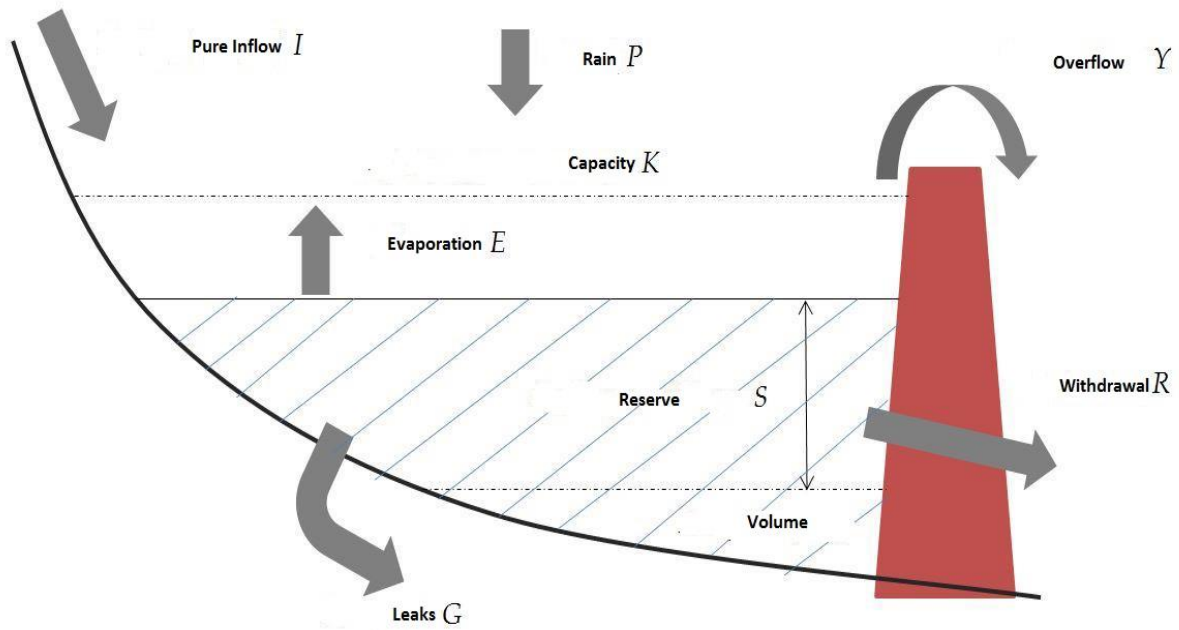


Figure 3.1: Diagram of the water balance components for a single reservoir [15,16]

All components described above are shown schematically in Figure 3.1. After by discretization of the equation (3.2) gives the equation of the water balance as it is customary to use the water resources management problems in general form:

$$S_{t+1} = S_t + I_t + P_t - G_t - E_t - O_t \quad (3.3)$$

Where:

- S_{t+1} : the storage in time $t + 1$
- S_t : the storage in time t
- I_t, P, E_t, O_t o corresponding volume of water passed by the reservoir in time t

The using equation (3.3) assumes the parallel inclusion of operational and physical restrictions

I. Limitation of reservoir capacity:

$$S_{\min} \leq S_t \leq K \quad (3.4)$$

Where

- S_{\min} the dead volume and K the capacity.

II. Limitation resulting from the discharge of supply pipes:

$$0 \leq R_t \leq R_{\max} \quad (3.5)$$

Where

- the discharge

In the case of a hydro system which constituted of several individual reservoirs, despite the apparent complexity, their interaction is reduced to combinations of the simple equation (3.3).

3.3 General Description of Hydroelectric Plants

Hydroelectric plants work on the principle of converting the potential energy between two water levels, first into mechanical power and later into electrical power [17]. Below in the figure the main components of a plant are shown. The basic principle is that water flows from a reservoir or river through a penstock and powers a turbine which creates a mechanical torque and rotational speed which generates electrical power from a generator. Gross power, P_{gross} [m] generated by the plant is dependent on the discharge Q [m³/s] and the gross water head H_{gross} [m] .

$$P_{gross} = \rho Q g H_{gross} n \quad (3.6)$$

Where:

- ρ is the density of water.
- g is the gravity constant (9.81 Newton).
- n is the turbine efficiency.
- The gross head H_{gross} in a plant is defined as the height between the water level of the reservoir and water level of the outlet destination, in Figure 3.1 this would be reservoir level minus the water level of the river. There is also a net head:

$$H_n = H_{gross} - H_L \quad (3.7)$$

Where:

H_L is the sum of all the losses in head throughout the system due to friction, turbulence and so forth. The net power P_n [W] acting on the turbine then becomes:

$$P_n = \rho Q g H_n n \quad (3.8)$$

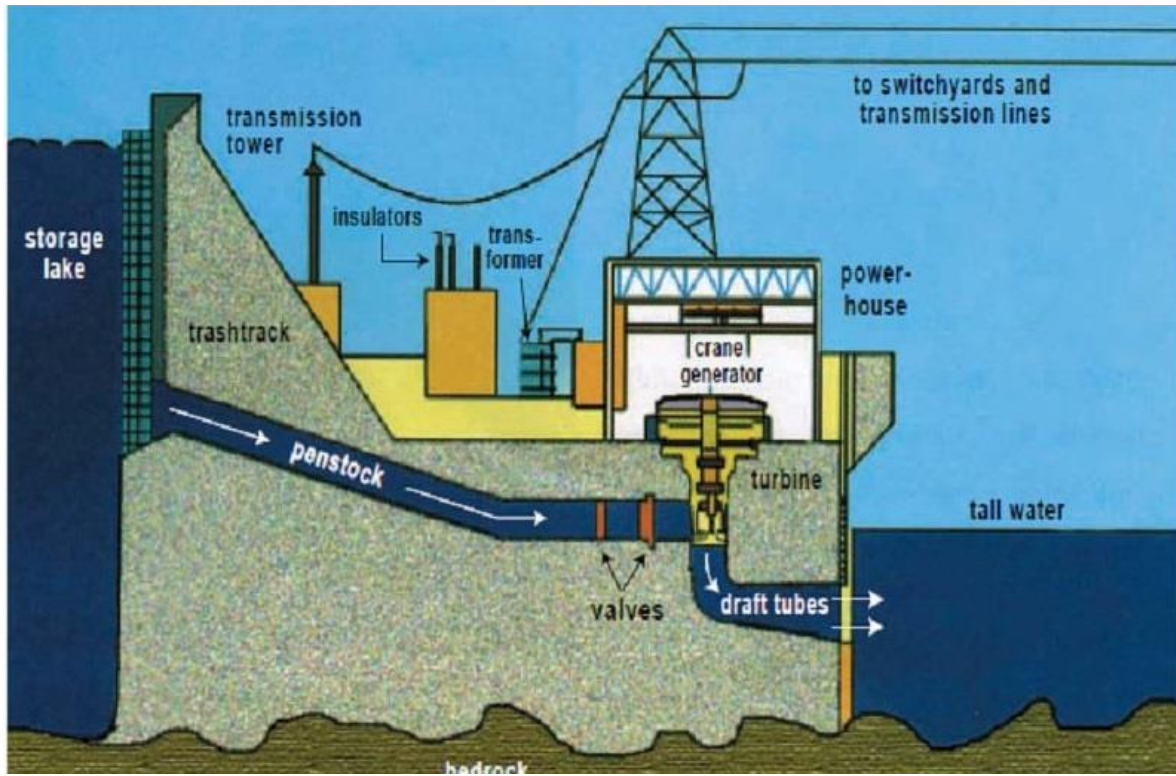


Figure 3.2: Principle of a Hydropower Plant. [18]

As Figure 3.2 shows this potential energy will turn into kinetic energy when the water falls down over the head through the pipeline. This kinetic energy is kind of pressure which will rotate the shaft of hydraulic turbine. Mechanical energy from turbine then will drive synchronous generator to produce electricity in term of alternating current (AC). The electricity will then be distributed to residences.

The other basic relationship of hydropower production is as follows:

$$E_t = \psi V_t H_t \quad (3.9)$$

Where:

- E_t : The energy generated at time step t [GWh].
- V_t : The passing of the turbine water volume at time step t [hm^3].
- H_t : The total height of fall in step t [m].
- ψ : The specific energy, i.e. the energy output per unit of height of the fall and of the transmitted volume [GWh/hm^4].

The specific energy ψ expressed as a function of the power factor of the turbine n of total and net drop height H , H_n respectively:

$$\psi = 0.2725n \frac{H_n}{H} \quad (3.10)$$

The net drop height obtained by the removal of linear and local losses (h_f , h_t respectively) of the flow line from the total drop height.

$$H_n = H + h_f + h_t \quad (3.11)$$

The value 0.2725 shown in relations (3.9) is the limit value of specific energy as shown in a hypothetical system zero losses and maximum efficiency ($n = 1$, $H_n = H$).

3.4 Flow Rate

The amount of Water flow is calculated by:

$$FR = \frac{\pi}{4} d^2 \sqrt{2gz} \quad (3.12)$$

Where:

- z is the specific head height in meters.

3.5 Capacity Factor

“It is the ratio of actual output to its potential output over a period of time”.

The annual energy output of the HPP is calculated as follows:

$$\text{Annual generated energy (KWh / year)} = P \text{ (KW)} * 365 \text{ (days)} * 24 \text{ (hrs)} * CF \quad (3.13)$$

Where:

- CF is the rate of return on hydropower (Capacity Factor) and is expressed as the ratio between the generated power of HPP to maximum power.

$$CF (\%) = \text{annual energy produced (KWh / y)} / P \text{ (KW)} * 365 \text{ (days)} * 24 \text{ (hrs)} \quad (3.14)$$

The Capacity Factor is very important factor, which describes and expresses the performance and the operation of the project.

3.6 Penstocks

A hydroelectric plant is usually located in the downstream of a body of flowing water, such as a river or an artificial lake. A reservoir is not necessary but often constructed to create a buffer of energy,

thus eliminating the dependency of a steady flow. Pipelines are used to feed water to the turbine in micro hydro system. The water should pass first through a simple filter to block debris that may clog up or damage the machine. It is important to use a penstock of sufficiently large diameter to minimize friction losses from the moving water. The water conduit between the turbine and reservoir is called a penstock. It can vary in length from 20 to several thousands of meters and be in the form of open canals, tunnels, pipes or combinations and be constructed in several different materials such as PVC or polyethylene although metal, concrete or steel are used. The penstock is responsible for the major part of a hydroelectric plant system's dynamics.

The unsteady flow behavior in a pipe system due to a regulatory disturbance is called surge. Surge occurs when the volumetric flow rate is changed, and due to the inertia of the masses of moving water. The positive pressure surge due to closing equipment, such as valves and turbines, is also referred to as water hammer.

The characteristics that describe a fall pipe is:

- The material that the conduit has constructed and describes the resistance, the life, the friction coefficient and the cost of purchase and installation.
- The diameter of the pipeline, which is determined by the amount of water to be passed from the duct.
- The thickness of the pipe wall which is selected according to the maximum hydraulic pressure to accept.

Generally, the friction coefficients of the conduits about pressure and resistance are given by manufacturer specifications.

3.6.1 Water Hammer

Water hammering is caused by the rapid loss of momentum of the water in the pipe and this kinetic energy must go somewhere so the pipe contorts, expands and bangs against the interior of the walls to absorb the stress. The same effect will take place in a penstock with long runs with a high rate of flow. Therefore, ensure the pipe and gate valves are able to withstand these forces. When possible, the pipeline should be buried in order to stabilize the pipe and prevents critters from chewing it. In order to counteract the momentum of this retardation, kinetic energy is transferred to pressure energy, causing pressure to increase. The magnitude of theoretical water hammer is given:

$$\Delta H = \frac{\alpha \Delta Q}{g A} \quad (3.15)$$

Where:

- A : Tunnel area [m^2].
- Q : Flow [m^3/s].
- L : Tunnel length [m].
- a : constant speed of sound.

For a conduit with constant speed of sound, this reflection time is:

$$T_r = \frac{2L}{a} \quad (3.16)$$

(3.14) is valid for immediate closure, defined as closure time T_c faster than the wave reflection time given by (3.15). For closures over a time $T_c \gg T_r$.

$$\Delta H = \frac{\alpha \Delta Q T_r}{g A T_c} \quad (3.17)$$

It becomes evident from (3.14) and (3.16) that the largest magnitude of water hammer occurs with a total retardation of the water. It is also dependent on tunnel cross-sectional area. A negative water hammer will occur for an acceleration of the water.

3.7 Reservoirs, Wicket Gate

When opening and closing the wicket gate it takes time for the body of water in the penstock to accelerate or decelerate and this may create pressure hammers or lag time in the system. Water elasticity may also have to be taken into account if the penstock is large enough. Depending on the design and material the penstock creates a loss in head due to friction and turbulence in the water. The connection between the reservoir and penstock is called a water intake, must be taken into consideration since it is a major source of turbulence and friction. The reason for this is mostly because of its design which often includes edges and a trash rack.

3.8 Generators

The conversion of mechanical energy to electricity is through generators. The generators now used in hydro works are three-phase alternating current (AC), while the first generators were (DC). There are two options generators, depending on the existing network to connect the power plant.

Synchronous generators: they are equipped with an induction system connected to a voltage regulator for controlling the voltage, frequency and phase angle before connecting the generator to the grid. By stopping the parallel connection, the synchronous generator will continue to produce voltage and frequency determined by the control equipment. Synchronous generators can operate independently from the grid and generate power since the excitation power does not depend on the network.

Asynchronous generators: Simple electric induction cage motors without adjustable voltage, operating at a speed directly related to system frequency. They draw their excitation current from the

grid, absorbing reactive power. They cannot generate when disconnected from the network when you are not capable of providing their own excitation current.

Synchronous generators are used more frequently, even though it is expensive, in sizes in the range up to 3 MW.

Asynchronous generators used in large networks, while their efficiency is less than, 2% to 4% of that of synchronous. In wind turbines usually asynchronous induction generators used DFIG or permanent magnet synchronous generators (PMSG). But in this thesis we are only concerned with the synchronous machine as electricity generator power, and it has been used for modeling to examine the hydroelectric plants in Kastraki and Stratos I, as we will see below.

3.9 Synchronous generators

This generator is much more expensive and more complex machining of a similar magnitude induction generator. Nevertheless, there is a clear advantage over the induction generator, that need not reactive magnetization current. The magnetic field in the synchronous generator can be created by the use of permanent magnets or a conventional field winding. If the synchronous generator has an appropriate number of poles can be used for direct drive applications without gearbox.

A synchronous machine, is probably the most suitable for a full-power control, as it is connected to the network, via a power electronic transformer. The transformer has two primary objectives: (1) to act as an energy regulator for power fluctuations caused by a native wind gust energy and for transients coming from the side of the network, and (2) to monitor magnetization and avoid problems, remaining synchronous with the mains frequency.

The stator of a synchronous machine consists of a stack of laminated ferromagnetic core with internal slots, a set of three-phase distributed stator windings placed in the core slots, and an outer framework with end shields and bearings for the rotor shaft. The turns of the stator windings are equally distributed over pole-pairs, and the phase axes are spaced $2\pi/3$ electrical radians apart.

The cross-sectional shape of the rotor can be salient or cylindrical. Salient pole construction is mostly used in low-speed applications where the diameter to length ratio of the rotor can be made larger to accommodate the high pole number. Salient pole synchronous machines are often used in hydro generators to match the low operating speed of the hydraulic turbines. The short, pancake-like rotor has separate pole pieces bolted onto the periphery of a spider-web-like hub. Salient here, refers to the protruding poles, the alternating arrangement of pole iron and interpolar gap results in preferred directions of magnetic flux paths or magnetic conductivity.

The cylindrical or round rotor construction is favored in high-speed applications where the diameter to length ratio of the rotor has to be kept small to keep the mechanical stresses from centrifugal forces within acceptable limits. Two- and four-pole cylindrical rotor synchronous machines are used in turbo generators to efficiently match the high operating speed of steam turbines. The long cylindrical rotors are usually produced from solid castings of chromium-nickel-molybdenum steel, with axial slots for the field winding on both sides of a main pole.

Direct current excitation of the field winding can be supplied through a pair of insulated slip rings mounted on the rotor shaft. Alternatively, the DC excitation can be obtained from the rectified output of a small alternator mounted on the same rotor shaft of the synchronous machine. The second excitation method eliminates the slip rings and it is called brushless excitation.

In the basic two-pole representation of a synchronous machine (see Figure 3.3), the axis of the poles is called the direct or d-axis. The quadrature, or q-axis, is defined in the direction 90 electrical degrees ahead of the direct axis. Under no-load operation with only field excitation, the field EMF (Electromagnetic Force) will be along the d-axis, and the stator internal voltage, $d\lambda_{af}/dt$, will be along the q-axis. The field is located on the rotor which is the rotating part of the generator connected to the shaft of for example a turbine on a hydro plant. The armature is located on the stator which is the static part of the machine. The armature and the field can also be fitted in opposite positions, but since the armature windings usually operate at a considerably higher voltage than the field windings and thus they require more space for insulation. The armature windings are also subject to much higher transient currents and must have sufficient mechanical strength. Therefore, the normal case is to have the armature on the stator. The three-phase armature windings are distributed 120° apart from each other in space. This means that with uniform rotation of the magnetic field, the voltages produced in the windings will be displaced by 120° in the time phase [19].

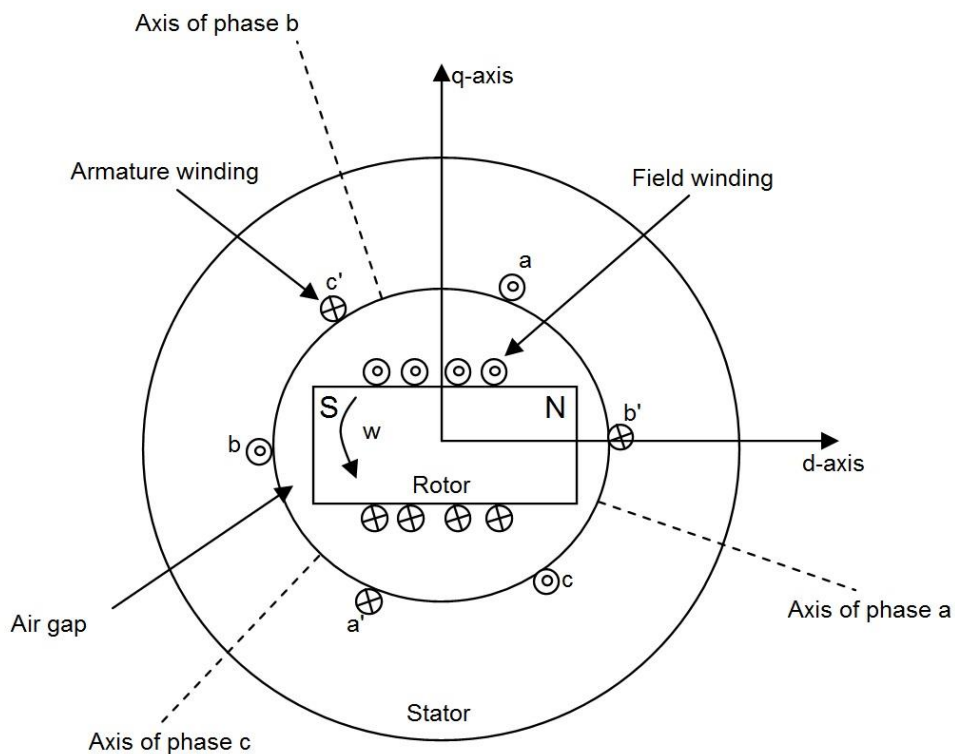


Figure 3.3: Schematic diagram over a three phase synchronous machine [17]

A direct current goes through the field windings and induces a magnetic field ϕ_r which induces alternative voltage(EMF) E_r in the armature windings when rotating. This EMF is 90° after the induced magnetic field ϕ_r (see Figure 3.4). The armature current I_a also induces a magnetic field

Having defined the positive direction of currents leaving the machine for generator operation, the actual P_G power and reactive power Q_G are positive quantities.

$$S = P_G + jQ_G = V_t I_a \quad (3.20)$$

For synchronous machine that uses salient pole rotor, the actual and reactive power is given by the following relationships:

$$P_G = \frac{|E||V_t|}{X_d} \sin \delta_m + \frac{|V_t|^2}{2} \left(\frac{1}{X_q} - \frac{1}{X_d} \right) \sin 2\delta_m \quad (3.21)$$

$$Q_G = \frac{|E||V_t|}{X_d} \sin \delta_m + \frac{|V_t|^2}{2} \left(\frac{\cos^2 \delta_m}{X_d} - \frac{\sin^2 \delta_m}{X_q} \right) \quad (3.22)$$

While a machine with a cylindrical rotor, wherein $X_d = X_q$, the above relationships take simple form and made:

$$P_G = \frac{|E||V_t|}{X_d} \sin \delta_m \quad Q_G = \frac{|V_t|(|E| \delta_m - |V_t|)}{X_d} \quad (3.23)$$

If E , V_t sizes expressed in phasic values, the above relationships give the per phase real and reactive power of the generator, while if the E , V_t expressed in polar values, giving the total three-phase powers.

Assuming that the generator is connected to a large and stable grid, the terminal voltage V_t of the balance amount is constant. If we also consider that the field current is constant, then and EMF E is constant and therefore the real and reactive power of generator are functions only of the power angle δ_m . As power angle is defined as the phase difference between the EMF E and the voltage V_t on the bus. On machines with rotor salient pole maximum active power provided in a δ_m angle $< 90^\circ$, while in the cylindrical rotor machines for $\delta_m = 90^\circ$. If we try to raise the actual power beyond its maximum value, the generator desynchronized from network. To avoid this problem, usually operate generators in small power angles, around the 20° , power factor less than the maximum. This gives us the advantage of ensuring non de-synchronization of the generator if suddenly is required more power from the network. The reactive power $P_G > 0$, the machine produces reactive power and it acts as transverse capacitor network. This is large values of EMF E . In this case we say that the machine is in hyper stimulation. In the opposite case the $P_G < 0$, the machine consumes reactive power from the grid, that acts as a cross coil. In this case we say that the machine is in under excited. Overstimulation and under excited are conditions they have nothing to do with whether the machine operates as motor or generator. From the above summarized that we can control sufficiently the production or

consumption of reactive power from a machine, by simply regulating the EMF E . This method is used and modern equalizers of electricity networks.

3.9.1 Generator Control

A generator supplies the network with complex power $S_G = P_G + Q_G$ connected to a voltage bus $|V|$ and in sync with the network which has frequency f .

The production of reactive and active power is controlled through two control inputs, which are:

1) The field current to the rotor i_f , 2) The mechanical torque to the generator shaft T_m

while the four outputs to be controlled are: P_G , Q_G , V and f . Actually if we change an entry, then, because of interactions within the engine are changed and the four outputs generator. The only case where these interactions are minimal and each input controls one output, is the connection in a stable and large grid. Such a network has very high inertia with respect to a generator, so any changing in the generator inputs does not affect the frequency f , and voltage V . This results essentially having two variables input and two output variables, P_G and Q_G .

Although if initially the mechanical torque T_m changes to the axis of generator, for example by adjusting suitably the water gate in a hydroelectric power station, would tend to change and kinetic situation of the generator rotor. The angular speed of the rotor but is determined by the frequency f of the strong network and therefore it can not be changed. According to the above relationships for the power in a generator, the only can be changed is the active power of the generator and as a consequence the power angle δ_m . The change of power angle in turn seems to pose change in reactive power Q_G . The change will be very small as negligible as for small values of δ_m angle usually the generators $\cos \delta_m$ is nowhere sensitive to changes. If it changes the i_f excitation current will change accordingly EMF E and the reactive power Q_G . To not be changed the active power, should the product $|E| \sin \delta_m$ to be kept stable. In summary, I have seen that when the generator is connected in an infinite network, changing the mechanical torque on the shaft generator mainly influence the actual power P_G , while changing the excitation current (or field current) i_f influence mainly reactive power Q_G .

If the generator is connected to non-infinite bus, the behavior of the change in the two control inputs are more complicated, because now the voltage V on the bus is not stable, but varies as a function of the generated complex S_G power. With regard to changes in the two other controlled output variables, P_G and Q_G , are made with the same logic as before, just now varies with them and the tendency of the bus V [20].

3.10 Hydroturbines

Generating power is a long standing issue due to the disadvantages of many of the modern techniques that require large amounts of energy or fuel. Energy consumption and population are always increasing, so it is essential for engineers and scientists to come up with natural and affordable ways

to produce power with minimal effect on the environment. One of these methods includes utilizing the physical properties of water and how it naturally acts in our environment. This is known as hydropower, or hydroelectric power, and is an environmentally friendly and efficient way to supply surrounding areas with power and electricity to live their daily lives.

Engineers have the ability to produce mechanisms or create environments that cause water to produce energy naturally, which can be transferred directly to an object to cause mechanical work. This work can be transferred into a generator to produce electricity. One way of producing this water energy is through use of a turbine. A turbine is a mechanism that accepts moving water, and contains a wheel or rotor that spins as the water impacts one of its blades. The faster the flow rate of water, the higher the frequency of the wheel or rotor. This rotation drives a shaft connected to the generator which ultimately produces power. There are often guide vanes or wicket gates that can control the flow of water impacting the blades and therefore output power, which ultimately controls the efficiency of the turbine.

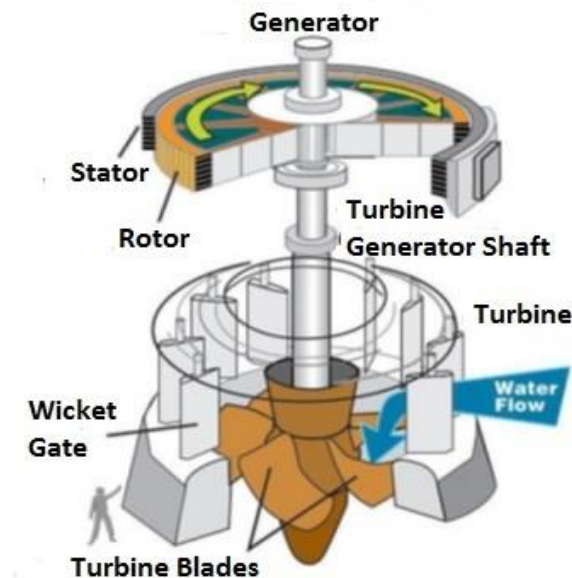


Figure 3.6: Kaplan turbine and electrical generator cut-away view [24]

All components of a hydropower system revolve around the turbine. The turbine converts hydraulic power from the water flowing from the reservoirs into mechanical shaft-power for the generator. There are two main types, impulse and reaction turbines, and the Francis belong to the latter. What differs them a part is the way the energy conversion carried out. In an impulse turbine water flows through a nozzle and hits the turbine. Thus, the energy flow is converted into kinetic energy which affects the turbine runner. In a reaction type turbine there are two types of energy conversions. First, the turbine is completely submerged in water, which creates a pressure drop between the inlet and the outlet that is converted into axial power, also called the reactive part. Secondly, impulse forces are created because of changes in velocity vectors when the water flows between the turbine blades. The most common reaction turbines used are Francis, Bulb and Kaplan, while the only impulse turbine really used today is the Pelton. three types of turbines are in widespread commercial use, Kaplan, Francis and Pelton. The selection of turbine depends mainly on the plant's head and available flow.

Table 3.1 Types of Turbines

Kaplan	Used for low head, high flow plants
Pelton	Used for high head, low to medium flow plants
Francis	Used for medium to high head, medium flow plants

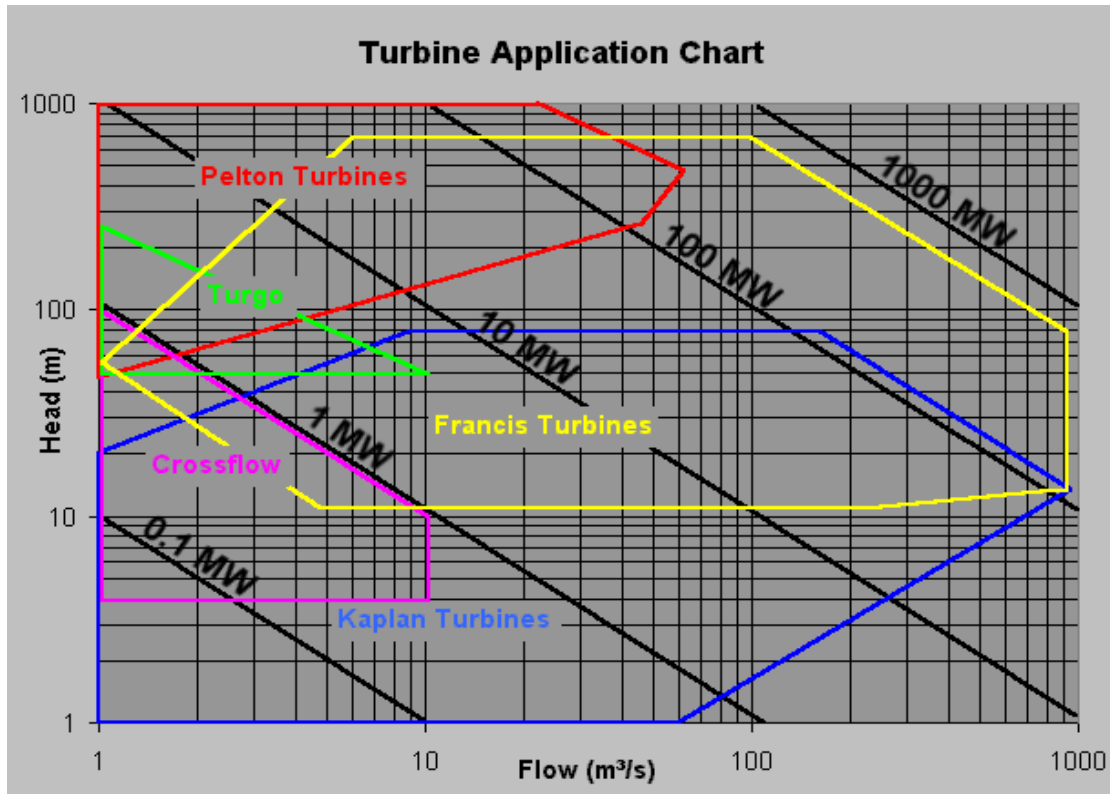


Figure 3.7: Turbine suitability diagram [25]

The Figure 3.7 shows the range of operation of various types of water turbines in line with the drop height(Head) and flow. The drop height itself is the first criterion for choosing the appropriate turbine type.

In this thesis, an investigation into the use of a model for Francis type turbines will be given. Subsequently, this type of turbine will be the focus in this section as in both Hydroelectric plants in Kastraki and in Stratos I this type is used.

3.10.1 Francis Turbine (Reaction Turbine)

The reaction turbine consists of fixed guide vanes called stay vanes, adjustable guide vanes called wicket gates, and rotating blades called runner blades. Flow enters tangentially at high pressure, is turned toward the runner by the stay vanes as it moves along the spiral casing or volute, and then passes through the wicket gates with a large tangential velocity component. Momentum is exchanged between the fluid and the runner as the runner rotates, and there is a large pressure drop.

Unlike the impulse turbine, the water completely fills the casing of a reaction turbine. For this reason, a reaction turbine generally produces more power than an impulse turbine of the same diameter, net head, and volume flow rate. The angle of the wicket gates is adjustable so as to control the volume flow rate through the runner. In most designs the wicket gates can close on each other, cutting off the flow of water into the runner. At design conditions the flow leaving the wicket gates impinges parallel to the runner blade leading edge to avoid shock losses.

The most common and preferred type of turbine is the Francis turbine, invented by James Francis in Lowell, MA in 1848. Francis turbines are used to generate about 60% of the global hydropower in the world, making them the most widely used type of turbine (Alstom). This type of turbine receives water at high pressure and causes the water exiting the turbine to leave at a much lower pressure. This change in momentum is transferred to the blades and causes the shaft to rotate at a much greater frequency. This causes the Francis turbine to be capable of much greater power output and therefore higher efficiency than other types of turbines as seen above in Figure 3.7.

In Francis turbine, a reaction turbine, there is a drop in static pressure and a drop in velocity head during energy transfer in the runner. Only part of the total head presented to the machine is converted to velocity head before entering the runner. This is achieved in the adjustable guide vanes, shown in Figure 3.8.

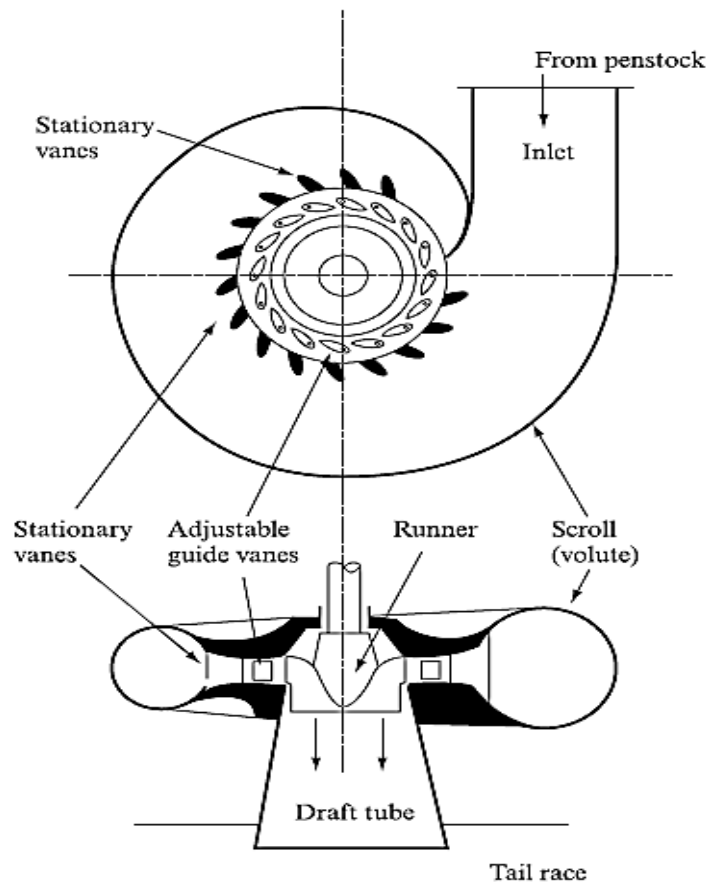


Figure 3.8: Configuration of a Francis Turbine [26]

Similarly, to Pelton wheel, Francis turbine usually drives an alternator and, hence, its speed must be constant. Since the total head available is constant and dissipation of energy by throttling is undesirable, the regulation at part load is achieved by varying the guide vane angle. This is possible because there is no requirement for the speed ratio to remain constant. In Francis turbines, sudden load changes are catered for either by a bypass valve or by a surge tank.

3.10.2 Spiral casing

Most of these machines have vertical shafts although some smaller machines of this type have horizontal shaft. The fluid enters from the penstock (pipeline leading to the turbine from the reservoir at high altitude) to a spiral casing which completely surrounds the runner. This casing is known as scroll casing or volute. The cross-sectional area of this casing decreases uniformly along the circumference to keep the fluid velocity constant in magnitude along its path towards the stay vane. This is so because the rate of flow along the fluid path in the volute decreases due to continuous entry of the fluid to the runner through the openings of the stay vanes. This is one of the main features that differentiate a Francis from other turbine types, only a part of the total specific energy at the inlet of the turbine is converted to kinetic energy before the runner is reached. The guide vanes can also be used to regulate the flow rate.

3.10.3 Stay Vanes and Wicket Gates

Water flow is directed toward the runner by the stay vanes as it moves along the spiral casing, and then it passes through the wicket gates. The basic purpose of the wicket gate is to convert a part of pressure energy of the fluid to the kinetic energy and then to direct the fluid on to the runner blades at the angle appropriate to the design. Moreover, they are pivoted and can be turned by a suitable governing mechanism to regulate the flow while the load changes. The wicket gates impart a tangential velocity and hence an angular momentum to the water before its entry to the runner.

3.10.4 Runner

It is the main part of the turbine that has blades on its periphery. During operation, runner rotates and produces power. For a mixed flow type Francis Turbine, the flow in the runner is not purely radial but a combination of radial and axial. The flow is inward, i.e. from the periphery towards the centre. The main direction of flow changes as water passes through the runner and is finally turned into the axial direction while entering the draft tube.

3.10.5 Power and Efficiency Expressions

Considering runner generates a torque of T with a rotational speed of N (rev/s), then power obtained from the runner can be expressed as: *Power Output = (Torque)(Angular velocity)*

$$P_{out} = T\omega \text{ [W]} \quad (3.24)$$

$$T = Fr \quad (3.25)$$

$$\omega = 2\pi N \text{ [rad/s]} \quad (3.26)$$

Where:

- F is the force in pounds or newtons.
- r is the radius or distance from the center to the edge in feet or meters.

The total head available at the nozzle is equal to gross head less losses in the pipeline leading to the nozzle (in the penstock) and denoted by H . Then available power input to the turbine becomes:

$$P_{in} = \rho g Q H \quad (3.27)$$

Where:

- P_{in} power input to turbine.
- H total available head at turbine inlet [m].
- ρ density of water [kg/m^3].
- Q volume flow rate of water [m^3/s].
- g gravitational acceleration [m/s^2].

During conversion of energy (hydraulic energy to mechanic energy or vice versa) there occur some losses. They can be in many form and main causes of them are friction, separation and leakage [26,27].

For a turbine:

$$\text{Fluid Input Power} = (\text{Mechanical loss}) + (\text{Hydraulic losses}) + (\text{Useful shaft power output}) \quad (3.28)$$

Where:

$$\text{Hydraulic Losses} = (\text{Impeller loss}) + (\text{Casing loss}) + (\text{Leakage loss}) \quad (3.29)$$

Considering all losses as one term:

$$P_{in} = P_{lost} + P_{out} \quad (3.30)$$

Then, overall efficiency of turbine becomes:

$$n_o = \frac{P_{out}}{P_{in}} = \frac{T\omega}{\rho g Q H} \quad (3.31)$$

3.10.6 Self governing

For fully submerged turbines such as Francis type, a phenomenon called selfgoverning occurs. This occurs due to flow in the turbine channels being dependent on the rotational speed. When the generator is disconnected from the grid, the runner is allowed to rotate faster than its design parameters. This will result in a throttling of the turbine due to increased centripetal force acting on the water as it flows through the runner. This results in lower efficiency, and any further increase in rotational speed will be reduced. This increases stability during load rejections.

3.10.7 Draft Tube

After passing through the turbine runner, the exiting fluid still has appreciable kinetic energy. To recover some of this kinetic energy the flow enters an expanding area (diffuser) called draft tube, which slows down the flow speed, while increasing the pressure prior to discharge into the downstream water. Therefore, the primary function of the draft tube is to reduce the velocity of the discharged water to minimize the loss of kinetic energy at the outlet. This permits the turbine to be set above the tail water without any appreciable drop of available head. Moreover, careful design of draft tube is vital, otherwise cavitation can occur inside the tube. The purpose of the draft tube is to convert residual kinetic energy in the spent water back to pressure energy, in order to increase the pressure differential over the turbine, hence increasing efficiency.

3.10.8 Turbine Losses

A modern hydro turbine is a very efficient machine, however it is not able to extract all the energy from the flowing water. There are several sources of loss that influence the overall efficiency.

- **Friction losses** occur due to contact friction between rotating and stationary parts, as well as friction from the water enclosing the turbine. These losses act as a resistance against rotation.
- **Losses due to undesirable inflow conditions** occurs when the turbine is operating outside its design parameters.
- **Draft tube loss** occurs as a result of undesirable flow angle out of the runner, causing swirl. Due to this swirl, the draft tube fails to regenerate some kinetic energy from the flow. Both draft tube loss and inflow angle losses are caused by flow angles being out of optimum design point.
- **Viscous loss** occurs throughout the turbine in the same way as in pipes.
- **Leakage loss** is a reduction in output power due to the loss of water mass. This usually occurs as the water is flowing from the spiral casing into the runner, by leakage via the small gap between them.

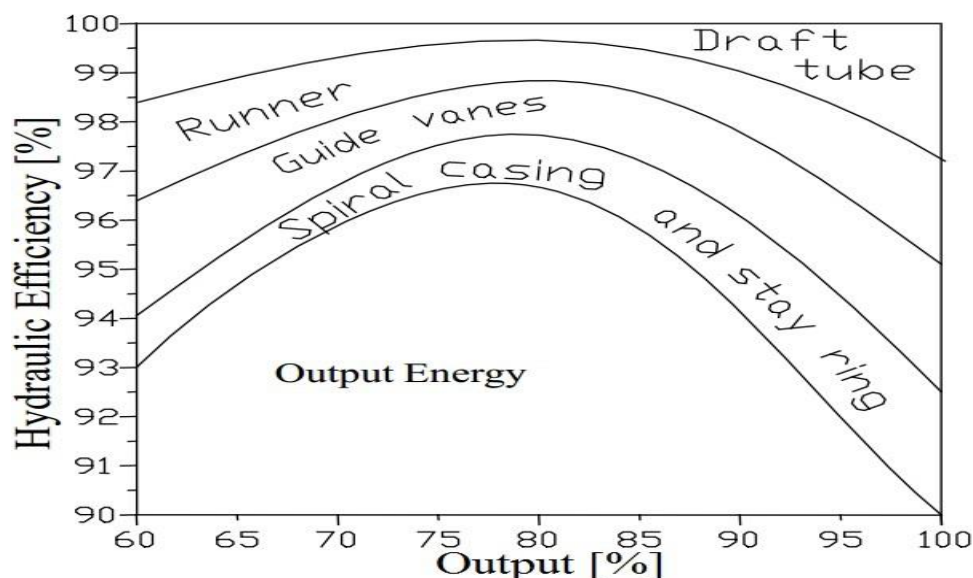


Figure 3.9: The sum of all losses creates the efficiency diagram [27]

Typically, largest energy losses occur in the runner and guide vanes. As velocity head decreases, these losses, as well as losses due to friction, remain relatively constant. Losses in the draft tube are more variable due to pressure decreases with low flow. Variability of losses with respect to total head is shown in Figure 3.9.

3.11 Turbine-Generator relationship

The generator needs to generate an alternating voltage signal with a frequency specified by grid-users, usually a small interval around 50 or 60 Hz (50 Hz in Greece). In order to achieve this, the generator rotor needs to have the correct amount of rotor poles with regards to the turbine optimal rotational speed. For a 2-pole generator, the voltage completes one period per revolution of the rotor. The voltage angular frequency for steady-state operation is then described by:

$$\omega_{grid} = \omega_{generator} = \frac{P}{2} \omega_t \quad (3.32)$$

Where:

- ω_{grid} - Grid angular frequency.
- P - Generator poles.
- ω_t - Turbine angular frequency.

This means that the generator must yield a variable power output at a constant rotational speed. It must also operate within a reasonably constant voltage. The output power (and torque) is then a function of the output current.

$$P_{electric} = \omega_{grid} T = EI \quad (3.33)$$

The output is increased by adjusting the rotor magnetization current. When the generator is producing power at a steady-state condition, the rotor will rotate at an angular displacement located in front of the synchronous reference frame of the stator. This can be viewed as the rotor "pulling" the magnetic field along with the rotation. This angle is a function of the generator output, the larger the output, the larger the displacement. Should either the output power or grid frequency change, so will the magnetic displacement angle, thus allowing the turbine to accelerate the rotor slightly despite being grid-connected. Shifting the synchronous machine power angle requires torque. This will act as a magnetic spring that resists sudden changes in rotational speed, hence acting in the direction opposite of rotational acceleration. All of these factors must be accounted for in the simulation model.

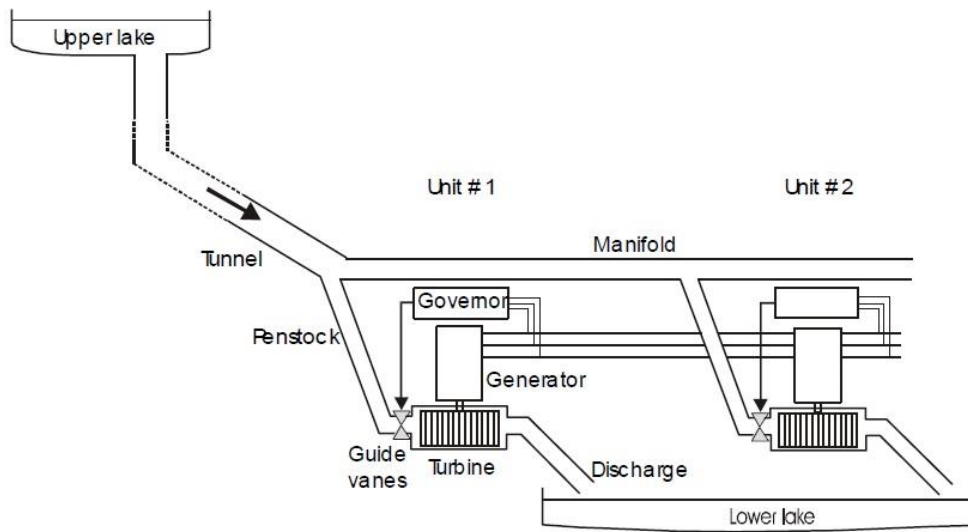


Figure 3.10: Schematic of a hydroelectric power plant of multiple parallel units [33]

3.12 Power System and Grid

A power plant has two tasks. As Figure 3.11 shows the first is to supply energy to the clients attached to the system via the grid. The other is to aid in overall grid stability. In this term, stability is focused around grid frequency and voltage.

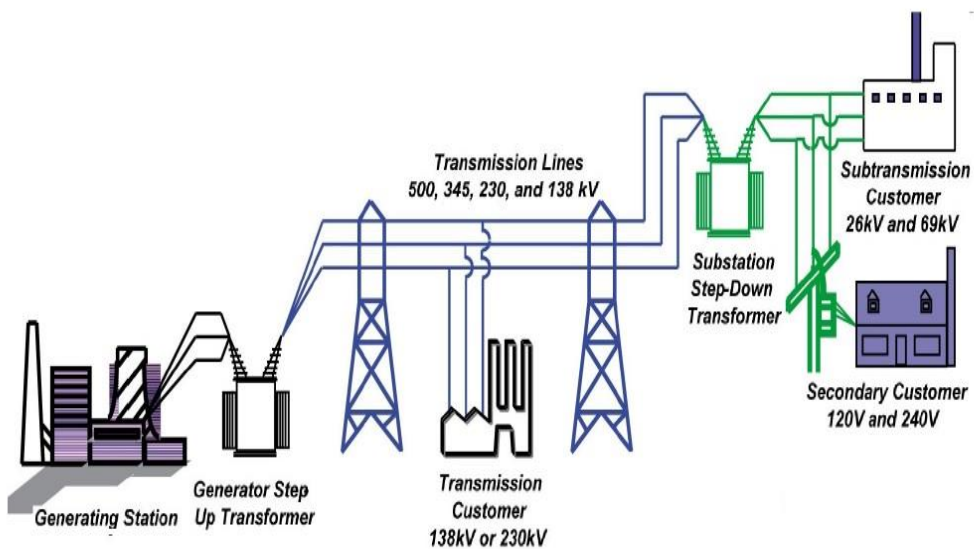


Figure 3.11: Power system illustration [3]

3.12.1 Frequency

All components and appliances connected to the grid is designed to operate at a specific frequency or set of frequencies, thus it must not be allowed to significantly drop or increase. Variations in the frequency are caused by changes in the supply/demand balance. This can be explained by the combined rotating flywheel mass of all synchronous rotating units. All rotating units have mass attached to them, most is due to the machine components themselves. However, extra flywheel mass is also added. While rotating, this mass can store large amounts of energy, hence acting as a buffer.

When the energy demand increases, energy is drained from this mass and actually allows the units to deliver more energy than is actually produced for a short period of time. As a consequence, the collective rotational speed of all units will drop this will result in a drop in frequency. To counteract this, some units will need to increase production in order to meet the increased demand as well as to "recharge" the drained mass.

3.12.2 Load distribution and permanent Speed Droop

When the load changes, some units are more suited to handle this variation than others. Examples are thermal plants versus hydropower plants. Thermal plants are very slow, and does not change load easily. On the other hand, hydropower plants can change load almost instantly and are therefore more suited to keep grid stability. In Kastraki and Stratos I hydroelectric power plants, every few minutes there is a change of load. To determine which plant will handle changes in load, the governors that regulate generator output has a property called "permanent speed droop. This property sets a slope between variations in load versus frequency, illustrated in Figure 3.12.

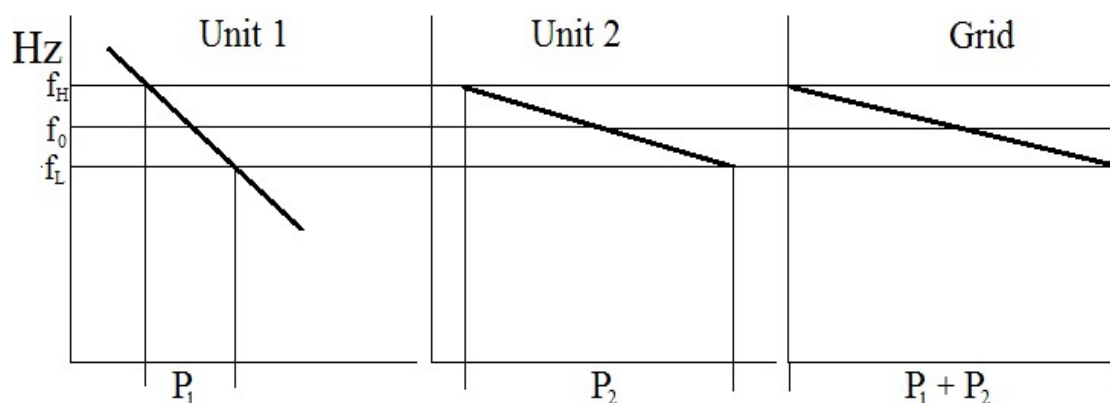


Figure 3.12: Speed droop and power distribution line for two units creating their own grid [3]

Setting a steep load variation line will mean the plant output is independent of grid frequency (typical of large thermal plants), and a flat line gives large load variations with change in frequency (typical of agile hydropower plants). The sum of all responses will set the total grid frequency as a function of load demand. Depending on the size during the load changes the rate at which decreases the frequency changes to be as possible gets closer to the normal operation frequency.



Figure 3.13: Kastraki Hydroelectric Power Plant (personal archive)

3.13 Per Unit System

In this Diploma Thesis all the generator and network models are in per-unit, which means that all the values are normalized to a common MVA base. This is standard practice in power system analysis and usually the generator parameters are given in per-unit from the manufacturer. For example, by normalizing the generator equations it will be easier to understand the generator performance due to that the parameters will be of same type. The per-unit value is calculated in the following way [44].

Where:

$$PerUnit_{value} = \frac{actual_{value}}{base_{value}} \quad (3.34)$$

Chapter 4

Modeling of a Hydroelectric Power Plant.

4.1 Introduction

Hydroelectricity is an important component of the world's renewable energy supply. Electricity generation in the world has been on the increase over the last few decades especially in the developing nations where hydropower remains the major source of electricity generation. Also Hydro-electric power is a form of renewable energy resource, which comes from the flowing water. To generate electricity, water must be in motion. When the water is falling by the force of gravity, its potential energy converts into kinetic energy. This kinetic energy of the flowing water turns blades or vanes in a hydraulic turbine, the form of energy is changed to mechanical energy. The turbine turns the generator rotor which then converts this mechanical energy into electrical energy. The electrical energy to be supplied to the end users is then transformed from mechanical energy by the synchronous generators. The speed governing system adjusts the generator speed based on the input signals of the deviations of both system frequency and interchanged power with respect to the reference settings. This is to ensure that the generator operates at or near nominal speed at all times.

4.2 Hydroelectric Power Plant components

The hydropower plant is basically made of a generator, a turbine, a penstock and wicket gates. In Kastraki HPP and in Stratos I HPP, the type of turbines is used: reaction turbine Francis in this case. The generator and turbine are mostly connected directly by a vertical shaft. The existence of high head produces fast-flowing water that flows through the penstock and arrives to the turbine. The flow of water into the turbine is controlled by the wicket gates. Wicket gates can be adjusted together with the opening of pivot around the periphery of the turbine to control the quantity of water that flows into the turbine. Servo-actuators, controlled by the governor, help to adjust these gates. The water drives the turbine-generator set and the rotating generator produces electricity. At the initial stage, the stored water with clear hydraulic head, possesses potential energy. As it flows through the penstock it gradually loses potential energy and gain kinetic energy before reaching the turbine. A critical look at the process of energy generation by hydropower plant shows that hydropower plant models are highly influenced by the penstock-turbine system, the electric generator and numerous control systems.

In this thesis accurate mathematical representation of power system components is significant for dynamic and transient stability studies. Therefore, some standard dynamic models for prime movers were introduced previously for simulation programs and other purposes in the literature. The parameters of these models need to be determined by operators and engineers as accurate as possible to take into account the behavior of such elements in power system dynamic simulations.

Furthermore, one important application of such modeling is tuning of the parameters of the unit controller such as governor. In order to guarantee good performance of electric power generation process in different conditions, the parameters of the controllers of the components have to be properly tuned. In this chapter I am trying to analyze the mathematical system modeling of the basic components of hydroelectric power plant so as I can use them to build our hydroelectric power plants in Kastraki and Stratos I in the software program we will choose.

4.3 Non-Linear Mathematical Modeling

There are many models that are used to describe the various power system components. As a result, the study of the dynamic behavior of the system depends upon the nature of the differential equations.

- **Small System:** If the system equations are linear, the techniques of linear system analysis are used to study dynamic behavior. Each component is simulated by transfer function and these transfer functions blocks are connected to represent the system under study.
- **Large System:** Here state-space model will be used for system studies described by linear differential equations. However, for transient stability study the nonlinear differential equations are used.

In general, linear models are used for small signal performance of turbine whereas non-linear models are more appropriate for large domain signal-time simulations

So in this thesis I will use the non-linear mathematic approximation for the construction of our models. Appropriate nonlinear model is required for large signal time-domain simulations such as islanding, load rejection, system restoration, etc. Hydrodynamics and mechanic-electric dynamics are included in nonlinear models. Nonlinear models can be generally represented by the block diagram. Also nonlinear models are required where speed and power changes are large. For governor, mathematical equations of ordinary differential equations representing the dynamic behavior are used. Here the regulator consists of two parts electrical (PID Controller) and electro-hydraulic parts. The generator model is derived starting from the basic circuit equations and the use of Park's transformation. The Park transformation maps the synchronous machine equations to the rotating reference frame with respect to the electrical angle. The Park transformation is used to define the per-unit synchronous machine equations. For excitors ordinary differential equations are used.

4.4 Model of Hydropower plant

An ideal modeling of HPP components, such as synchronous machine, turbine and its governing system is necessary to analysis the power system response during any disturbance on the system. Power system performance is affected by dynamic characteristics of hydraulic turbine and its governor system during any disturbance, such as presence of a fault, harmonics on the network, rapid change of load and loss of a line. The block diagram of the Hydraulic Turbine with governor, servomotor, synchronous machine and the generator excitation is shown in Figure 4.1.

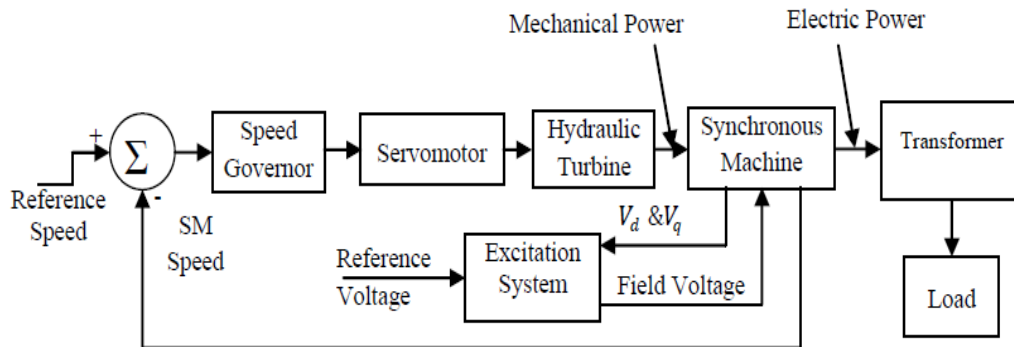


Figure 4.1: Block Diagram for Hydro power plant [34]

The stored water at certain head contains potential energy. This energy is converted to kinetic energy. When it is allowed to pass through the penstock, this kinetic energy is converted to mechanical energy (rotational energy) which allows water to fall on the runner blades of the turbine. As the shaft of the generator is coupled to the turbine, the generator produces electrical energy by converting the mechanical energy into electrical energy.

The speed governing system of turbine adjusts the generator speed based on the feedback signals of the deviations of both system frequency and power with respect to their reference settings. This ensures power generation at synchronous frequency.

In this simulation model, the reference speed signal is obtained from the kinetic energy of the falling water through the penstock. The measured synchronous machine speed is fed back to compare with the reference speed signal. The speed deviation produced by comparing reference and synchronous generator speed is used as input for PID based speed governor. Usually PID is used as turbine governor because this control has simple structure, stability, strong robustness and non-steady state error. The governor produces the control signal, causing a change in the gate opening. The turbine in turn produces the torque, driving the synchronous machine that generates the electrical power output. The speed governor constantly checks speed deviation to take action.

4.5 Synchronous machine model

The Synchronous Machine model operates in generator or motor modes. The operating mode is dictated by the sign of the mechanical power (positive for generator mode, negative for motor mode). The electrical part of the machine is represented by a sixth-order state-space model and the mechanical part is the same as in the Simplified Synchronous Machine block.

The model takes into account the dynamics of the stator, field, and damper windings. The equivalent circuit of the model is represented in the rotor reference frame (qd frame). All rotor parameters and electrical quantities are viewed from the stator. They are identified by primed variables. The subscripts used are defined as follows:

- d, q : d and q axis quantity.
- R, s : Rotor and stator quantity.

- l, m : Leakage and magnetizing inductance.
- f, k : Field and damper winding quantity.

The electrical model of the machine is as follow:

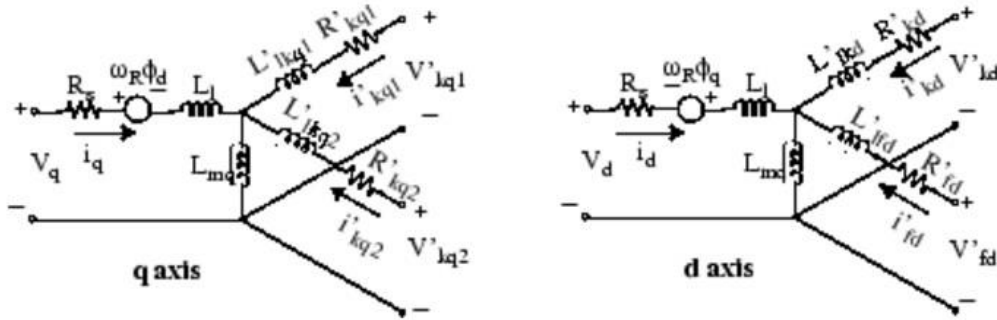


Figure 4.2: Electrical model of synchronous machine with the following equations. [36]

$$V_d = R_s i_d + \frac{d}{dt} \phi_d - \omega_R \phi_q \quad \phi_d = L_d i_d + L_{md} (i'_{fd} + i'_{kd}) \quad (4.1)$$

$$V_q = R_s i_q + \frac{d}{dt} \phi_q - \omega_R \phi_d \quad \phi_q = L_q i_q + L_{mq} i'_{kq} \quad (4.2)$$

$$V'_{fd} = R'_{fd} i'_{fd} + \frac{d}{dt} \phi'_{fd} \quad \phi'_{fd} = L'_{fd} i'_{fd} + L_{md} (i_d + i'_{kd}) \quad (4.3)$$

$$V'_{kd} = R'_{kd} i'_{kd} + \frac{d}{dt} \phi'_{kd} \quad \phi'_{kd} = L'_{kd} i'_{kd} + L_{md} (i_d + i'_{fd}) \quad (4.4)$$

$$V'_{kq1} = R'_{kq1} i'_{kq1} + \frac{d}{dt} \phi'_{kq1} \quad \phi'_{kq1} = L'_{kq1} i'_{kq1} + L_{mq} i_{kq} \quad (4.5)$$

$$V'_{kq2} = R'_{kq2} i'_{kq2} + \frac{d}{dt} \phi'_{kq2} \quad \phi'_{kq2} = L'_{kq2} i'_{kq2} + L_{mq} i_{kq} \quad (4.6)$$

This model assumes currents flowing into the stator windings. The measured stator currents returned by the Synchronous Machine block (I_a, I_b, I_c, I_d, I_q) are the currents flowing out of the machine.

4.6 Hydro Turbine and Governor

When water flows from high elevation to the hydro turbine, gravitational potential energy is converted into kinetic energy. Then, the turbine shaft, obtaining mechanical energy from the conversion, drives the machine to generate electricity. In a turbine, the power is controlled by regulating the flow into the turbine using the position of the gates or nozzles. This regulation is realized by the turbine governor, which is also called the speed governing system, or turbine governing system.

Generally, hydro turbine governors can be classified in two types: mechanical hydraulic or electro hydraulic, depending on if there are electronic apparatus participating in sensing and measuring work

in the turbine governor. Figure 4.3 shows the relationship of the turbine and governor, indicated by the red block, with the power system.

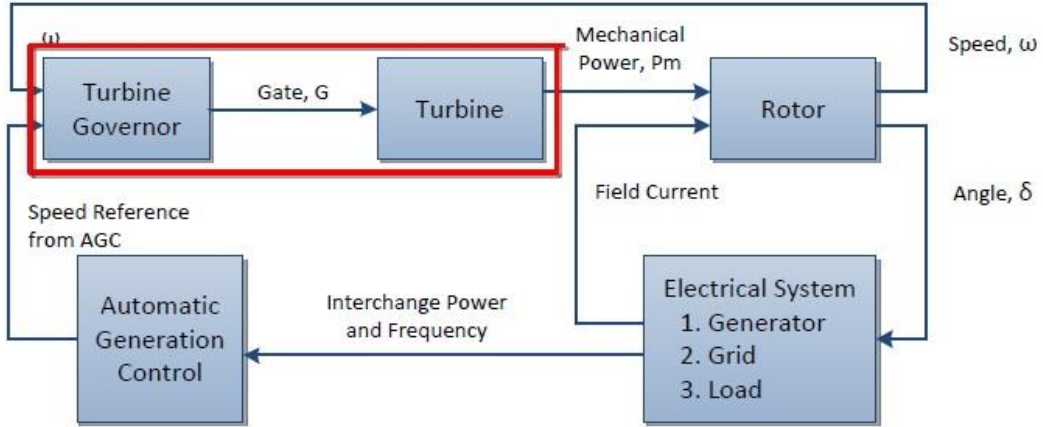


Figure 4.3: Block diagram showing relationship of the turbine and governor with the overall power system where speed of rotor is an input in the governor in order to regulate the opening of the gate and we have as a result the proportionate produced energy. [37]

4.6.1 Hydro Turbine Model

The penstock is modeled by assuming that the flow is incompressible when the rate of change of flow in the penstock is obtained by equating the rate of change of momentum of the water in the penstock to the net force on the water in the penstock when:

$$\rho L \frac{dQ}{dt} = F_{net} \quad (4.7)$$

Where

- Q :is the volumetric flow rate.
- L the penstock length.
- ρ the mass density of water.

The net force on the water can be obtained by considering the pressure head at the conduit. On entry to the penstock the force on the water is simply proportional to the static head H_s , while at the wicket gate it is proportional to the head H across the turbine. Due to friction effects in the conduit, there is also a friction force on the water represented by the head loss so that the net force on the water in the penstock is:

$$F_{net} = (H_s - H_l - H) A \rho g \quad (4.8)$$

Where:

- A is the penstock cross-sectional area.
- g is the acceleration due to gravity.

Substituting the net force into Equation (4.8) gives:

$$\rho L \frac{dQ}{dt} = (H_s - H_l - H) A \rho g \quad (4.9)$$

It is usual to normalize this equation to a convenient base. Although this base system is arbitrary, the base head h_{base} is taken as the static head above the turbine, in this case, while the base flowrate q_{base} is taken as the flowrate through the turbine with the gates fully open and the head at the turbine equal to h_{base} (IEEE Committee Report, 1992). Dividing both sides of Equation (4.9) by $q_{base} * h_{base}$ gives:

$$\frac{dq}{dt} = (1 - h_l - h) \frac{1}{T_w} \quad (4.10)$$

Where:

- q , h are the normalized flowrates and pressure heads respectively.

$$q = \frac{Q}{q_{base}} \quad (4.11)$$

$$h = \frac{H}{h_{base}}$$

$$T_w = \frac{L q_{base}}{A g h_{base}} \quad (4.12)$$

Where:

- T_w is the water starting time, which is theoretically defined as the time taken for the flowrate in the penstock to change by a value equal to q_{base} when the head term in brackets changes by a value equal to h_{base} .
- The head loss is proportional to the flowrate squared and depends on the conduit dimensions and friction factor. It suffices here to assume that $h_l = k_f q^2$ and can often be neglected. This equation defines the penstock model.

In modeling the turbine, itself both its hydraulic characteristics and mechanical power output must be modeled. Firstly, the pressure head across the turbine is related to the flowrate by assuming that the turbine can be represented by the valve characteristic:

$$Q = kG\sqrt{H} \quad (4.13)$$

Where:

- G is the gate position between 0 and 1.
- k is a constant.

With the gate fully open $G = 1$ and this equation can be normalized by dividing both sides by:

$$q = G\sqrt{H} \quad (4.14)$$

Secondly, the power developed by the turbine is proportional to the product of the flowrate and the head and depends on the efficiency. To account for the turbine not being 100% efficient the no-load flow q_{nl} is subtracted from the actual flow to give, in normalized parameters:

$$P_m = h(q - q_{nl}) \quad (4.15)$$

Unfortunately, this expression is in a different per-unit system to that used for the generator whose parameters are normalized to the generator MVA base so that last equation is written as:

$$P_m = A_t h(q - q_{nl}) \quad (4.16)$$

Where:

- the factor A_t is introduced to account for the difference in the bases.

The value of the factor A_t can be obtained by considering the operation of the turbine at rated load when:

$$P_m = A_t h(q - q_{nl}) = \frac{\text{turbinepower}(MW)}{\text{generatorMVArating}} \quad (4.17)$$

and the suffix 'r' indicates the value of the parameters at rated load. Rearranging the equation gives:

$$A_t = \frac{\text{turbinepower}(MW)}{\text{generatorMVArating}} \frac{1}{h_r(q_r - q_{nl})} \quad (4.18)$$

A damping effect is also present that is dependent on gate opening so that at any load condition the turbine power can be expressed by:

$$P_m = A_t h(q - q_{nl}) - DG\Delta_\omega \quad (4.19)$$

Where:

- D is the damping coefficient [19].
- Π is the symbol for the multiplication and Σ the symbol for the summation.

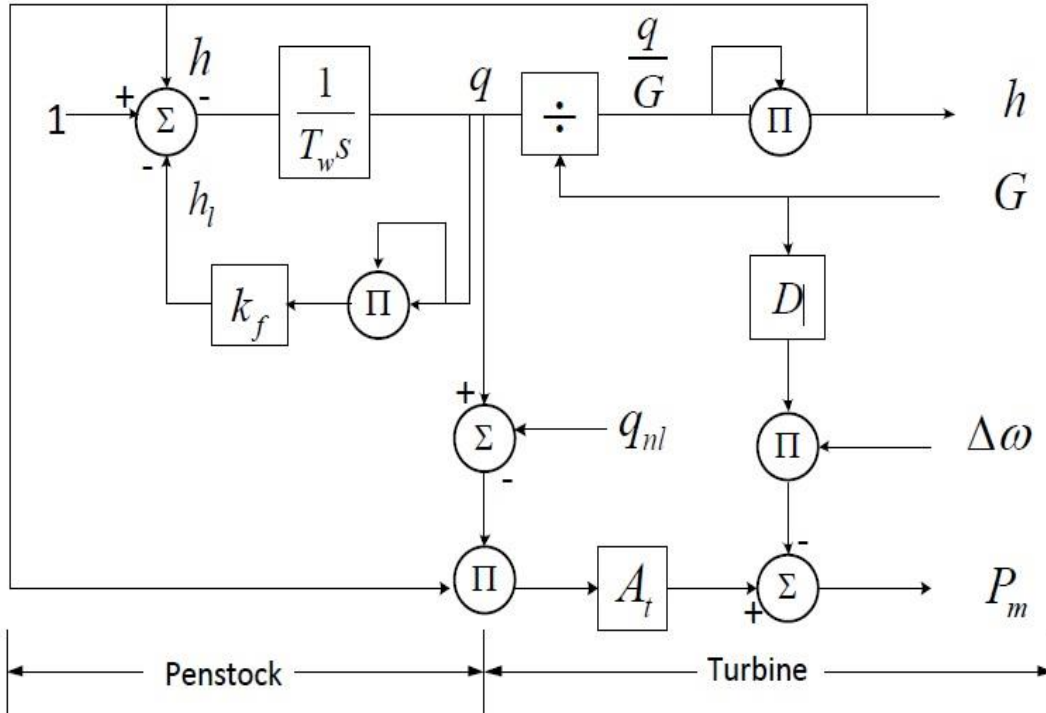


Figure 4.4: Hydraulic turbine non-linear model [37]

4.6.2 Hydraulic Turbine Governor Systems

A governor regulates the speed and power output of a prime mover as a control system. The governor includes mainly a controller function, and one or more control actuators. It should be mentioned that hydro turbines have initial inverse response characteristics of power to gate changes due to water inertia. Therefore, a hydro governor needs to provide a transient droop in speed controls to limit the overshoot of turbine gate servomotor during a transient condition. This means that for fast deviations in frequency, the governor should exhibit high regulation (low gain) while in slow changes and steady state, it should exhibit the normal low regulation (high gain). Therefore, a large transient droop with a long resetting time is required. This feedback limits the movement of the gate blades until the water flow and mechanical power output has time to overtake.

4.6.2.1 Hydraulic-Mechanical Governor

Hydro turbines have a peculiar response due to water inertia: a change in gate position produces an initial turbine power change which is opposite to that sought. For stable control performance, a large transient (temporary) droop with a long resetting time is therefore required. This is accomplished by the provision of a rate feedback or transient gain reduction compensation as shown in Figure 4.5 The rate feedback retards or limits the gate movement until the water flow and power output have time to

catch up. The result is a governor which exhibits a high droop (low gain) for fast speed deviations, and the normal low droop (high gain) in the steady state. On older units the governing function is realized using mechanical and hydraulic components.

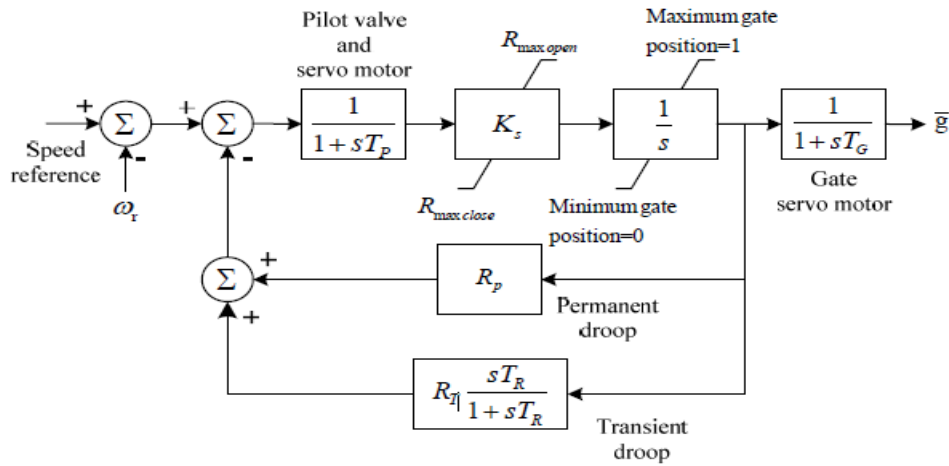


Figure 4.5: Hydraulic turbine governor model [38]

4.6.2.2 Electro hydraulic governor

Electro hydraulic governor is more widely used in modern hydro speed governors. The dynamic behavior, structure, and operation are essentially similar to that of the mechanical hydraulic governor except that:

- Speed sensing, permanent droop, temporary droop, and other measuring and computer functions are performed electrically.
- The electric components provide more flexibility and better performance.

Three-terms controller with proportion-integral-derivative (PID) action is often implemented in electro hydraulic governors [6]. It calculates the error" values between the measured process variable and a desired set point of $\Delta\omega$. The controller attempts to minimize the error by adjusting the process control input. The Proportional Integral Derivative regulator is regulating process, usually formulated:

$$u(t) = K_p D(t) + K_i \int_0^t D(t) d(t) + K_d \frac{d}{dt} D(t) \quad (4.20)$$

Where:

- $u(t)$ - Output signal.
- $D(t)$ - Deviation from desired operating point.
- K_p - Proportional gain.
- K_i - Integral gain.
- K_d - Derivative gain.

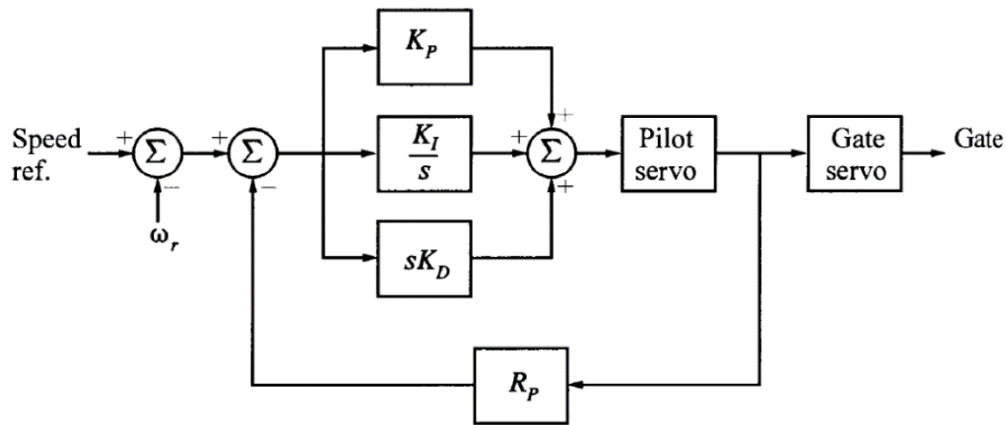


Figure 4.6: PID governor [19]

The output signal is a superposition of the three terms:

Proportional uses the deviation D along with the gain K_p to calculate control signal output. The contribution from the proportional term is only dependent on the magnitude of deviation, hence there will always be a small steady-state deviation called droop.

Integral corrects for droop by accounting for duration of previous deviation, in addition to the magnitude. The integral contribution thus increases as long as a deviation exist. In this way the integral term accounts for accumulated deviation, multiplies this by the integral gain K_i , then adds this to the proportional contribution.

Derivative calculates the rate of change, or slope of the deviation, thus anticipating future deviation. This slope is then multiplied by the derivative gain K_d and added to the other terms. The derivative gain is often small (or even zero) as this term is highly sensitive towards measurement noise.

The proportional term controls the present state by means of multiplying the error with a negative constant K_p and adding to the desired set point. The integral term controls the past state. The sum of the instantaneous error over time multiplies with a negative constant K_i , and adds to the desired set point, which eliminates the error between the process variable and the desired set point. As a result, the PID system can reach the steady state of the desired set point. The derivative term controls the future state by multiplying the error with a negative constant K_d and adding it to the desired set point. The derivative controller responds to system changes, the larger the derivative value is, the faster the response becomes.

The derivative action is beneficial for isolated operation, particularly for plants with larger water starting time ($T_w = 3$ s or more). However, higher derivative gain may result in excessive oscillations and governor loop instability. This is the reason for the minimum limit imposed on the value of $K_p = K_d$ or directly setting K_d to zero. The following formulas from reference [46] illustrate how to choose suitable parameters for PID controller; typical values are $K_p = 3.0$, $K_i = 0.7$, $K_d = 0.5$ [37].

$$\frac{1}{K_p} = \frac{0.625T_w}{H} \quad (4.21)$$

$$\frac{K_p}{K_i} = 3.33T_w \quad (4.22)$$

$$\frac{K_p}{K_d} > 3T_w \quad (4.23)$$

4.7 Stability and PID coefficients limits

The dynamic stability of a Hydroelectric Power Plant mainly is affected to a greater extent from the operation of the hydro turbine governor and the setting of PID-PI coefficients. So the study of the transfer function in the unit can give more accurate values for the coefficients, in order to reduce the oscillations, which are indication of instability in the station as I see later in the chapter 7. (T_m) is the rotating machine inertia.

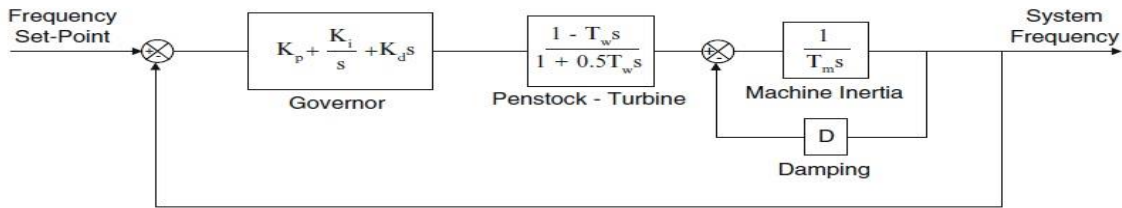


Figure 4.7: Block diagram of a hydraulic turbine generating system [67]

Where the system transfer function is:

$$G(s) = \frac{(K_p s + K_i + K_d s^2)(1 - T_w s)}{s(1 + 0.5T_w s)(T_m s + D)} \quad (4.24)$$

Through the criterion Ruth-Hurwitz I will find some helpful restrictions for the PID coefficients, studying the stability of the unit in the HPP and in which conditions the stability is possible [67].

The criterion Ruth-Hurwitz is based on the provision of rates of the characteristic equation

$$a_n s^n + a_{n-1} s^{n-1} + a_{n-2} s^{n-2} + \dots + a_1 s + a_0 = 0 \quad (4.25)$$

According to the criterion Ruth-Hurwitz the number of the roots of $q(s)$ that have positive real part equal to the sign changes in the first column of the table Ruth. Therefore a system is stable when there are not sign changes in the first column of the table. This condition is necessary and sufficient.

So

$$q(s) = 1 + G(s)H(s) = 0 \Leftrightarrow [K_p + K_d s + \frac{K_i}{s}] [\frac{1 - T_w s}{1 + 0.5 T_w s}] [\frac{1}{T_m s + D}] + 1 = 0 \quad (4.26)$$

in the form of (4.25) is:

$$a(s) = s^3(0.5 - X_3) + s^2(X_3 - X_1 + 1 + 0.5X_4) + s(X_1 - X_1X_2 + X_4) + X_1X_2 = 0 \quad (4.27)$$

Where:

- $X_1 = K_p T_w / T_m$
- $X_2 = K_i T_w / K_p$
- $X_3 = K_d / T_m$
- $X_4 = D(T_w / T_m)$

4.7.1 Routh's Test

The coefficients of the characteristic Eq. 4.27 are arranged in two rows in order to determine the Routh array, beginning with the first and the second coefficients and followed by the even numbered and odd-numbered coefficients. Hence, the array for the system can be constructed as:

s^3 :	A_0	A_2
s^2 :	A_1	A_3
s :	$B_1 = -\frac{\det \begin{bmatrix} A_0 & A_2 \\ A_1 & A_3 \end{bmatrix}}{A_1}$	0
s^0 :	$C_1 = -\frac{\det \begin{bmatrix} A_1 & A_3 \\ B_1 & 0 \end{bmatrix}}{B_1}$	

Figure 4.8: Routh Table

To ensure a stable response all the elements of the array $A_0, A_1, A_2, A_3, B_1, C_1$ must be positive, then the following criteria must be fulfilled:

- A_0 will be positive if $0.5 - X_3 > 0$, which means that $0.5 > X_3$, therefore, the derivative gain must be set to $K_d < 0.5 T_m$.
- A_1 will be positive if $1 - X_1 + X_3 + 0.5 X_4 > 0$, which results in $X_1 < 1 + X_3 + 0.5 X_4$.
- A_2 will be positive if $X_1 - X_1 X_2 + X_4 > 0$, which results in $1 + (X_4 / X_1) > X_2$.
- A_3 (C_1) will be positive if $X_1 X_2 > 0$.
- B_1 will be positive if $A_1 A_2 - A_0 A_3 > 0$, which results in:

$$(1 - X_1 + X_3 + 0.5X_4)(X_1 - X_1X_2 + X_4) - (0.5 - X_3)(X_1X_2) > 0 \quad (4.28)$$

If all the former conditions are satisfied, the stability boundaries of the system can be established by setting Eq. 4.28 to be equal to zero which results in:

$$X_1^2(X_2 - 1) + X_1(1 - 1.5X_2 + X_3 - 0.5X_4 - 0.5X_4X_2) + (X_4 + X_4X_3 + 0.5X_4^2) = 0 \quad (4.29)$$

4.8 Model of Excitation

An excitation system model is described Type DC excitation system, without the exciter's saturation, which utilize a direct current generator with a commutator as the source of excitation system power. An excitation system model is used to generate the excitation voltage that supplies the synchronous generator. Feedback systems are used through PID controllers to regulate both the generated excitation voltage as well as mechanical power produced by the turbine. Figure 4.6 presents the model of excitation system, which utilizes a direct current generator with a commutator as the source of excitation system. The principal input to this model is the output V_c , from the terminal voltage transducer and load compensator model. At the summing junction, terminal voltage transducer output, V_c is subtracted from the set point reference V_{REF} . The stabilizing feedback V_F is subtracted, and the power system stabilizing signal V_S is added to produce an error voltage. In the steady-state, these last two signals are zero, leaving only the terminal voltage error signal. The resulting signal is amplified in the regulator. The major time constant T_A and gain K_A associated with the voltage regulator, These voltage regulators utilize power sources that are essentially unaffected by brief transients on the synchronous machine or auxiliaries buses. The time constants, T_C and T_B may be used to model equivalent time constants inherent in the voltage regulator but these time constants are frequently small enough to be neglected, and provision should be made for zero input data. The exciter is represented by the following transfer function between the exciter voltage V_R and the regulator output E_{FD} . A signal derived from field voltage is normally used to provide excitation system stabilization V_F via the rate feedback with gain K_F and time constant T_F .

$$\frac{V_R}{E_{FD}} = \frac{1}{K_E + sT_E} \quad (4.30)$$

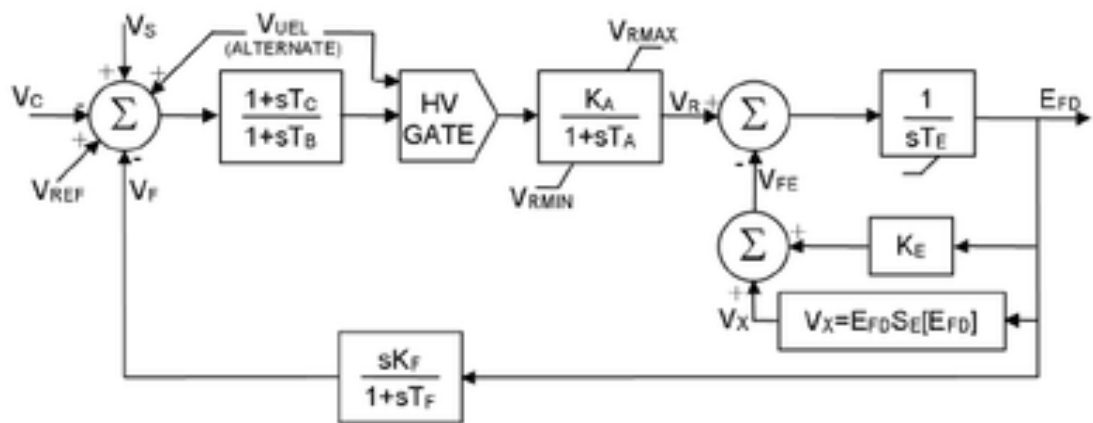


Figure 4.9: Excitation system with stabilizing circuit [35]

Chapter 5

Software Implementation

Now that the hydro turbine, governor, synchronous machine and excitation models have been established, they now can be implemented, simulated and studied using the software programs that we chose. This thesis focuses on the implementation of two simulation software: SimPowerSystems (SPS) | a proprietary software and PowerSim.

Although in this chapter is explored the literature to find which software is the best solution for our purposes. In this thesis the basic target is the modeling of the hydroelectric power plants in Kastraki and Stratos I so as to examine their dynamic stability and secondly there is an effort to optimize the operation of these two stations. Here are presented some of the other available software programs.

5.1 Dymola software

Dymola which is an object oriented graphical simulation program that uses the simulation language Modelica. Also, Dymola is an equation-based simulation tool unlike block-oriented tools such as Simulink. In Dymola you can both use graphical code and also manually entered row-based code. If graphical code is used Dymola will convert all the graphical code into Modelica code before simulation. The simulation environment is divided into two parts: the modeling part and the simulation part. The modeling part is where you draw the models and check them regarding to syntax and structure. In the simulation part the code is first converted into C-code and then simulated. In the simulation editor it is possible to look at plots of all variables in the model. An example of a model in Dymola is showed in Figure 5.1 where a graphical view of the model is showed in the left window and the simulation tool is showed in the right window [17].

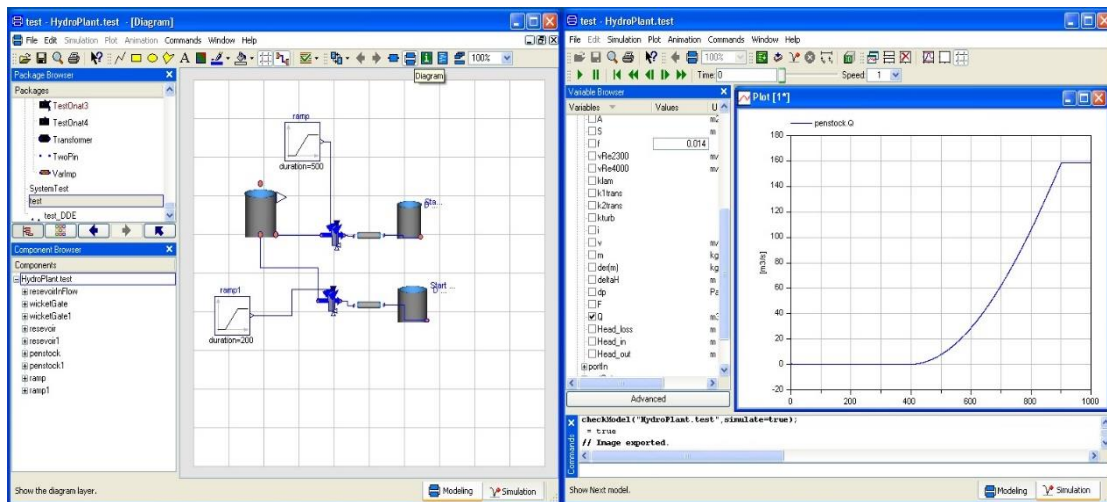


Figure 5.1: Modeling window (left side) and Simulation window (right side). [17]

5.2 TOPSYS software

A mathematical model of hydro power units, especially the governor system model for different operating conditions, based on the existing basic version of software TOPSYS by applying Visual C++ can be constructed. The graphical user interface of TOPSYS is shown in Figure 5.2. Various components of HPPs are represented in different blocks, and the corresponding equations are contained within the blocks. Users could build an HPP model conveniently by dragging and dropping the icons and inputting the parameters. It is worth noting that this study focuses on the model of hydro power units, especially the governor system. Models of other components (e.g., pipeline system) in the HPP system are only shortly presented. In the basic version of TOPSYS, the model of waterway systems and hydraulic turbines has the following characteristics: (1) equations for compressible flow are applied in the draw water tunnel and penstock, considering the elasticity of water and pipe wall; (2) different types of surge tanks and tunnels are included; and (3) characteristic curves of the turbine are utilized, instead of applying simplified transmission coefficients. These characteristics lay a solid foundation for this study to achieve efficient and accurate simulation results [40].

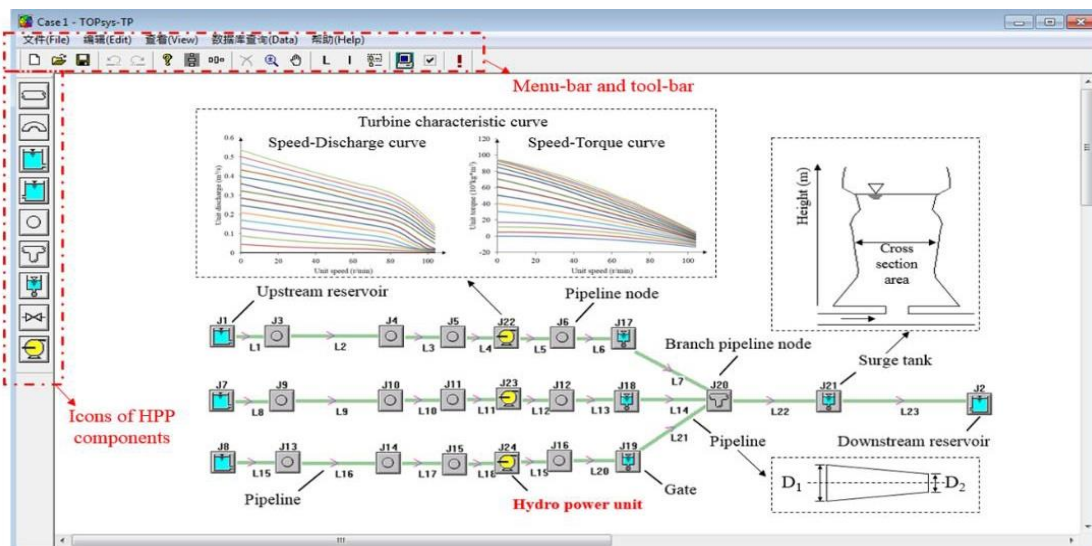


Figure 5.2: Graphical user interface of TOPSYS and a model of a Swedish hydro power plant (HPP)[40]

5.3 Labview Transient, Lvtrans

Lvtrans, Lab View transient pipe analysis, is a simulation and calculation tool for liquid filled ducts. The program is applicable to any liquid filled system, but the program was originally developed for studying the dynamics of hydro power plants. The program contains a broad range of components found in hydro power plants. This allows the user to create models of specific power plants by using the built in graphical user interface, GUI. The source code of LVtrans is object orientated, meaning that changes can be done to a specific set up of a plant without changing the source code of the program.

The program relies on the method of characteristic for solving the equations.

The method allows a system of partial differential equations, PDE to be solved fast and accurate. The **transients** due to the water hammer effect described are thus included in the solution, meaning that the program is able to provide an accurate solution of the actual systems. The version number used in the master thesis in [41] is LVtrans86 1.31.T. This version includes a module that makes it possible to perform a frequency scan of a system created with the program's GUI [41].

5.4 Simpow software

Simpow is a software for simulation of power systems developed by STRI AB. The software enables the user to simulate power systems **in the steady state, time and frequency domain**. A built in library simplifies the process of modeling systems. The built in Dynamic Simulation Language, DSL, enables the user to define components and models. The user defined components and models can interact with components from the internal library during simulation. Simulations entirely based on user defined components are also possible. Such simulations can be set up by altering the DSL files to run independently from the internal library. This enables the user to extract data and study relationships that are not included in the standard library. Tools for viewing, extracting and plotting results are provided. For analysis in the frequency domain the software contains helpful tools. The frequency scanning module enables the user to study the small signal stability by exiting the system with a sinusoidal signal in the desired frequency range. The amplitude of the perturbation can be selected. Studies of modal swings are simplified by a built in package. A tool for extraction and plotting eigenvalues are also provided [41].

5.5 Simsen software

This software is based on a modular structure, which enables the numerical simulation **in transient or steady-state** modes of systems with arbitrary topologies. It is composed of units, each representing a specific cell in the network: electrical machine, mechanical system taking into account mechanical masses connected with damping and springs, transformer, voltage supply, transmission line, load, static converter, regulator. The originality of this package lies within its ability to simulate classical three phase power networks for the generation, transmission, distribution and networks involving semi-conductor units as well. Each unit includes a set of differential equations based on the network element modelling. An original algorithm has been developed in order to generate the main set of differential equations solved by fourth order Runge-Kutta. The variable time-step used for the integration of the governing equations allows detecting the exact sequence of events like the on-off switching of semi-conductor or circuit-breakers phase on-off switching.

The hydraulic elements are modelled as an assembly of RLC components and the whole installation is modelled like an electrical network where the variables are:

- the piezometric head H at the node
- the discharge Q through each of components respectively corresponding to voltage U and current i .

Thus, the differential equations can be generated by “SIMSEN” using Kirchhoff’s law. The main differential set of equations contains electric, hydraulic and regulation equations that are solved simultaneously. An example of hydroelectric power plant, which will be created with “SIMSEN” is shown in Figure 5.3 [42].

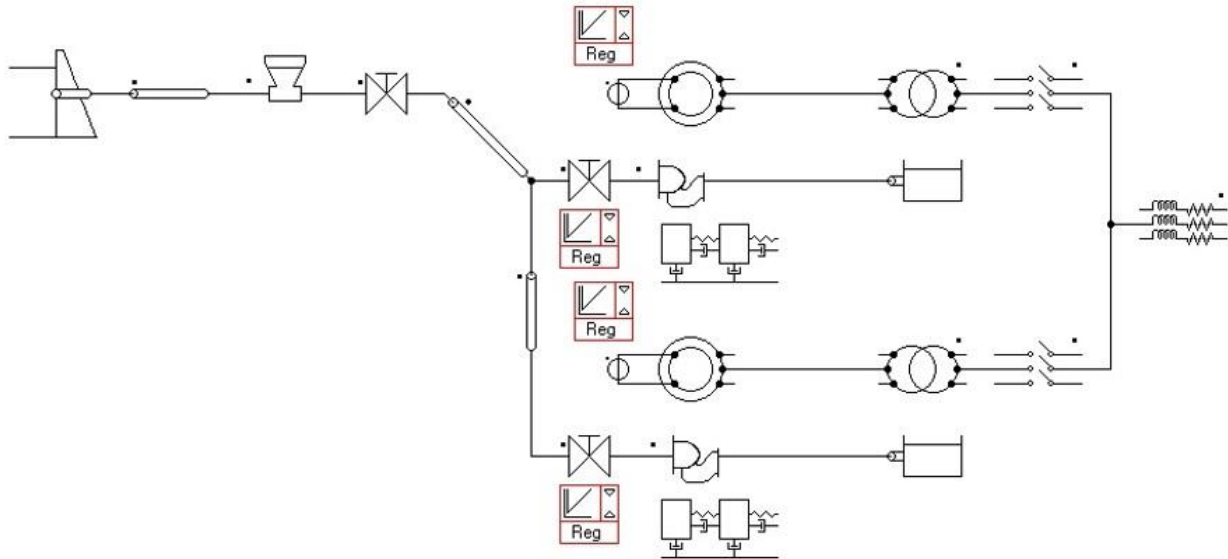


Figure 5.3: Hydroelectric power plant modelled with SIMSEN including the hydraulic module [42]

5.6 PowerSim

If the optimization that we wanted to achieve in this diploma thesis was the improving water management so as to increase the efficiency of utilization of dam reservoirs, because even small improvement in reservoir operation can lead to large benefits then the tool that we could have used is Powersim Simulation software. Powersim simulation software: It is windows-based software for creating **system dynamics models**. It is an object-oriented package that is used for hierarchical modeling with an unlimited depth of sub models. Its packages allow for the on-screen construction of a flow-chart style representation of a simulation model. It has a wide variety of objects for presentation of simulation results in graphs, simple numeric display, or tables. Powersim supports Dynamic Data Exchange (DDE) using standard Windows protocol and boasts an Application Programmers' Interface (API) which allows programmers to connect Powersim applications to programs developed in C++, Visual Basic, or Delphi (D. Chapman, UniServe Science, News Volume 8 November 1997).

Powersim can be used to model an imaginary or real system. It enables the user to create a visual image of the problem. By running the model, the user can observe the effects of decisions over time, discover potential problem areas and make adjustments in a risk-free environment. It utilizes the system dynamics method to model the system and simulate its behavior over time. It offers the user a wide array of options to control the simulation’s behavior. It has been successfully used to create simulations across a wide spectrum of industries and business such as strategic planning, resources

management, crisis planning and management and process re-engineering (Daene, 2004; Powersim Corporation, 1997). In the paper of Brosona and Gebresenbet they used the mean monthly data of reservoir inflow, evaporation rate, recorded energy production, recorded discharge (turbine flow) and recorded reservoir elevation as time series input data, they defined different variables and relationships between variables along with the constraints. Their main purpose was to optimize the Melka Wakena Hydropower Plant System in Ethiopia. After developing and calibrating the model successfully, they achieved a detailed simulation analysis by controlling reservoir releases for energy production, taking into consideration the increasing yearly energy production and improving the uniformity of monthly energy production. The results of the simulation analysis indicated that the yearly energy production was increased by 5.67% while evaporation loss was reduced by 38.33%. But this power plant still produces below its design capacity by 12.21%. The uniformity of monthly energy production from this plant was also improved [48].

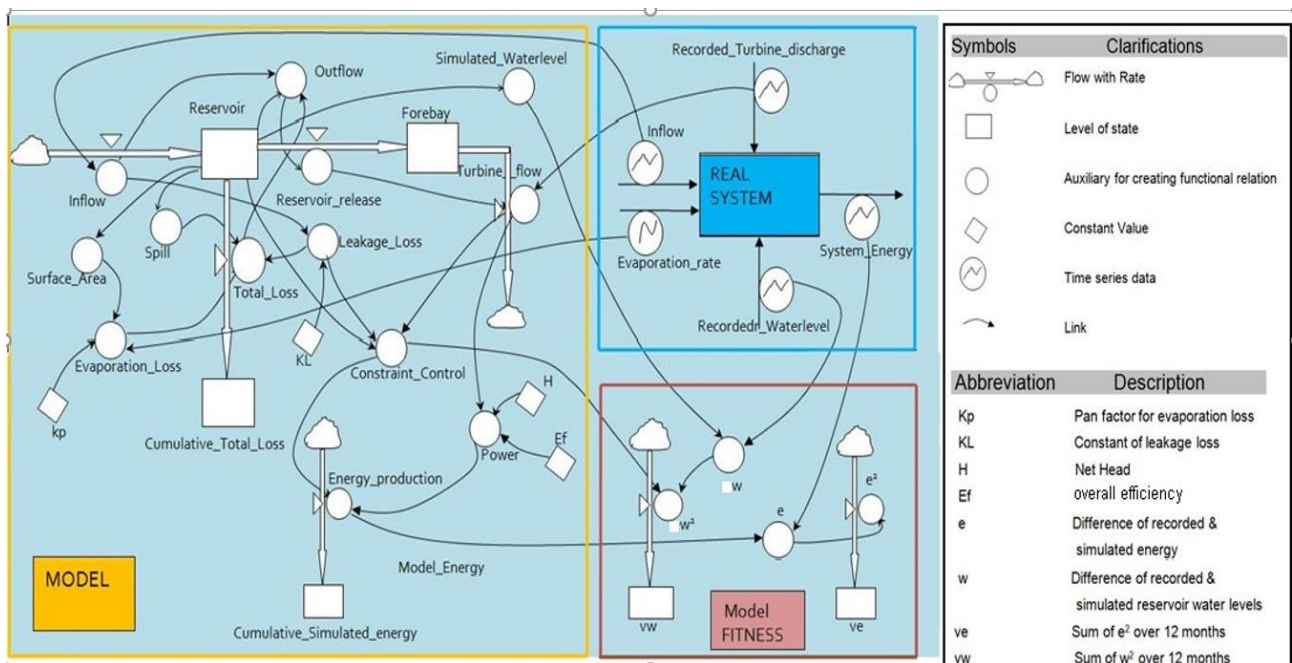


Figure 5.4: Powersim diagram of Melka Wakena Hydropower Plant System [48]

5.7 Matlab/Simulink Simscape PowerSystems Implementation

In this thesis is used the software Matlab and more specifically the Simulink Simscape PowerSystems tool, so as to represent the nonlinear models that is analyzed in 4th chapter. My main purpose is the modeling of a Hydropower plant in order to study the dynamic stability of Stratos I HPP and Kastraki HPP.

5.7.1 Simulink

Simulink (Simulation and Link) is an extension of MATLAB by Mathworks Inc. It works with MATLAB to offer modelling, simulation, and analysis of dynamical systems under a graphical user interface (GUI) environment. The construction of a model is simplified with click and drag mouse

operations. Simulink includes a comprehensive block library of toolboxes for both linear and nonlinear analyses. Models are hierarchical, which allow using both top down and bottom up approaches. As Simulink is an integral part of MATLAB, it is easy to switch back and forth during the analysis process and thus, the user may take full advantage of features offered in both environments.

5.7.2 Simscape PowerSystems

Simscape Power Systems™ (formerly SimPowerSystems™) provides component libraries and analysis tools for modeling and simulating electrical power systems. It includes models of electrical power components, including three-phase machines, electric drives, and components for applications such as flexible AC transmission systems (FACTS) and renewable energy systems (RES). Harmonic analysis, calculation of total harmonic distortion (THD), load flow, and other key electrical power system analyses are automated, helping to investigate the performance of a design. Simscape Power Systems helps to develop control systems and test system-level performance. It can parameterize the models using MATLAB® variables and expressions, and design control systems for its electrical power system in Simulink®. It can integrate mechanical, hydraulic, thermal, and other physical systems into a model using components from the Simscape™ family of products. To deploy models to other simulation environments, including hardware-in-the-loop (HIL) systems, Simscape Power Systems supports C-code generation.

5.7.3 Hydropower Plant in Simscape Power Systems

This diploma thesis discusses the use of SIMULINK software of MATLAB, in the dynamic modeling of the hydropower plant components. The main advantage of Simscape Power Systems over other programming software is that, instead of compilation of program code, the simulation model is built up systematically by means of basic function blocks. The models of Stratos I HPP and Kastraki HPP are developed using existing Simulink blocks contained in the Simscape PowerSystems blockset. In the simulation models, the reference speed signal is obtained from the kinetic energy of the falling water through the penstock (see Figure 4.1). The measured synchronous machine speed is fed back to compare with the reference speed signal. The speed deviation produced by comparing reference and synchronous generator speed is used as input for PID based speed governor. PID is used as turbine governor because this control has simple structure, stability, strong robustness and non-steady state error. The governor produces the control signal, causing a change in the gate opening. The turbine in turn produces the torque, driving the synchronous machine that generates the electrical power output. The speed governor constantly checks speed deviation to take action.

5.7.4 Hydraulic Turbine and Governor Simulation

The block that is used as Hydroturbine and Governor is block that implements a nonlinear hydraulic turbine model, a PID governor system, and a servomotor. The hydraulic turbine is modeled by the following nonlinear system. The gate servomotor is modeled by a second-order system.

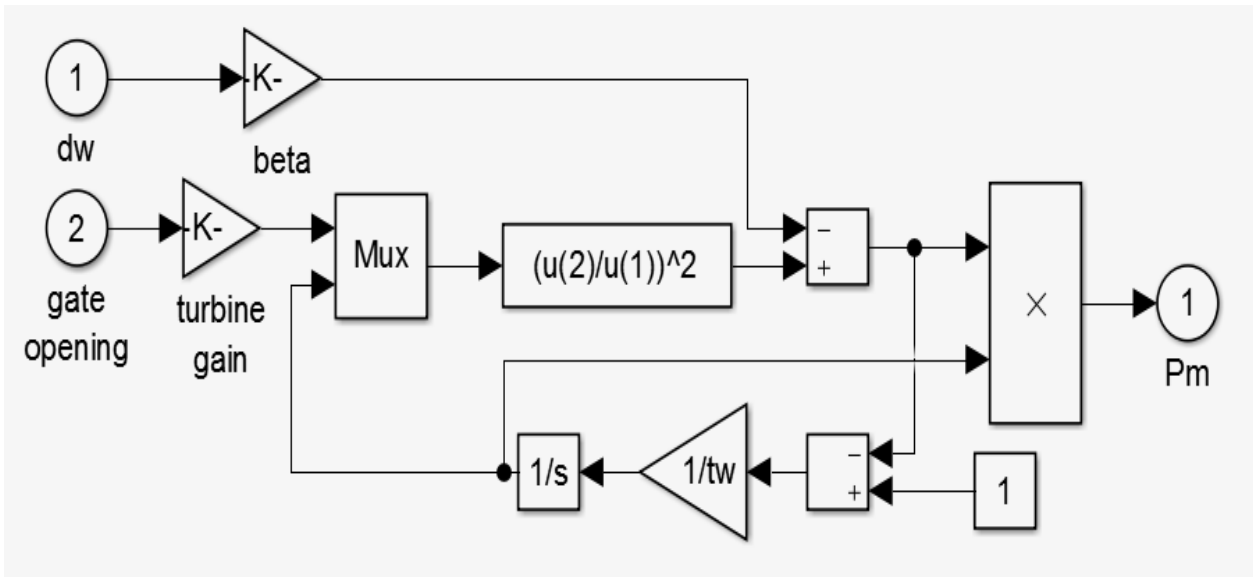


Figure 5.7: The hydraulic turbine block in Simulink

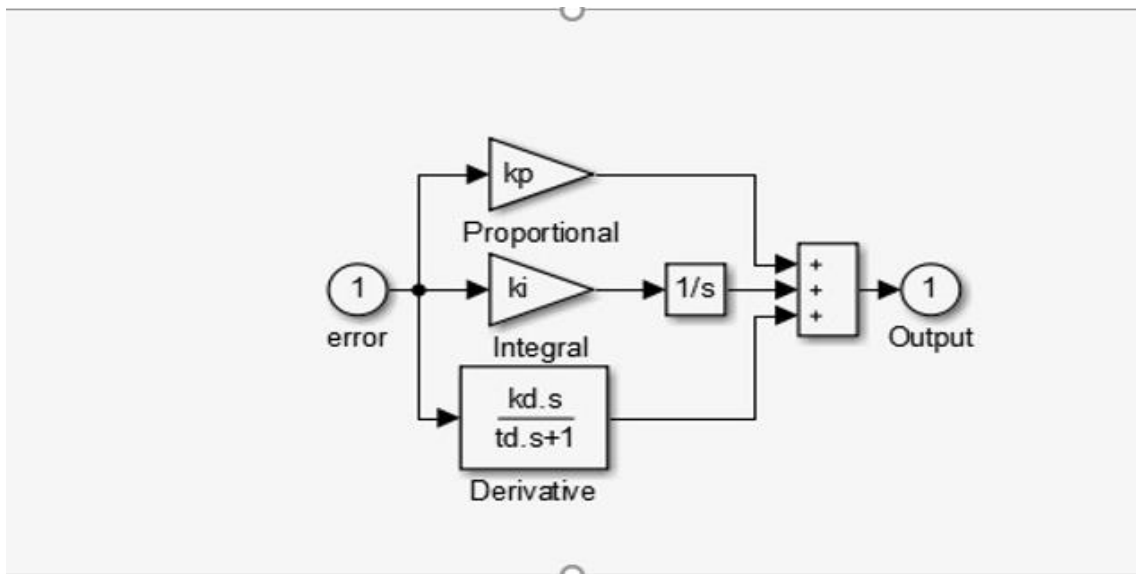


Figure 5.8: PID

The block parameters are:

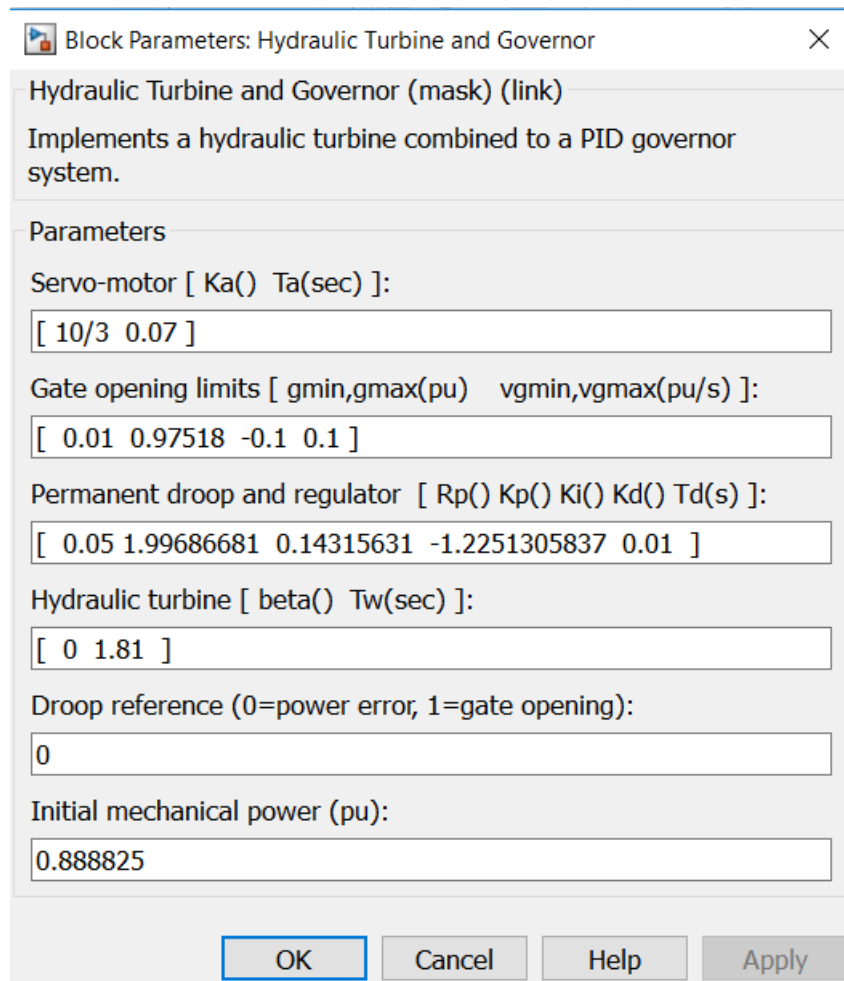


Figure 5.9: HTG: Block Parameters (Kastraki HPP parameters for 0.9 pu power load)

- **Servo-motor**

The gain K_a and time constant T_a , in seconds (s), of the first-order system representing the servomotor.

- **Gate opening limits**

The limits g_{\min} and g_{\max} (pu) imposed on the gate opening, and vg_{\min} and vg_{\max} (pu/s) imposed on gate speed.

- **Permanent droop and regulator**

The static gain of the governor is equal to the inverse of the permanent droop R_p in the feedback loop. The PID regulator has a proportional gain K_p , an integral gain K_i , and a derivative gain K_d . The high-frequency gain of the PID is limited by a first-order low-pass filter with time constant T_d (s).

- **Hydraulic turbine**

The speed deviation damping coefficient β and water starting time T_w (s).

- **Droop reference**
Specifies the input of the feedback loop: gate position (set to 1) or electrical power deviation (set to 0).
- **Initial mechanical power**
The initial mechanical power $Pm0$ (pu) at the machine's shaft. This value is automatically updated by the load flow utility of the Powergui block.

Inputs and Outputs

- ***wref***
Reference speed, in pu.
- ***Pref***
Reference mechanical power in pu. This input can be left unconnected if you want to use the gate position as input to the feedback loop instead of the power deviation.
- ***we***
Machine actual speed, in pu.
- ***Pe0***
Machine actual electrical power in pu. This input can be left unconnected if you want to use the gate position as input to the feedback loop instead of the power deviation.
- ***dw***
Speed deviation, in pu.
- ***Pm***
Mechanical power Pm for the Synchronous Machine block, in pu.
- ***gate***
Gate opening, in pu.

5.7.5 Synchronous Machine pu Standard block

The block of Synchronous Machine pu Standard, is used although are existing other Synchronoys Machine blocks like: Synchronous Machine SI Fundamental, Synchronous Machine pu Fundamental. In Configuration Tab of the block I select Mechanical Power Pm to specify a mechanical power input, in W or in pu, and change labeling of the block input to Pm . The machine speed is determined by the machine Inertia J (or inertia constant H for the pu machine) and by the difference between the mechanical torque Tm , resulting from the applied mechanical power Pm , and the internal electromagnetic torque Te . The sign convention for the mechanical power is when the speed is positive, a positive mechanical power signal indicates generator mode and a negative signal indicates motor mode. In the section Rotor type we select. Salient-pole because in Stratos I HPP and Kastraki HPP the type of generetors is this type. This choice affects the number of rotor circuits in the q-axis (damper windings).

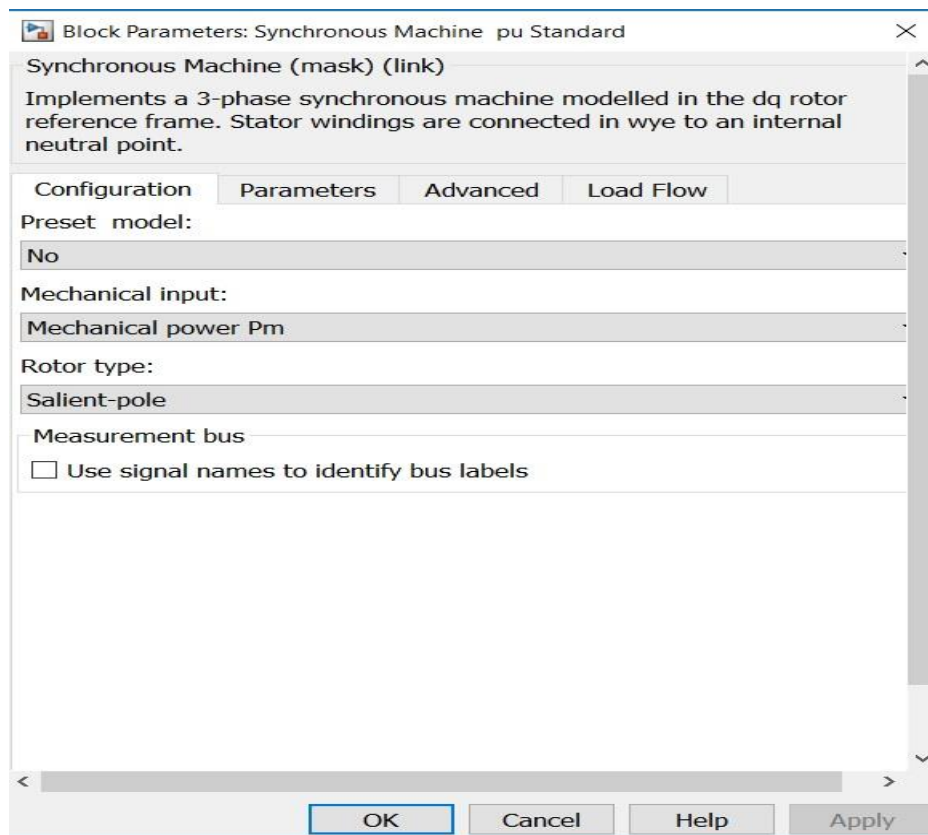


Figure 5.10: Configuration Tab of Synchronous Machine pu Standard block

In the parameters tab of Synchronous Machine pu Standard block:

- Nominal power, line-to-line voltage, and frequency**
 Total three-phase apparent power (VA), RMS line-to-line voltage (V), frequency (Hz), and field current (A).
 This line is identical to the first line of the fundamental parameters in SI dialog box, except that you do not specify a nominal field current. This value is not required here because we do not need the transformation ratio. Since rotor quantities are viewed from the stator, they are converted to pu using the stator base quantities derived from the preceding three nominal parameters.
- Reactances**
 The d-axis synchronous reactance X_d , transient reactance X_d' , and subtransient reactance X_d'' , the q-axis synchronous reactance X_q , transient reactance X_q' (only if round rotor), and subtransient reactance X_q'' , and finally the leakage reactance X_l (all in pu).
- d-axis time constants, q-axis time constant(s)**

Specify the time constants you supply for each axis: either open-circuit or short-circuit.

- **Time constants**

The d-axis and q-axis time constants (all in s). These values must be consistent with choices made on the two previous lines: d-axis transient open-circuit (T_{do}') or short-circuit (T_d') time constant, d-axis subtransient open-circuit (T_{do}'') or short-circuit (T_d'') time constant, q-axis transient open-circuit (T_{qo}') or short-circuit (T_q') time constant (only if round rotor), q-axis subtransient open-circuit (T_{qo}'') or short-circuit (T_q'') time constant.

- **Stator resistance**

The stator resistance R_s (pu).

- **Inertia coefficient, friction factor, pole pairs, Initial conditions, Simulate saturation, Saturation parameters**

The same initial conditions and saturation parameters as in the SI units' dialog box, but all values are expressed in pu instead of SI units. For saturation, the nominal field current and nominal RMS line-to-line voltage are the base values for the field current and terminal voltage, respectively.

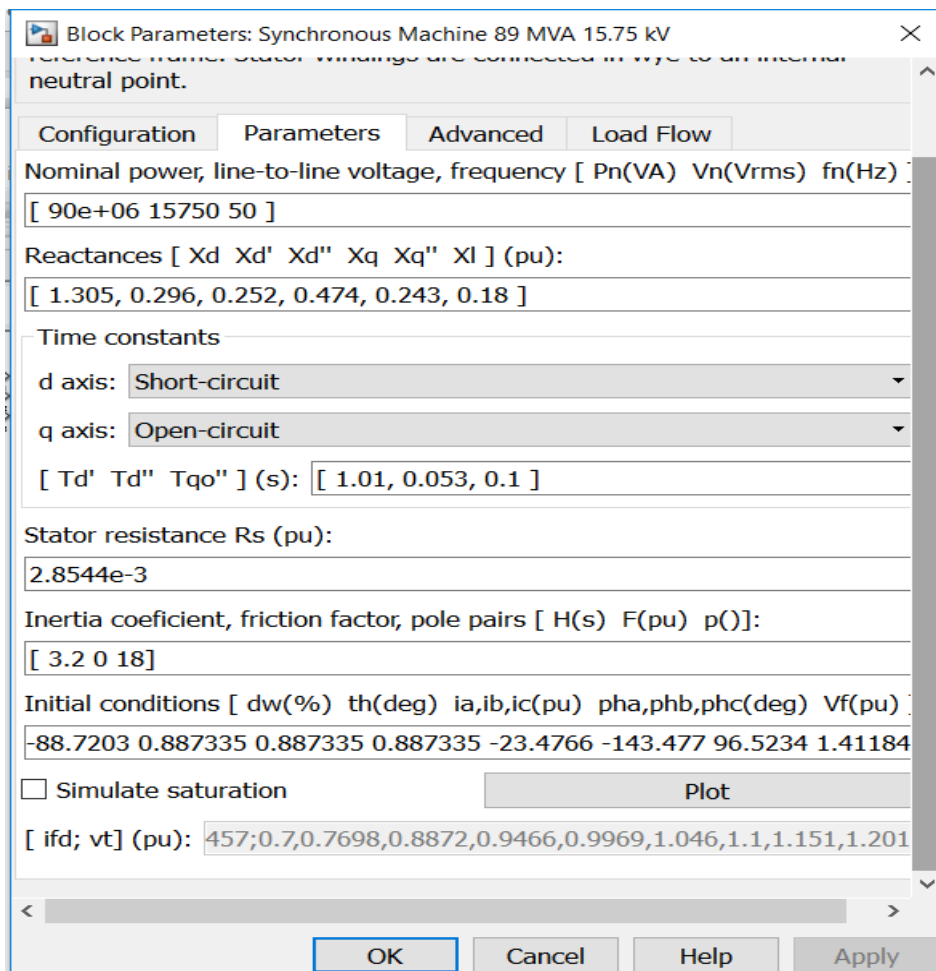


Figure 5.11: Parameters Tab of Synchronous Machine pu Standard block (Kastraki HPP parameters for 0.9 pu power load)

The load flow parameters are used to define block parameters for use with the Load Flow tool of the Powergui block. These load flow parameters are used for model initialization only. They have no impact on the block model and on the simulation performance.

The configuration of the Load Flow tab depends on the option selected for the Generator type parameter.

In section Generator type parameter, we Select PV to implement a generator controlling its output active power P and voltage magnitude V . P is specified by the Active power generation P parameter of the block. V is specified by the Swing bus or PV bus voltage parameter of the Load Flow Bus block connected to the machine terminals. You can control the minimum and maximum reactive power generated by the block by using the Minimum reactive power Q_{min} and Maximum reactive power Q_{max} parameters.

Inputs and Outputs

The units of inputs and outputs vary according to which dialog box you use to enter the block parameters. If the fundamental parameters in SI units is used, the inputs and outputs are in SI units (except for d_w in the vector of internal variables, which is always in pu, and angle Θ , which is always in rad). Otherwise, the inputs and outputs are in pu.

- **P_m**

The first Simulink input is the mechanical power at the machine's shaft, in Watts or pu. In generating mode, this input can be a positive constant or function or the output of a prime mover block (see the Hydraulic Turbine and Governor or Steam Turbine and Governor blocks). In motoring mode, this input is usually a negative constant or function.

- **w**

The alternative block input instead of P_m (depending on the value of the Mechanical input parameter) is the machine speed, in rad/s.

- **V_f**

The second Simulink input of the block is the field voltage. This voltage can be supplied by a voltage regulator in generator mode (see the Excitation System block). It is usually a constant in motor mode.

If the is used model in SI fundamental units, the field voltage V_f must be entered in volts DC if nominal field current I_{fn} is specified, or in volts referred to stator if I_{fn} is not specified. To obtain the V_{fd} producing nominal voltage, select the Display nominal field current and voltage producing 1 pu stator voltage check box in the Advanced tab. If the model is in pu Standard or in pu Fundamental units, V_f must be entered in pu (1 pu of field voltage producing 1 pu of terminal voltage at no load).

- **m**

The Simulink output of the block is a vector containing measurement signals. To demultiplex these signals the Bus Selector block provided in the Simulink library can be used. Depending on the type of mask that it is used, the units are in SI or in pu.

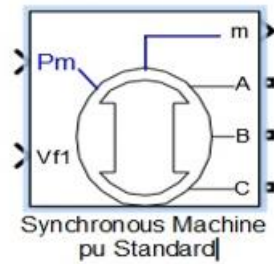


Figure 5.12: Block of Synchronous Machine pu Standard

5.7.6 Excitation System

Provide excitation system for synchronous machine and regulate its terminal voltage in generating mode

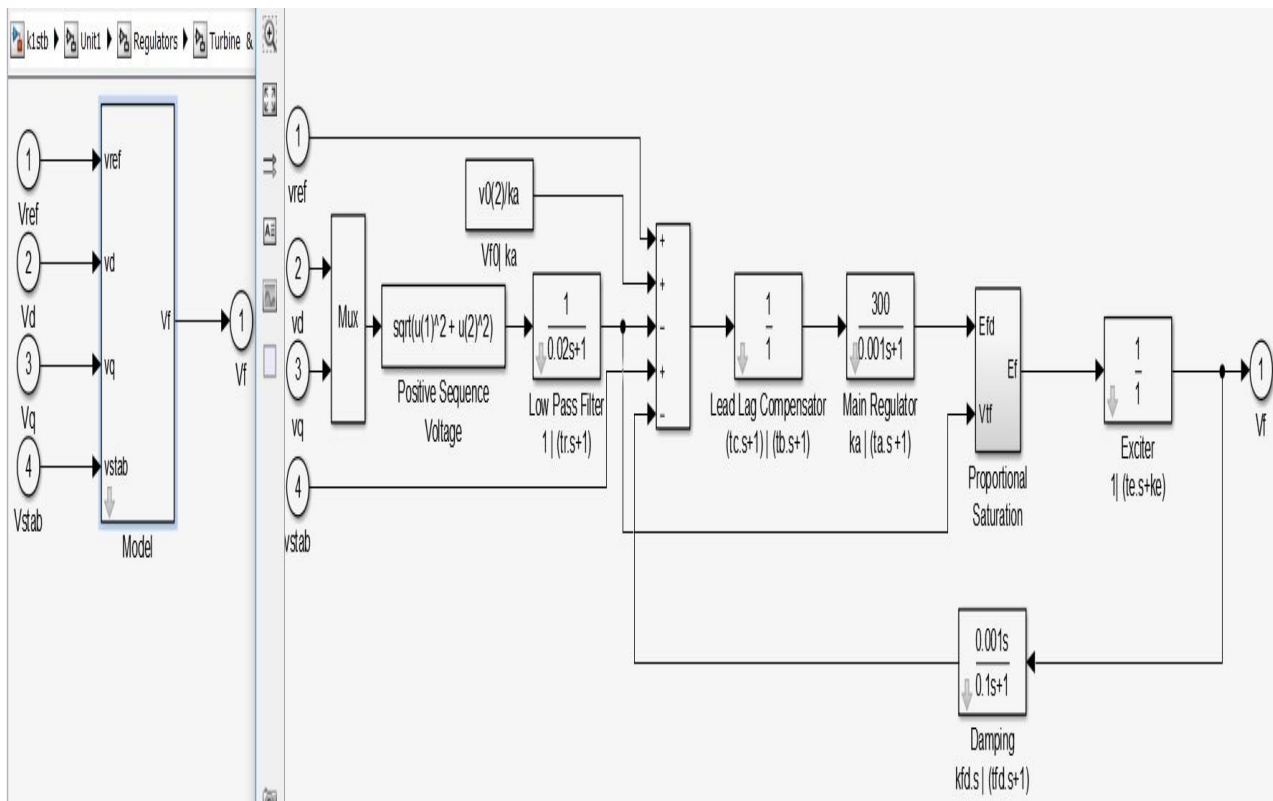


Figure 5.13: The basic elements that form the Excitation System block are the voltage regulator and the exciter

The parameters of Excitation System block:

- **Low-pass filter time constant**

The time constant T_r , in seconds (s), of the first-order system that represents the stator terminal voltage transducer.

- **Regulator gain and time constant**

The gain K_a and time constant T_a , in seconds (s), of the first-order system representing the main regulator.

- **Exciter**

The gain K_e and time constant T_e , in seconds (s), of the first-order system representing the exciter.

- **Transient gain reduction**

The time constants T_b , in seconds (s), and T_c , in seconds (s), of the first-order system representing a lead-lag compensator.

- **Damping filter gain and time constant**

The gain K_f and time constant T_f , in seconds (s), of the first-order system representing a derivative feedback.

- **Regulator output limits and gain**

Limits E_{fmin} and E_{fmax} are imposed on the output of the voltage regulator. The upper limit can be constant and equal to E_{fmax} , or variable and equal to the rectified stator terminal voltage V_{tf} times a proportional gain K_p . If K_p is set to 0, the former applies. If K_p is set to a positive value, the latter applies.

- **Initial values of terminal voltage and field voltage**

The initial values of terminal voltage V_{t0} (pu) and field voltage V_{f0} (pu). When set correctly, they allow you to start the simulation in steady state. Initial terminal voltage should normally be set to 1 pu. Both V_{t0} and V_{f0} values are automatically updated by the load flow utility of the Powergui block.

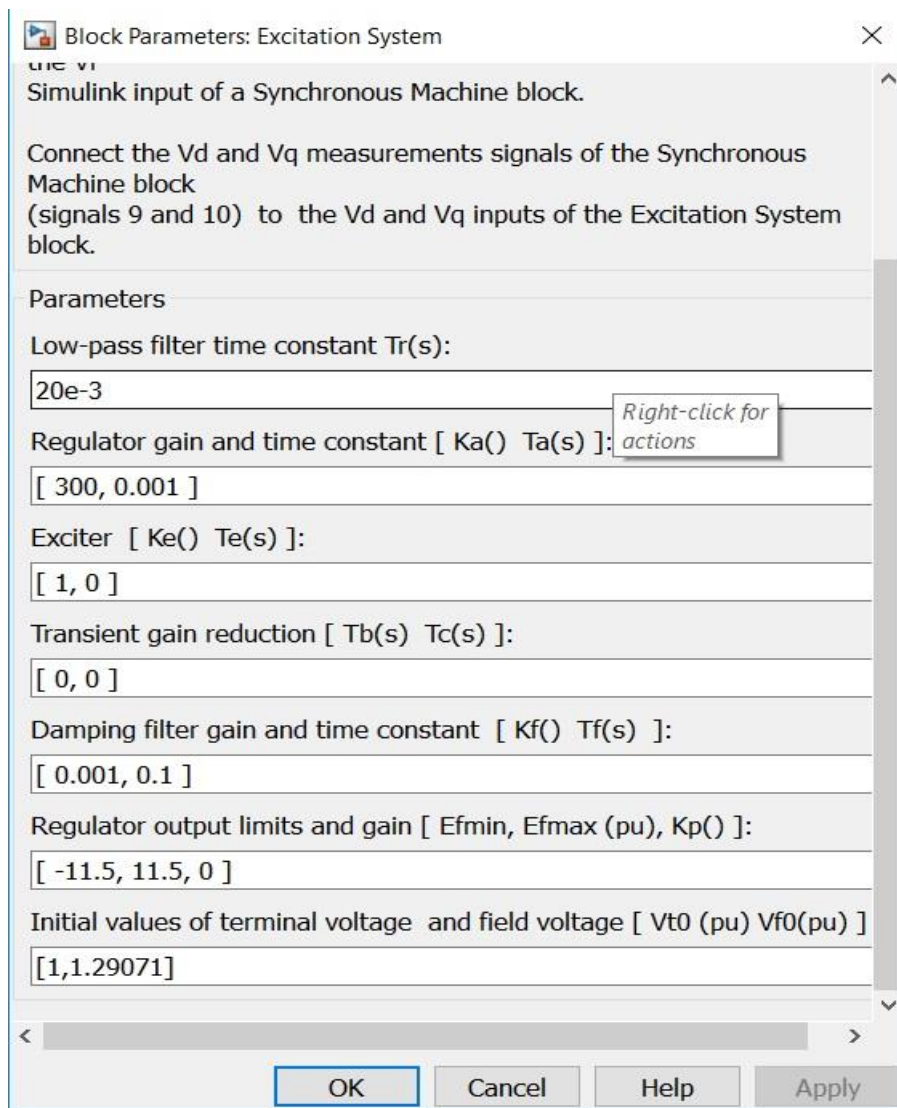


Figure 5.14: Parameters of Excitation System block applied to Stratos I HPP and Kastraki HPP

Inputs and Outputs

- ***vref***
The desired value, in pu, of the stator terminal voltage.
- ***vd***
 v_d component, in pu, of the terminal voltage.
- ***vq***
 v_q component, in pu, of the terminal voltage.
- ***vstab***
Connect this input to a power system stabilizer to provide additional stabilization of power system oscillations.

- V_f
The field voltage, in pu, for the Synchronous Machine block.

Chapter 6

Kastraki and Stratos I model in Simulink/Matlab

6.1 Parallel Operation

In today's world, an isolated generator supplying its own load independently is very rare. The usual situation is that the generators are operating in parallel (synchronised) sharing the load of the power system. Operating in this manner increases the reliability of the power system because the failure of any generator will not lead to total power loss. Moreover, having a large number of generators in parallel allows a bigger load to be supplied and permits the shutdown of some generators for maintenance. In Kastraki HPP there are four units parallel and in Stratos I there are two units parallel.

6.2 Kastraki HPP Simscape Power Systems Model

Kastraki HPP and Stratos I Models can be represented as a single-machine infinite-bus system (SMIB).

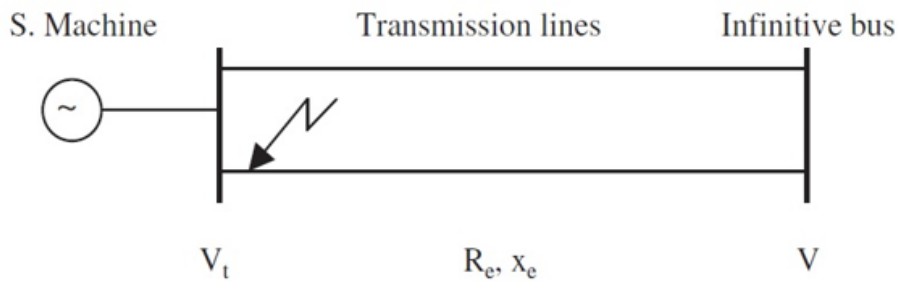


Figure 6.1: The considered single machine-infinite bus system

Figure 6.1 shows a common SMIB system. For my purposes the infinite bus is represented by an infinite generator (or source) with 100.000 MVA, 161.25 kV (an infinite bus). The base voltage V_{rms} ($ph-ph$) in the infinite bus block is $161.25 e^3$.

The model of Kastraki HPP using Matlab/Simulink is presented in Figure 6.10, the generating station consists of four generating units with P_{mech} of the turbine 80 MW (0.888 pu) each and P of the generator 79.792 MW (0.8866 pu) each, since the performance level of the Francis turbine at each unit is $n=0.9974$.

The line frequency of the system is 50 Hz. The model consists of hydraulic turbine, synchronous machine, excitation system blocks, three-phase transformers blocks and RLC blocks. RLC blocks (1 MW at each unit) in the left side of the figure represent the locally consumed power that the generators consume so as to be in continuous operation. In addition, the RLC block of 10 MW in right side

between infinite bus and transformer represents the power need of city of Agrinio, which is the main consumer in the area. This value is not constant value it can be changing.

The Kastraki HPP model is a 319.88 MW (totally from all 4 units) station with 89 MVA, 15.75 kV three phase generator at each unit with 18 pair poles (36) , that means from the equation (3.18) that the speed is 166.66 rpm and is connected to a 161.25 kV network through a $\Delta-Y$ 90 MVA transformer with forced cooling. In the section Rotor type I select Salient-pole because in Kastraki HPP the type of generators is this type.

In the model, the synchronous generator is driven by mechanical power generated by the hydraulic turbine block. In addition, an excitation system is used to generate the excitation voltage that supplies the synchronous generator. The generated excitation voltage from the excitation system block and the mechanical power produced by the turbine are both regulated through the PID controller employed in feedback systems. The PID coefficients are determined by the ZN method chapter ($P_{mech}=0.9 \Rightarrow K_p=1.99686681, K_i=0.14315631, K_d=-1.2251305837$).

Each of the generating unit has an output of 79.792MW, and each unit generator has an output voltage of 15.75 kV which is fed to a step up transformer that feeds 161.25 kV transmission line.

To achieve a steady state of continuous production of power in our Simulink model I need to use the Powergui to initialize the currents of the synchronous machines of the generators. I am opening the Powergui and I select 'Machine Initialization'. A new window appears. The machine 'Bus type' is initialized as 'PV generator', indicating that the initialization is performed with the machine controlling the active power and its terminal voltage. The desired terminal voltage parameter is set to 15.750 and the Active Power to $7.9792 e^7$. The Reactive Power is $Q=3.2996$ MVar (0.0366 pu) . The initial terminal voltage and field voltage is set to 1 and 1.4 per unit respectively for the excitation system block. The base Power is 100 MVA as I am measuring in pu.

Table 6.1 Hydraulic Turbine and Governor

Type	Vertical shaft
	Francis
Effective head	75.70 m.
Max	
Nor.	74.50 m.
Min.	75.20 m.
Output at normal head	80 MW
Discharge at normal head	120 m ³ /sec
Revolving speed	166.66 rpm
Water starting time T_w	1.81 s
Permanent droop R_p	0.05
Servo gain K_a	10/3
Servo time constant T_a	0.07 s

Table 6.2 Three Phase Transformer Parameters

Nominal Power	90 MVA
Rated frequency	50 Hz
Rated voltage	15.75 kV
Resistance	0.002 Ω
Inductance	0.08 H
Rated voltage	161.25 kV
Resistance	0.002 Ω
Inductance	0.08 H

Table 6.3 Generator Parameters

Type	synchronous generator, vertical shaft
Rotor type	Salient pole
Nominal power	89 MVA
Rated power factor	0.886578
Rated frequency	50 Hz
Rated voltage	15.75 kV
Rated speed	166.66 rpm
Stator winding resistance	0.0028544 Ω
Rotor winding resistance	0.0857 Ω
Rotor pole pairs	18

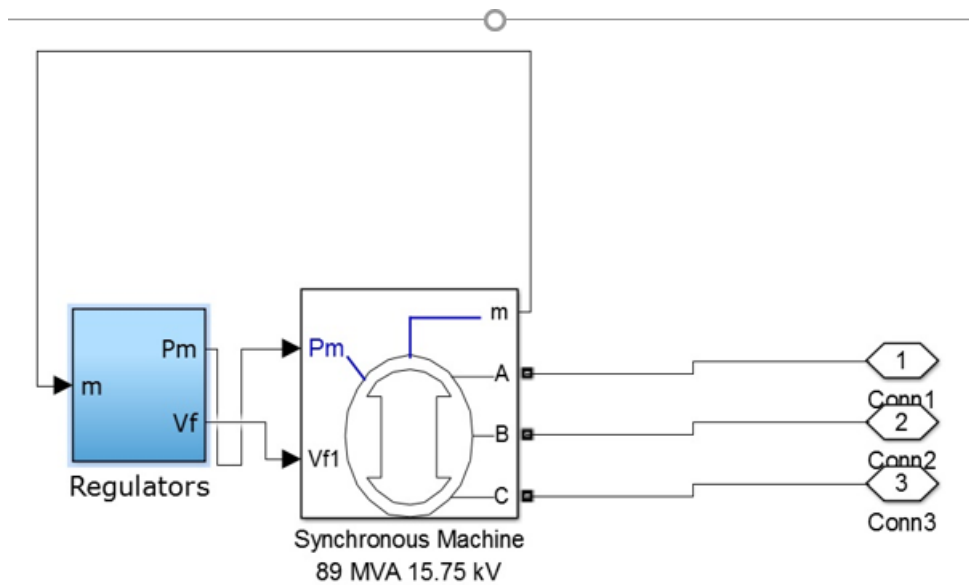


Figure 6.3: Model of Generating Unit of Kastraki using Matlab/Simulink

Inertia coefficient in the block of Synchronous machine is 3.2 and is given by Mr.Georgios Lappas who is electrical engineer in the division of Kastraki HPP & Stratos I HPP in PPC S.A.

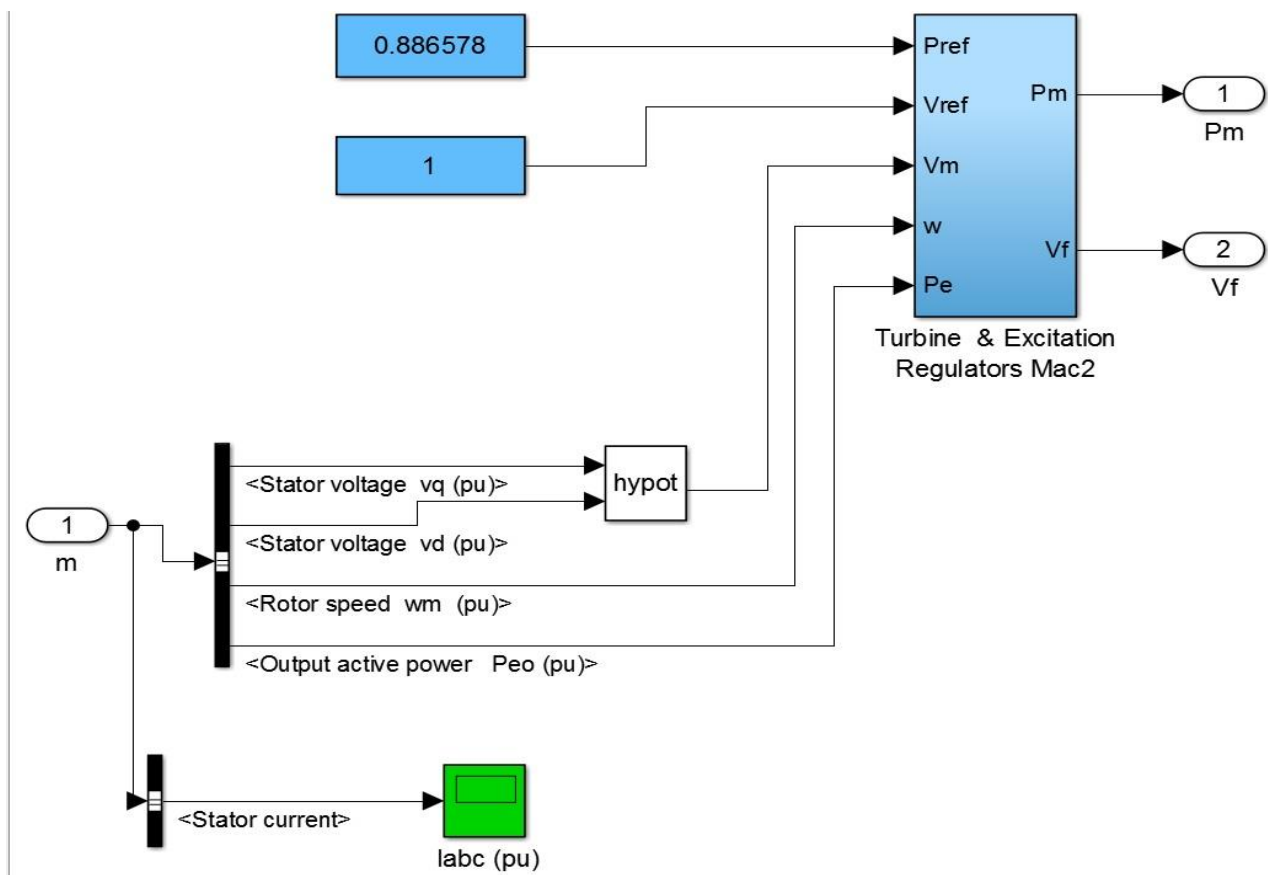


Figure 6.4: Model of Regulators of Kastraki using Matlab/Simulink

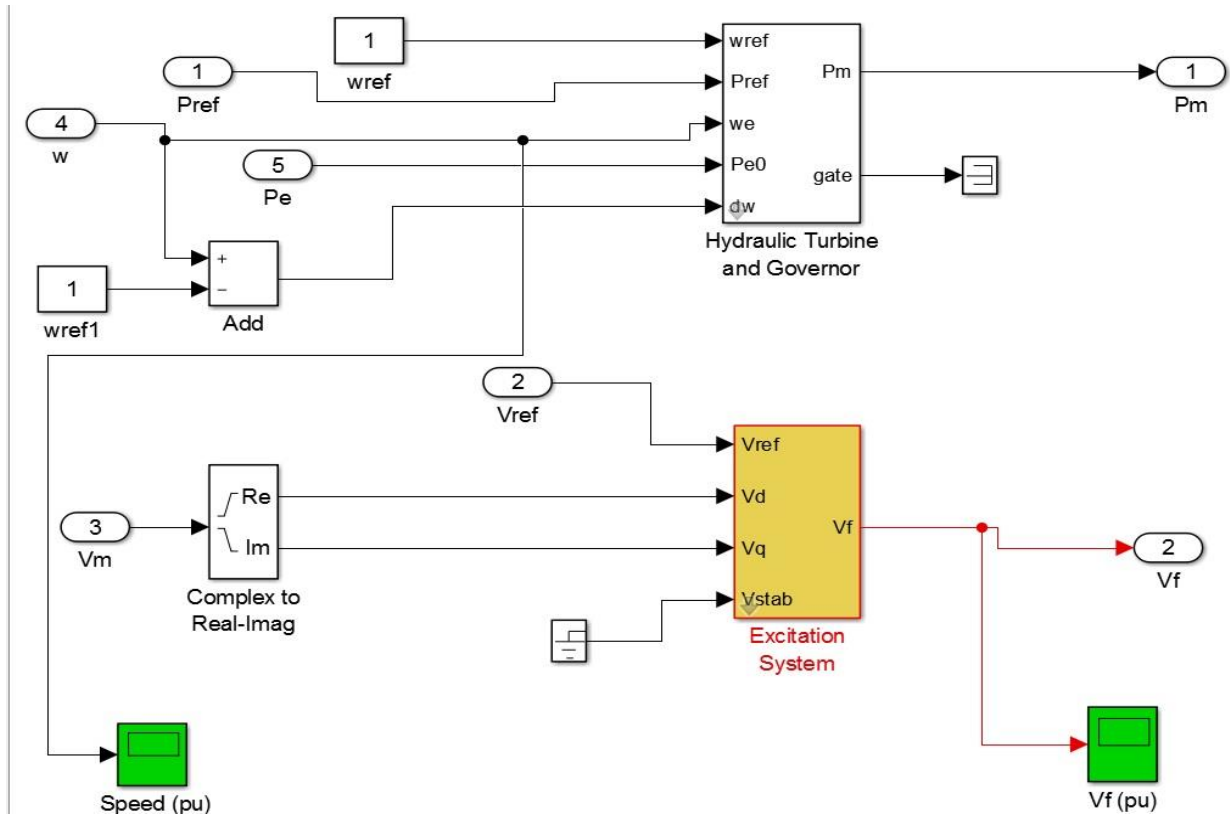


Figure 6.5: Model of Turbine & Excitation Regulators of Kastraki using Matlab/Simulink

In the Hydraulic Turbine the water starting time T_w is calculated by the type:

$$T_w = \frac{L \frac{Q_r}{\pi(D/2)^2}}{a_g H_r} = \frac{242.55 * \frac{120}{3.14 * (5.365/2)^2}}{9.8 * 72.40} = 1.81 \text{ s} \quad (6.1)$$

which is a variation of the equation in (4.12)

Where:

- $Q_r = 120 \text{ m}^3/\text{s}$ is the water discharge in when the level of reservoir is at the maximum level. In this thesis I assume that the water discharge is in maximum because I don't examine the behavior of the reservoir characteristics of the HPP but I examine the dynamic stability of the station instead.
- $H_r = 72.40 \text{ m}$ is the maximum height of fall of the water so as the mechanical Power of the turbine to be 80 MW.
- $L = 242.55 \text{ m}$ is the length of each of four pipelines.
- $D = 5.365 \text{ m}$ is the diameter of each of four pipelines.

6.3 Stratos I HPP Simscape Power Systems Model

The model of Stratos I HPP using Matlab/Simulink is presented in Figure 6.6, the generating station consists of four generating units with P_{mech} of the turbine 75 MW (0.8928 pu) each and P of the generator 74.808 MW (0.8906 pu) each, since the performance level of the Francis turbine at each unit is $n=0.99744$. The turbine losses in the Francis turbine of each unit in Stratos I HPP are the same as in Francis turbine in Kastraki HPP that's the reason why the performance level of the turbines in these two stations are the same. The line frequency of the system is 50 Hz as is usual in Power System in Europe and more specifically in Greece. The model consists of hydraulic turbine, synchronous machine, excitation system blocks, three-phase transformers blocks and RLC blocks. RLC blocks (1 MW at each unit) in the left side of the figure represent the locally consumed power that the generators consume so as to be in continuous operation. In addition, the RLC block of 10 MW in right side between infinite bus and transformer represents the power need of city of Agrinio, which is the main consumer in the area. In this chapter I don't examine how is the power demand from Agrinio exactly, I analyze that later in other chapter Also, the infinite bus is represented by an infinite generator (or source) with 100.000 MVA, 150 kV (an infinite bus). The base voltage $V_{rms} (ph - ph)$ in the infinite bus block is $150 e^3$. This value is not constant value it can be changing.

The Stratos I HPP model is a 149.616 MW (totally from all 2 units) station with 84 MVA, 15.75 kV three phase generator at each unit with 28 pair poles (56), that means from the equation (3.18) that the speed is 107.14 rpm and is connected to a 150 kV network through a $\Delta - Y$ 84 MVA transformer with forced cooling. In the section Rotor type I select Salient-pole because in Stratos I HPP the type of generators is this type. In the model, the synchronous generator is driven by mechanical power generated by the hydraulic turbine block.

In addition, an excitation system is used to generate the excitation voltage that supplies the synchronous generator. The generated excitation voltage from the excitation system block and the mechanical power produced by the turbine are both regulated through the PID controller employed in feedback systems. The PID coefficients are designated by the ZN method ($P_{mech}=0.9 \Rightarrow K_p = 1.99686681$, $K_i = 0.14315631$, $K_d = -1.2251305837$). Each of the two generating unit has an output of 74.808 MW, and each unit generator has an output voltage of 15.75 kV which is fed to a step up transformer that feeds 150 kV transmission line.

To achieve a steady state of continuous production of power in our Simulink model I need to use the Powergui to initialize the currents of the synchronous machines of the generators. I am opening the Powergui and I select 'Machine Initialization'. A new window appears. The machine 'Bus type' is initialized as 'PV generator', indicating that the initialization is performed with the machine controlling the active power and its terminal voltage. The desired terminal voltage parameter is set to 15750 and the Active Power to $7.4808e7$.

The initial terminal voltage and field voltage is set to 1 and 1.4307 per unit respectively for the excitation system block. The Reactive Power is $Q = 4.254$ MVar (0.05065 pu). The base Power is 100 MVA as I am measuring in pu.

Inertia coefficient in the block of Synchronous machine of Stratos I model is 3.2 and is given by Mr. Georgios Lappas who is electrical engineer in the division of Kastraki HPP & Stratos I HPP in PPC S.A.

In the Hydraulic Turbine the water starting time T_w is calculated by the type:

$$T_w = \frac{LU_r}{a_g H_r} = \frac{L \frac{Q_r}{\pi(D/2)^2}}{a_g H_r} = \frac{74.45 * \frac{120}{3.14 * (7.30/2)^2}}{9.8 * 36.6} = 0.595 \text{ s} \quad (6.2)$$

which is a variation of the equation in (4.12)

Where:

- $Q_r = 120 \text{ m}^3/\text{s}$ is the water discharge in when the level of reservoir is at the maximum level. In this thesis I assume that the water discharge is in maximum because I don't examine the behavior of the reservoir characteristics of the HPP but I examine the dynamic stability of the station instead.
- $H_r = 36.6 \text{ m}$ is the maximum height of fall of the water so as the mechanical Power of the turbine to be 75 MW.
- $L = 74.45 \text{ m}$ is the length of each of two pipelines.
- $D = 7.3 \text{ m}$ is the diameter of each of two pipelines.

Table 6.4 Hydraulic Turbine and Governor

Type	Vertical shaft
Nor.effective Head	Francis
Output at normal head	36.60 m.
Discharge at normal head	75 MW
Revolving speed	120 m ³ /sec
Water starting time T_w	107.14 rpm
Permanent droop	0.595 s
Servo gain K_a	0.05
Servo time constant T_a	10/3
	0.07 s

Table 6.5 Three Phase Transformer Parameters

Nominal Power	84 MVA
Rated frequency	50 Hz
Rated voltage	15.75 kV
Resistance	0.002 Ω
Inductance	0.08 H
Rated voltage	150 kV
Resistance	0.002 Ω
Inductance	0.08 H

Table 6.6 Generator Parameters

Type	synchronous generator, vertical shaft
Rotor type	Salient pole
Nominal power	89 MVA
Rated power factor	0.886578
Rated frequency	50 Hz
Rated voltage	15.75 kV
Rated speed	107.14 rpm
Stator winding resistance	0.0028544 Ω
Rotor winding resistance	0.0857 Ω
Rotor pole pairs	28

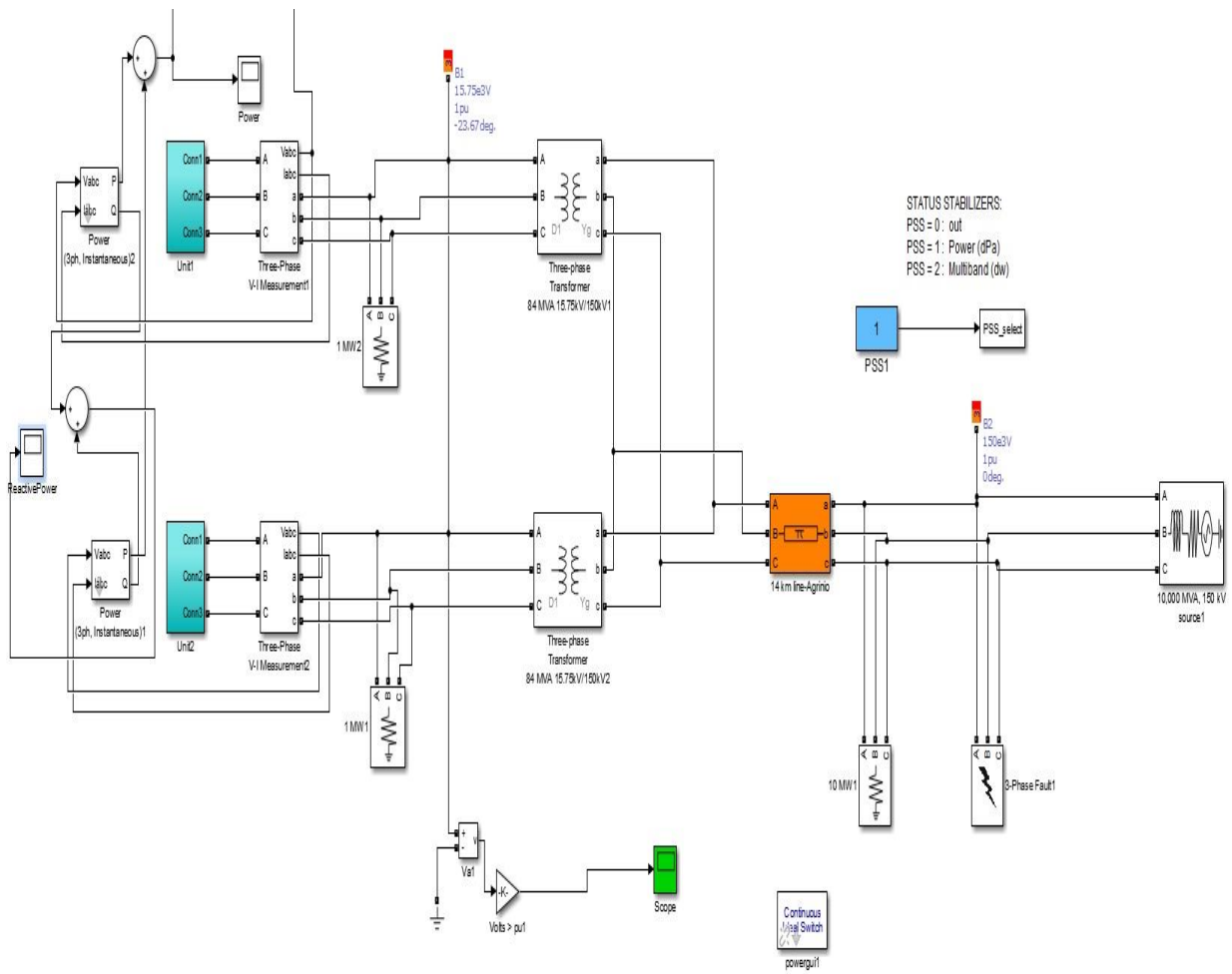


Figure 6.6: Model of Stratos Hydro Power Plant using Matlab/Simulink.

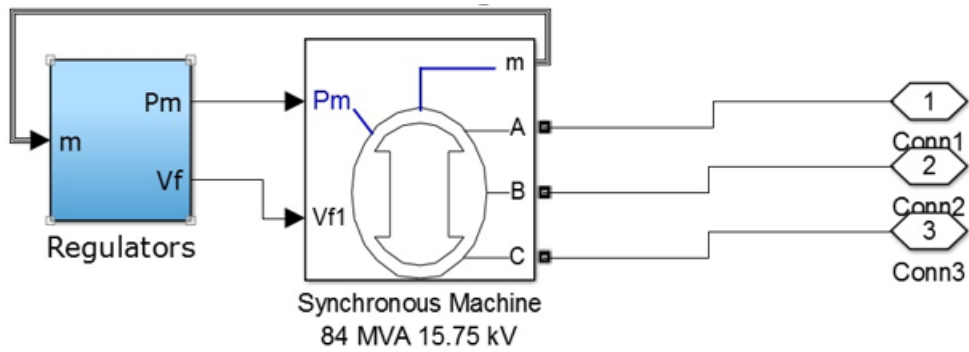


Figure 6.7: Model of Generating Unit of Stratos I using Matlab/Simulink

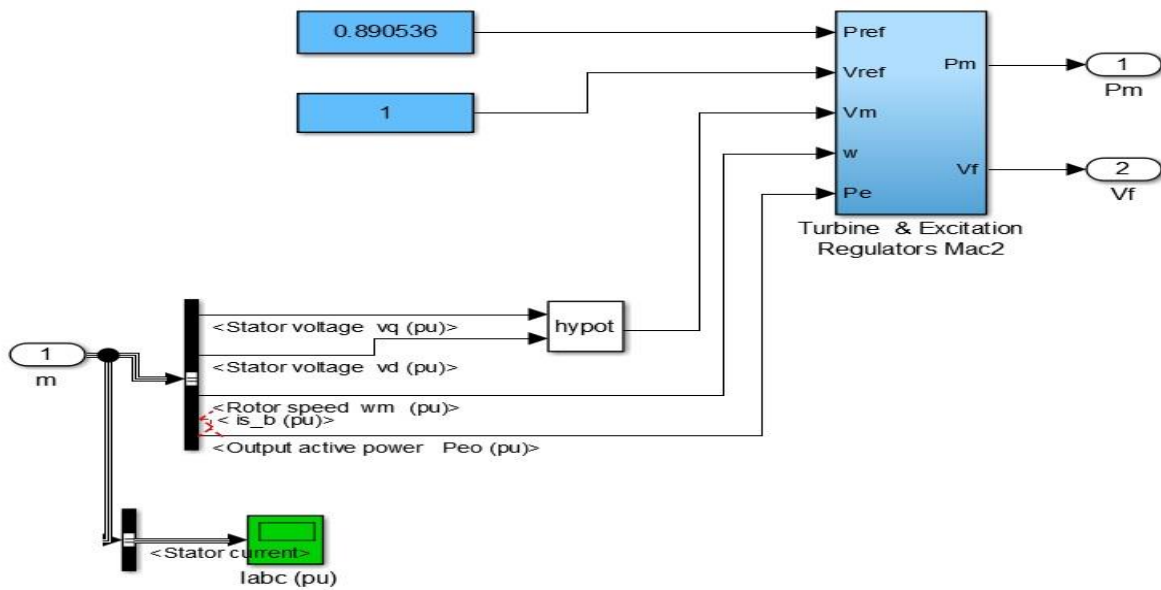


Figure 6.8: Model of Regulators of Stratos I using Matlab/Simulink

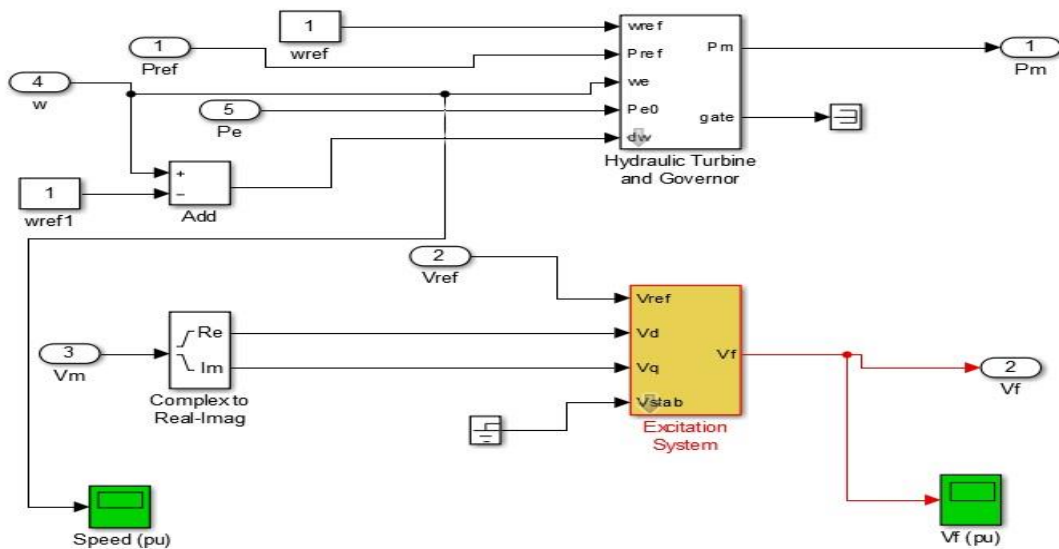


Figure 6.9: Model of Turbine & Excitation Regulators of Stratos I using Matlab/Simulink

6.4 Summary

I constructed the models of Kastraki HPP and Stratos I HPP in Simulink/Matlab. The production load of 0.8866 pu (79.792 MW) in each of four units in Kastraki Hydroelectric Power plant is not the maximum ability of production in the station, neither the production load of 0.8928 pu (75 MW) is the maximum ability of energy production in each of two units in Stratos I HPP. That's the reason why the values are near at 0.9 pu and not 1 pu. The two Hydropower Power plants don't use the max

of their ability so as they can cope successfully in cases of high demand and in high peak situations which require using the actual maximum of generator. This limit in the generator operates as a mean of saving for security reasons and for maintenance and energy conservation reasons.

Chapter 7

Tuning PI and PID coefficients in governor

In the previous chapter, I modeled the HPPs in Stratos I and in Kastraki. The modelling of dynamic behavior of the system was analyzed to investigate the output of magnitudes (output active power, rotor speed, reactive power, excitation voltage, current of synchronous machine, output voltage) under normal conditions. The modelling of dynamic behavior of the 2 HPPs was designed by using the Matlab /Simulink and Simscape Power Systems Toolbox. I designed the transient model of synchronous generator with excitation system model and hydraulic turbine model were applied. The simulated excitation system is DC exciter type excitation system with considering saturation characteristic. Non-linear hydraulic turbine model was applied with PID control of the gate servomotor. I used a power system stabilizer (PSS block) on the system so as to improve as it is possible the stability. In this section I am going to determine between the hydraulic governor and the electro-hydraulic governor. This decision will be made by presenting the systems in various simulation tests. From here and beyond all the simulations models have a PSS stabilizer.

7.1 PI and PID controllers

There are two kinds of governors the mechanical hydraulic governor which in Simulink I can represent with a PI governor which does not have a derivation action, hence it is equivalent to a hydraulic governor and the electro-hydraulic governors. The electro-hydraulic governors are provided with three-term controllers with proportional-integral-derivative (PID) action. These governors provide higher response speeds by providing both transient gain decrement and transient gain increment. The proportional and integral gains can be adjusted to obtain desired temporary droop and reset-time. The derivative action is beneficial for isolated operation. As in many other industrial applications, the PID (proportional-integral-derivative) type controller is one of the most widely used control laws in hydro power station governing. Although the derivative term in the control action is important in case of isolated operation. Its use results in excessive oscillation in interconnected system. The transfer function of PID without derivative effect in action is equivalent to that of the hydraulicmechanical governor. The design is based on linear control theory at one load condition and then de-tuned for worst operating conditions. This controller design does not guarantee the close loop system to remain stable at all operating conditions.

For purpose of limiting the occurring oscillations within the acceptable tolerance value, parameters of the PID controller that controlled the mechanic energy input or turbine speed according to loading statutes were determined by the ZN method. By means of the PID controller that regulated the speed of hydro turbine, operating voltage and frequency reached to desired value in the shortest time and steady and stable working condition of the system was realized. We are going to design the PI controllers of the corresponding HPP in each case (Stratos I and Kastraki) using the ZN method and

table 7.1. The table 7.1 is based in the Ziegler-Nichols method which is a heuristic method of tuning a PID controller.

7.2 Ziegler-Nichols Tuning method table

The process of setting the optimal gains for P, I and D to get an ideal response from a control system is called tuning. There are different methods of tuning of which the “guess and check” method and the Ziegler Nichols method will be discussed. The gains of a PID controller can be obtained by trial and error method. Once an engineer understands the significance of each gain parameter, this method becomes relatively easy. In this method, the I and D terms are set to zero first and the proportional gain is increased until the output of the loop oscillates. As one increases the proportional gain, the system becomes faster, but care must be taken not make the system unstable. Once P has been set to obtain a desired fast response, the integral term is increased to stop the oscillations. The integral term reduces the steady state error, but increases overshoot. Some amount of overshoot is always necessary for a fast system so that it could respond to changes immediately. The integral term is tweaked to achieve a minimal steady state error. Once the P and I have been set to get the desired fast control system with minimal steady state error, the derivative term is increased until the loop is acceptably quick to its set point. Increasing derivative term decreases overshoot and yields higher gain with stability but would cause the system to be highly sensitive to noise. Often times, engineers need to tradeoff one characteristic of a control system for another to better meet their requirements. As a result, the Ziegler-Nichols method is another popular method of tuning a PID controller. It is very similar to the trial and error method wherein I and D are set to zero and P is increased until the loop starts to oscillate. Once oscillation starts, the critical gain K_c and the period of oscillations P_c are noted. The P, I and D are then adjusted as per the tabular column shown below. Knowing the PID coefficients for each load I can calculate with the help of table 7.1 the coefficients of PI. The electro-hydraulic governors can be represented in Simulink by a PID block.

The PID block which is in the block path in the Figure 5.5 is projected in the Figure 5.8. The PI is presented in the block path in Figure 7.1 .The block of PI is the same with the PID block in Figure 5.8 with the difference that the K_p and K_i values are different and the K_d has zero value [66].

Table 7.1 Ziegler-Nichols tuning, using the oscillation method.

Control	P	Ti	Td
P	$0.5K_c$	-	-
PI	$0.45K_c$	$P_c/1.2$	-
PID	$0.60K_c$	$0.5P_c$	$P_c/8$

Where:

- the critical gain K_c .
- the period of oscillations P_c .

These 3 parameters are used to establish the correction from the error via the equation:

$$u(t) = K_p(e(t) + \frac{1}{T_i} \int_0^t e(\tau) d\tau + T_d \frac{de(t)}{dt}) = K_p e(t) + K_i \int_0^t e(\tau) d\tau + K_d \frac{de(t)}{dt} \quad (7.1)$$

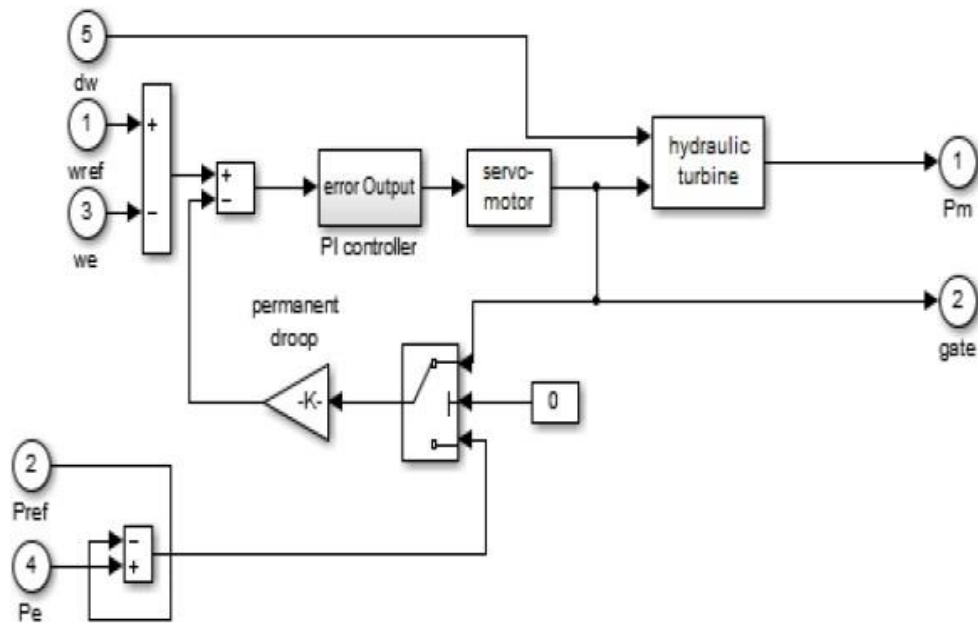


Figure 7.1: Simulink model of PI Governor

Chapter 8

Simulation of the HPP with PI and PID controller

8.1 Simulation Results under normal conditions in Kastraki HPP

Now I am going to see the simulation of Kastraki Model under normal conditions in order to check if the Hydropower Plant in Kastraki that I modelled, is in steady state. I will check the dynamic stability of the station. The simulation is continuous. The time of simulation is 20 s. We have PID controller with gains from ZN method for 0.9 pu mechanical power.

Table 8.1 PID coefficients in Kastraki HPP for 0.9 pu

K_p	K_i	K_d
1.99686681	0.14315631	-1.2251305837

The following figure shows the generated voltage of the station of this model in steady state. The simulation results show that with proper choice of turbine design for micro hydro power plant leads to constant voltage output. The output voltage of Kastraki HPP ranges between 1.2 to -1.2 pu.

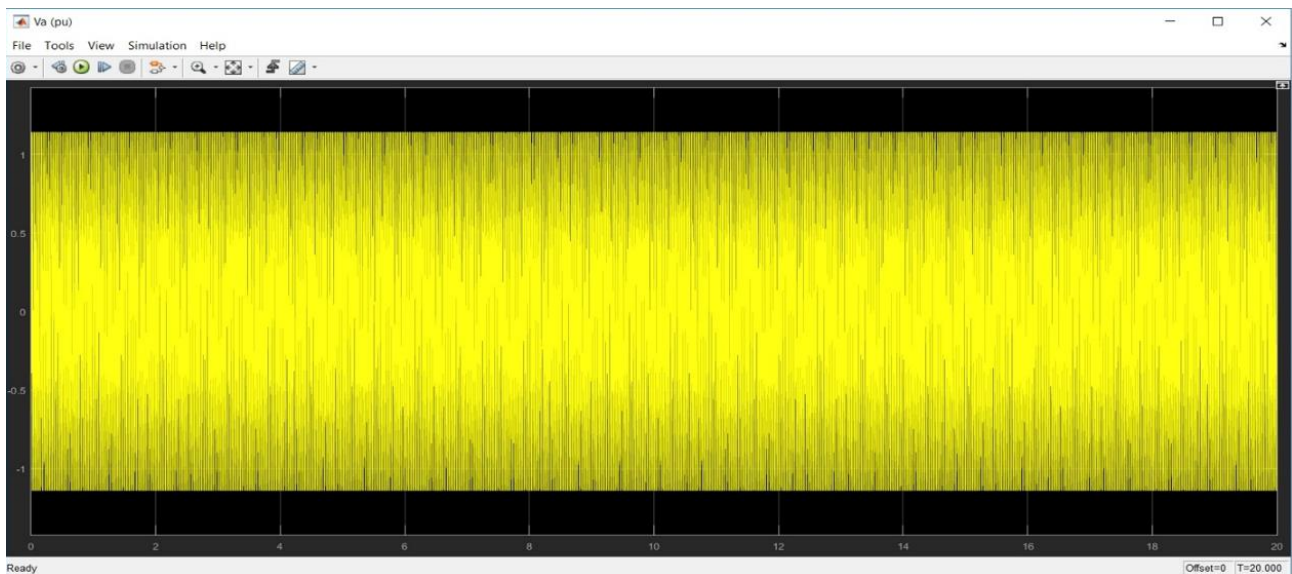


Figure 8.1: Output Voltage Characteristics of Kastraki station for 0.8866 pu (in y-Axis pu Voltage in Volt and in x-Axis Time in s)

The following figure shows the current I_{abc} of each machine of the station of this model in steady state. The simulation results show that with proper choice of turbine design for micro hydro power

plant leads to constant current without oscillations. The I_{abc} current of Kastraki HPP ranges between 0.9 to -0.9 pu.

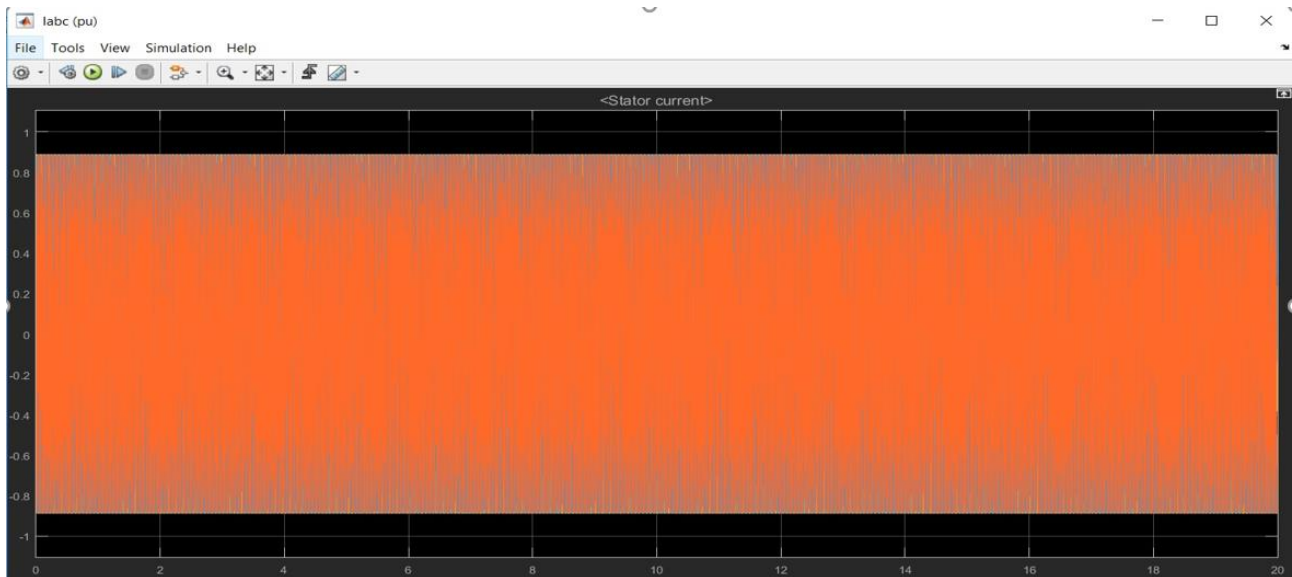


Figure 8.2: Stator Three Phase Current Characteristics of Hydro Power Plant in Kastraki for 0.8866 pu (in y pu and in x-Axis Time in s)

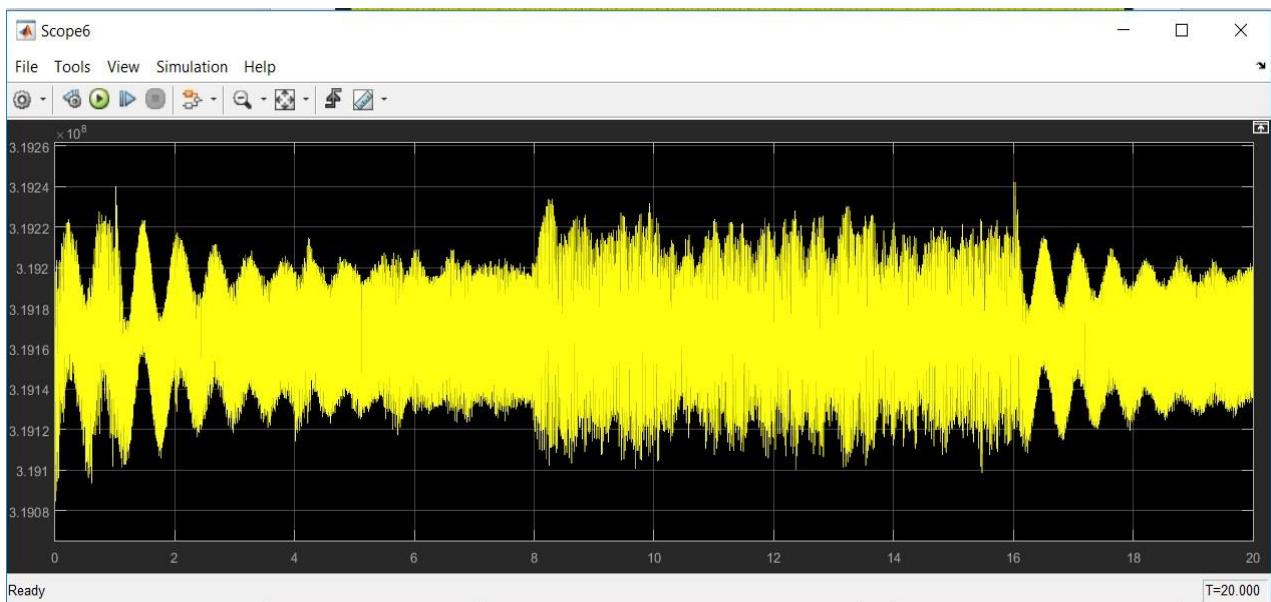


Figure 8.3: Output active power of the Hydropower Plant in Kastraki for 0.8866 pu (in y MW and in x-Axis Time in s)

In Figure 8.3 I see the total Active Power of the station and I notice that is between 319.11 to 319.24 MW.

First of all, I am satisfied with the value of the power but I don't like the multiple oscillations of the power in the duration of simulation time. Even the deviation between the values of the power is small, it's not right to have changes in the value all the time.

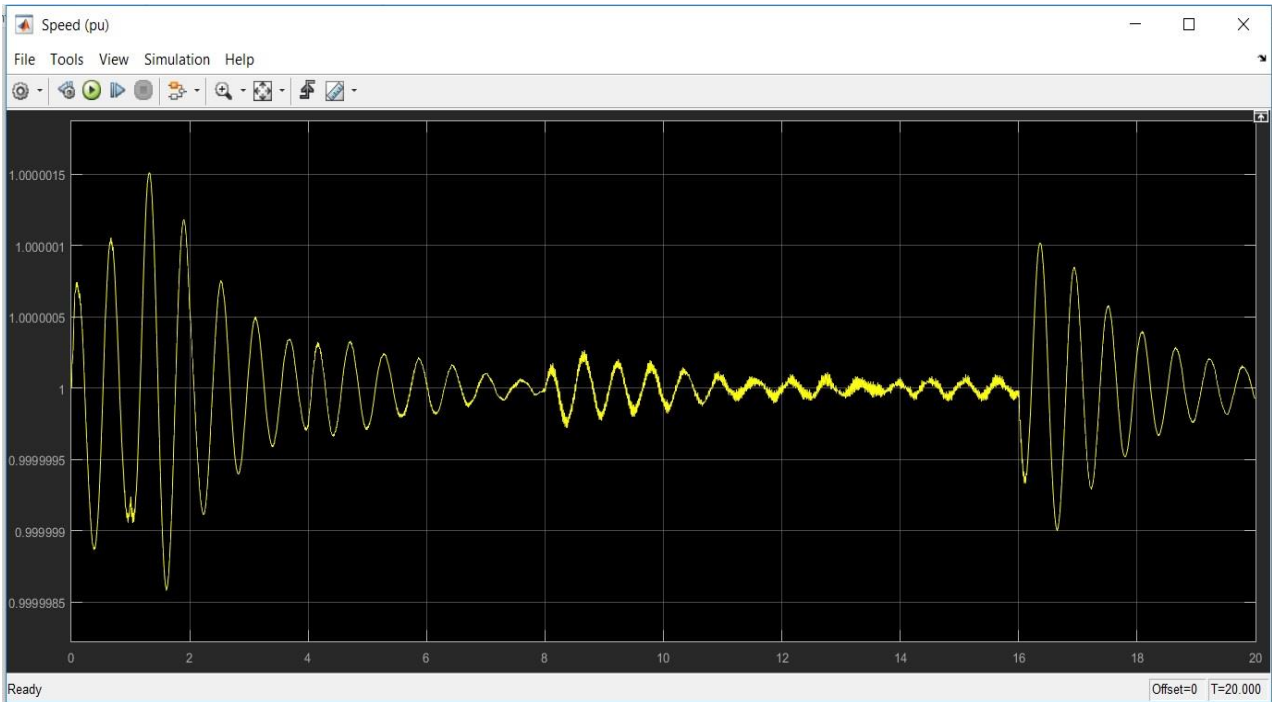


Figure 8.4: Synchronous Generator Speed Characteristics in Kastraki for 0.8866 pu (in y-Axis Speed in pu and in x-Axis Time in s)

The under damped rotor speed characteristic of hydro (synchronous) generator is shown in Figure 8.4. From the characteristics, it is observed that at the time 8 s the value is more stable but after in time 16 s the big oscillations start again like the beginning, it seems almost like a periodic signal.

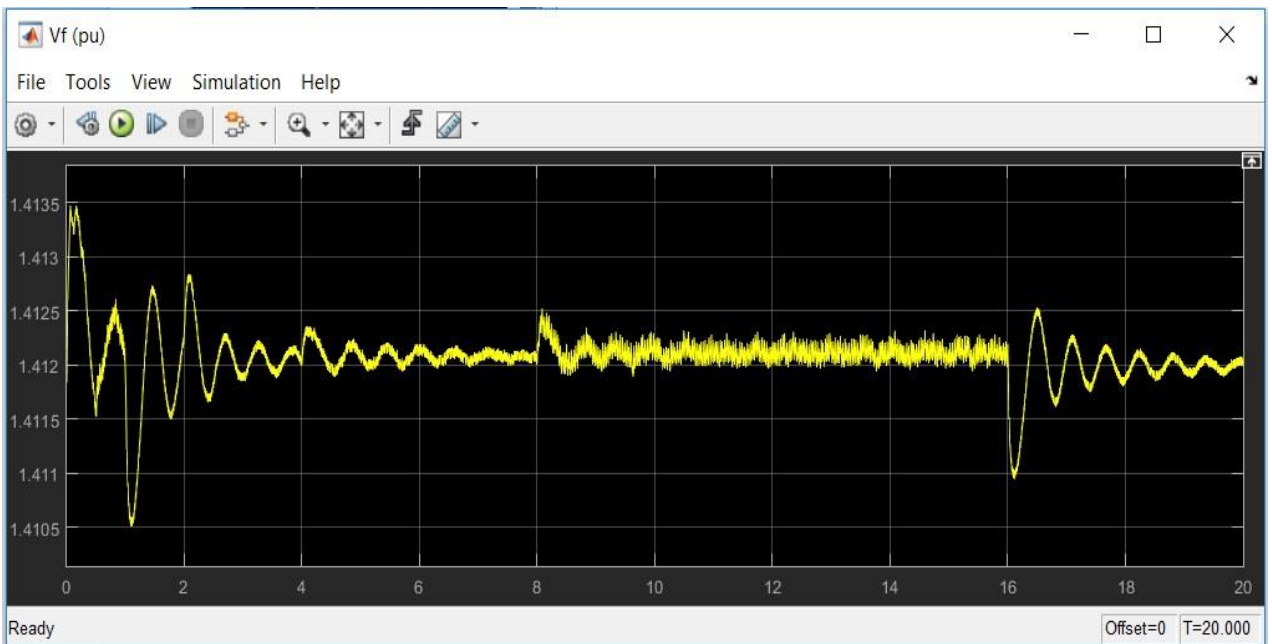


Figure 8.5: Excitation Voltage of Generator Speed in Kastraki for 0.8866 pu (in y-Axis Volts in pu and in x-Axis Time in s)

In figure 8.5 I see the excitation voltage of each unit.

I notice that starts with oscillation and in time 8 s like the speed is more stable but again in 16 s like in the figure of speed starts again big oscillations.

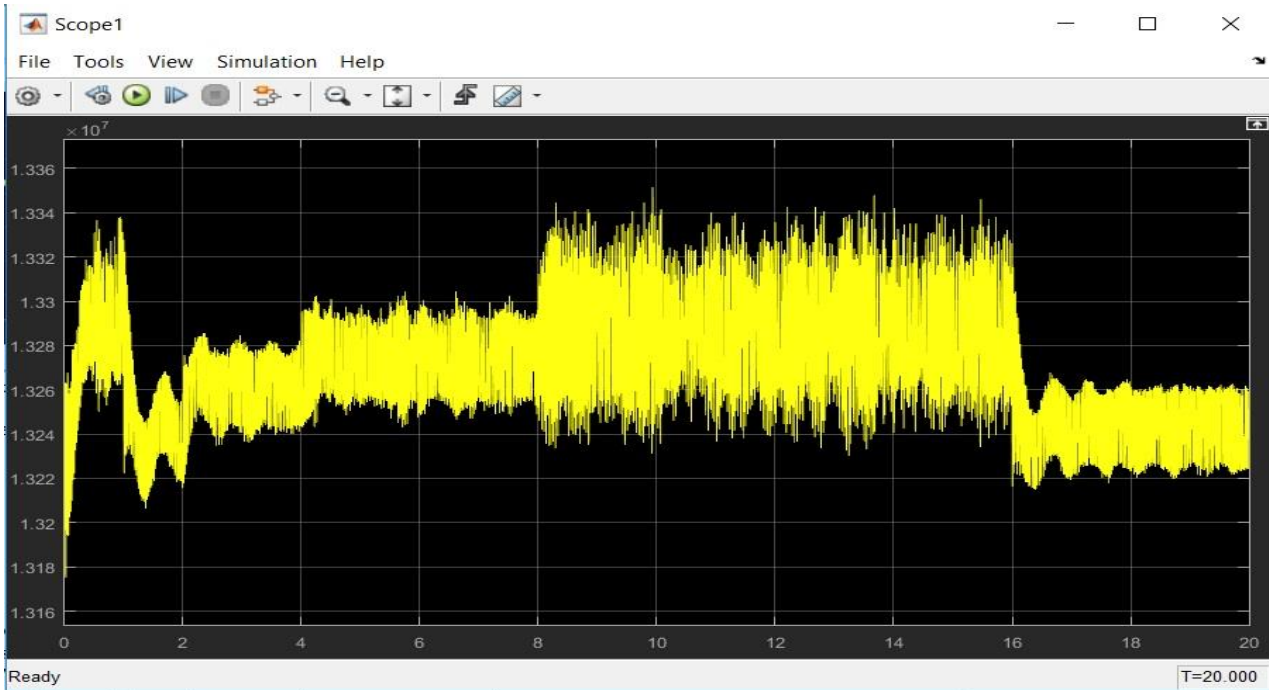


Figure 8.6: Reactive Power of the station in Kastraki for 0.8866 pu (in y-Axis M var and in x-Axis Time in s)

In Figure 8.6 I see the Reactive Power Q of the Hydropower Plant in Kastraki . I notice that the value is between 13.34 to 13.21 MVar.

8.1.1 PSS implementation in Kastraki HPP model

As I have mentioned already my purpose is the operation of our HydroPower Plant in Kastraki, being in a steady state. I am okay with the figures of the output voltage and the current of synchronous machine because these signals have not any oscillations, but all the other figures have.

So I am going to optimize our model so as not having these oscillations. My first thought is to implement a PSS stabilizer. The stabilize connects the excitation system with the Hydraulic Turbine and Governor. Though generator output power is decided by a turbine's mechanical torque, it can be changed by transiently changing the excitation value. A PSS detects the change in generator output power, controls the excitation value, and reduces the rapid power fluctuation.

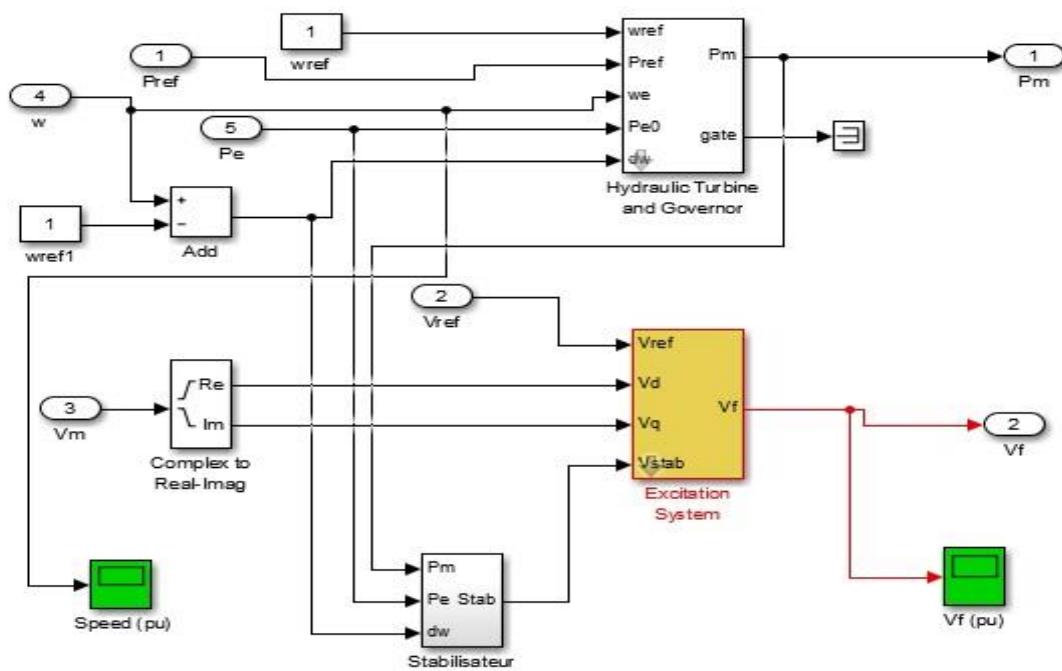


Figure 8.7: PSS Stabilizer in model of Kastraki HPP

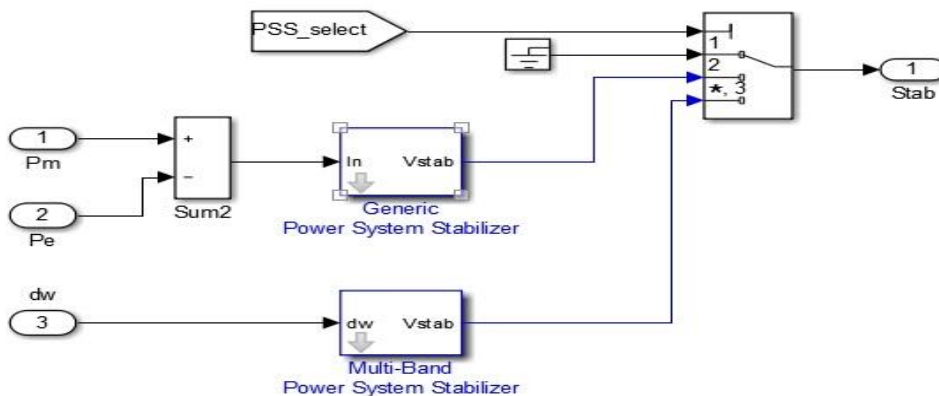


Figure 8.8: PSS stabilizer model

I am going to see the effect of using power system stabilizer on the system stability. I will present the same figures after the implementation of the PSS stabilizer.

The output voltage and current of synchronous machine signals are the same as before (8.1, 8.2) the implementation of the PSS Stabilizer block. The stabilizer can only optimize the performance of the system stability but these two signals were already in their optimal version, so they are the same.

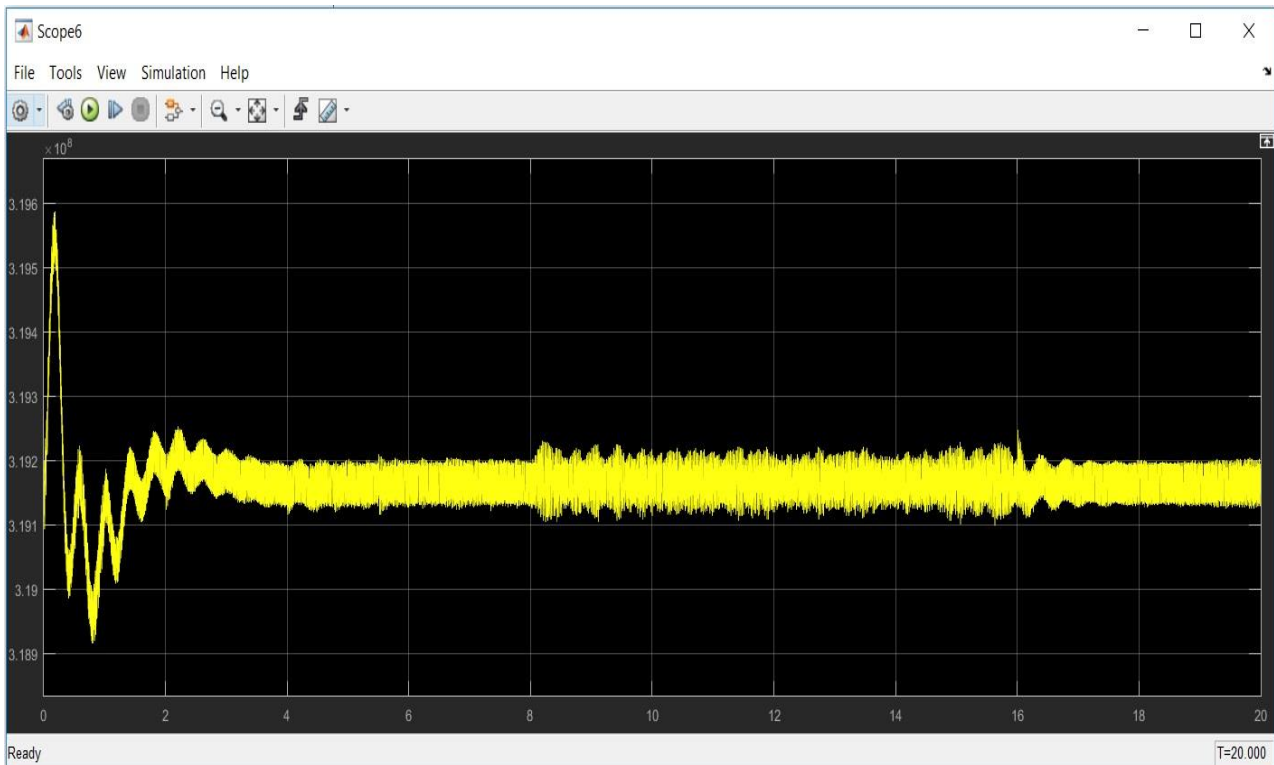


Figure 8.9: Output active power of the Hydropower Plant in Kastraki with PSS for 0.8866 pu (in y MW and in x-Axis Time in s)

I notice that huge difference before and after the implementation of the PSS stabilizer in the output active power. The values of the active power are 319.6 MW to 318.9 MW. I have heavy oscillations only in the first 2.5 s and after in time 3 s I have a steady state as I see that the output active power remains stable at 319.2 MW. It is observed that the steady state is obtained around 3 s. To reach the stable operating point on power - angle characteristics, few oscillations around this point occurs. This leads to initial overshoots and undershoots of the power characteristics. This figure is better than Figure 8.3.

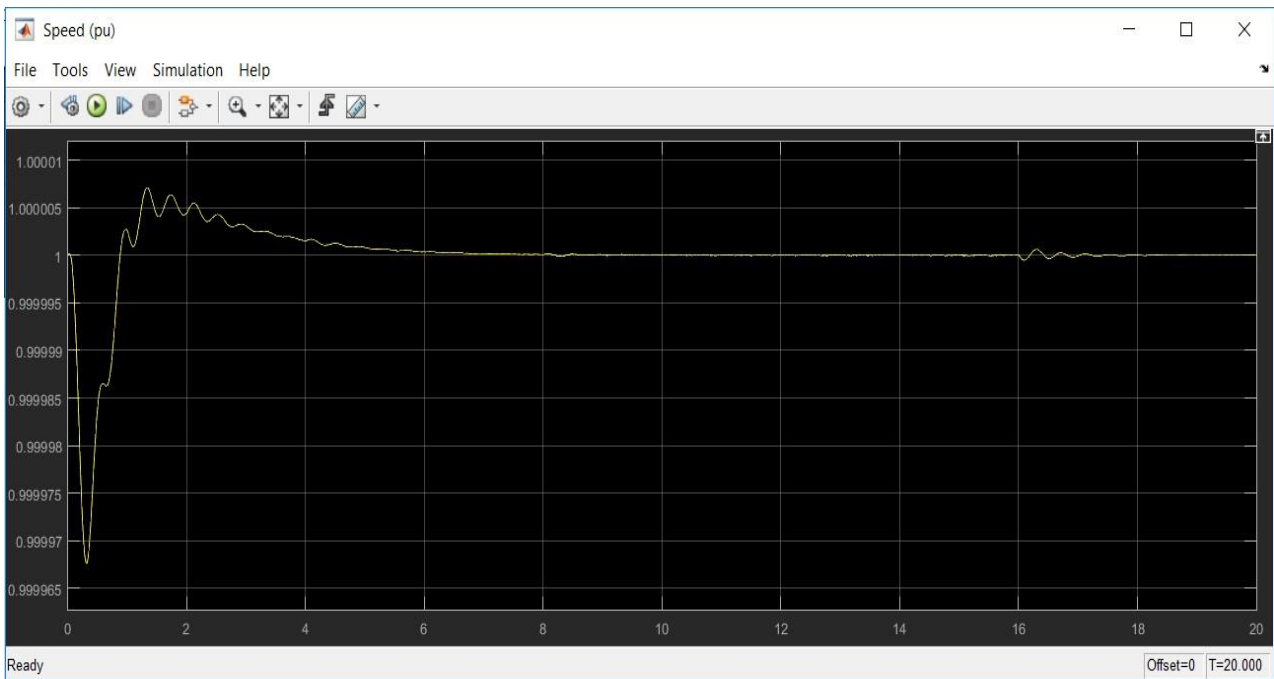


Figure 8.10: Synchronous Generator Speed Characteristics in Kastraki with PSS for 0.8866 pu (in y-Axis Speed in pu and in x-Axis Time in s)

In the Figure 8.10 from the characteristics, it is observed that the transient time is 8 s. After 6 s its speed reaches steady state at synchronous speed. With sudden application of mechanical torque input to the shaft of alternator, the load angle settles to a steady state value after few oscillations owing to system damping following the swing equation and power angle characteristics. Moreover, for the governor setting $K_p = 1.99686681$, $K_i = 0.14315631$, $K_d = -1.2251305837$) I used the ZN method and error method helps to keep the speed near synchronous speed (1.02 pu). Also this figure is better than the Figure 8.4.

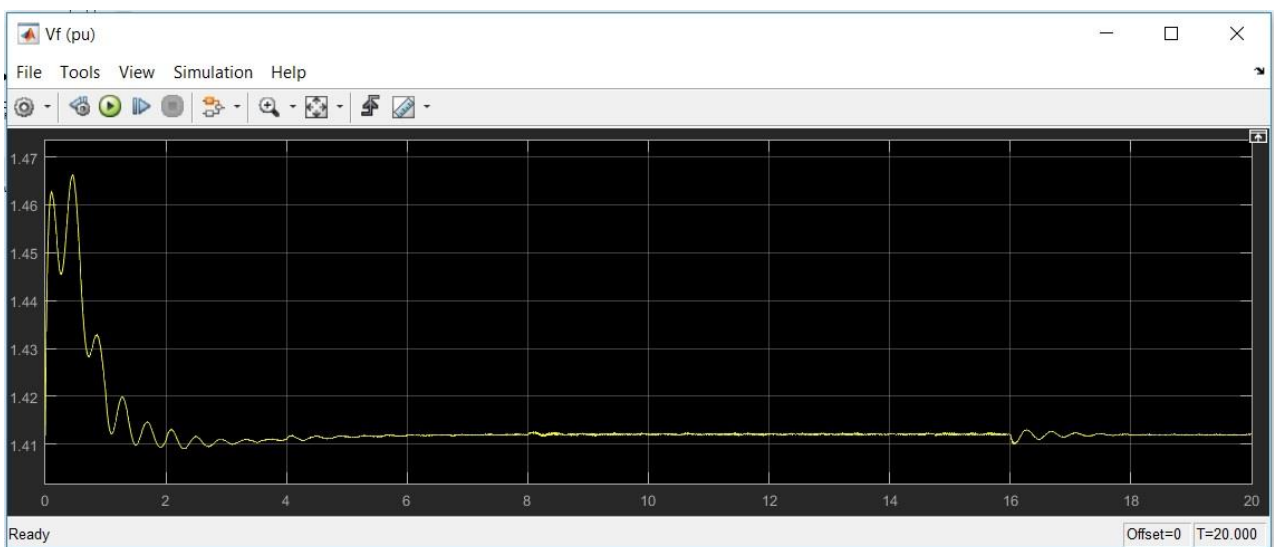


Figure 8.11: Excitation Voltage of Generator Speed in Kastraki with PSS for 0.8866 pu (in y-Axis Volts in pu and in x-Axis Time in s)

In the Figure 8.11 from the characteristics, it is observed that the transient time is 8 s. After 6 s its speed reaches steady state at excitation voltage. In the steady state it helps to keep the excitation voltage near the initial field voltage (1.42 pu). Also this figure is better than the Figure 8.5.

In the Figure 8.12 below shows that the reactive power characteristics complete its transient period in 8 s and steady state value achieved is 13 MVar in time 7 s and is obtained which matches the actual reactive load connected. Also this figure is better than the Figure 8.6.

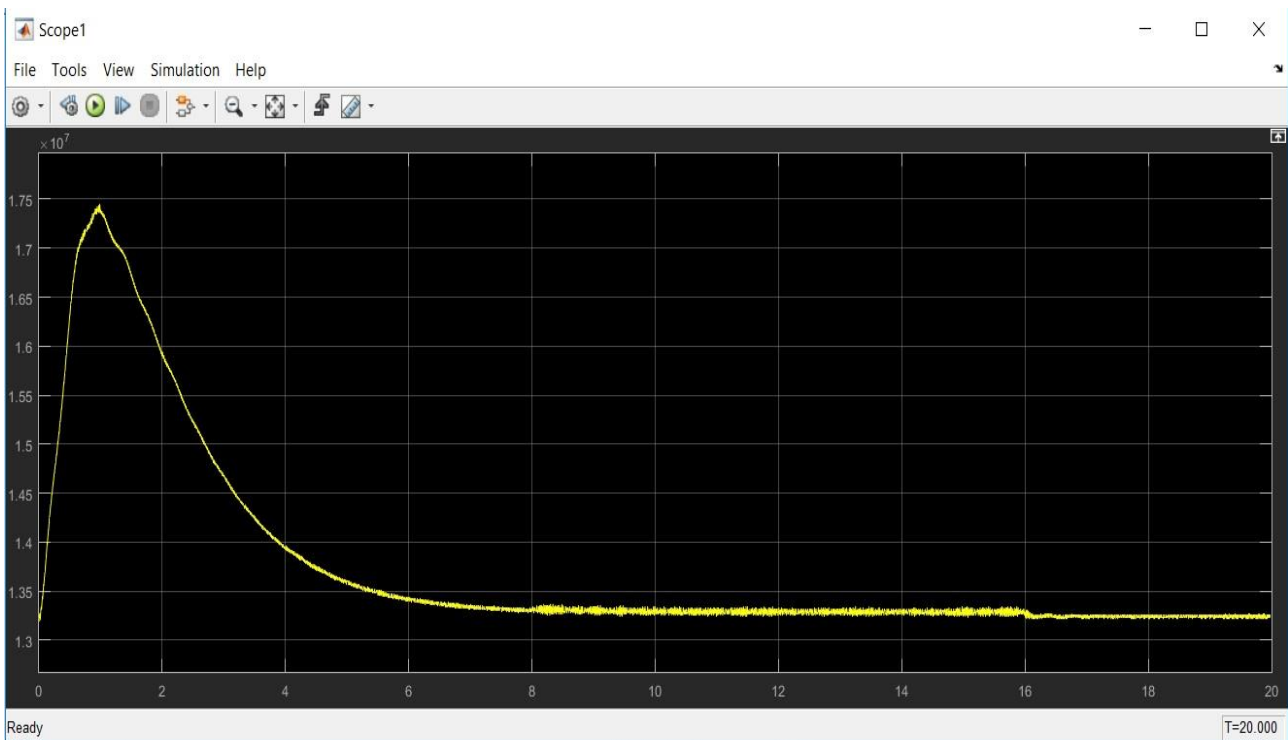


Figure 8.12: Reactive Power of the station in Kastraki with PSS for 0.8866 pu (in y-Axis M var and in x-Axis Time in s)

I understand that the PSS stabilizer helps the HydroPower Plant of Kastraki reach its dynamic stability more quickly and in a more efficient way.

8.2 Simulation Results under normal conditions in Stratos I HPP

In this section I am going to test the simulation of Stratos I Model under normal conditions in order to check if the Hydropower Plant in Stratos I that I modelled, is in steady state. Moreover, I will check the dynamic stability of the station. The simulation is continuous.

The time of simulation is 20 s like the simulation of Kastraki under of these circumstances.

I have PID controller with gains from ZN method for 0.9 pu mechanical power ($P_{mech} = 0.9 \Rightarrow K_p = 1.25387312, K_i = 0.13126167, K_d = -0.71356127$).

Table 8.2 PID coefficients 0.9 pu

K_p	K_i	K_d
1.25387312	0.13126167	-0.71356127

The following figure shows the generated voltage of the station of this model in steady state under normal condition. The simulation results show that with proper choice of turbine design for micro hydro power plant leads to constant voltage output. The voltage is measured in the A phase of the three-phase line between generator and transformer of Stratos I HPP.

I observe that the value of output voltage ranges between 1 to 1 pu, while in output voltage figure of Kastraki HPP we had 1.2 to -1.2 pu. Both figures are a sine response which is stable in entire simulation but the smaller amplitude of Stratos I HPP shows that the output voltage remains closer to 1 pu.

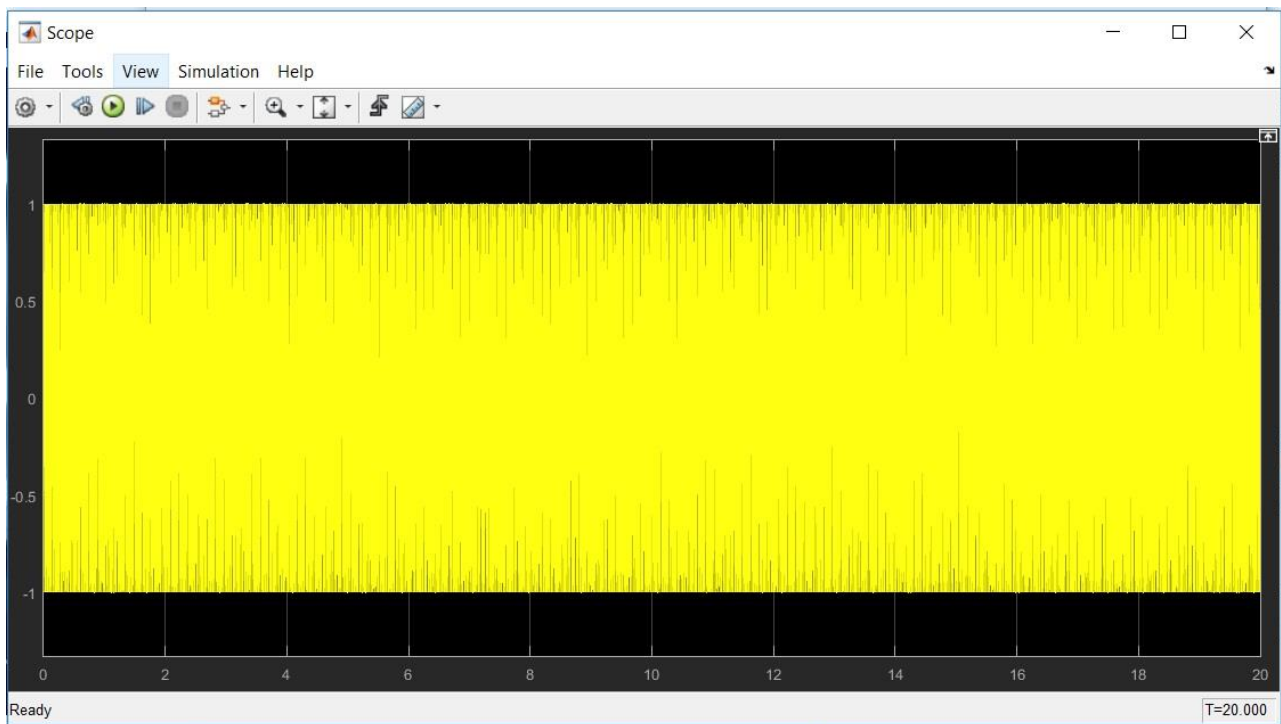


Figure 8.13: Output Voltage Characteristics of Stratos I station for 0.8906 pu (in y-Axis pu Voltage in Volt and in x-Axis Time in s)

The figure below 8.14 shows the current I_{abc} of each unit that comes from each synchronous machine of Stratos I HPP of this model in steady state. The simulation results show that with proper choice of turbine design for micro hydro power plant leads to constant current without oscillations. The I_{abc} current of Stratos I HPP ranges between 0.9 to -0.9 pu as it also happens in the three-phase current response in Kastraki HPP.

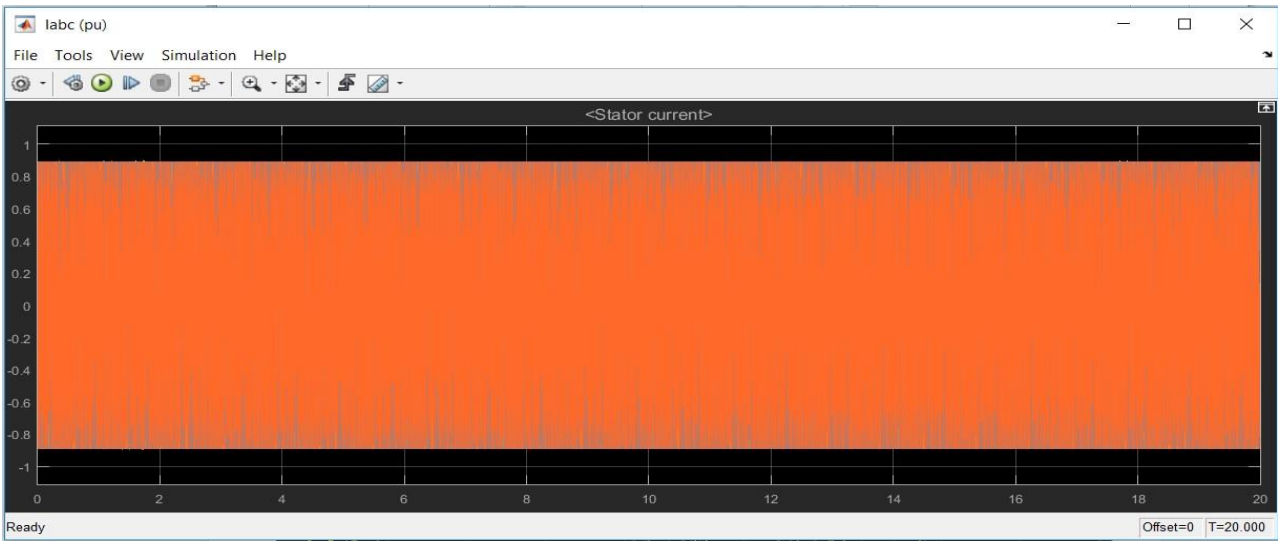


Figure 8.14: Stator Three Phase Current Characteristics of Hydro Power Plant in Stratos I for 0.8906 pu (in y pu and in x-Axis Time in s)

In Figure 8.15 I see the total Active Power of the station and I notice that is between 150.3 to 149.10 MW in the first 1.8 seconds and after 2 seconds the value ranges mainly between 149.9 to 149.3. First and foremost, I am satisfied with the value of the active power because I expected from our HPP to produce 149.616 MW but I don't like the multiple oscillations of the power in the duration of simulation time, my aim is to make smaller the amplitude as it is possible with less oscillations in the figure, I will check later if the PSS stabilizer will help. Even the deviation between the values of the power is small, it's not right to have such fluctuations in the value all the time. In transient signal analysis I want as it is possible more stability.

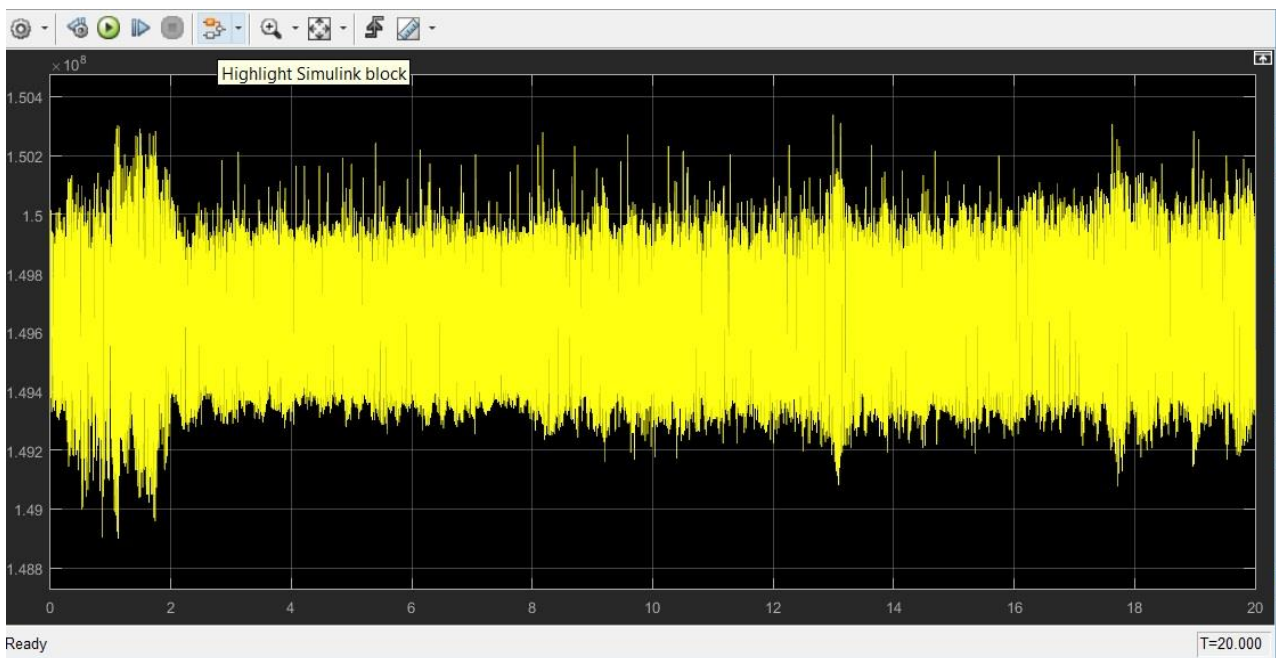


Figure 8.15: Output active power of the Hydropower Plant in Stratos I for 0.8906 pu (in y MW and in x-Axis Time in s)

Concerning the rotor speed characteristic of hydro (synchronous) generator is shown in Figure 8.16. From the characteristics, it is observed that at the time 5 s the value is more stable but after in time 16 s the big oscillations start again like the beginning, it seems almost like a periodic signal like the speed of Kastraki but the time difference here is about 9 s and in Kastraki HPP was about 4 s.

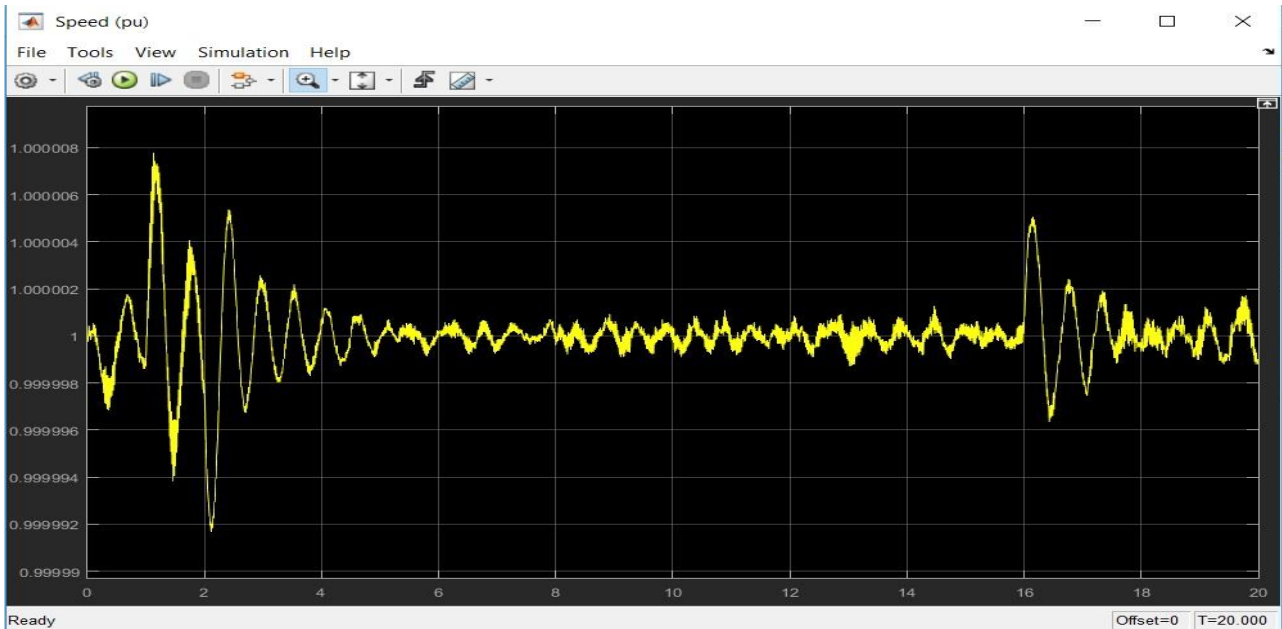


Figure 8.16: Synchronous Generator Speed Characteristics in Stratos I for 0.8906 pu (in y-Axis Speed in pu and in x-Axis Time in s)

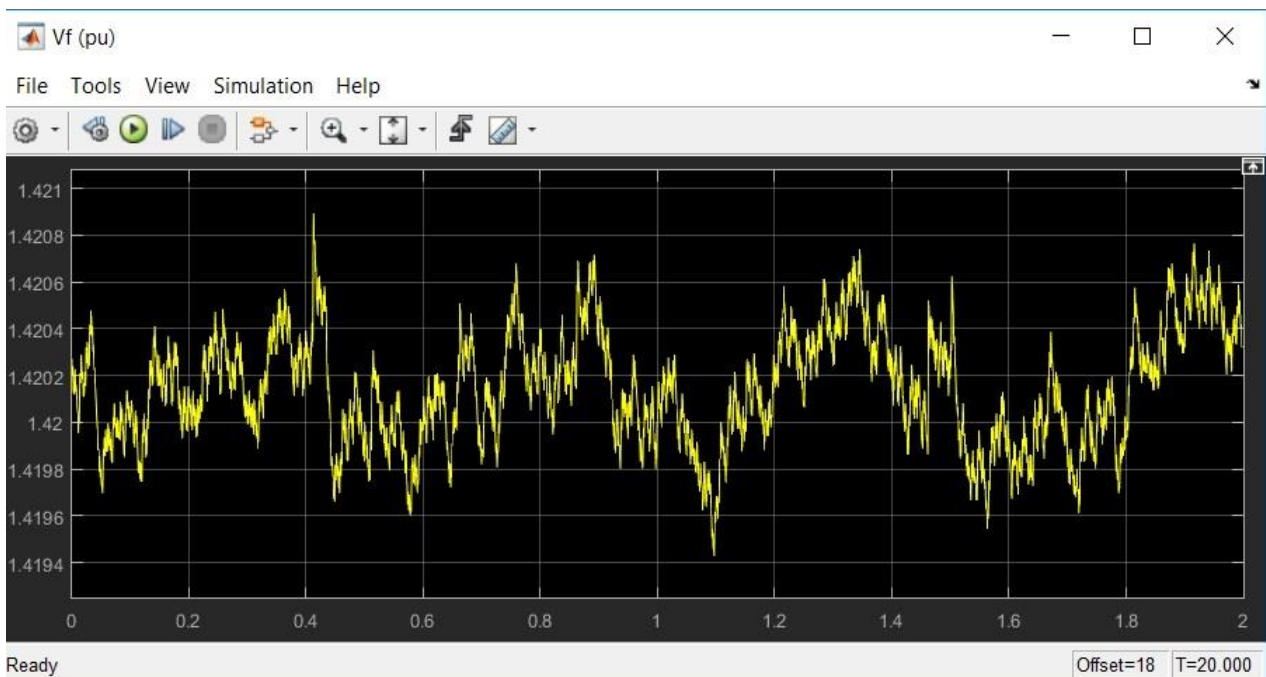


Figure 8.17: Excitation Voltage of Generator Speed in Stratos I for 0.8906 pu (in y-Axis Volts in pu and in x-Axis Time in s)

In figure 8.17 I observe the excitation voltage of each unit of Stratos I HPP. I notice that the signal response it's almost like a periodic signal with period 0.4 s. The value is between 1.421 to 1.4195 pu.

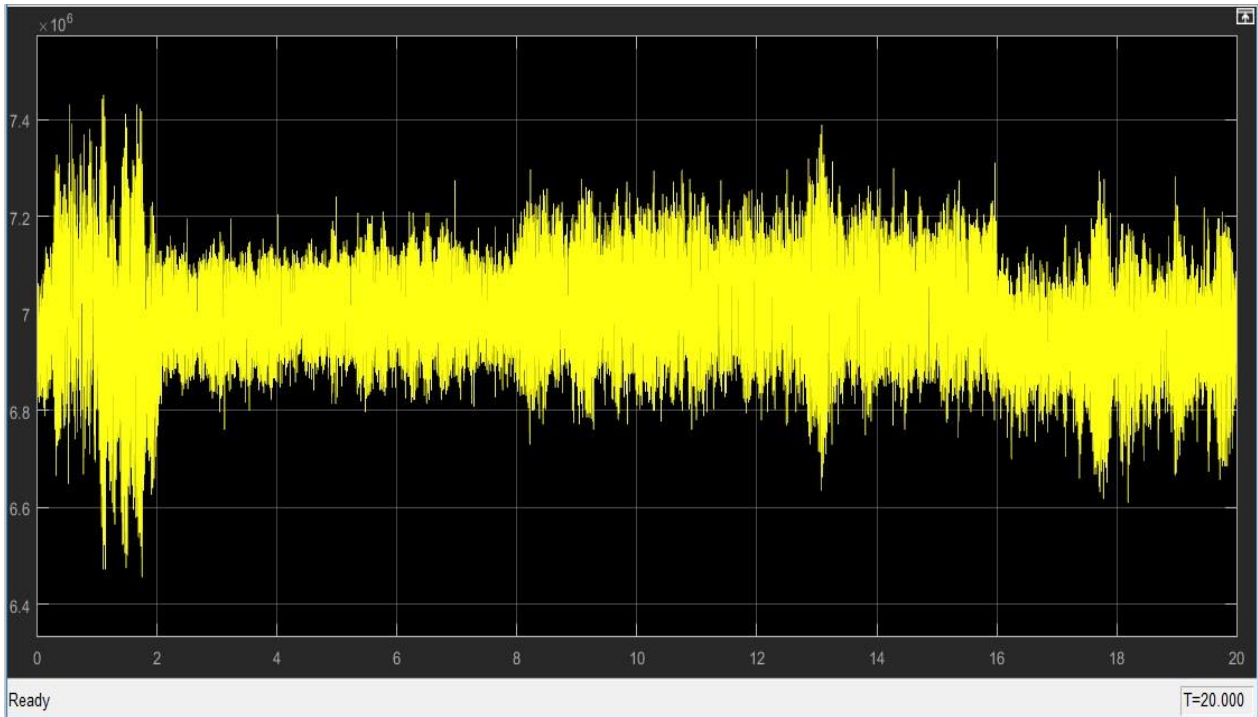


Figure 8.18: Reactive Power of the station in Stratos I for 0.8906 pu (in y-Axis M var and in x-Axis Time in Sec)

In Figure 8.18 I see the Reactive Power Q of the Hydropower Plant in Stratos I has same form as the figure of Active Power in Stratos I but with different amplitude and different values . I notice that the value is between 6.5 to 7.4 MVar in the first 2 seconds and for the rest of simulation is the peak to peak value is smaller 6.7 to 7.2 MVar but still with a lot of oscillations at each second.

8.2.1 PSS implementation in Stratos I HPP model

In the rest of this section I am going to check the same figures although this time with the implementation of the PSS stabilizer in Stratos I HPP model. The PSS stabilizer block is the same block as in the Kastraki HPP model (see Figure 8.8). Also the PSS stabilizer is placed in the same block path as in Kastraki HPP and connects the t excitation system block with the HTG block (see Figure 8.7).

I will present the figures to see the effect of using power system stabilizer on the system stability. I will notice the differences if there is any in the same figures after the implementation of the PSS stabilizer.

The output voltage and current of synchronous machine signals are the same as before (Figures 8.13 , 8.14) the implementation of the PSS Stabilizer block in the Stratos I HPP model in Simulink. The

stabilizer can only optimize the performance of the system stability but these two signals were already in their optimal version, so they are the same.

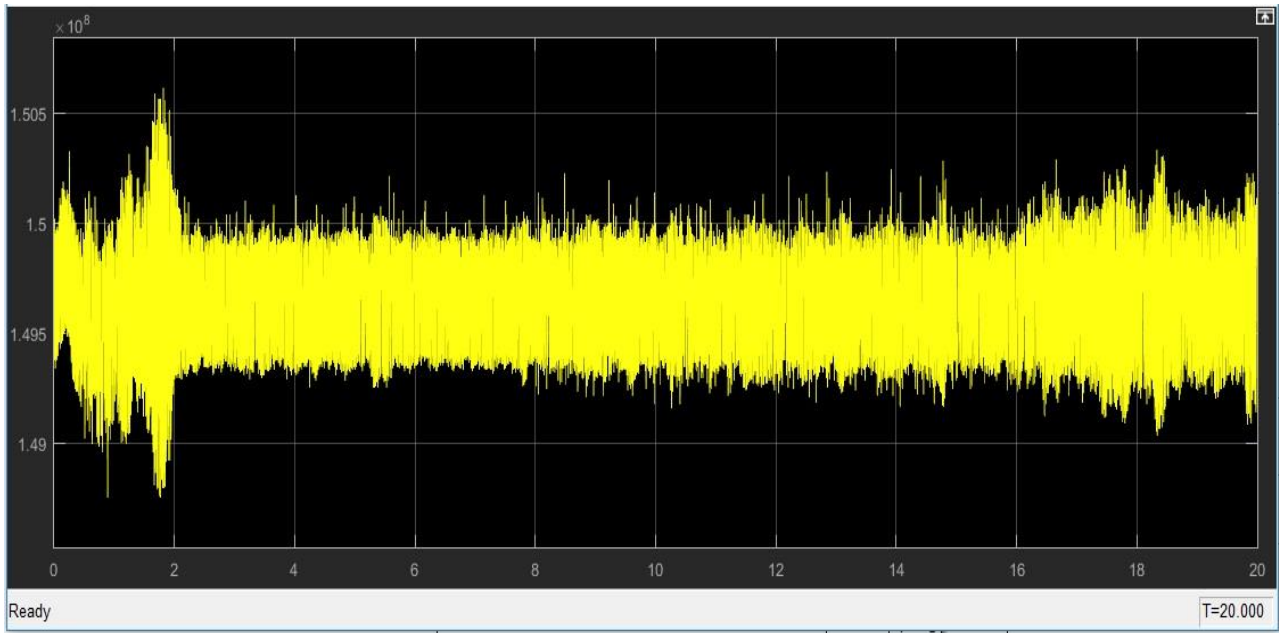


Figure 8.19: Output active power of the Hydropower Plant in Stratos I with PSS for 0.8906 pu (in y MW and in x-Axis Time in s)

In Figure 8.19 I notice that small difference before and after the implementation of the PSS stabilizer in the output active power. The values of the active power are 149.0 MW to 150.5 MW. This response in this Figure has big oscillations only in the first 1.7 to 2 s and after in time 2 s I have a steadier state as I see that the output active power remains stable at 149.5 to 150.0 MW. It is observed that the steady situation with lesser oscillations than the Stratos I HPP without the PSS is obtained around 16 s. This figure is better than Figure 8.15.

About the speed of each unit I see in the Figure 8.20 below from the characteristics, it is observed that the transient time is 6 s. After 3.8 s its speed reaches steady state at synchronous speed. With sudden application of mechanical torque input to the shaft of alternator, the load angle settles to a steady state value after few oscillations owing to system damping following the swing equation and power angle characteristics. Moreover, the governor settings ($K_p = 1.25387312$, $K_i = 0.13126167$, $K_d = -0.71356127$) chosen by the ZN method and error method helps to keep the speed near synchronous speed (1.0 pu). Also this figure is better than the Figure 8.15 because I see in Figure 8.16 that in 16 s I have again big oscillations like the start of the response until secs, but in Figure 8.20 I never see again big oscillations we have a far steadier state without almost any fluctuation

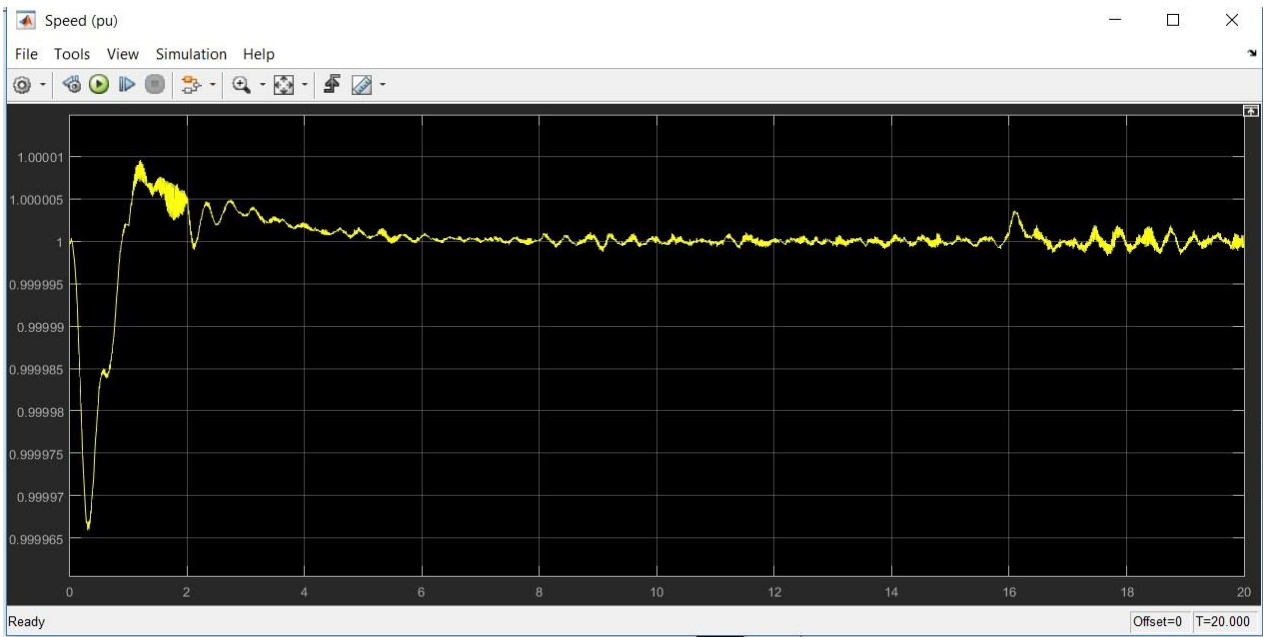


Figure 8.20: Synchronous Generator Speed Characteristics in Stratos I with PSS for 0.8906 pu (in y-Axis Speed in pu and in x-Axis Time in s)

In the Figure 8.21 below from the characteristics, it is observed that the transient time is 4 s. After 3 s its speed reaches steady state at excitation voltage. In the steady state it helps to keep the excitation voltage near the initial field voltage (1.42 pu). Also this figure is better than the Figure 8.17 because we see that in 4 s I have a stable condition without almost periodic big oscillations like the Figure 8.17 response.

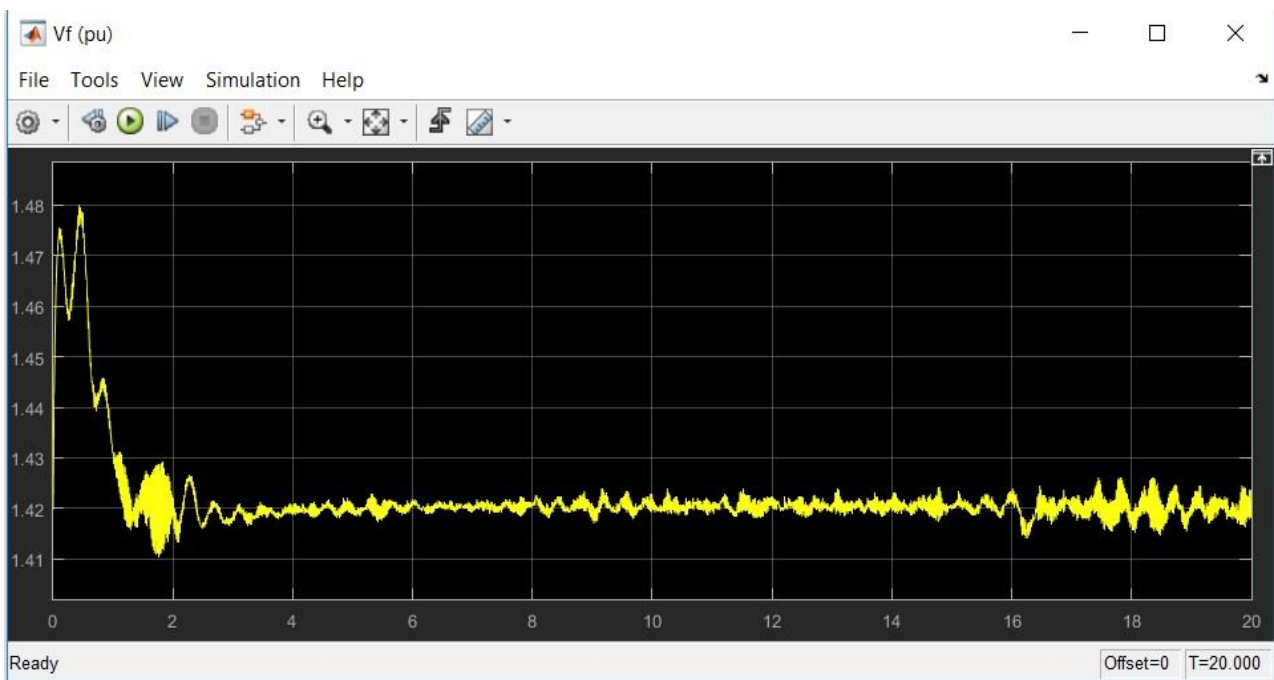


Figure 8.21: Excitation Voltage of Generator Speed in Kastraki with PSS for 0.8906 pu (in y-Axis Volts in pu and in x-Axis Time in s)

In the Figure 8.22 I notice a huge difference with the Figure 8.18. It shows that the reactive power characteristics complete its transient period in 8 seconds and steady state value achieved is 7 MVar in time 7 s and is obtained which matches the actual reactive load connected. Also this figure is better than the Figure 8.18.

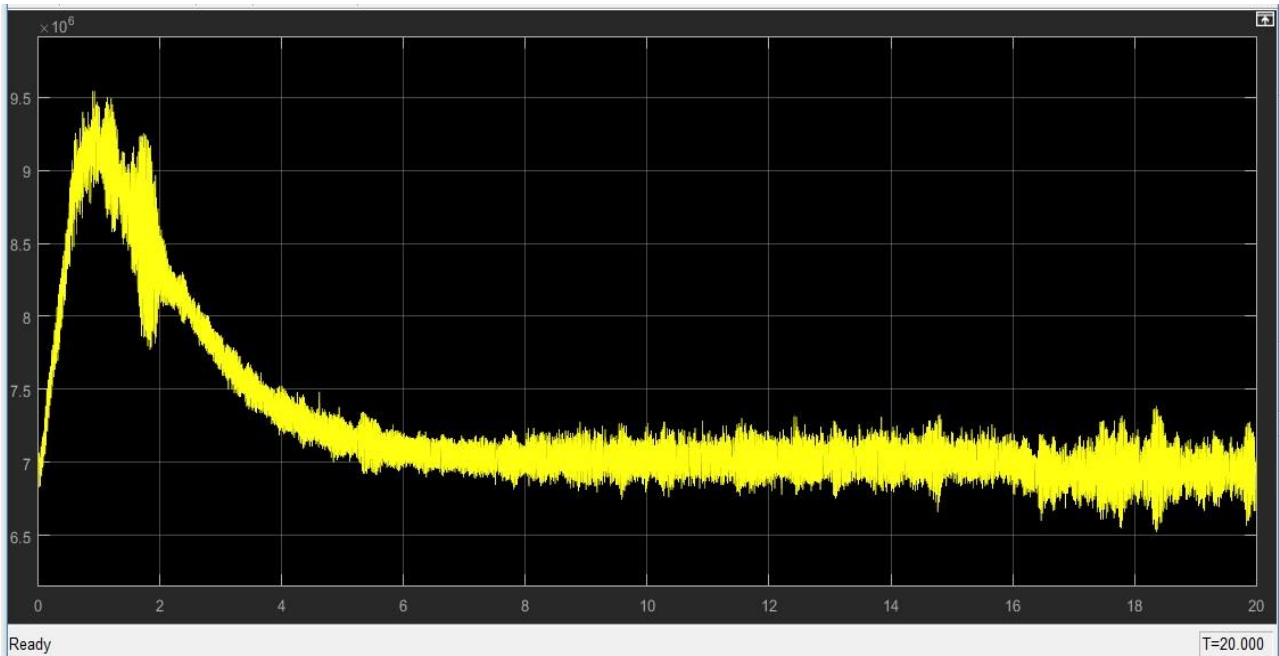


Figure 8.22: Reactive Power of the station in Stratos I with PSS for 0.8906 pu (in y-Axis M var and in x-Axis Time in s)

I understand here too as in Kastraki HPP simulations that the PSS stabilizer helps the HydroPower Plant of Stratos I reach its dynamic stability more quickly and in a more efficient way.

8.3 Conclusions about normal responses and PSS

I showed the models of the two HPP in Kastraki and in Stratos I. Later I tested with simulations to see if the systems have good dynamic stability. As I expected both in Stratos I and in Kastraki I observed good stable responses in the figures, because these two stations are two existent projects that I study for this thesis. So I tried to minimize the peak-peak values of the figures and to minimize the amplitude of the oscillation as possible it is. I managed with the implementation of a PSS stabilizer to see different results. Even these small optimizations can have benefits for the consumer of the produced energy and for the PPC S.A. In the figures of output voltage and I_{abc} current of each synchronous machines in both HPPs I didn't noticed differences before and after the PSS block as they were already optimal before because the PSS block doesn't affect them. About the speed and excitation voltage I see in both stations that after the PSS block i have better steady states with almost zero oscillation and I managed to eliminate the periodic repeats of the signal responses as I saw the station had in these two figures before the PSS block. In the case of Active Power and Reactive Power I see a little better results in Kastraki HPP as the oscillation of the Active Power in the steady state

after the PSS block have a peak-peak value less than 0.001 MW (1000 W) but in the Stratos I HPP the same value is 6000 W. In the reactive power the oscillation in the steady state after the PSS block have a peak-peak value less than 5000 Var but in the Stratos I HPP the same value is bigger than 6000 Var. So both in Active and Reactive powers I have optimizations after the PSS block in both of the 2 stations but in Kastraki HPP are a little sharper.

8.4 No controller in the HPPs

To understand the significance of the PID and PI governors I simulate the Stratos I HPP and Kastraki HPP models in Simulink without controllers. When no controller is used in turbine governor circuit, the electrical changes in output size of the system were obtained as a result of the simulation processed. Electrical quantities were measured as the signals of consumer total output power (watts), the terminal voltage (volts) and load current (amps).

8.4.1 Kastraki HPP with no controller

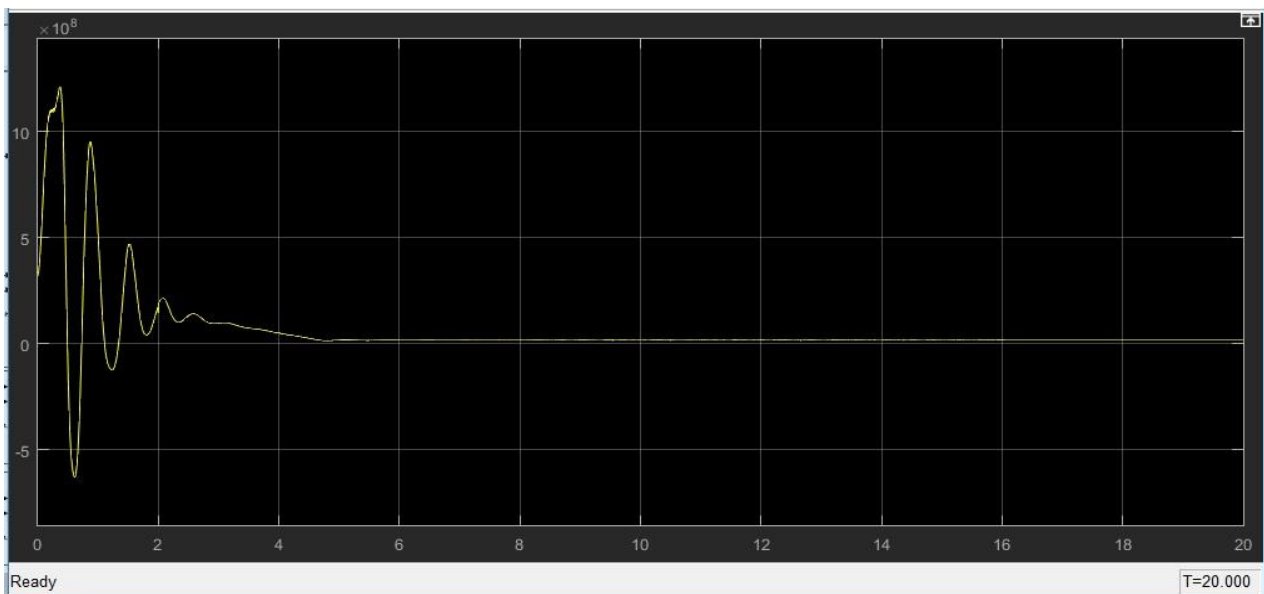


Figure 8.23: Change in electrical output power without controller in Kastraki HPP for 0.8866 pu

Each of the 4 synchronous generators did not meet the demanded power and as a result it was seen that system started to collapse after 2 seconds as the total output active power falls to zero MW, when the power generation system in Figure 8.23 in which the graphics were fed with 79.792 MW (0.8866 pu) at each unit. I expected the total active power to be 319.88 MW but this is not happening instead it is 0 MW definitively at 4.3 s.

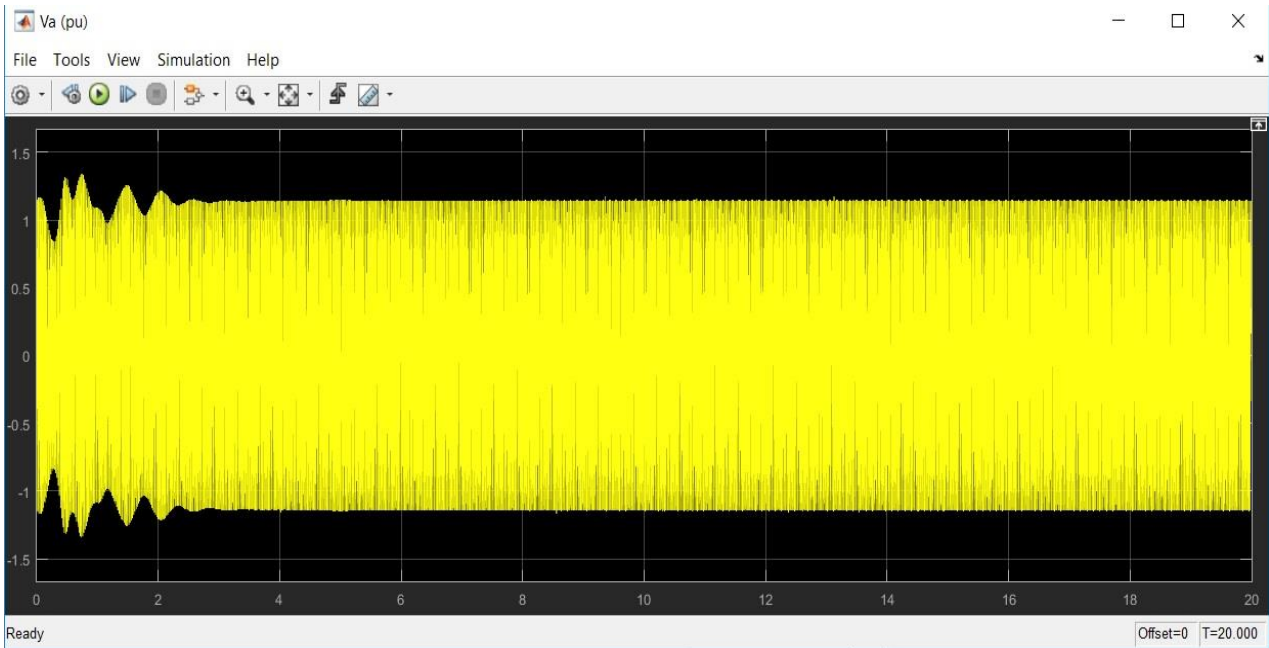


Figure 8.24: Change in output voltage without controller in Kastraki HPP for 0.8866 pu

The output or terminal voltage in the figure, has big oscillations until 2.6 s and later has a more stable form with peak to peak value -1.2 to 1.2 pu.

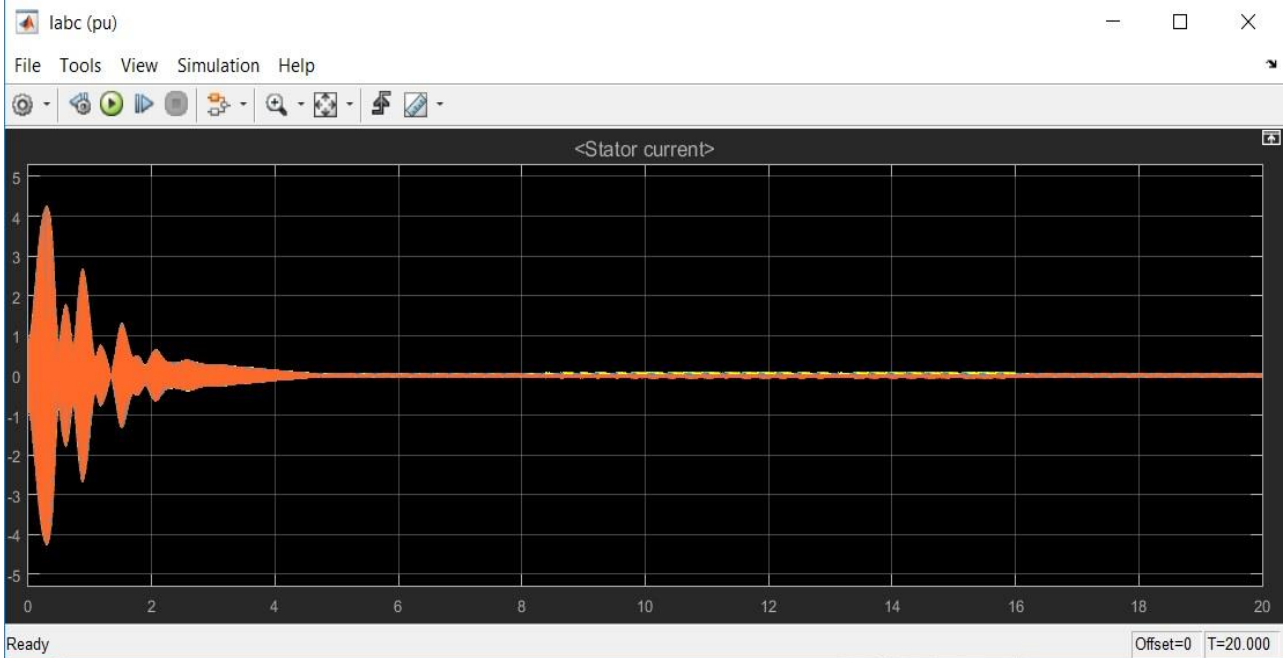


Figure 8.25: Change in stator current without controller in Kastraki HPP for 0.8866 pu

Likewise, in the case of total output power, the current of each synchronous machine in each unit of the four in the start is the duration of the first second the figure had peak value 4 pu. But in the 4 s of the simulation it seems that current I_{abc} has zero value.

8.4.2 Stratos I HPP with no controller

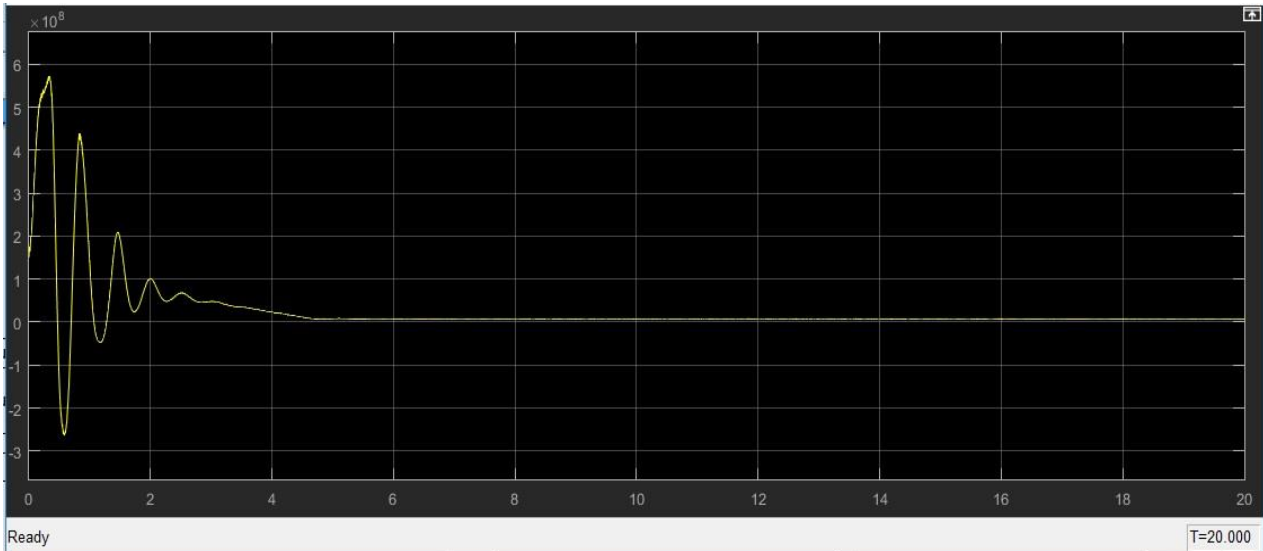


Figure 8.26: Change in electrical output power without controller in Stratos I HPP for 0.8906 pu

In Stratos I HPP each of the 2 synchronous generators obviously did not meet the demanded power and as a result it was seen that system started to collapse after 2 seconds as the total output active power falls to zero MW, when the power generation system in Figure 8.26 in which the graphics were fed with 79.792 MW (0.8866 pu) at each unit. I expected the total active power to be 319.88 MW but this is not happening instead it is 0 MW definitively 4.3 s.

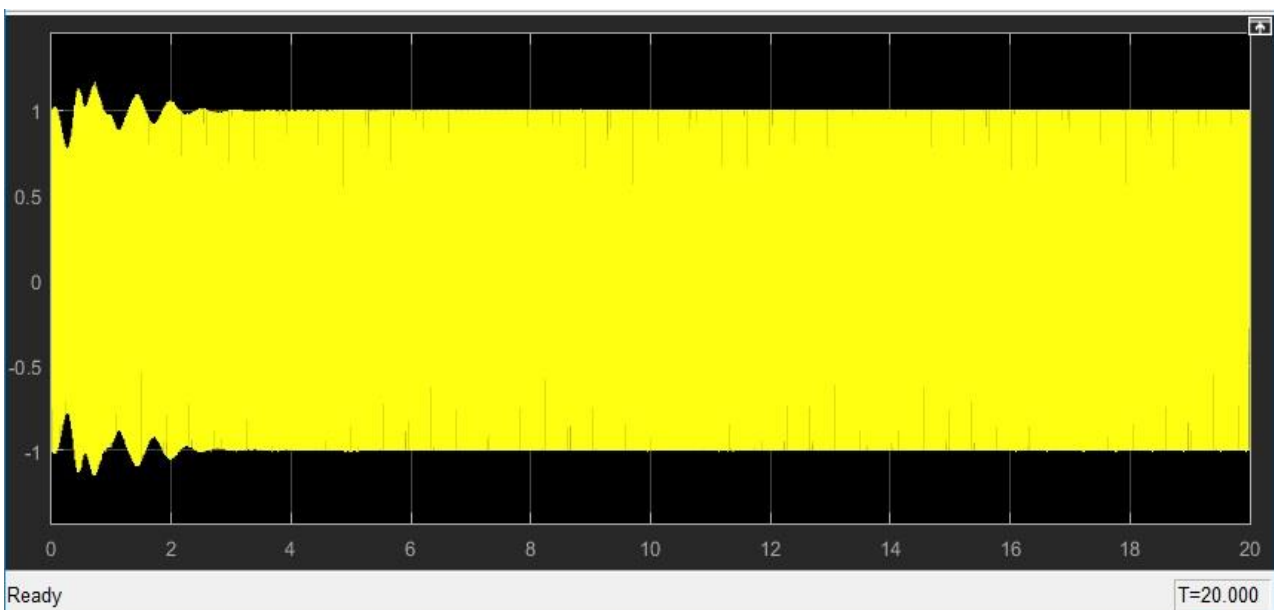


Figure 8.27: Change in output voltage without controller in Stratos I HPP for 0.8906 pu

The output or terminal voltage of Stratos I HPP in the Figure 8.27, has big oscillations until 2.5 s and later has a more stable form with peak to peak value -1.16 to 1.15 pu.

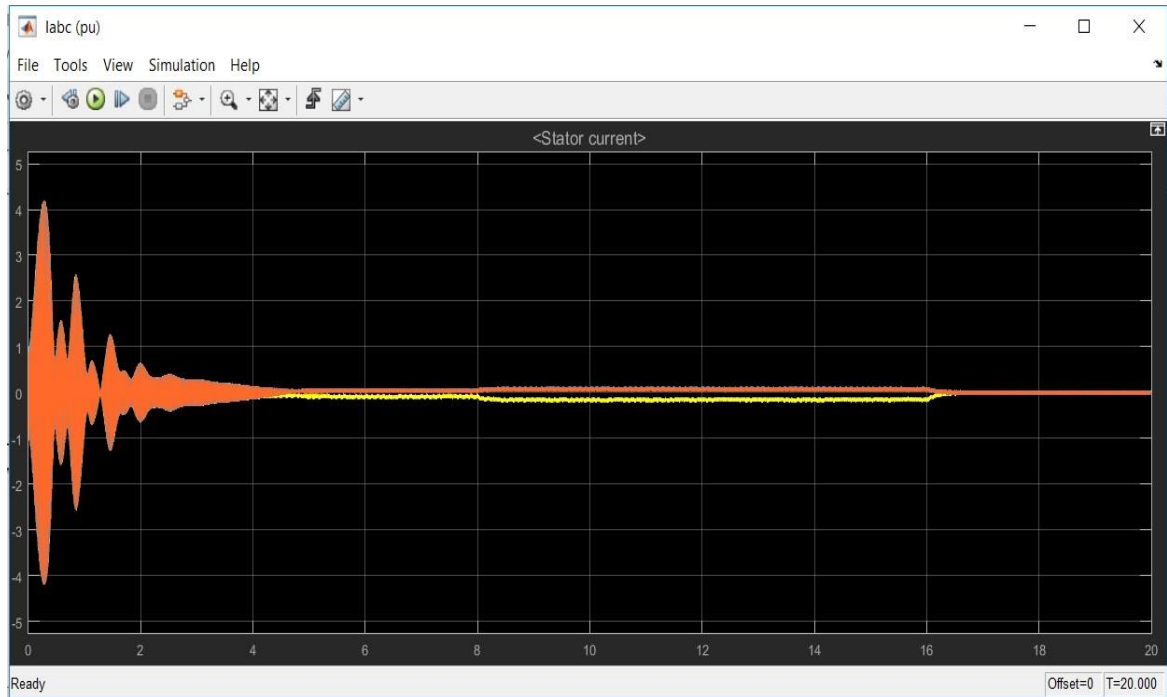


Figure 8.28: Change in stator current without controller in Stratos I HPP for 0.8906 pu

In Stratos I HPP in the case of total output power I observe in Figure 8.28, that the current of each synchronous machine in each unit of the two units in the start is the duration of the first second the figure had peak value 4.2 pu. But in the 4 s of the simulation it seems that current I_{abc} is decreased to the minimum value which is zero. Also I notice that the yellow color which represents one of the current phase of three phase current (3 colors, yellow, blue, red) is below zero from 8 s to 16 s.

8.4.3 Conclusions

The result of this analysis reads as running an uncontrolled power generation system is not possible, both in terms of business and use of clean energy by consumers. It is clear that the quality of the power generated in an uncontrolled system is out of question and will cost huge financial losses to customers and to PPC S.A. Also the frequency is decreased to the minimum value both in Kastraki HPP and Stratos I HPP. So I understand the value of controller in our governor and that for the good operation of a Hydropower Plant their existence is necessary.

8.5 Transient Stability Analysis and Simulations Tests

Transient (large disturbance) stability is the ability of the power system to maintain synchronism when subjected to a severe transient disturbance, such as a fault on transmission line or a load change. In the sections below I am trying to understand which controller is better the PI or the PID. Our

models in Simulink of our HPPs in Kastraki and Stratos I are going to pass through some simulation tests so as to understand their behavior of each one with PID and PI controller. These simulation tests are a three phase to ground fault in the three phase line, RLC (Agrinio power demand) increase, RLC (Agrinio power demand) decrease, and different power load values in the units. So I am going to see the 5 figures versus simulation time (output total active power of the station, output or terminal voltage of the station, excitation or field voltage of each unit of the station, rotor speed of each unit of the station and current of synchronous machine of each unit of the station). In this way the below sections constitute a comparison between PID and PI controller and a recording of these figures as I mentioned for each HPP with each controller (PI or PID).

I am trying to understand and compare which controller is better the PI or the PID. My models in Simulink of my HPPs in Kastraki and Stratos I are going to pass through some simulation tests so as to understand their behavior of each one with PID and PI controller.

These simulation tests are:

- A. a three phase to ground fault in the three phase line.
- B. RLC (Agrinio power demand) increase, decrease.
- C. and different power load values in the units.

In order to achieve this comparison, I use the following 5 figures versus simulation time

1. output total active power of the station
2. output or terminal voltage of the station.
3. current of synchronous machine of each unit of the station.
4. rotor speed of each unit of the station.
5. excitation or field voltage of each unit of the station,

Important Clarification : If the RLC load between the transformer and the infinite bus changes (increase or decrease) i.e. the demand of power from Agrinio area changes it doesn't mean that automatically each unit of the HPP has the needed load to cover the demand. For example, in case of Katsraki HPP which has 4 units each of them can produce almost 80 MW (maximum production). If the demand in a certain hour is 40 MW and changes to 80 MW it doesn't mean that the unit in the next seconds produce that amount of active power. As Mr. Georgios Lappas (Electrical Engineer in PPC S.A. in Kastraki and Stratos I) when the demand of Agrinio area changes it take a little time to change the load of each turbine because the load changes are made from PPC S.A. in Athens. So when we say that I am going to examine the behavior of the HPP with PI or PID when the RLC load changes, I am mentioning to this case I described earlier.

In electrical engineering and mechanical engineering, a transient response or natural response is the response of a system to a change from an equilibrium or a steady state. The transient response is not necessarily tied to "on/off" events but to any event that affects the equilibrium of the system. The events incurred by the system and are useful for us for the recording of the behavior of our stations are the fault in the three phase line of the transmission, the RLC increases and decreases and the load changes in our units. The impulse response and step response are transient responses to a specific input (an impulse and a step, respectively).

8.6 Three Phase Fault

A three-phase fault is applied at $t=10.1$ s and removed at $t=10.2$ s. After computing the power flow, time-domain simulations show the models responses in Simscape Power Systems. The three-phase fault block in Simulink represents a disturbance which is possible to occur in the three phase line in our stations. The time that is needing to return my power generating systems in the proper situation before the fault is very important and one of the characteristics that determine the reliability of the Hydropower Plants.

8.6.1 Kastraki HPP in Three Phase Fault case

I present the figures of Kastraki HPP for the 4 simulations tests with PID and PI controller. A three phase short circuit fault was introduced into the HPP model in order to determine the response of the system during and after fault conditions and how effectively the entire system network can regain its stability after the three phase fault occur.

8.6.1.1 PID controller in Kastraki HPP in Three Phase Fault case

The PID coefficients for the below simulations in the case of a fault from the ZN method are $K_p = 1.99686681$, $K_i = 0.14315631$, $K_d = -1.2251305837$ for load 0.8866 pu. These are the data for Kastraki HPP with PID.

Table 8.2 PID coefficients in Kastraki HPP for 0.9 pu

K_p	K_i	K_d
1.99686681	0.14315631	-1.2251305837

A close look at the graphs provided in Figures 8.30, 8.32 and 8.33 respectively show that before the introduction of the fault, the system was in steady state with nominal speed of 1 pu, an output voltage of amplitude 1.1 pu and an excitation voltage of about 1.5 to 2 pu. The fault lasted for about 0.1 s, that is from 10.1 s to 10.2 s and during the fault there was a significant drop in the output voltage which became 0.4-0.5 pu in amplitude. In addition, the excitation voltage in Figure 8.33 increased highly to an average of 11.5-12 pu and the speed also increased slightly to 1.01 pu. The increase in the excitation voltage is a very positive response of the system vis-a-vis the fault because it leads to an increase in the flux value which further relates to the induced voltage by the famous equation

$$E = k\Phi n \quad (8.1)$$

Where:

- k is a constant related to the machine.
- Φ is the flux per pole.
- n is the speed.

In the equation 8.1, it can be seen that the induced voltage is proportional to the flux and therefore an increase in flux will have the effect of bringing the voltage back to its previous value as it was highly reduced by the fault. To achieve more increase in the induced voltage the speed can also be increased

and this is controlled by the governor from the opening and closing of wicket gates. But, the increase in speed in Figure 8.32 did not yield a big change as it can be observed that the increase was only about 0.01 pu due to the fact that it is dependent on the availability of the flowing water. Furthermore, after the fault was removed at $t=10.2$ s, the system of Kastraki HPP quickly regain stability with an output voltage of 1 pu which is equivalent to the previous steady state value. Automatically the excitation voltage drops and continues with oscillations in order to maintain the output voltage constant. It can also be realized that the speed also oscillates around an average value of 1 pu. The oscillations of the speed took longer time to stabilize as compared to the ones of the voltage and this may be due to the rate of valve opening/closing in the governor system.

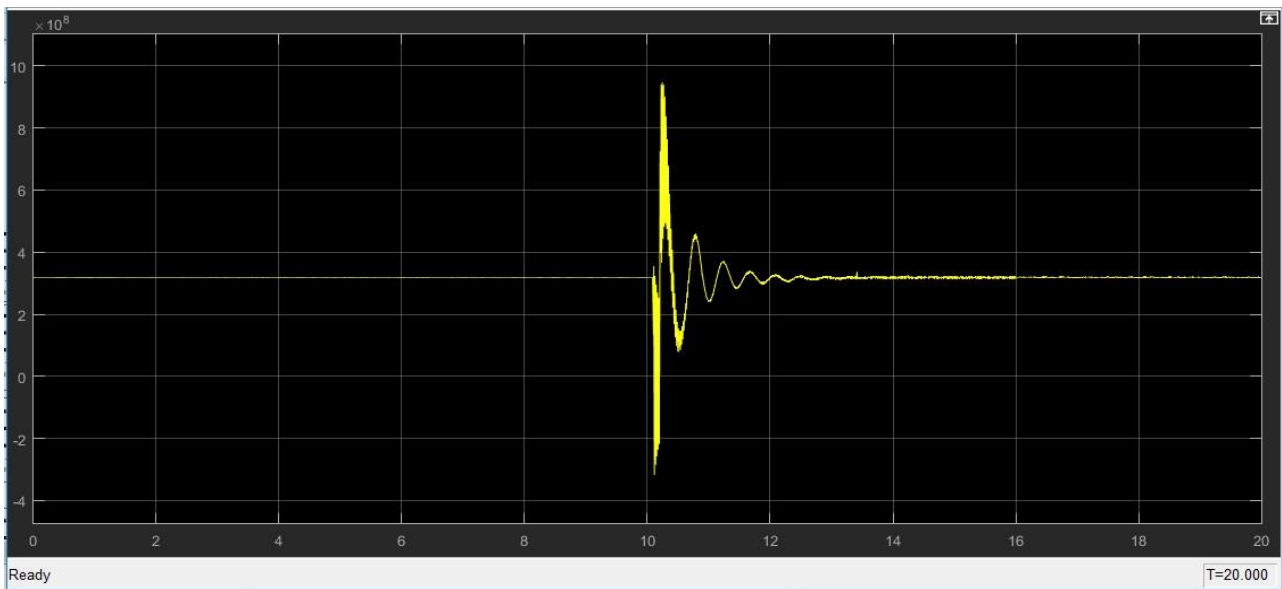


Figure 8.29: Output active power of the Hydropower Plant in Kastraki with transmission line fault at 10.1 s with PID for 0.8866 pu (in y MW and in x-Axis Time in s)-A1

When occurs the fault in time 10.1 s in Kastraki HPP with PID, the output active power of the station decreases from 3.2 to $-2.8 e^8$ W and then the highest peak is to $9.8 e^8$ W and comes again to the 80% of steady state at 12.2 s and the transient time is after the breaker switch is the period 13 s.

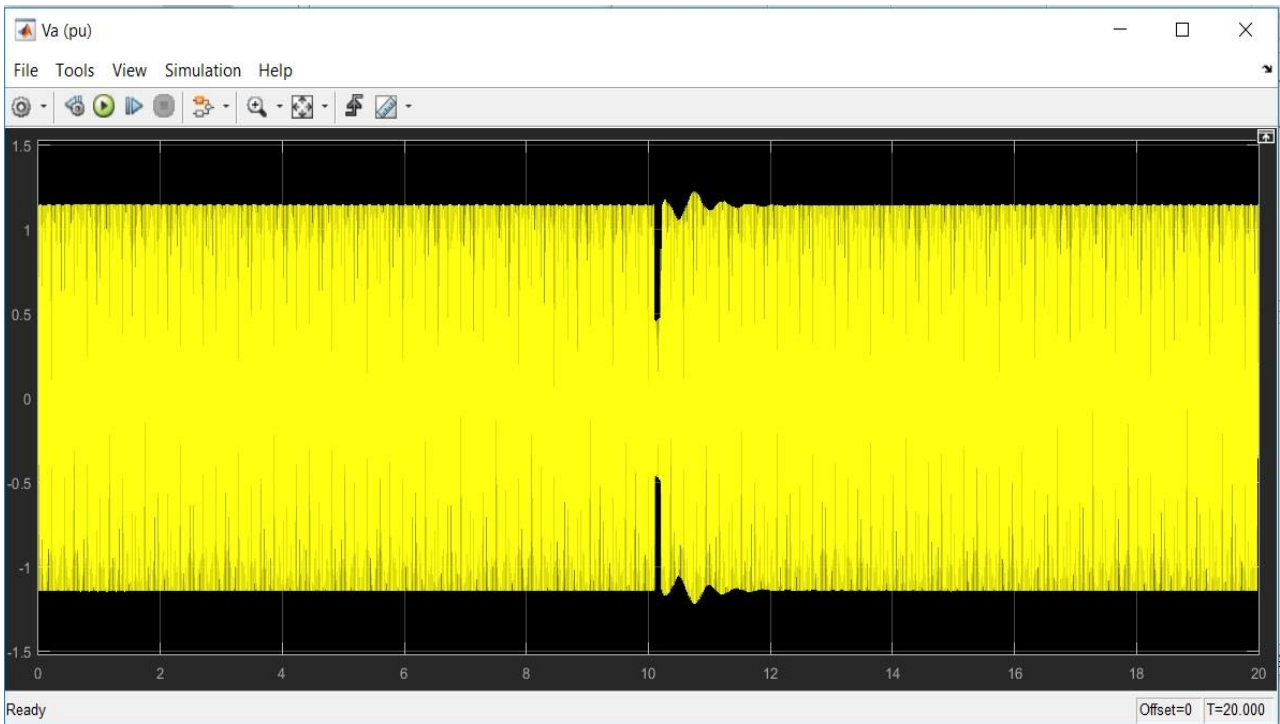


Figure 8.30: Output Voltage Characteristics of Kastraki station with transmission line fault at 10.1 s with PID for 0.8866 pu (in y-Axis pu Voltage in Volt and in x-Axis Time in s)-A2



Figure 8.31: Stator Three Phase Current Characteristics of Hydro Power Plant in Kastraki with transmission line fault at 10.1 s with PID for 0.8866 pu (in y pu and in x-Axis Time in s)-A3

It is observed that when the fault occurs at 10.1 s the current of stator increases highly at 4.5 pu, the value falls 0.4 pu at 10.5 s and after that starts immediately to rise so as to come back in steady state of 1 pu at 12.3 s.

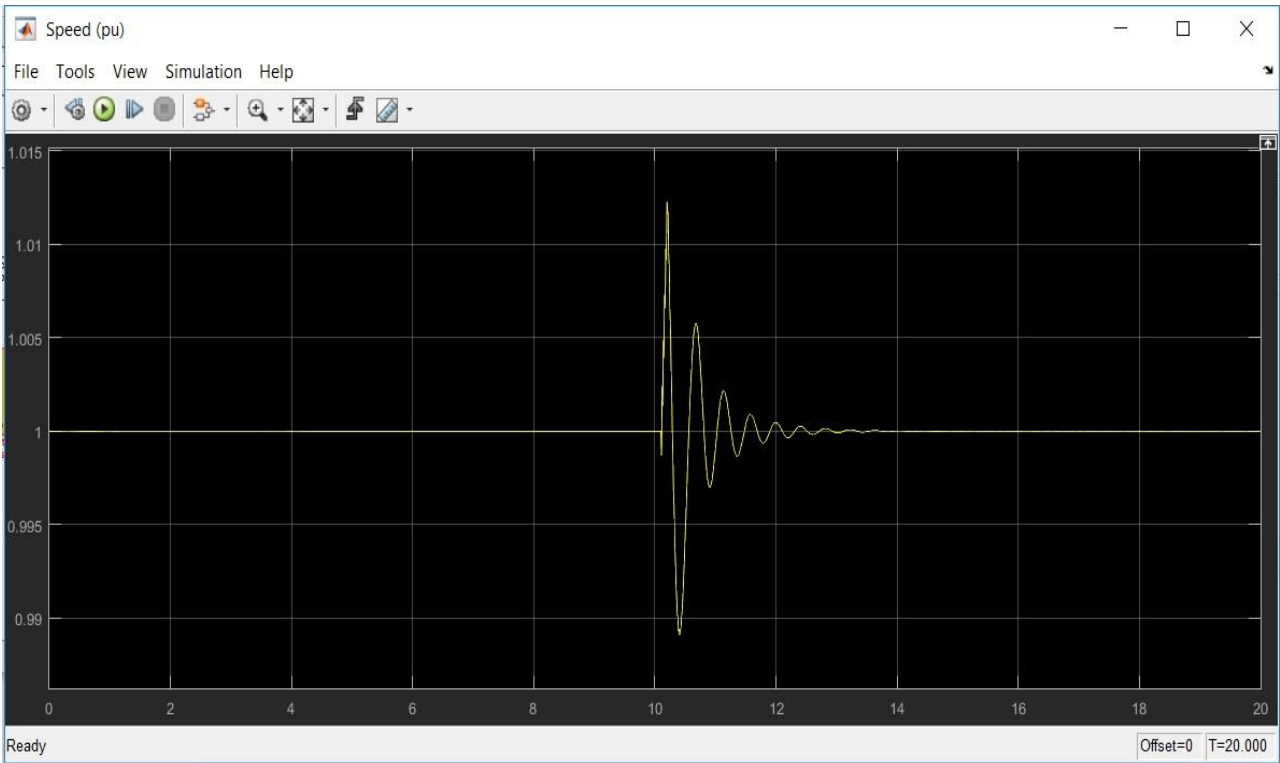


Figure 8.32: Synchronous Generator Speed Characteristics in Kastraki HPP with transmission line fault at 10.1 s with PID for 0.8866 pu (in y-Axis Speed in pu and in x-Axis Time in s)-A4

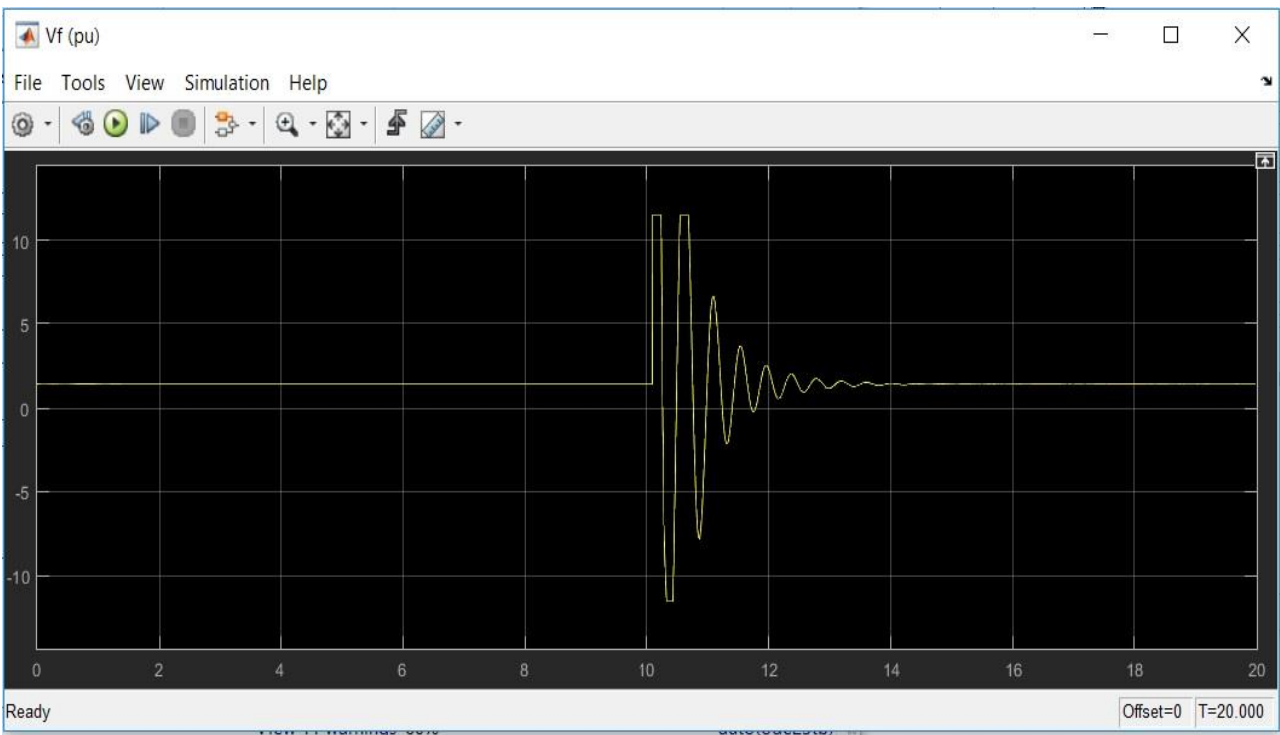


Figure 8.33: Excitation Voltage of Generator Speed in Kastraki HPP with transmission line fault at 10.1 s with PID for 0.8866 pu (in y-Axis Volts in pu and in x-Axis Time in s)-A5

8.6.1.2 PI controller in Kastraki HPP in Three Phase Fault case

The PI coefficients for the below simulations from the ZN method and table 7.1 are $K_p = 1.497650108$, $K_i = 0.23859385$ for load 0.8866 pu. These are the data for Kastraki HPP with PI.

Table 8.3 PI coefficients in Kastraki HPP for 0.9 pu

K_p	K_i
1.497650108	0.23859385

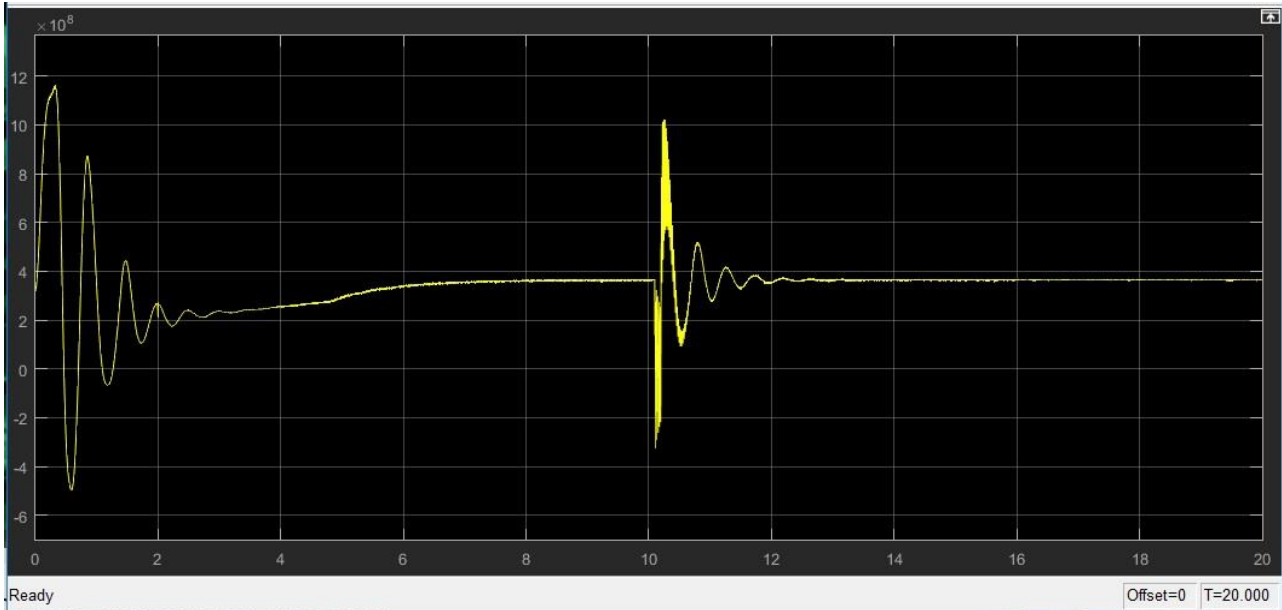


Figure 8.34: Output active power of the Hydropower Plant in Kastraki with transmission line fault at 10.1 s with PI for 0.8866 pu (in y MW and in x-Axis Time in Sec)-A1

In the start of the simulation I have oscillations for the reason I use PI controller for a period 0-6.8 s. When occurs the fault in time 10.1 s in Kastraki HPP with PI, the output active power of the station decreases from 4 to -3×10^8 W and then the highest peak is to 10.1×10^8 W and comes again to the 80% of steady state at 12 s and the transient time is after the breaker switch is the period 12.5 s.

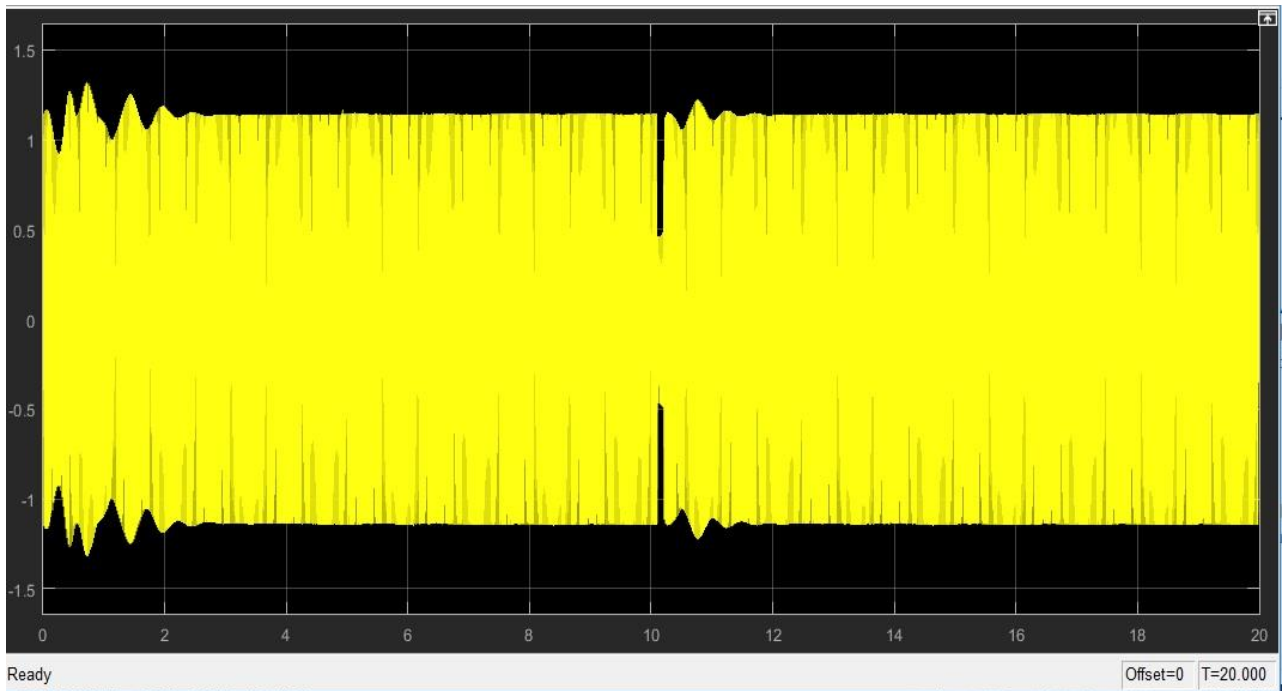


Figure 8.35: Output Voltage Characteristics of Kastraki station with transmission line fault at 10.1 s with PI for 0.8866 pu (in y-Axis pu Voltage in Volt and in x-Axis Time in s)-A2

The output or terminal voltage in the case of Kastraki model with PI controller the system was in steady state from 2.3 to 10.1 s with an output voltage of amplitude 1.1 pu. The fault lasted for about 0.1 s, that is from 10.1 s to 10.2 s and during the fault there was a significant drop in the output voltage which became 0.4 - 0.5 pu in amplitude.

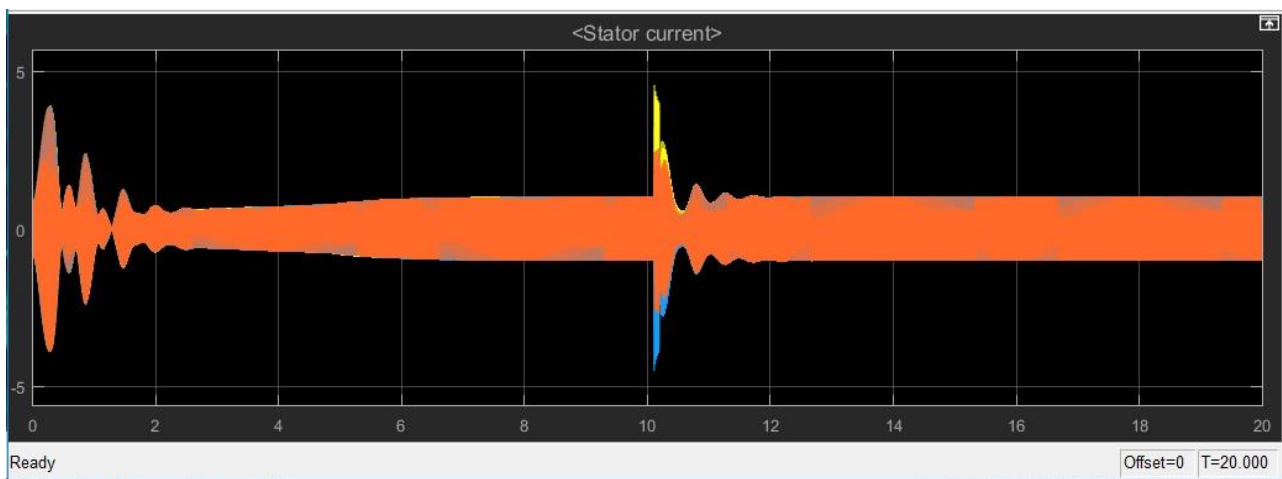


Figure 8.36: Stator Three Phase Current Characteristics of Hydro Power Plant in Kastraki with transmission line fault at 10.1 s with PI for 0.8866 pu (in y pu and in x-Axis Time in s)-A3

I can notice that when the fault occurs at 10.1 s the current of stator increases highly at 4.8 pu, the value falls 0.4 pu at 10.5 s and after that starts immediately to rise so as to come back in steady state of 1 pu at 12.1 s.

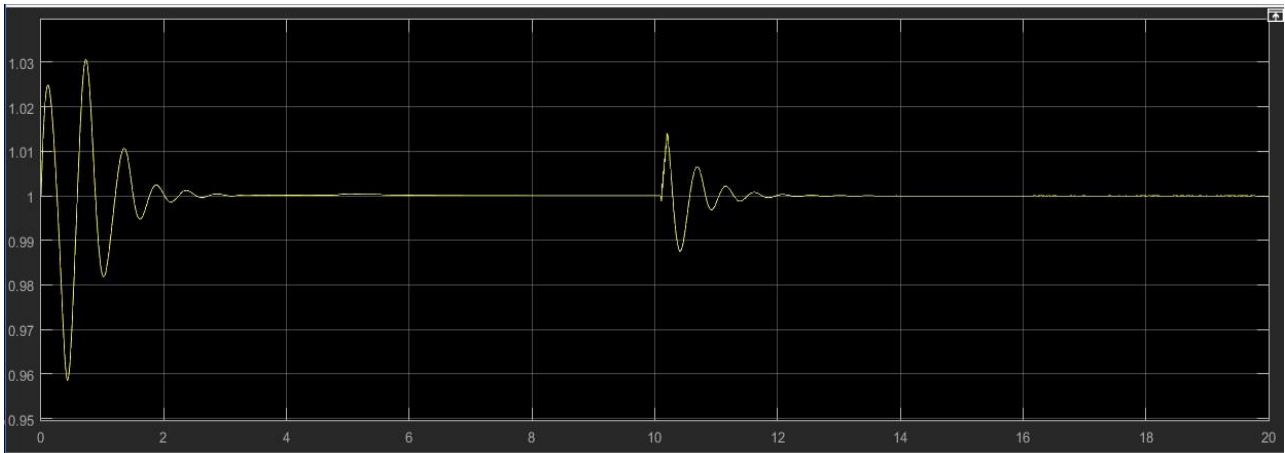


Figure 8.37: Synchronous Generator Speed Characteristics in Kastraki HPP with transmission line fault at 10.1 s with PI for 0.8866 pu (in y-Axis Speed in pu and in x-Axis Time in s)-A4

The fault occurred and I see in the Figure 8.37 of the rotor speed that in the start of the simulation I have oscillations until the time of 2.3 seconds then the response is in steady state. The value increases to 1.015 pu. The 80% of steady state comes at 11.8 s and the transient time is 12.3 s.

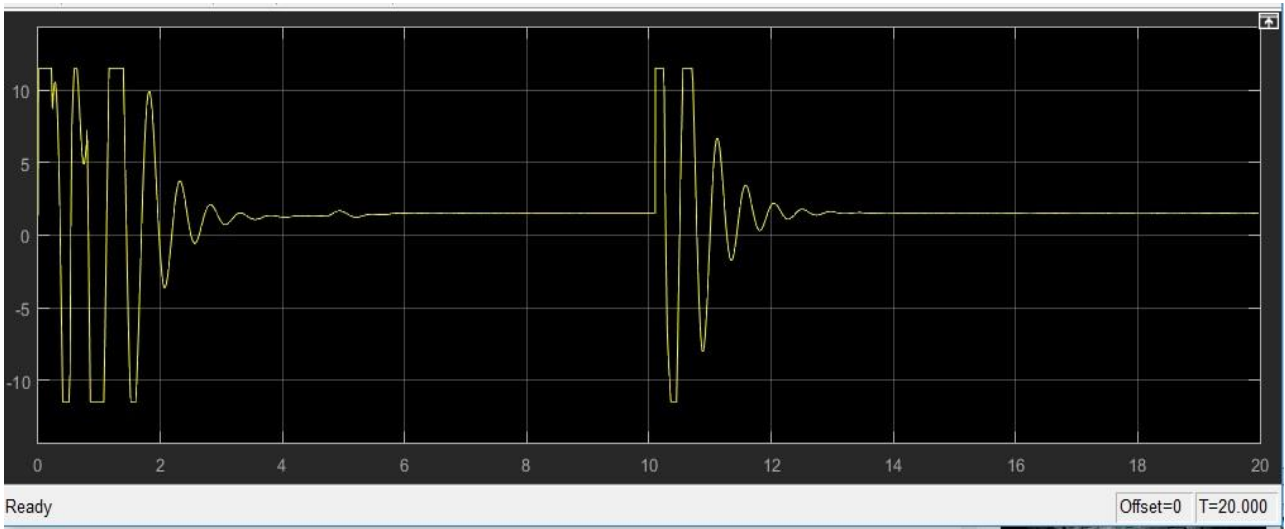


Figure 8.38: Excitation Voltage of Generator Speed in Kastraki HPP with transmission line fault at 10.1 s with PI for 0.8866 pu (in y-Axis Volts in pu and in x-Axis Time in s)-A5

In Figure 8.38 the response of the excitation voltage in each unit in Kastraki HPP station with PI I see that the implementation of the fault changes the signal of the response. I have some oscillations in the beginning in the simulation 0 to 3.8 s. The 80% of steady state comes at 3.8 s and the transient time is at 5.2 s.

8.6.2 Stratos I HPP in Three Phase Fault case

To analyze the simulation results of model of Stratos I HPP in Simulink, five graphs have been plotted:

- the speed characteristic.
- the output voltage characteristic.
- the excitation voltage.
- the output active power.
- the current characteristic of the synchronous machine with respect to time.

The reliability of the hydropower plant can only be tested by the plant's capacity of overcome fault quickly and effectively. For this matter I introduced a short-circuit fault into the system in order to analyze its response and conclude on the reliability. The fault, also known as three phase to ground fault [22] was introduced at a time $t=10.1$ s as I did in Kastraki station case.

8.6.2.1 PID controller in Stratos I in Three Phase Fault case

The PID coefficients for the below simulations from the ZN method are $K_p=1.25387312$, $K_i=0.13126167$, $K_d=-0.71356127$ for load 0.8905 pu. These are the data for Stratos I HPP with PID.

Table 8.4 PID coefficients in Stratos I HPP for 0.9 pu

K_p	K_i	K_d
1.25387312	0.13126167	-0.71356127

The simulation time for all the models is 20 s. Figures 8.43, 8.42, 8.41 and 8.40 present the waveforms of the excitation voltage (V_f) with respect to time in per unit, the speed of the rotor, the stator currents (I_{abc}) of the generator and the generated voltage (V_a) respectively. A three phase to ground fault was introduced into the model at a time of 10.1 s. It was observed from the graphs in Figures 8.43, 8.42, 8.41 and 8.40 the system experienced a steady state condition at the initial stage of the simulation with excitation voltage of 1 to 1.3 pu, an output voltage of about 1 pu, the nominal speed of amplitude of 1 pu and the stator currents of about 0.8 to 1.2 pu. A three phase fault was rotor become unstable during and after the introduction of three phase fault whereas excitation voltage returns to stable state after a long period at 12.2 s.

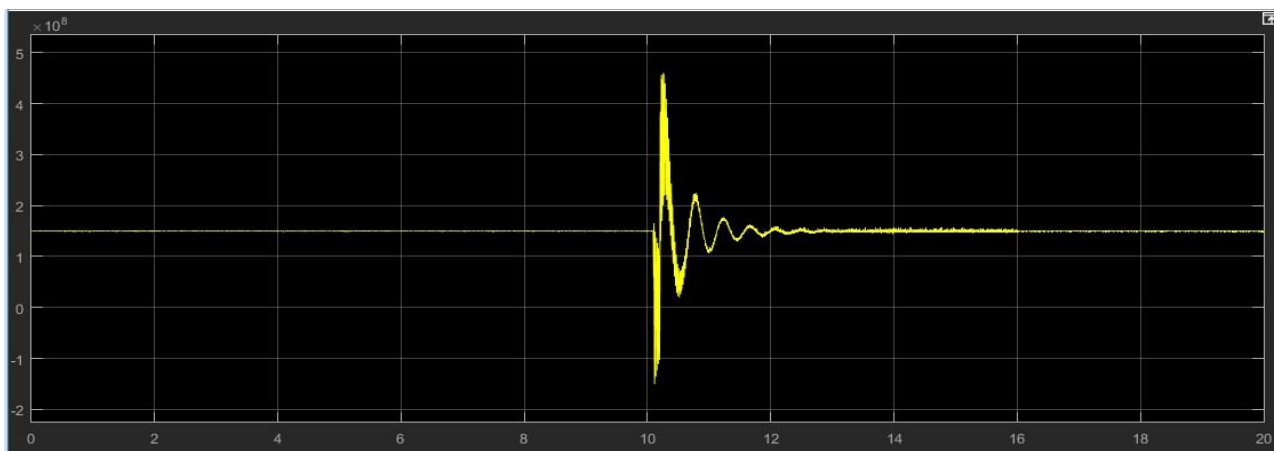


Figure 8.39: Output active power of the Hydropower Plant in Stratos I with transmission line fault at 10.1 s with PID for 0.8906 pu (in y MW and in x-Axis Time in s)-A1

When occurs the fault in time 10.1 s in Stratos I HPP with PID, the output active power of the station decreases from 1.5 to $-1.3 e^8$ W and then the highest peak is to $4.5 e^8$ W and comes again to the 80% of steady state at 12.2 s and the transient time is after the breaker switch is the period 12.8 s.

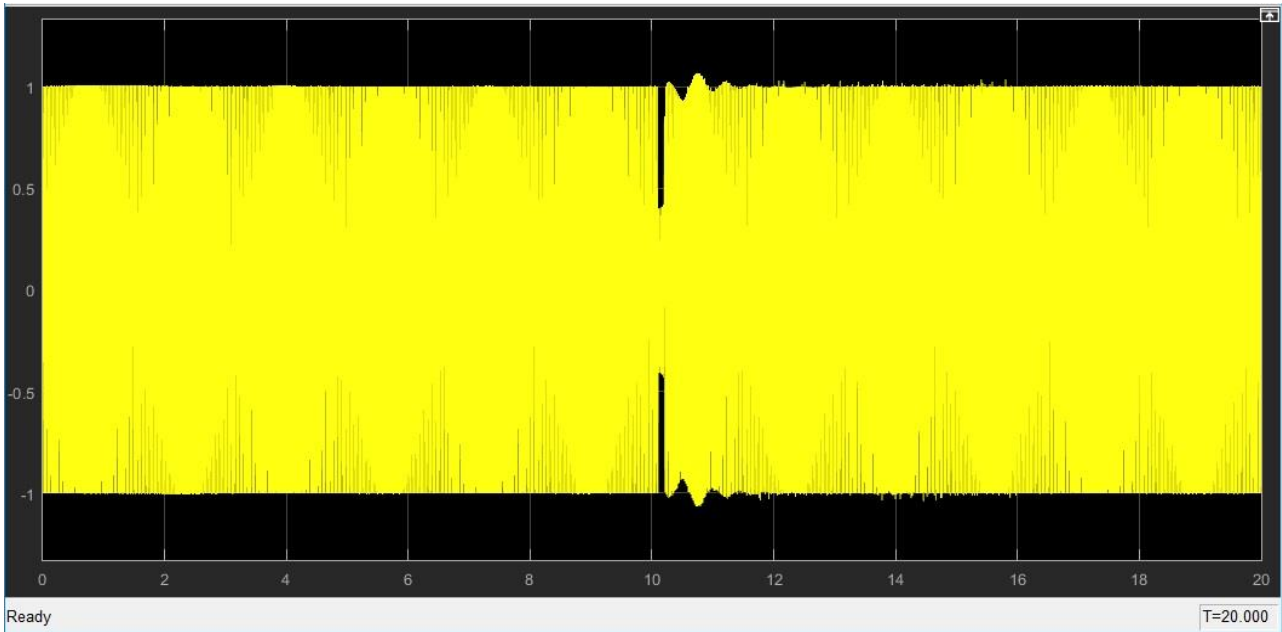


Figure 8.40: Output Voltage Characteristics of Stratos I station with transmission line fault at 10.1 s with PID for 0.8906 pu (in y-Axis pu Voltage in Volt and in x-Axis Time in s)-A2

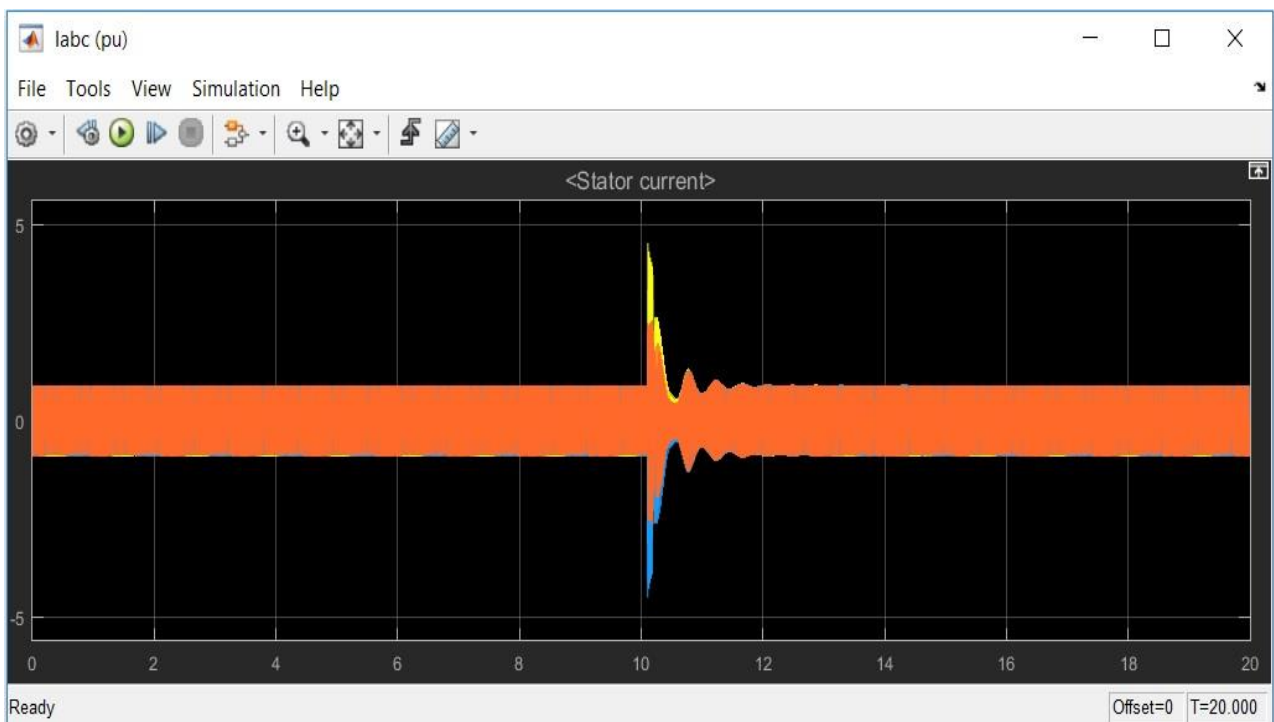


Figure 8.41: Stator Three Phase Current Characteristics of Hydro Power Plant in Stratos I with transmission line fault at 10.1 s with PID for 0.8906 pu (in y pu and in x-Axis Time in s)-A3

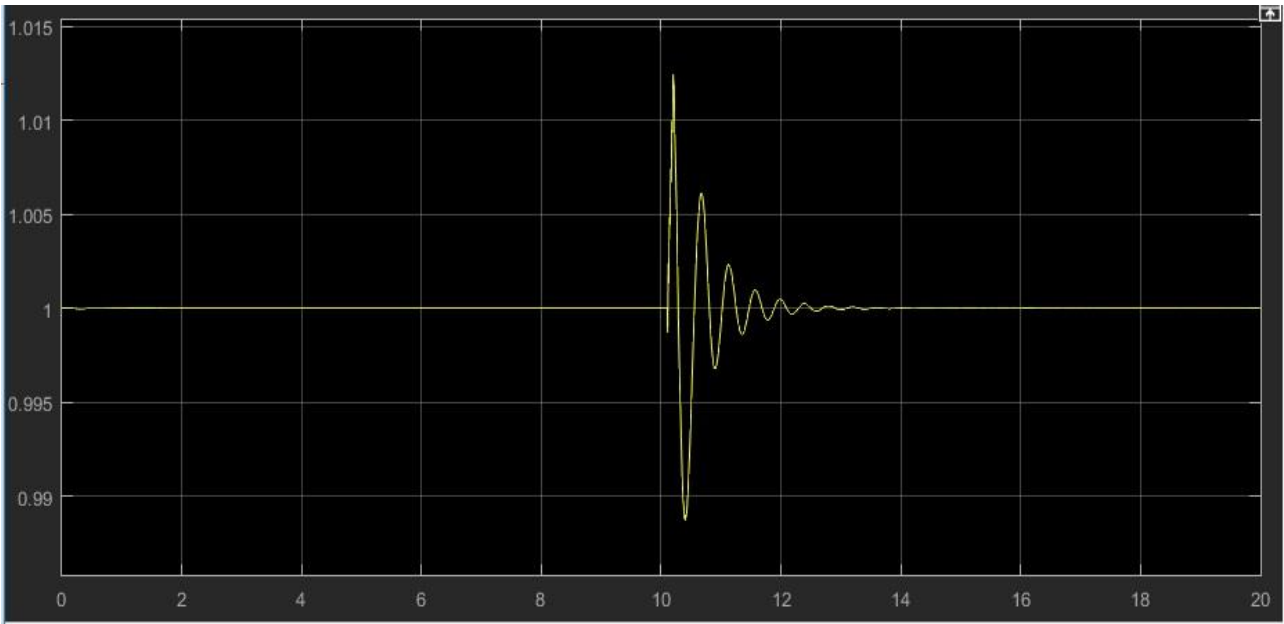


Figure 8.42: Synchronous Generator Speed Characteristics in Stratos I with transmission line fault at 10.1 s with PID for 0.8906 pu (in y-Axis Speed in pu and in x-Axis Time in s)-A4

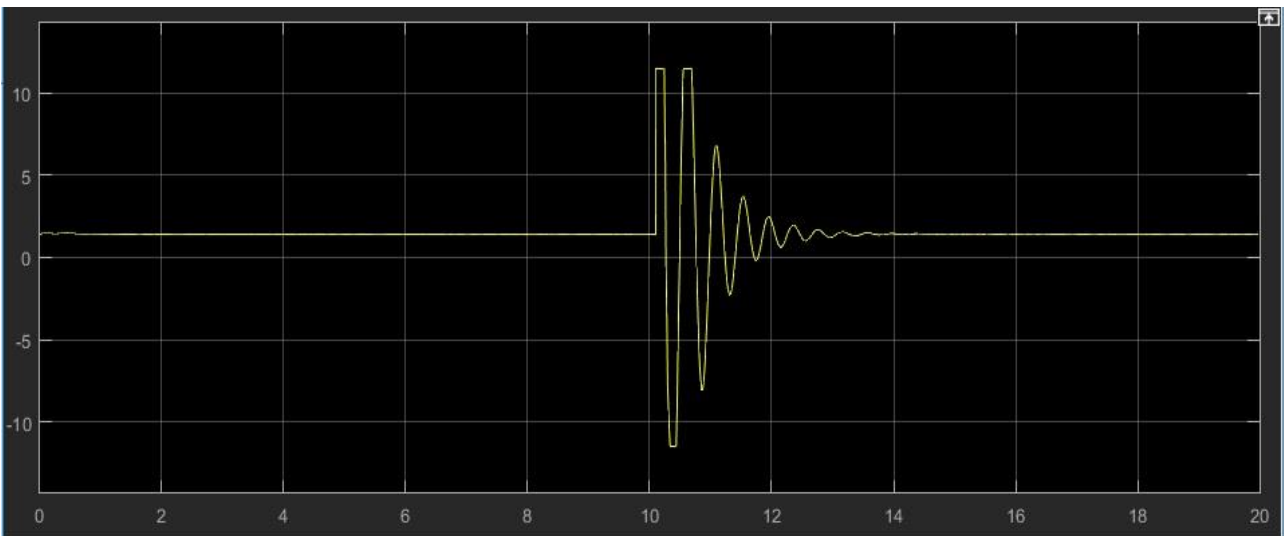


Figure 8.43: Excitation Voltage of Generator Speed in Stratos I HPP with transmission line fault at 10.1 s with PID for 0.8906 pu (in y-Axis Volts in pu and in x-Axis Time in s)-A5

8.6.2.2 PI controller in Stratos I HPP in Three Phase Fault case

The PI coefficients for the below simulations from the ZN method and the 7.1 are $K_p = 0.94040484$, $K_i = 0.52504668$ for load 0.8905 pu. These are the data for Stratos I HPP with PI

Table 8.5 PI coefficients for 0.9 pu

K_p	K_i
0.94040484	0.52504668

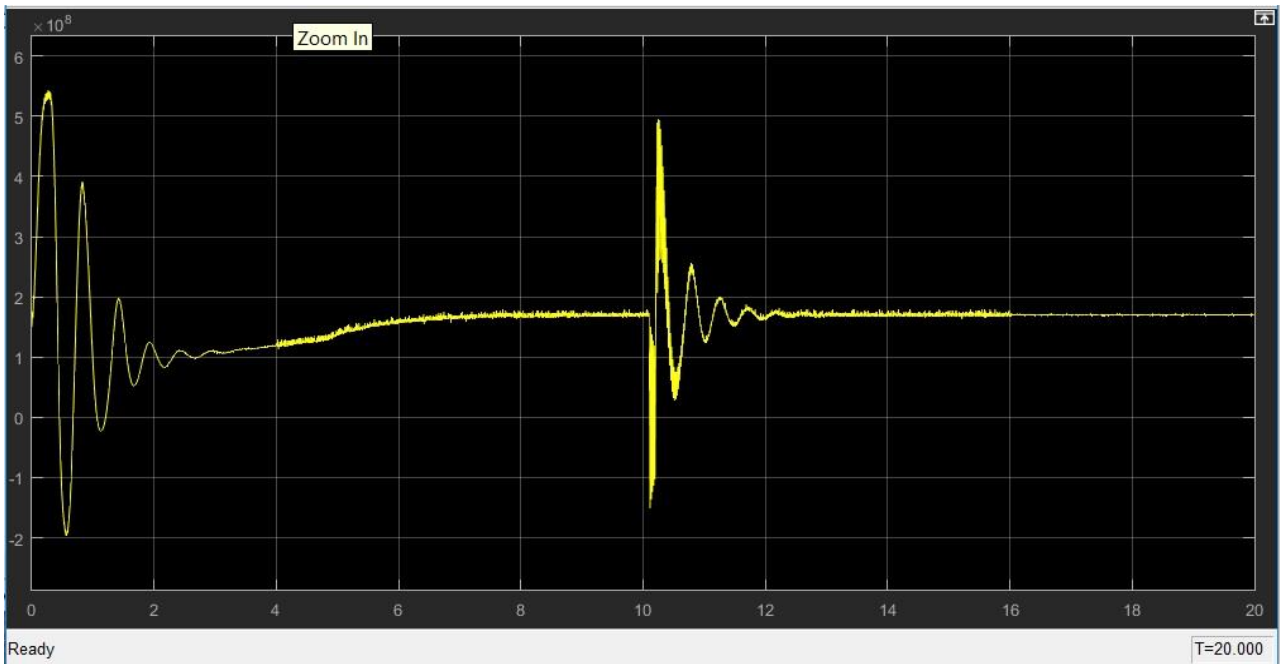


Figure 8.44: Output active power of the Hydropower Plant in Stratos I with transmission line fault at 10.1 s with PI for 0.8906 pu (in y MW and in x-Axis Time in s)-A1

In the Figure 8.44 I am presenting the output voltage of the Stratos I HPP. In the start of the simulation I have oscillations for the reason I use PI controller for a period 0 to 6.6 seconds. When occurs the fault in time 10.1 s, the output active power of the station decreases from 4 to $-3 e^8$ W and then the highest peak is to 10.1 e^8 W and comes again to be 80% of steady state at 12 seconds and the transient time is after the breaker switch is the period 12.5 s.

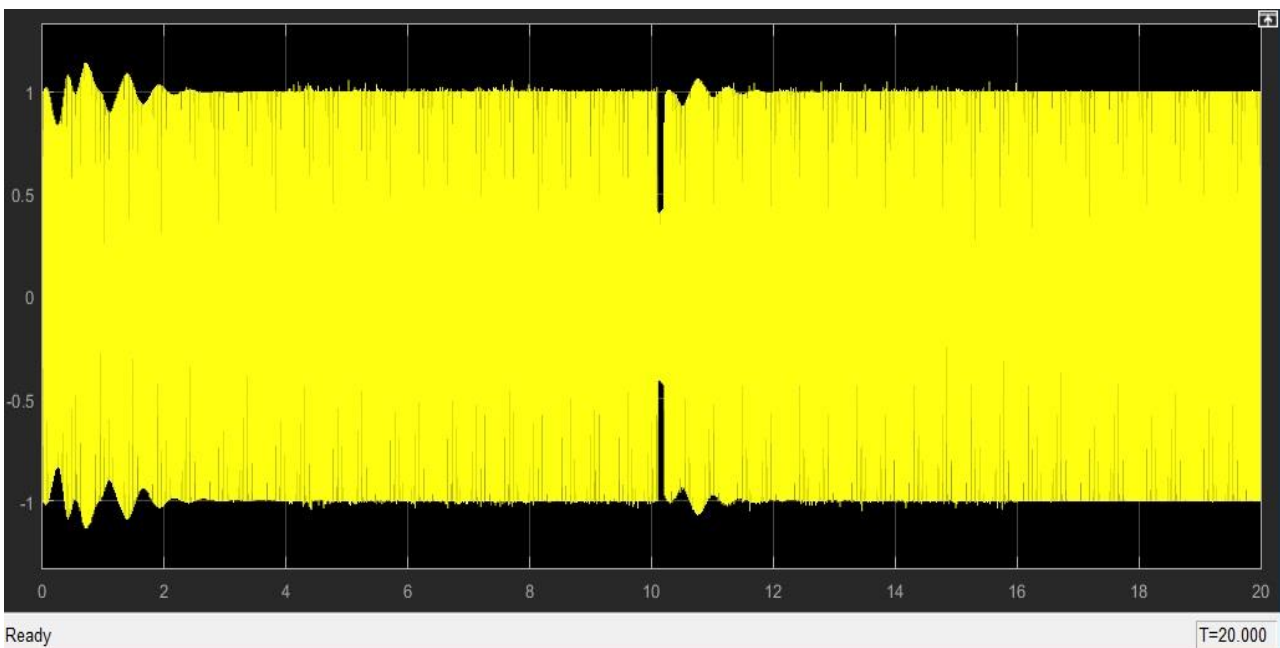


Figure 8.45: Output Voltage Characteristics of Stratos I station with transmission line fault at 10.1 s with PI for 0.8906 pu (in y-Axis pu Voltage in Volt and in x-Axis Time in s)-A2

The output or terminal voltage in the case of Stratos I model with PI controller in the Figure 8.45 the system was in steady state from 2.6 to 10.1 s with an output voltage of amplitude 1 pu. The fault lasted for about 0.1 s, that is from 10.1 s to 10.2 s and during the fault there was a significant drop in the output voltage which became 0.3 to 0.4 pu in amplitude.

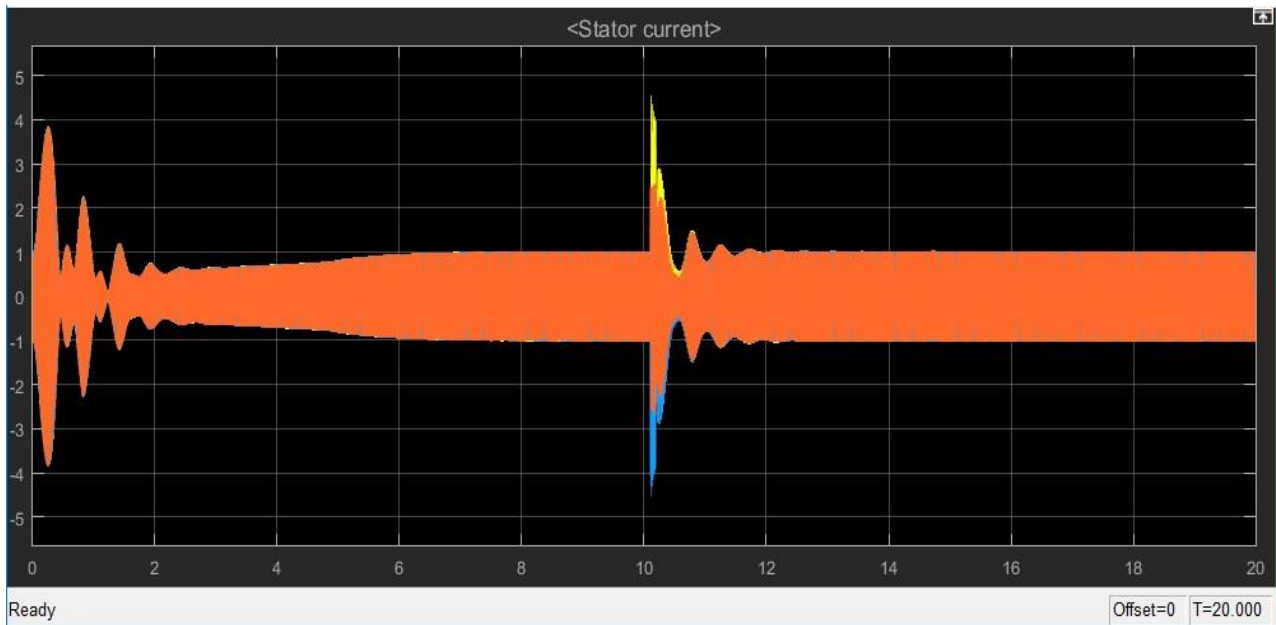


Figure 8.46: Stator Three Phase Current Characteristics of Hydro Power Plant in Stratos I with transmission line fault at 10.1 s with PI for 0.8906 pu (in y pu and in x-Axis Time in s)-A3

I can observe in the Figure 8.46 about the current of the synchronous machine in Stratos I HPP with PI controller that when the fault occurs at 10.1 s the current of stator increases highly at 4.6 pu, the value falls 0.3 pu at 10.5 s and after that starts immediately to rise so as to come back in steady state of 1 pu at 12.3 s.

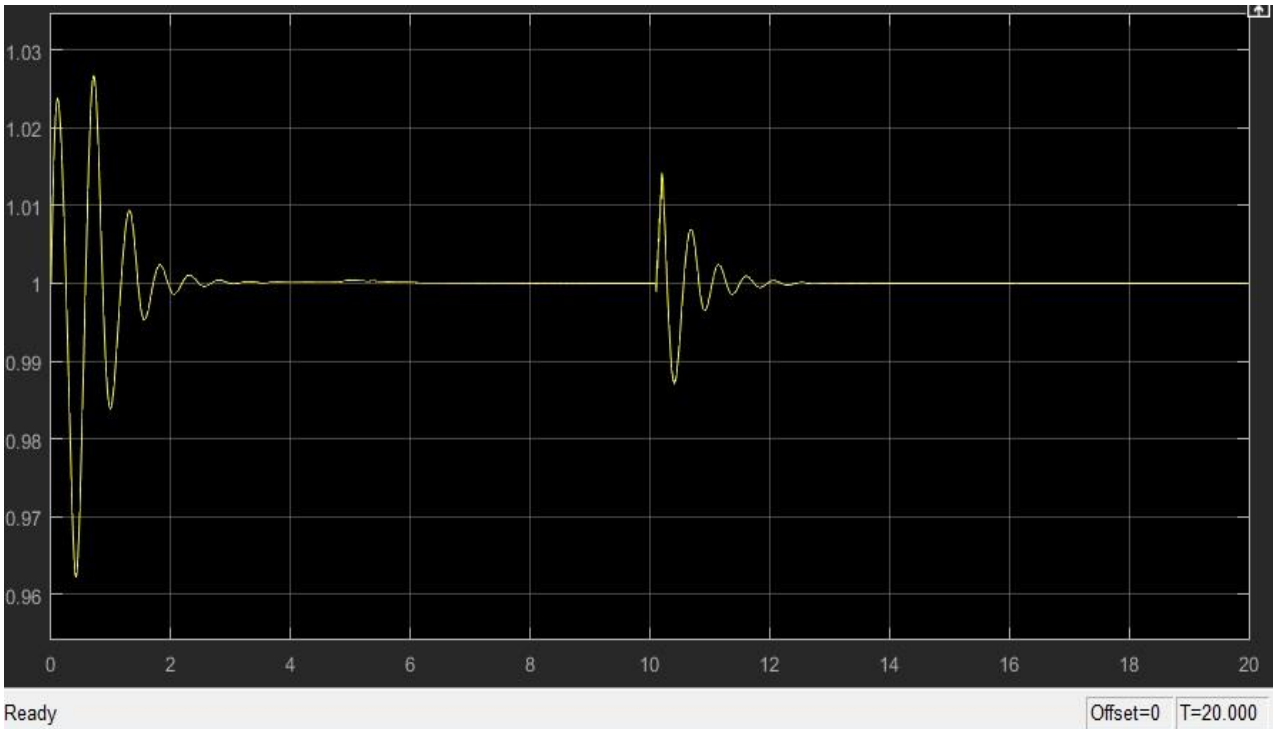


Figure 8.47: Synchronous Generator Speed Characteristics in Stratos I with transmission line fault at 10.1 s with PI for 0.8906 pu (in y-Axis Speed in pu and in x-Axis Time in s)-A4

The fault occurred and I see tin the Figure 8.47 of the speed of synchronous machine of each unit that in the start of the simulation I have oscillations until the time of 2.6 s then the response is in steady state. The value increases to 1.014 pu. The 80% of steady state after the fault comes at 12 s and the transient time is 12.3 s.

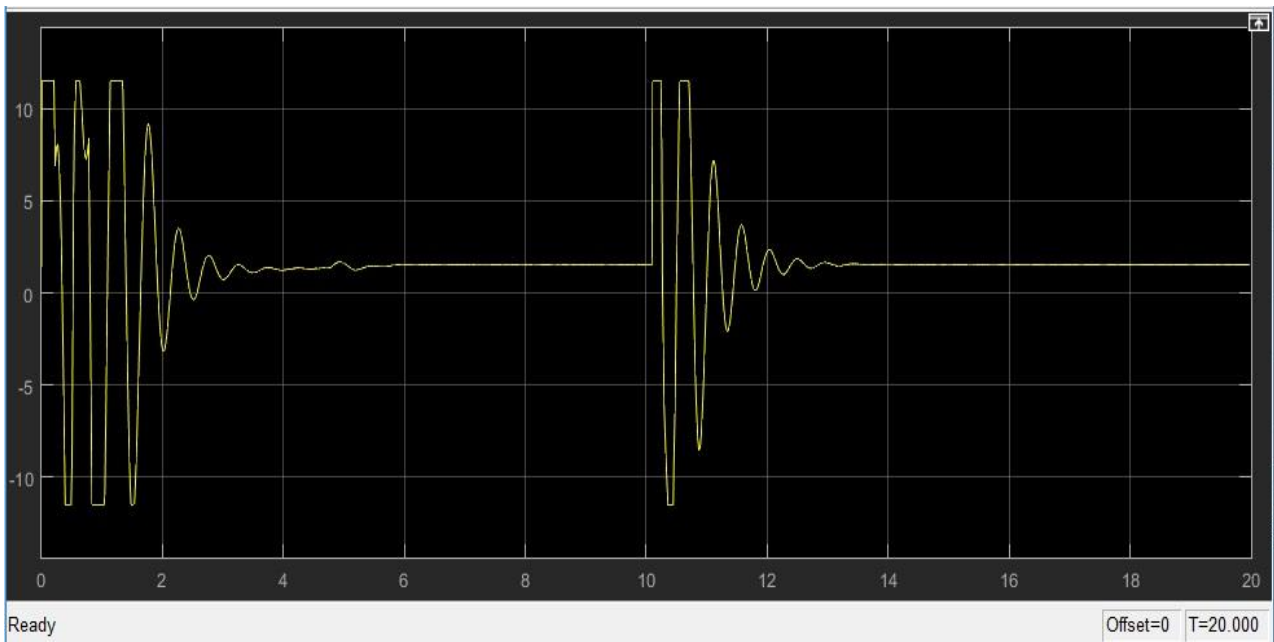


Figure 8.48: Excitation Voltage of Generator Speed in Stratos I HPP with transmission line fault at 10.1 s with PI for 0.8906 pu (in y-Axis Volts in pu and in x-Axis Time in s)-A5

In the case of excitation voltage of each of the two units I see in Figure 8.48 the response of the excitation voltage in each unit in Stratos I HPP station with PI I see that the implementation of the fault changes the signal of the response. I have some oscillations in the beginning in the simulation 0 to 4 s. The 80% of steady state comes at 4.2 s and the transient time is at 5.1 s.

8.6.3 Conclusions for Three Phae Fault Simulation Tests

I see that the implementation of the fault block affects both of the two stations in locations of Kastraki and Stratos I. In all of five figures there is smaller transient time and smaller amount of time to get to the steady state in the case of the PI controller. So the choice of a PI controller seems to be a wiser option to adress the three phase fault problems in the system of Kastraki and in system of Stratos I. Although the PID seems completely eliminates the starting oscillations which lasts for a significant period of about two seconds in any figure.

As a result, is a choice of engineering team in the HPP if they choose PI or PID. In system in which there is known that there are often errors in transmission lines the PI is a more efficient controller even if there is an instability in the first 2 seconds.

Kastraki HPP Three Phase Fault Simulation Tests

Table 8.6 A1 Simulation Test

Output Power	Starting Oscillations	Transient Time
PID	-	10.1-13 s
PI	0-6.8 s	10.1-12.5 s

Table 8.7 A2 Simulation Test

Output Voltage	Starting Oscillations	Transient Time
PID	-	10.1-12.2 s
PI	0-2.3 s	10.1-11.9 s

Table 8.8 A3 Simulation Test

Stator Current	Starting Oscillations	Transient Time
PID	-	10.1-12.3 s
PI	0-5.5 s	10.1-12.1 s

Table 8.9 A4 Simulation Test

Rotor Speed	Starting Oscillations	Transient Time
PID	-	10.1-13.8 s
PI	0-3 s	10.1-12.1 s

Table 8.10 A5 Simulation Test

Excitation Voltage	Starting Oscillations	Transient Time
PID	-	10.1-14.2 s
PI	0-5.2 s	10.1-12.9 s

Stratos I HPP Three Phase Fault Simulation Tests

Table 8.11 A1 Simulation Test

Output Power	Starting Oscillations	Transient Time
PID	-	10.1-12.8 s
PI	0-6.6 s	10.1-12.5 s

Table 8.12 A2 Simulation Test

Output Voltage	Starting Oscillations	Transient Time
PID	-	10.1-11.8 s
PI	0-2.6 s	10.1-11.5 s

Table 8.13 A3 Simulation Test

Stator Current	Starting Oscillations	Transient Time
PID	-	10.1-12.4 s
PI	0-6 s	10.1-12.3 s

Table 8.14 A4 Simulation Test

Rotor Speed	Starting Oscillations	Transient Time
PID	-	10.1-13.2 s
PI	0-2.6 s	10.1-12.3 s

Table 8.15 A5 Simulation Test

Excitation Voltage	Starting Oscillations	Transient Time
PID	-	10.1-13.8 s
PI	0-5.1 s	10.1-13 s

8.7 Load Demand Increase

I am testing the simulations responses of the two Hydropower plants with PI and with PID controllers. The simulation time in the models in the simulation test for different values of RLC load i.e. different values of Agrinio's demand in power is 20 s.

8.7.1 Kastraki HPP in Load Demand increase case

The generation system of Kastraki HPP runs in steady state. At $t = 6.0$ s the restive load is increased by 50 % where it was 100 MW and becomes 150 MW. This change is achieved with the use of a breaker line block in Simulink. In the start of simulation, the breaker is an open circuit and when the time is at 6 s closes and then opens again at 6.2 s. The effect of this RLC load variation (Agrinio demand).

8.7.1.1.1 PID controller in Kastraki HPP in Load Demand Increase Case

The PID coefficients for the below simulations from the ZN method are $K_p=1.99686681$, $K_i=0.14315631$, $K_d=-1.2251305837$ for load 0.8866 pu. These are the data for Kastraki HPP with PID

Table 8.16 PID in Kastraki HPP coefficients for 0.9 pu

K_p	K_i	K_d
1.99686681	0.14315631	-1.2251305837

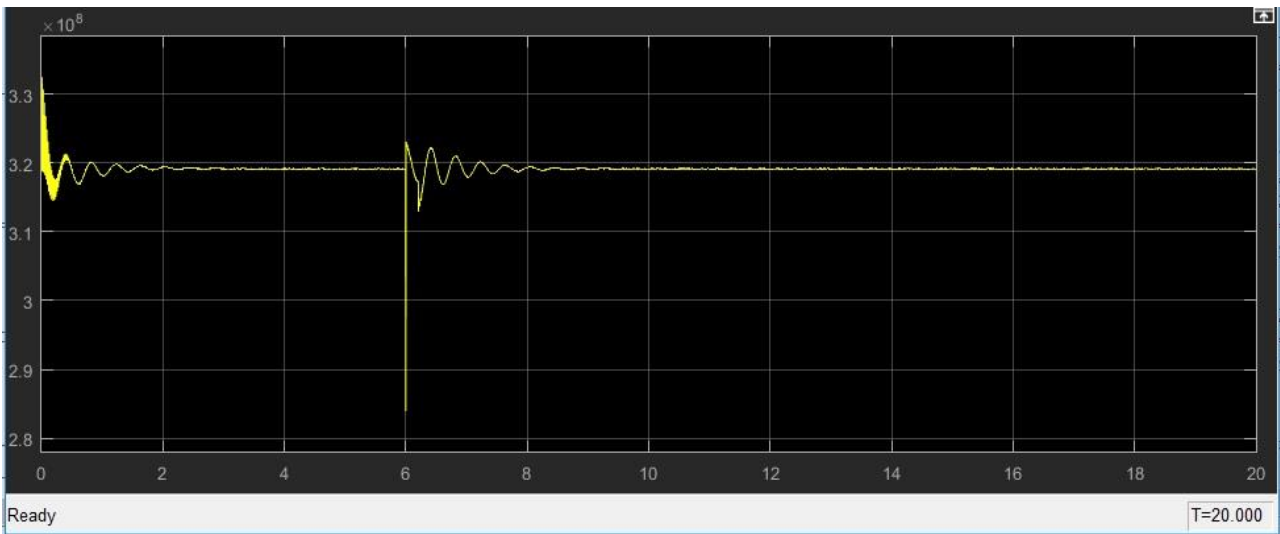


Figure 8.49: Output active power of the Hydropower Plant in Kastraki with RLC increase of 50% at 6 s with PID for 0.8866 pu (in y MW and in x-Axis Time in Sec)-B1

At occurrence RLC load variation in Kastraki HPP with PID, the output active power of the station decreases. The value falls from 3.2 to 2.7 e^8 W and comes again to the 80% of the steady state at 8 s and the transient time is after the breaker switch is the period 6 to 8.8 s.

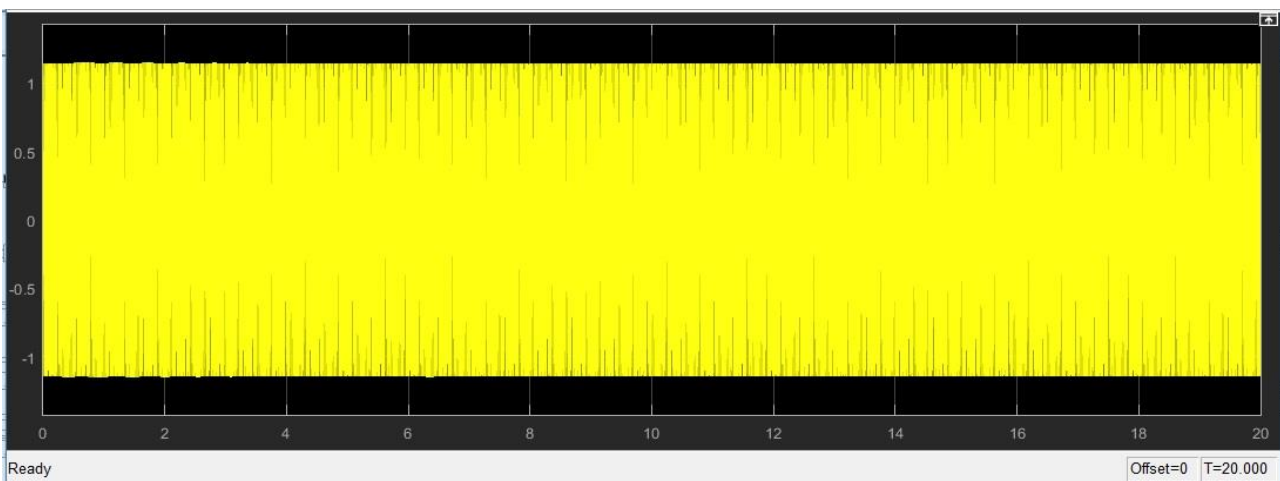


Figure 8.50: Output Voltage Characteristics of Kastraki station with RLC increase of 50% at 6 s with PID for 0.8866 pu (in y-Axis pu Voltage in Volt and in x-Axis Time in s)-B2

The terminal voltage of the total HPP station remains constant and I don't observe any oscillation at time 6 s. So I come to a conclusion that the RLC loads variations don't affect the output voltage.

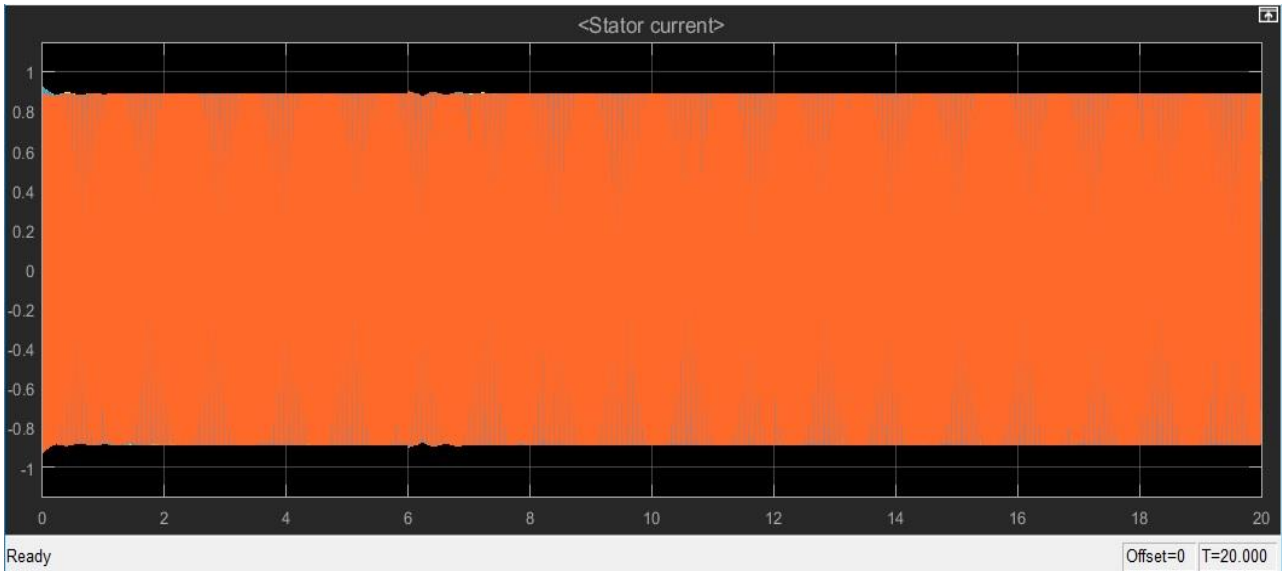


Figure 8.51: Stator Three Phase Current Characteristics of Hydro Power Plant in Kastraki with RLC increase of 50% at 6 s with PID for 0.8866 pu (in y pu and in x-Axis Time in s)-B3

About the stator current it shows that the signal response has small increment of the order of 0.1 pu i.e a small turmoil but not anything special. So I come to a conclusion that the RLC loads variations affect very little the current of synchronous machine.

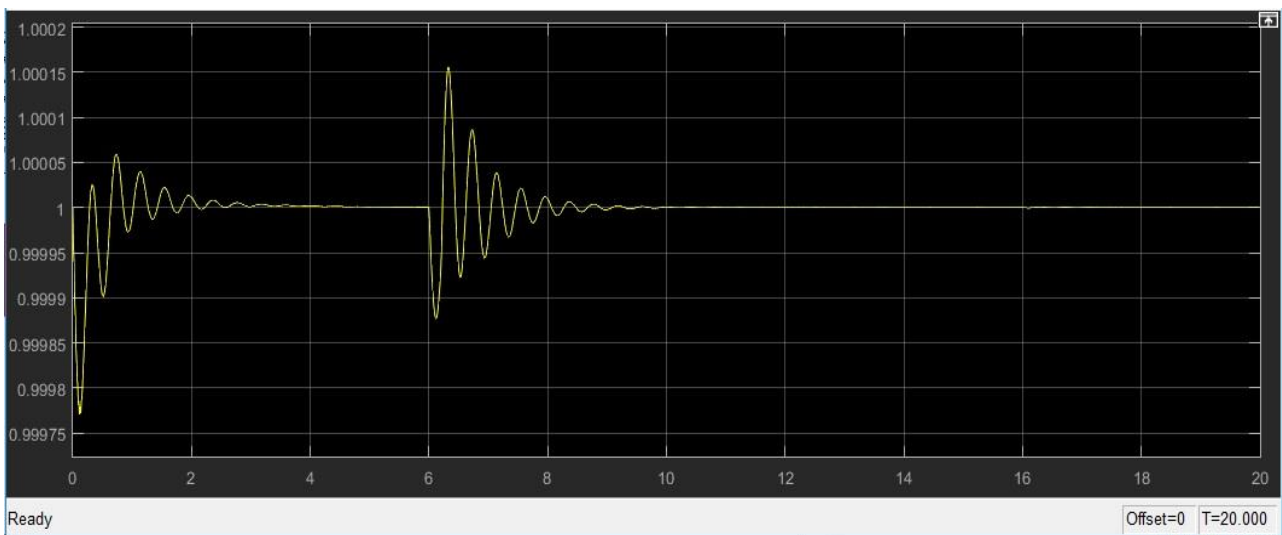


Figure 8.52: Synchronous Generator Speed Characteristics in Kastraki with RLC increase of 50% at 6 s with PID for 0.8866 pu (in y-Axis Speed in pu and in x-Axis Time in s)-B4

For the case of RLC load variation in Kastraki HPP with PID, the speed of rotor decreases. The value falls from 1 to 0.9998 pu then increase from 0.9998 to 1.015 pu and comes again to the 80% of the steady state at 9 s and the transient time is after the breaker switch is the period 6 to 9.8 s.

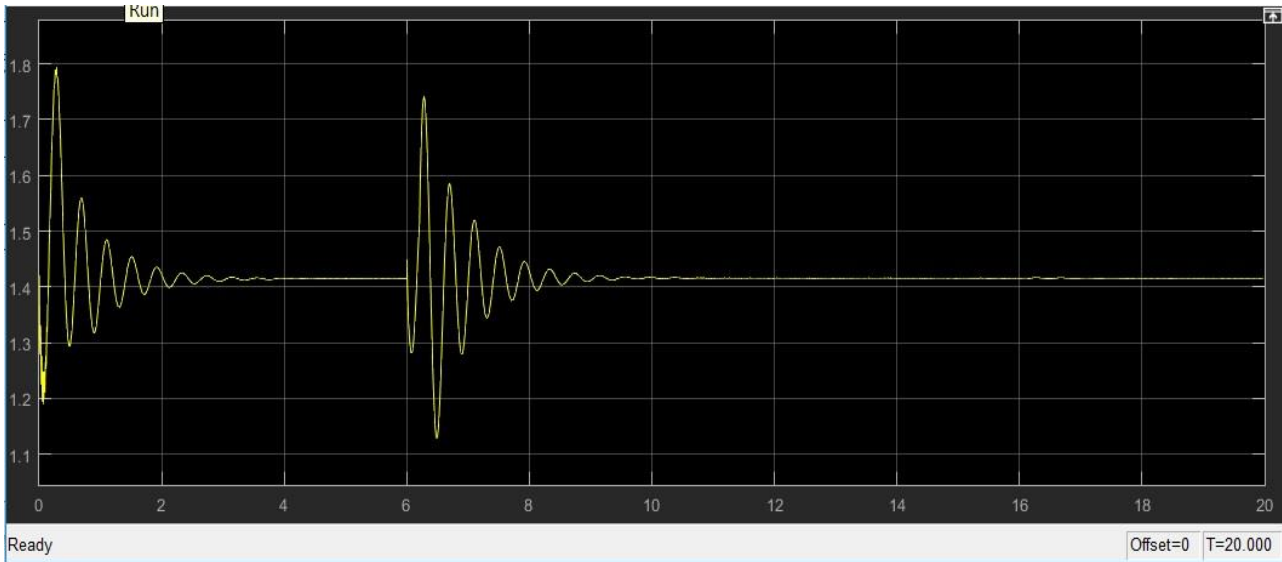


Figure 8.53: Excitation Voltage of Generator Speed in Kastraki with RLC increase of 50% at 6 s with PID for 0.8866 pu (in y-Axis Volts in pu and in x-Axis Time in s)-B5

The excitation voltage increases for a RLC load increase in Kastraki HPP with PID with a peak to peak value at 6.1 s of 0.7 pu. The value rises from 1.3 to 1.75 pu and comes again to the 80% of the steady state at 9 s and the transient time is after the breaker switch is the period 6 to 10 s.

8.7.1.1.2 PI controller in Kastraki HPP in Load Demand increase case

The PI coefficients for the below simulations from the ZN method and table 7.1 are $K_p = 1.497650108$, $K_i = 0.23859385$ for load 0.8866 pu. These are the data for Kastraki HPP with PI.

Table 8.17 PI coefficients in Kastraki HPP for 0.9 pu

K_p	K_i
1.497650108	0.23859385

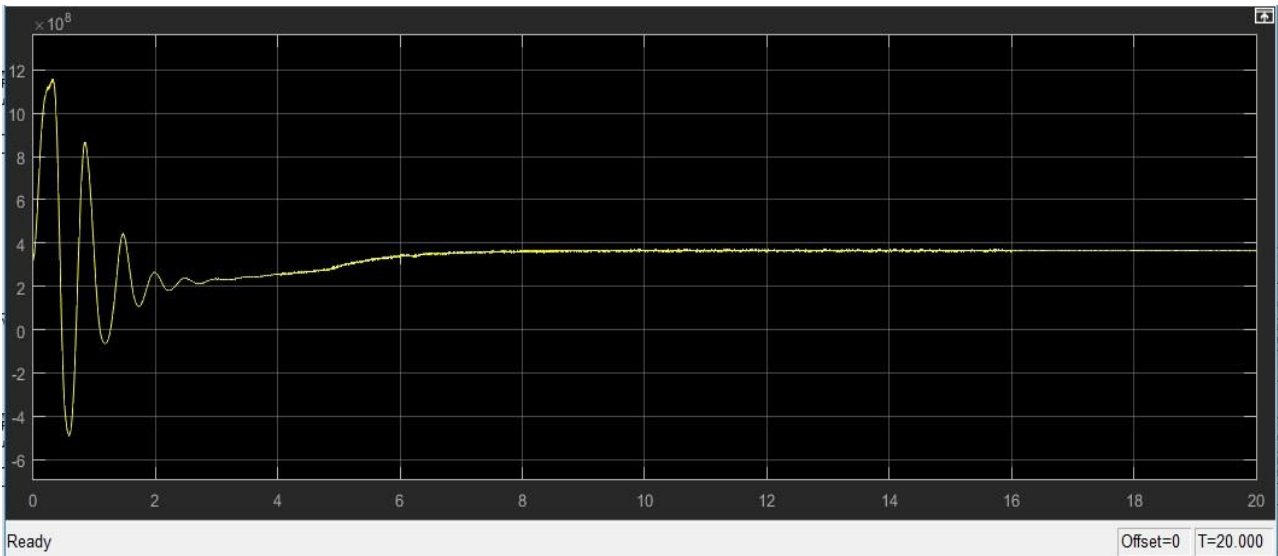


Figure 8.54: Output active power of the Hydropower Plant in Kastraki with RLC increase of 50% at 6 s with PI for 0.8866 pu (in y MW and in x-Axis Time in s)-B1

As I see in Figure 8.54 RLC load increase in Kastraki HPP with PI with PI controller, the output active power of the station as a result it hasn't any oscillations beside the starting period 0 to 2.8 s. The value increases from 2.1 to 4 e^8 W and comes again to the 80% of the steady state at 4 s and the transient time is the period 0 to 6 s.

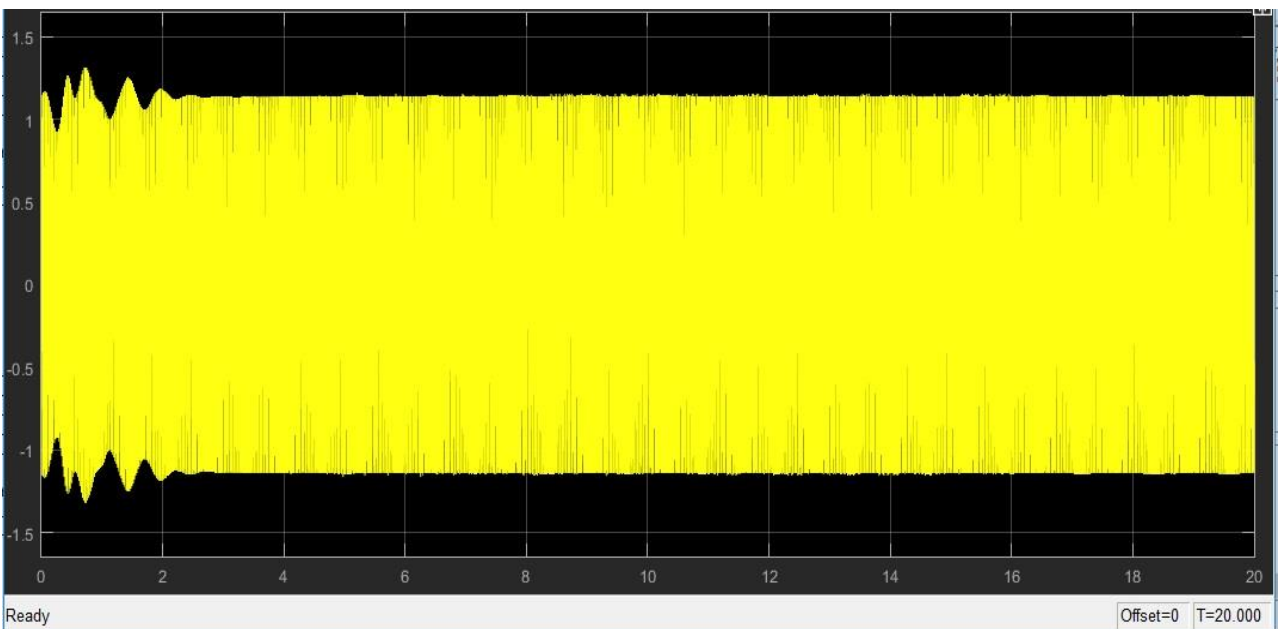


Figure 8.55: Output Voltage Characteristics of Kastraki station with RLC increase of 50% at 6 s with PI for 0.8866 pu (in y-Axis pu Voltage in Volt and in x-Axis Time in s)-B2

The terminal voltage of the total HPP in Kastraki with PI station remains constant and I don't observe any oscillation at time 6 s besides the first oscillations in the period 0 to 2 s which are a result that I

am using a PI controller. So I come to a conclusion that the RLC loads variations don't affect the output voltage

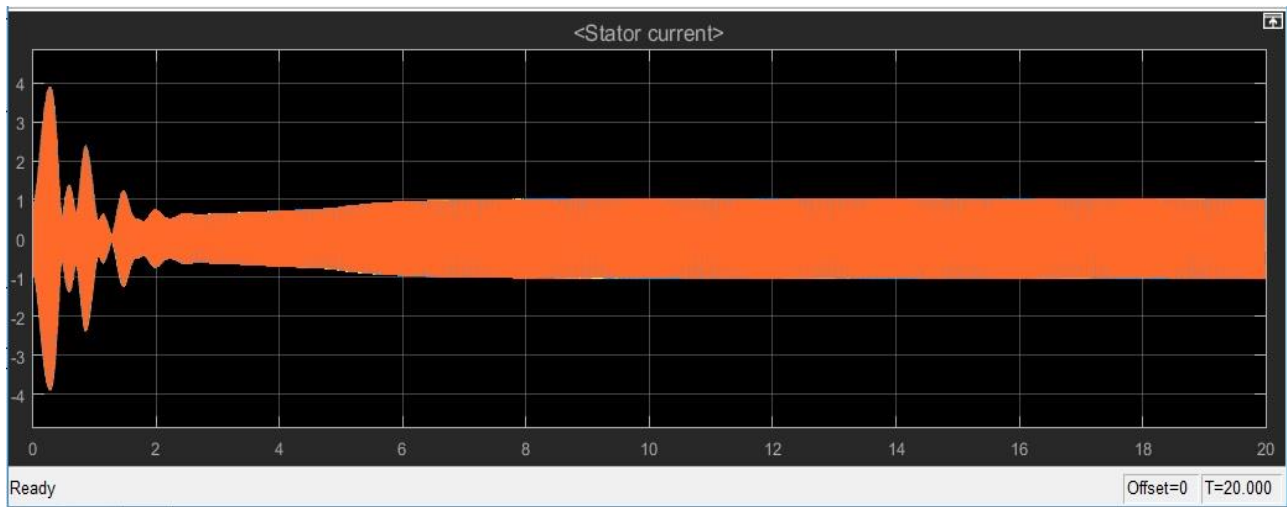


Figure 8.56: Stator Three Phase Current Characteristics of Hydro Power Plant in Kastraki with RLC increase of 50% at 6 s with PI for 0.8866 pu (in y pu and in x-Axis Time in s)-B3

In Figure 8.56 I am observing the response of the current of each synchronous machine has oscillation in the period 0 to 2.2 s and from the period 2.2 s to 5.8 s the amplitude of the stator current increases from 1.5 to 2 pu. It seems that the RLC increase at time 6 s don't affect the current of each unit.

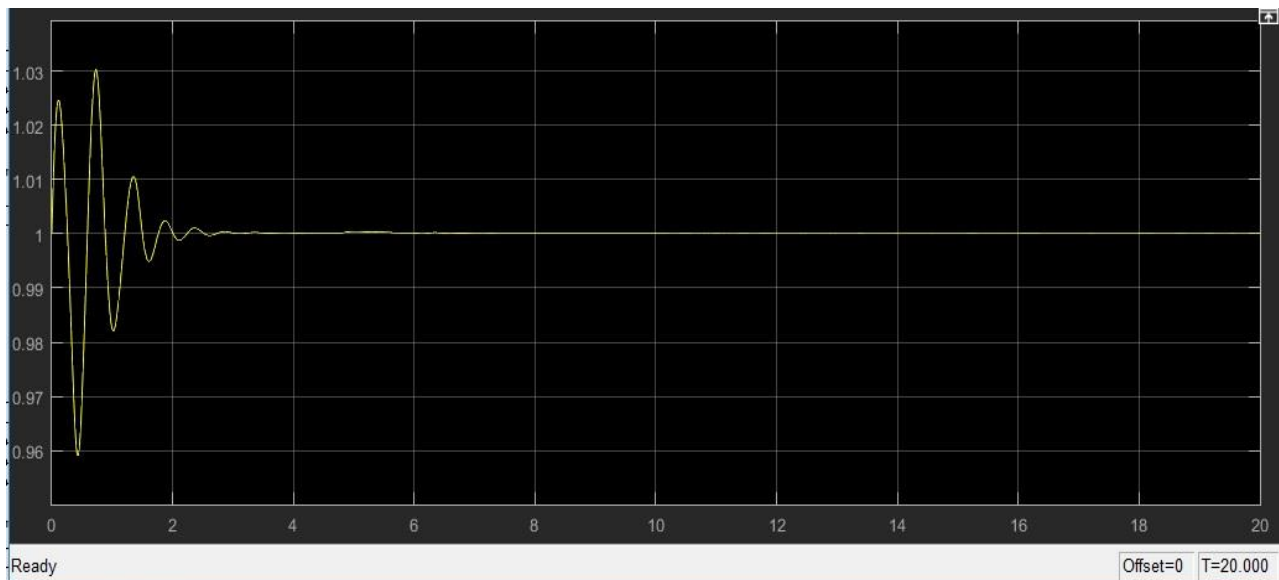


Figure 8.57: Synchronous Generator Speed Characteristics in Kastraki with RLC increase of 50% at 6 s with PI for 0.8866 pu (in y-Axis Speed in pu and in x-Axis Time in s)-B4

About the rotor speed in each unit in Kastraki HPP with PI station I see that the RLC load increase doesn't change the signal of the response. I have only oscillations in the beginning in the simulation 0 to 2.2 s. The 80% of the steady state comes at 2.2 s and the transient time is at 3 s.

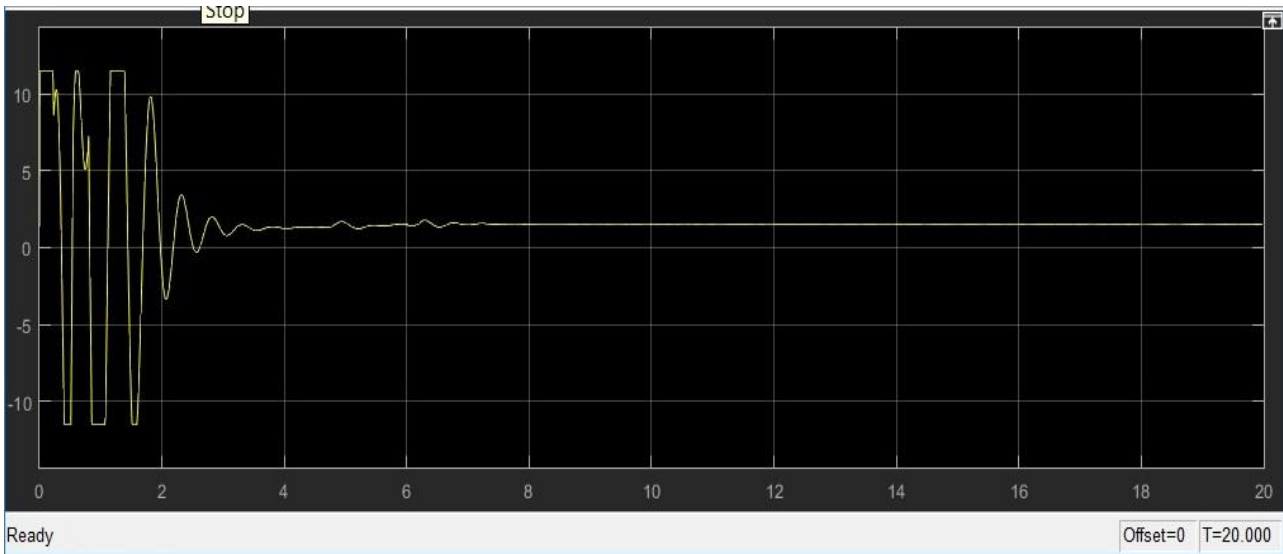


Figure 8.58: Excitation Voltage of Generator Speed in Kastraki with RLC increase of 50% at 6 s with PI for 0.8866 pu (in y-Axis Volts in pu and in x-Axis Time in s)-B5

In Figure 8.58 in the figure of the excitation voltage in each unit of the four units in Kastraki HPP station with PI controller I see that the RLC load increase doesn't change the signal of the response. I have only oscillations in the beginning in the simulation 0 to 4 s. The 80% of the steady state comes at 3.8 s and the transient time is at 6.6 s. The value in steady state is at 2 pu.

8.7.2 Stratos I HPP in Load Demand increase case

The Hydropower plant of Stratos I HPP is power generating system runs in steady state. At $t = 6.0$ s the restive load is increased by 50 % where it was 50 MW and becomes 75 MW. This change is achieved with the use of a breaker line block in Simulink. In the start of simulation, the breaker is an open circuit and when the time is at 6 s closes and then opens again at 6.2 s. The effect of this RLC load variation (Agrinio demand).

8.7.2.1 PID controller in Stratos I in Load Demand increase case

The PID coefficients for the below simulations from the ZN method are $K_p = 1.25387312$, $K_i = 0.13126167$, $K_d = -0.71356127$ for load 0.8905 pu. These are the data for Stratos I HPP with PID.

Table 8.18 PID coefficients in Stratos HPP for 0.9 pu

K_p	K_i	K_d
1.25387312	0.13126167	-0.71356127

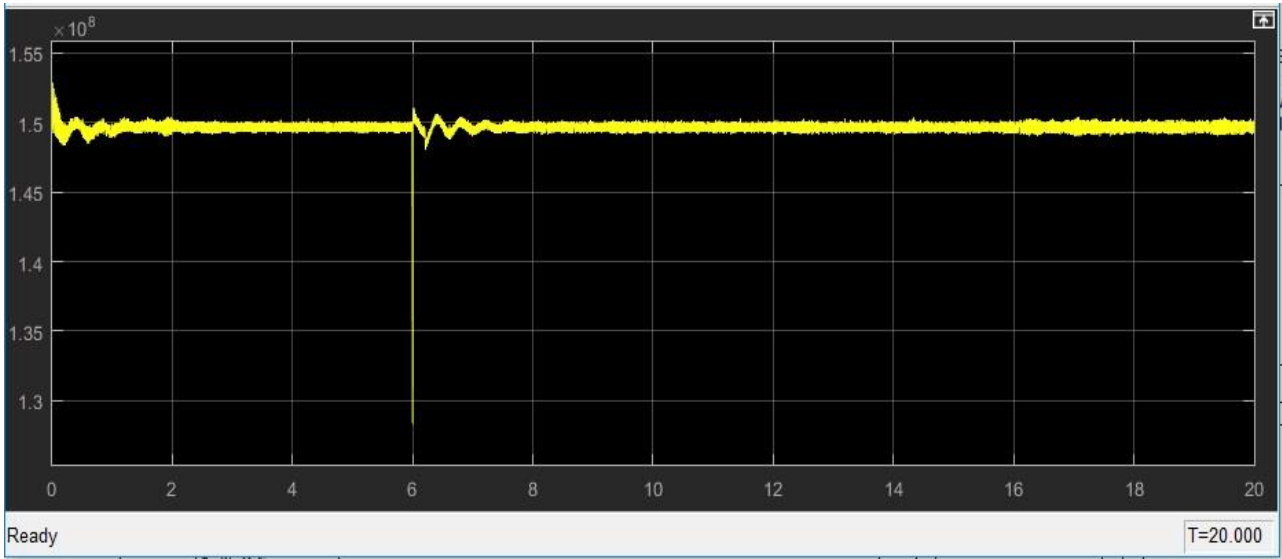


Figure 8.59: Output active power of the Hydropower Plant in Stratos I with RLC increase of 50% at 6 s with PID for 0.8906 pu (in y MW and in x-Axis Time in s)-B1

Regarding the RLC load variation in Stratos I HPP with PID, the output active power of the station decreases. The value falls from 1.5 to 1.28 e^8 W and comes again to the 80% of the steady state at 7.5 s and the transient time is after the breaker switch is the period 6 to 8 s.

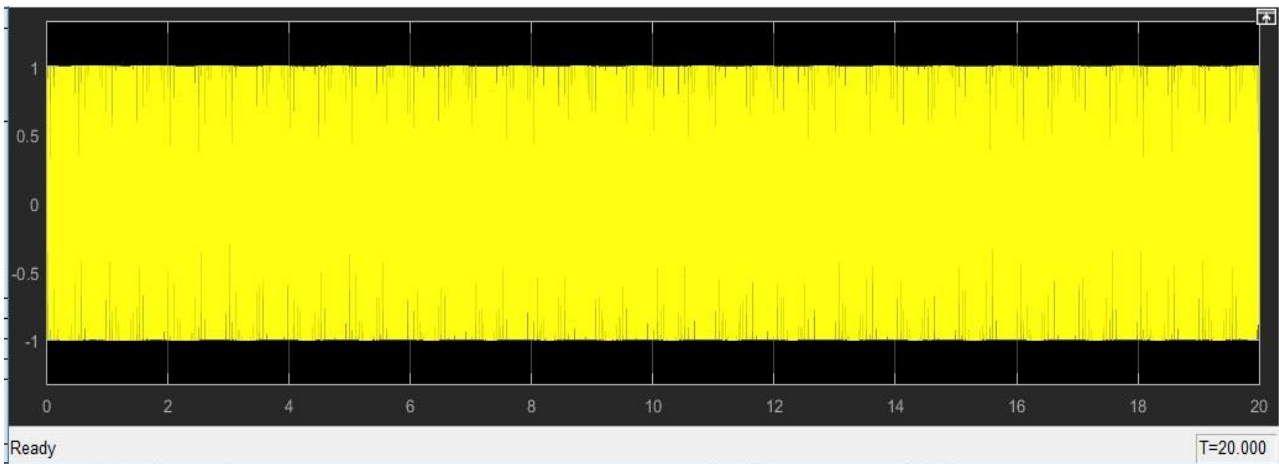


Figure 8.60: Output Voltage Characteristics of Stratos I station with RLC increase of 50% at 6 s with PID for 0.8906 pu (in y-Axis pu Voltage in Volt and in x-Axis Time in s)-B2

Also the terminal voltage of the total HPP station in Stratos I location remains constant and I don't observe any oscillation at time 6 s. So I come to a conclusion that the RLC loads variations don't affect the output voltage.

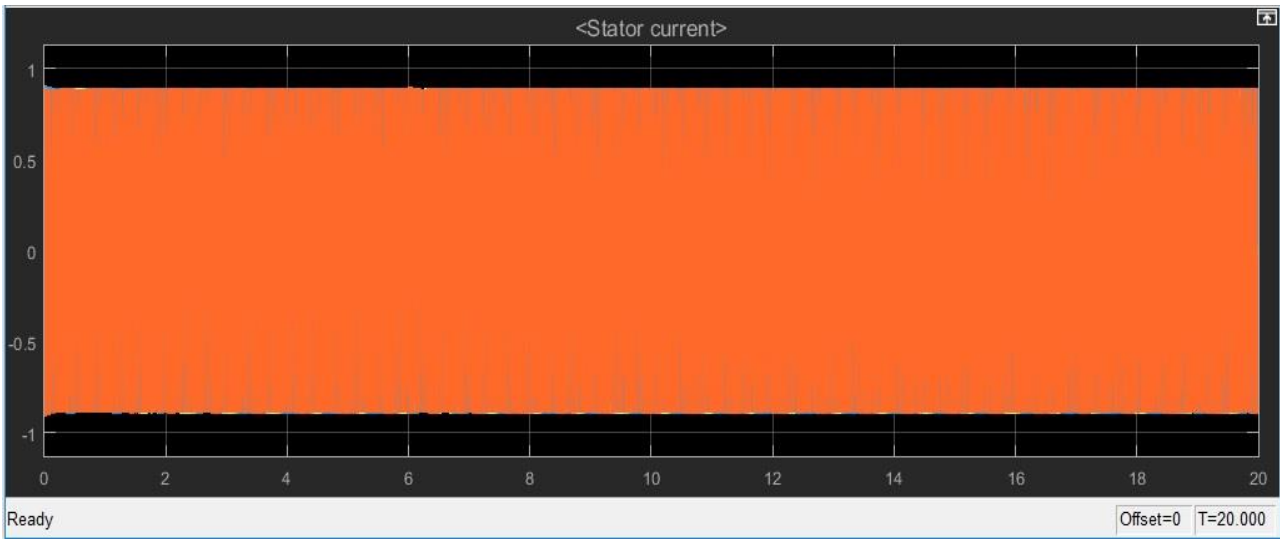


Figure 8.61: Stator Three Phase Current Characteristics of Hydro Power Plant in Stratos I with RLC increase of 50% at 6 s with PID for 0.8906 pu (in y pu and in x-Axis Time in s)-B3

In the Figure 8.61 of the synchronous machine current it shows that the signal response has almost at all any oscillation and is the same as the stator current figure of Stratos I HPP with operation under normal conditions. So I come to a conclusion that the RLC loads variations dont affect the current of synchronous machine.

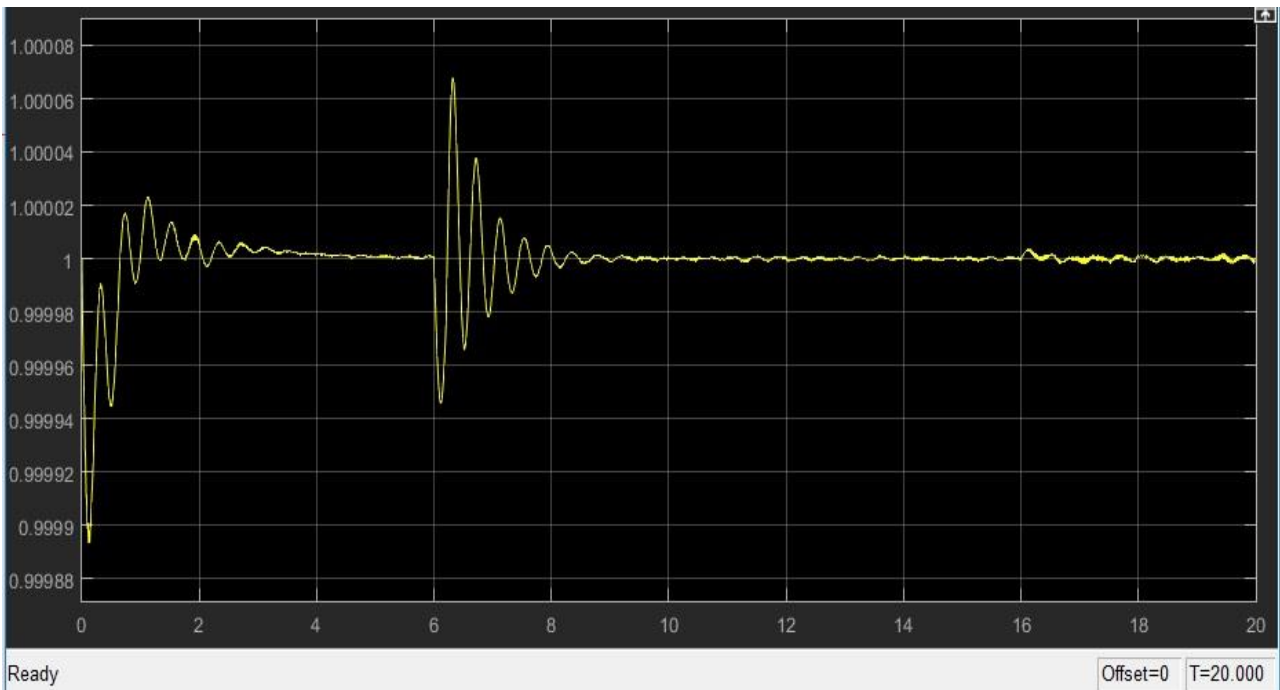


Figure 8.62: Synchronous Generator Speed Characteristics in in Stratos I with RLC increase of 50% at 6 s with PID for 0.8906 pu (in y-Axis Speed in pu and in x-Axis Time in s)-B4

In the case of RLC load increase in Stratos I HPP with PID, the speed of rotor decreases. As I notice in Figure 8.62 the value falls from 1 to 0.9995 pu then increase from 0.9995 to 1.00007 pu and comes again to the 80% of the steady state at 8.8 s and the transient time is after the breaker switch is the period 6 to 9.5 s.

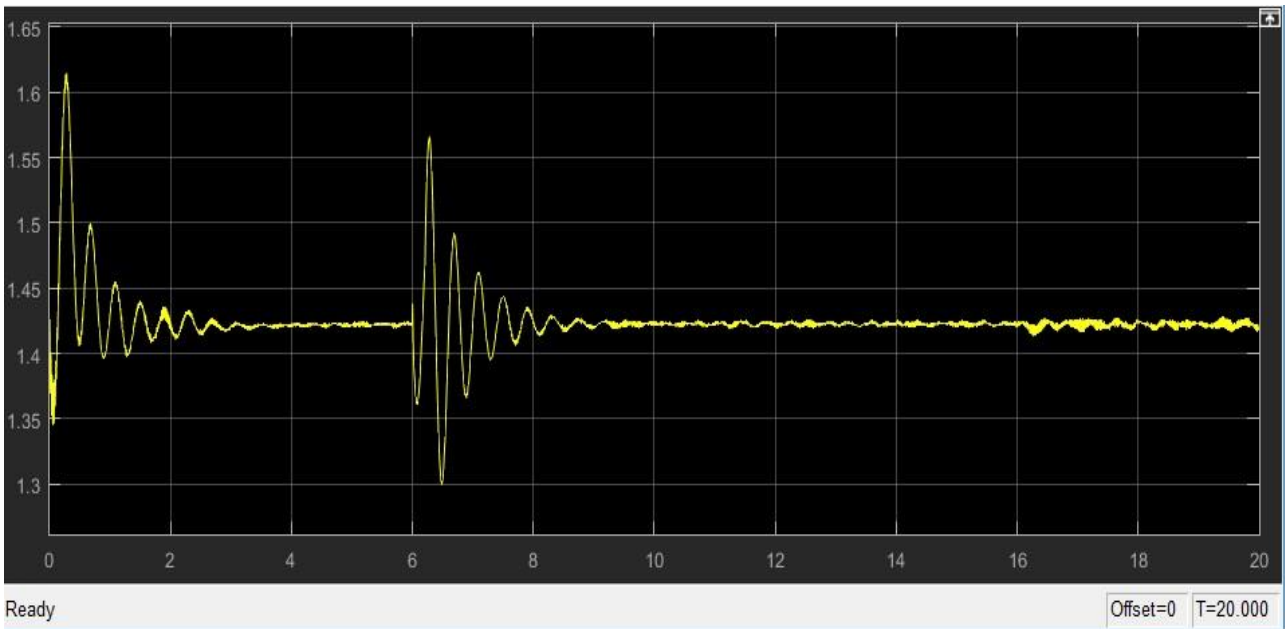


Figure 8.63: Excitation Voltage of Generator Speed in Stratos I with RLC increase of 50% at 6 s with PID for 0.8906 pu (in y-Axis Volts in pu and in x-Axis Time in s)-B5

For each of the 2 units the excitation voltage increases for a RLC load increase in Stratos I HPP with PID with a peak to peak value at 6.1 s of 0.27 pu. The value rises from 1.36 to 1.58 pu and comes again to the 80% of the steady state at 9.2 s and the transient time is after the breaker switch is the period 6 to 9.8 s.

8.7.2.2 PI controller in Stratos I in Load Demnad case

The PI coefficients for the below simulations from the ZN method and table 7.1 are $K_p = 0.94040484$, $K_i = 0.52504668$ for load 0.8905 pu. These are the data for Stratos I HPP with PI

Table 8.19 PI coefficients in Stratos I HPP for 0.9 pu

K_p	K_i
0.94040484	0.52504668

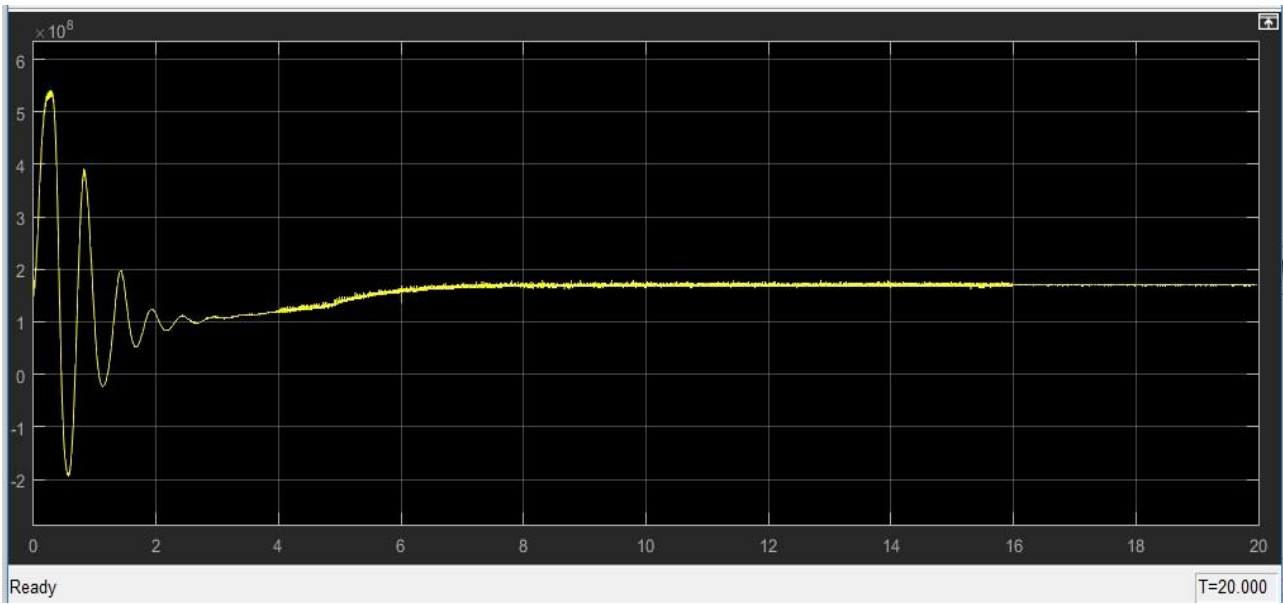


Figure 8.64: Output active power of the Hydropower Plant in Stratos I with RLC increase of 50% at 6 s with PI for 0.8906 pu (in y MW and in x-Axis Time in s)-B1

I am observing in Figure 8.64 RLC load increase in Stratos I HPP with PI controller, the output active power of the station as a result it hasn't any oscillations beside the starting period 0 to 3 s. The value increases from 1 to 1.7 to 1.8 e^8 W and comes to the 80% of the steady state at 3.2 s and the transient time is the period 0 to 6 s.

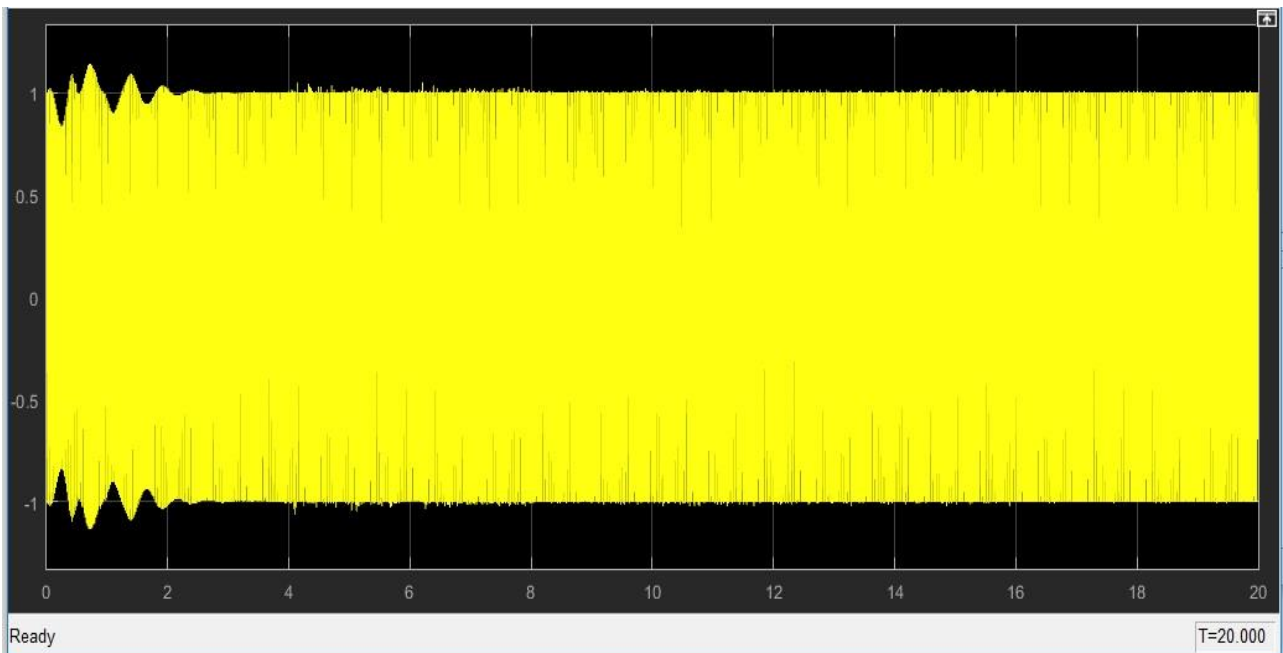


Figure 8.65: Output Voltage Characteristics of Stratos I station with RLC increase of 50% at 6 s with PI for 0.8906 pu (in y-Axis pu Voltage in Volt and in x-Axis Time in s)-B2

The Figure 8.65 shows that the total output or terminal voltage of the total HPP in Stratos I station with PI remains constant and I don't observe any oscillation at time 6 s besides the first oscillations in the period 0 to 2.2 s which are a result that I am using a PI controller. So I come to a conclusion that the RLC loads variations don't affect the output voltage.

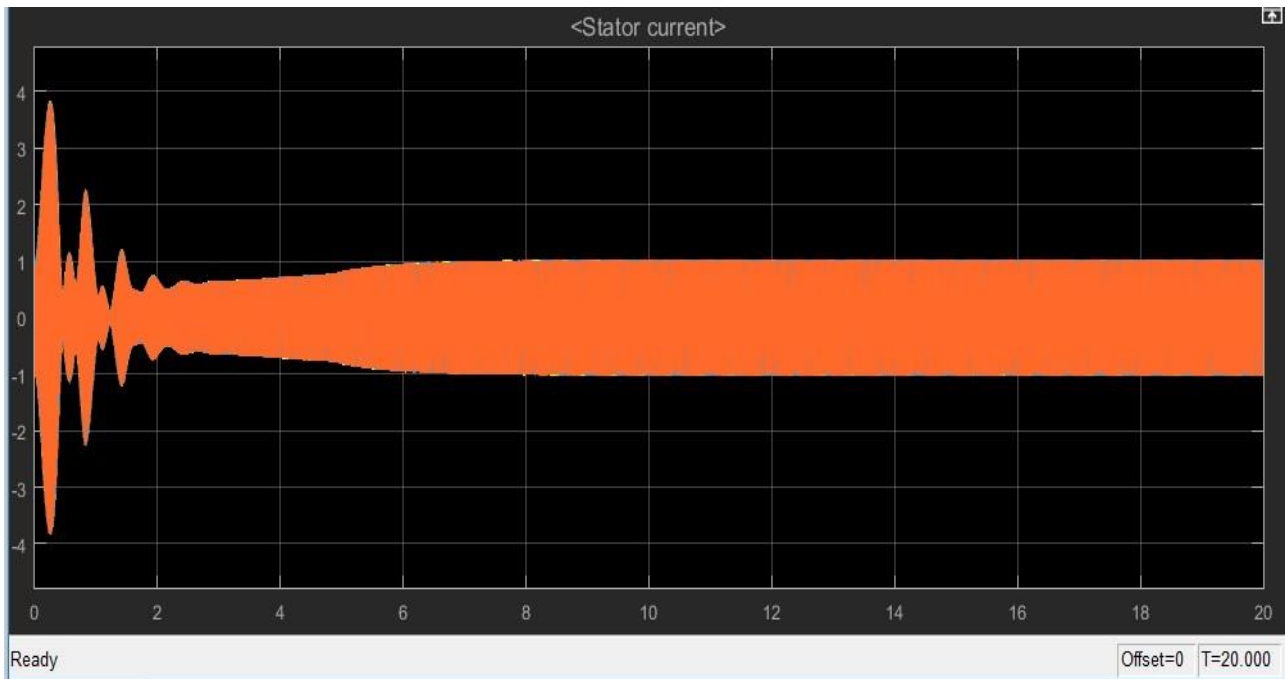


Figure 8.66: Stator Three Phase Current Characteristics of Hydro Power Plant in Stratos I with RLC increase of 50% at 6 s with PI for 0.8906 pu (in y pu and in x-Axis Time in s)-B3

Figure 8.66 which is the Stratos I with PI shows the response of the current of each synchronous machine has oscillation in the period 0 to 2.4 s and from the period 2.2 to 5.8 the amplitude of the stator current increases from 1.5 to 2 pu. It seems that the RLC increase at time 6 s don't affect the current of each unit.

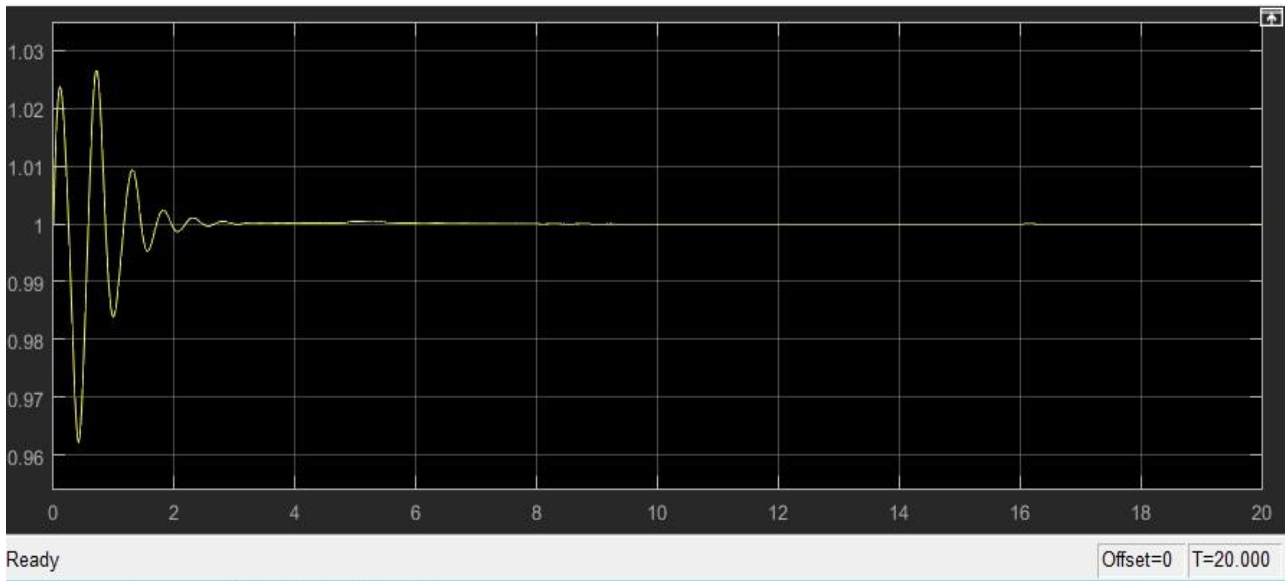


Figure 8.67: Synchronous Generator Speed Characteristics in in Stratos I with RLC increase of 50% at 6 s with PI for 0.8906 pu (in y-Axis Speed in pu and in x-Axis Time in s)-B4

In Figure 8.67 in the figure of the rotor speed in each unit in Stratos I HPP station with PI I see that the RLC load increase doesn't change the signal of the response. I have only oscillations in the beginning in the simulation 0 to 3.1 s. The 80% of the steady state comes at 3.1 s and the transient time is at 3.5 s.

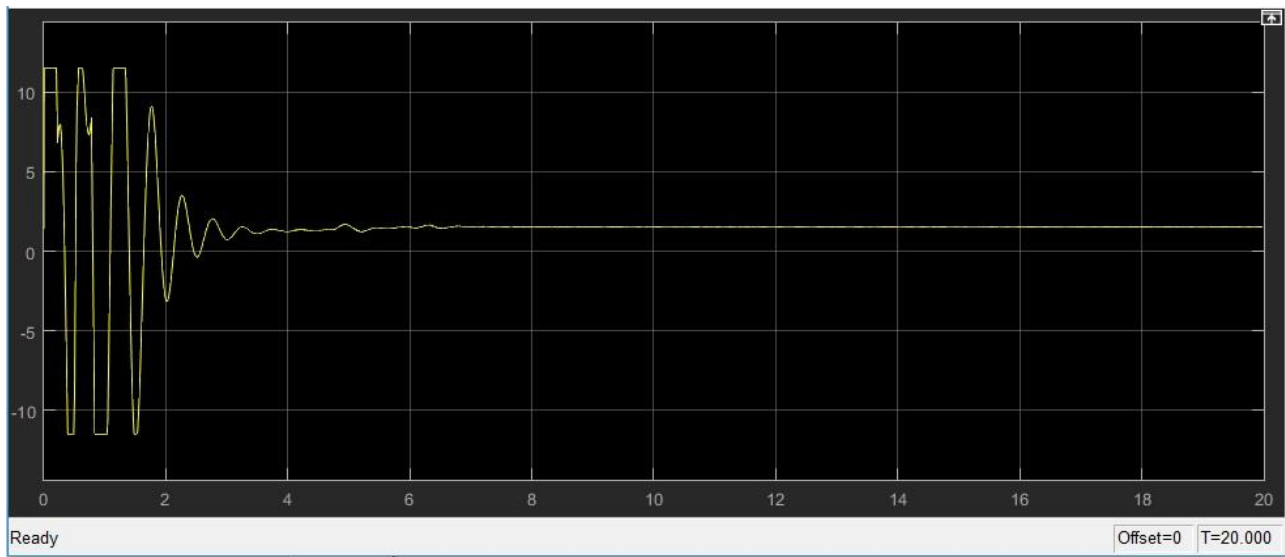


Figure 8.68: Excitation Voltage of Generator Speed in Stratos I with RLC increase of 50% at 6 s with PI for 0.8906 pu (in y-Axis Volts in pu and in x-Axis Time in s)-B5

In Figure 8.68 in the figure of the excitation voltage in each unit in Stratos I HPP station with PI I see that the RLC load increase doesn't change the signal of the response. I have only oscillations in the beginning in the simulation 0 to 5.2 s. The 80% of the steady state comes at 4 s and the transient time is at 6.2 s.

8.8 Load Demand Decrease

In both models of Simulink, I study the same 5 figures (output voltage, excitation voltage, rotor speed, active power, stator current) this time for RLC decreases. The decreases are achieved with the use of a breaker line block in Simulink. In the start of simulation, the breaker is a closed circuit and when the time is at 6 s opens and then closes again at 6.2 s. In the case of Kastraki HPP we have RLC load 100 MW and we decrease that about 50% to 50 MW, but in the case of Stratos I HPP we have RLC load 50 MW and we decrease that about 50% to 25 MW. The effect of this RLC load decrease (Agrinio demand) has the same result as in the case of the increase that's the reason why I don't show again the figures. The simulation time is again 20 s and the coefficients for PI and PID controller are the same because the testing loads in each unit are the same. So I understand each variation whether it is increase or decrease of the same magnitude have the same results. At occurrence of load increase, the speed of rotor decreases and excitation voltage increases. The terminal voltage remains constant but the stator current shows small increment. While at the occurrence of the load decrease the speed of rotor increases, excitation voltage decreases and set at its lower level and the terminal voltage remains constant but the stator current slightly decreases and become stable

8.8.1 Conclusions for Load Demand Increase/Decrease Simulation Tests

In general, in both Hydropower plants in Stratos I and in Kastraki locations I see that the PI has better results than PID because it seems that the changes in the RLC load (Agrinio demand) don't affect the stability or the equilibrium of the two generating systems who under normal conditions run in steady state. Just in the PI case have some starting oscillations and is needed some time to reach the steady state. But in the PID case I see that these changes affect the response and I am recording them along with the transient times and the time periods in which the stations have steady state.

Kastraki HPP Transient Times during Load Demand Increase/Decrease Simulation Tests

Table 8.20 B1 Simulation Test

Output Power	Starting Oscillations	Transient Time
PID	0-2.5 s	6-8.8 s
PI	0-6 s	-

Table 8.21 B2 Simulation Test

Output Voltage	Starting Oscillations	Transient Time
PID	-	-
PI	0-2.8 s	-

Table 8.22 B3 Simulation Test

Stator Current	Starting Oscillations	Transient Time
PID	0-0.4 s	6-6.8 s
PI	0-5.8 s	-

Table 8.23 B4 Simulation Test

Rotor Speed	Starting Oscillations	Transient Time
PID	0-3.1 s	6-9.8 s
PI	0-3 s	-

Table 8.24 B5 Simulation Test

Excitation Voltage	Starting Oscillations	Transient Time
PID	0-3.6 s	6-10 s
PI	0-6.6 s	-

Stratos I HPP Transient Times during Load Demand Increase/Decrease Simulation Tests**Table 8.25 B1 Simulation Test**

Output Power	Starting Oscillations	Transient Time
PID	0-2 s	6-8 s
PI	0-6 s	-

Table 8.26 B2 Simulation Test

Output Voltage	Starting Oscillations	Transient Time
PID	-	-
PI	0-2.6 s	-

Table 8.27 B3 Simulation Test

Stator Current	Starting Oscillations	Transient Time
PID	0-0.2 s	-
PI	0-6.1 s	-

Table 8.28 B4 Simulation Test

Rotor Speed	Starting Oscillations	Transient Time
PID	0-4 s	6-9.5 s
PI	0-2.9 s	-

Table 8.29 B5 Simulation Test

Excitation Voltage	Starting Oscillations	Transient Time
PID	0-3.7 s	6-9.8 s
PI	0-6.2 s	-

8.9 Power Load Change

8.9.1 Kastraki HPP in Power Load changes case

I am going to simulate the model of Kastraki HPP for 3 different loads i) 0.4, ii) 0.6, iii) 0.8866 pu with PI controller and with PID controller. The simulation time in the models in the simulation test for different values of load is 10 s.

8.9.1.1 PID in Kastraki HPP in Power Load changes case

Graphics in Figure 8.69 indicate which has taken from the synchronous generator terminals of one load of about 35.99 MW (0.4 pu) for each unit in system frequency within the desired limits, the effective terminal voltage is 15.750 kV and the $V_f = 1.081$ pu. The coefficients of PID for load 0.4 pu are taken from the ZN method ($K_p = 0.71591296$, $K_i = 0.04657833$, $K_d = -3.2007578307$). It is clear from given graphics that it was loaded with HEPP 35.99 MW load at each generator and 143.96 MW total output active power and came to stable state with minimization of oscillations in voltage and frequency in a short time in 2 s and came to steady state in time 7 s.

Table 8.30 PID coefficients in Kastraki HPP for 0.4 pu

K_p	K_i	K_d
0.71591296	0.04657833	-3.2007578307

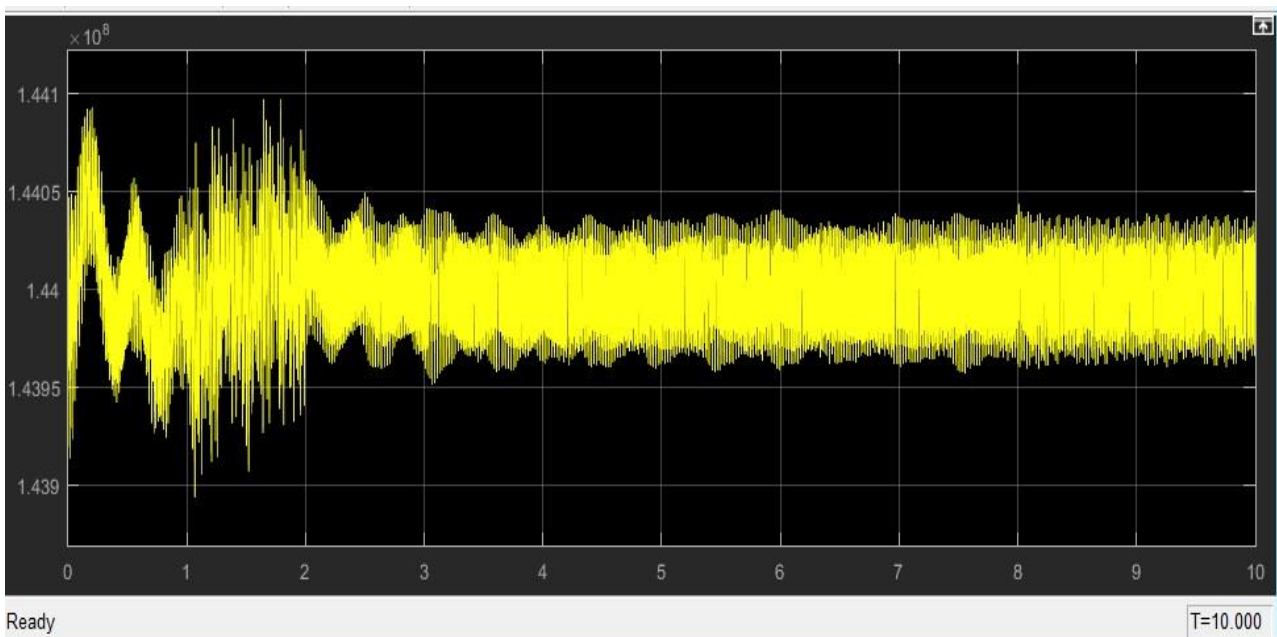


Figure 8.69: Output A. Power of the HPP in Kastraki with active power at 0.4 pu with PID-C1

In Figure. 8.70 below in which I am measuring the total active power of the station i.e. the synchronous generator has power production of about 53.99 MW (0.6 pu) .The frequency of the system is within the desired limits, the effective terminal voltage is 15.750 kV and the $V_f = 1.1943$ pu. The coefficients of PID for load 0.6 pu are taken from the ZN method ($K_p = 1.07148533$, $K_i = 0.09612619$, $K_d = -2.5605848591$) . It is obvious from given Figure 8.70 that it was loaded with HEPP 53.99 MW load at each generator and 215.96 MW total output active power and came to stable state with minimization of oscillations in voltage and frequency in a short time like 3.6 s and the transient time in which we have an undoubtedly steady state is in time 6.3 s. Also the value of the active power has very smaller variations than the case of 0.4 pu.

Table 8.31 PID coefficients in Kastraki HPP for 0.6 pu

K_p	K_i	K_d
1.07148533	0.09612619	-2.5605848591

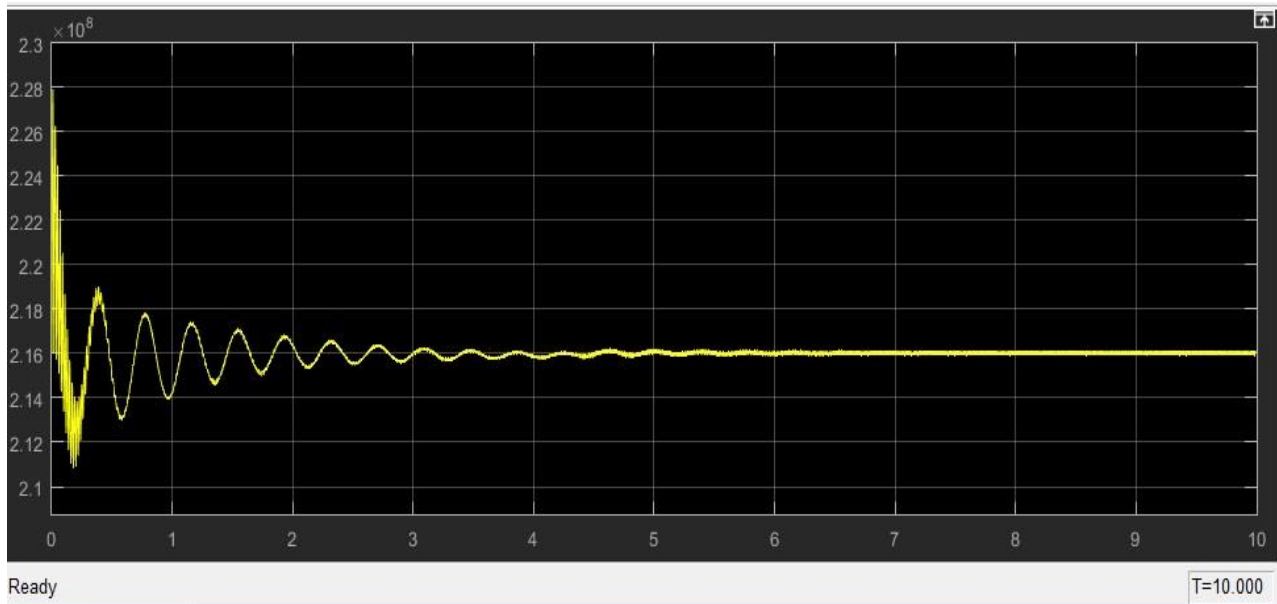


Figure 8.70: Output A. Power of the HPP in Kastraki with active power at 0.6 pu for each generator with PID-C1

Moreover the Figure 8.71 shows the same figures for Kastraki HPP when the load of the unit is in the synchronous generator terminals of 1 load of about 79.792 MW (0.8866 pu) which is the maximum at each unit ,in system frequency within the desired limits, the effective terminal voltage is 15.750 kV and the $V_f = 1.4157$ pu. The coefficients of PID for load 0.8866 pu are taken from the ZN method ($K_p = 1.99686681$, $K_i = 0.14315631$, $K_d = -1.2251305837$). It is clear from given graphics that it was loaded with HEPP 79.72 MW load at each generator and 318.88 MW total output active power and came to stable state with minimization of oscillations in voltage and frequency in a short time like 3 to 4 seconds and the transient time is 4.4 s. The variations of value which is not of course the same as Kastraki with load of active power 0.8866 pu have the almost same amplitude and a little bigger compared to the case of Kastraki with load 0.6 pu and smaller than the case of 0.4 pu.

Table 8.32 PID coefficients in Kastraki HPP for 0.9 pu

K_p	K_i	K_d
1.99686681	0.14315631	-1.2251305837

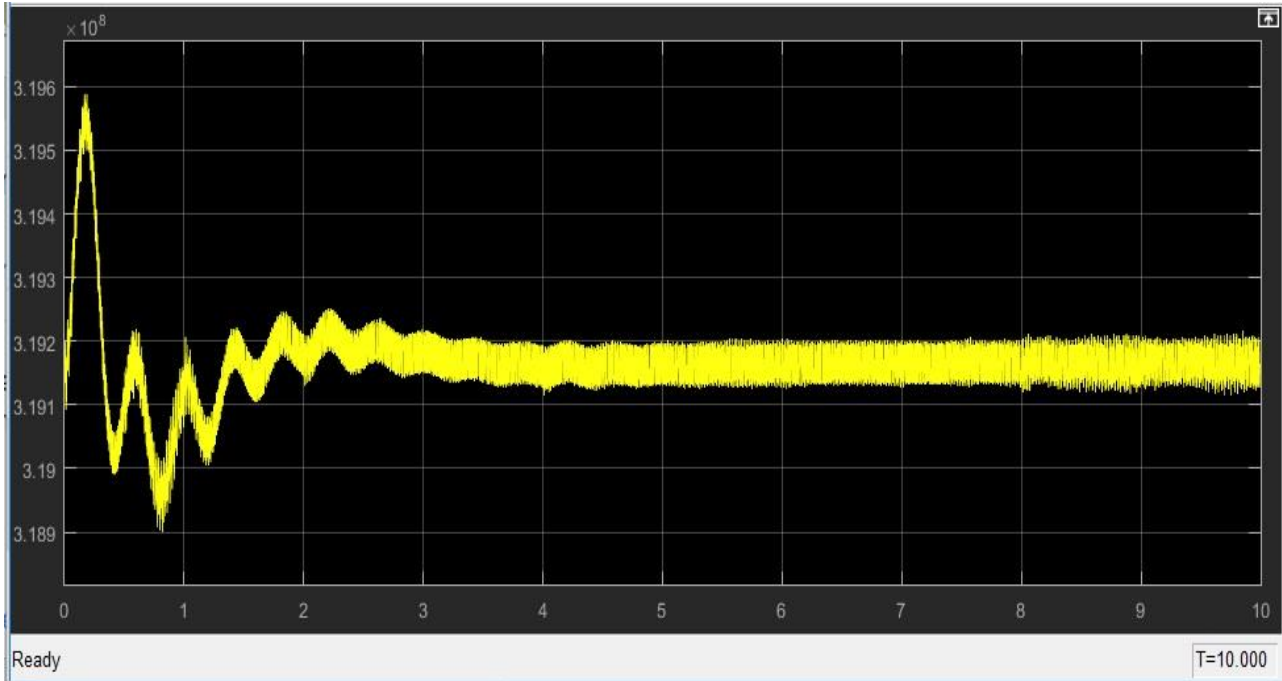


Figure 8.71: Output A. Power of the HPP in Kastraki with active power at 0.8866 pu for each generator with PID-C1

8.9.1.2 PI controller in Kastraki HPP in Power Load changes case

I show below the same figures for the 3 cases of different load but this time with PI controller.

The coefficients of PI controller are calculated for each different load (0.4,0.6,0.8866) according to the mathematical combination of the ZN method and the table 7.1.

For 0.4 pu load the coefficients are $K_p=0.53693472$ $K_i=0.07763055$

For 0.6 pu load the coefficients are $K_p=0.803613997$ $K_i=0.160210316$

For 0.8866 pu load the coefficients are $K_p=1.497650108$ $K_i=0.23859385$

Table 8.33 PI coefficients in Kastraki HPP for 0.4 pu

K_p	K_i
0.53693472	0.07763055

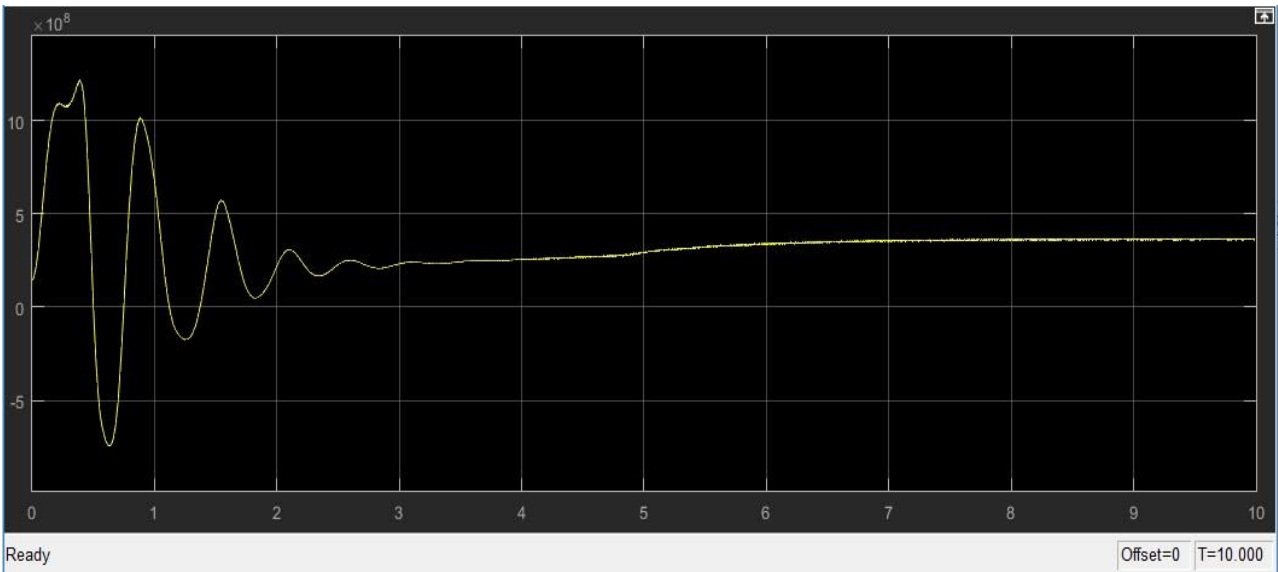


Figure 8.72: Output A. Power of the HPP in Kastraki with active power at 0.4 pu with PI-CI

Graphics in Figure 8.72 indicate which has taken from the synchronous generator terminals of 1 load of about 35.99 MW (0.4 pu) for each unit of the 4 in Kastraki HPP in system frequency within the desired limits, the effective terminal voltage is 15.750 kV and the $V_f = 1.081$ pu. The coefficients of PID for load 0.4 pu are taken from the ZN method and table 7.1 ($K_p = 0.53693472$, $K_i = 0.07763055$, $K_d = 0$). It is clear from given graphics that it was loaded with HEPP 35.99 MW load at each generator and 143.96 MW total output active power and came to stable state with minimization of oscillations in voltage and frequency in a short time in 3.2 s and came to steady state in time 6 s.

Table 8.34 PI coefficients in Kastraki HPP for 0.6 pu

K_p	K_i
0.803613997	0.160210316

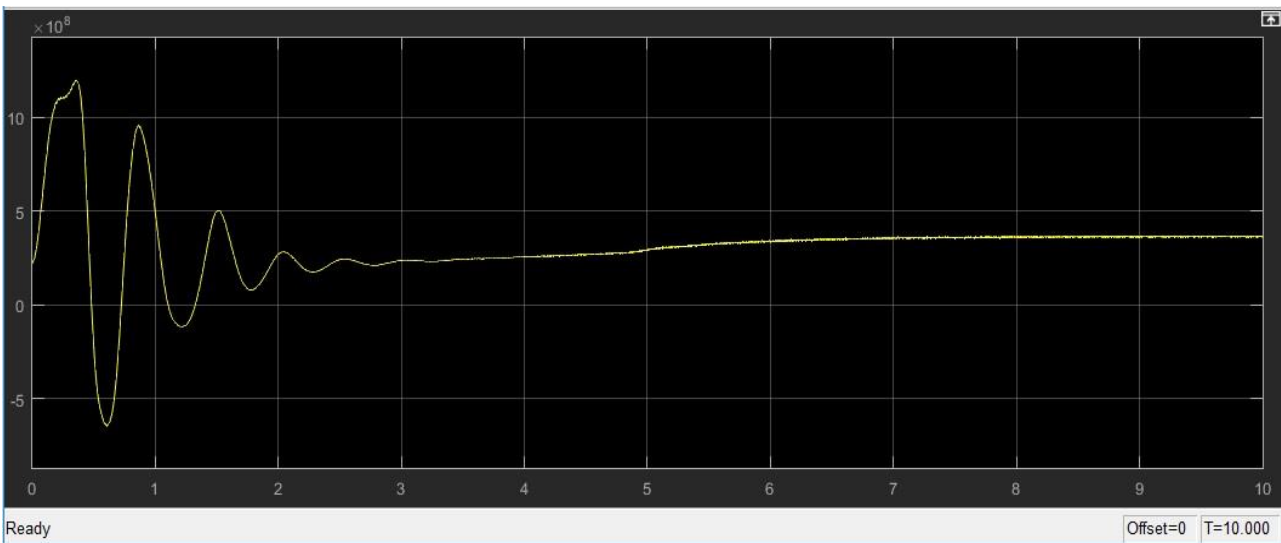


Figure 8.73: Output A. Power of the HPP in Kastraki with active power at 0.6 pu for each generator with PI

In Figure 8.73 in which I am measuring the total active power of the station i.e. the synchronous generator has power production of about 53.99 MW (0.6 pu) .The frequency of the system is within the desired limits, the effective terminal voltage is 15.750 kV and the $V_f = 1.1943$ pu. The coefficients of PID for load 0.6 pu are taken from the ZN method and table 7.1 ($K_p = 0.803613997$, $K_i = 0.160210316$, $K_d = 0$). It is visible from given Figure 8.70 that it was loaded with HEPP 53.99 MW load at each generator and 215.96 MW total output active power and came to stable state with minimization of oscillations in voltage and frequency in a short time like 3.1 s and the transient time in which I have an undoubtedly steady state is in time 5.3 s. I see that in 8 to 9 s I have a small decrease and then the active power comes again to the proper value.

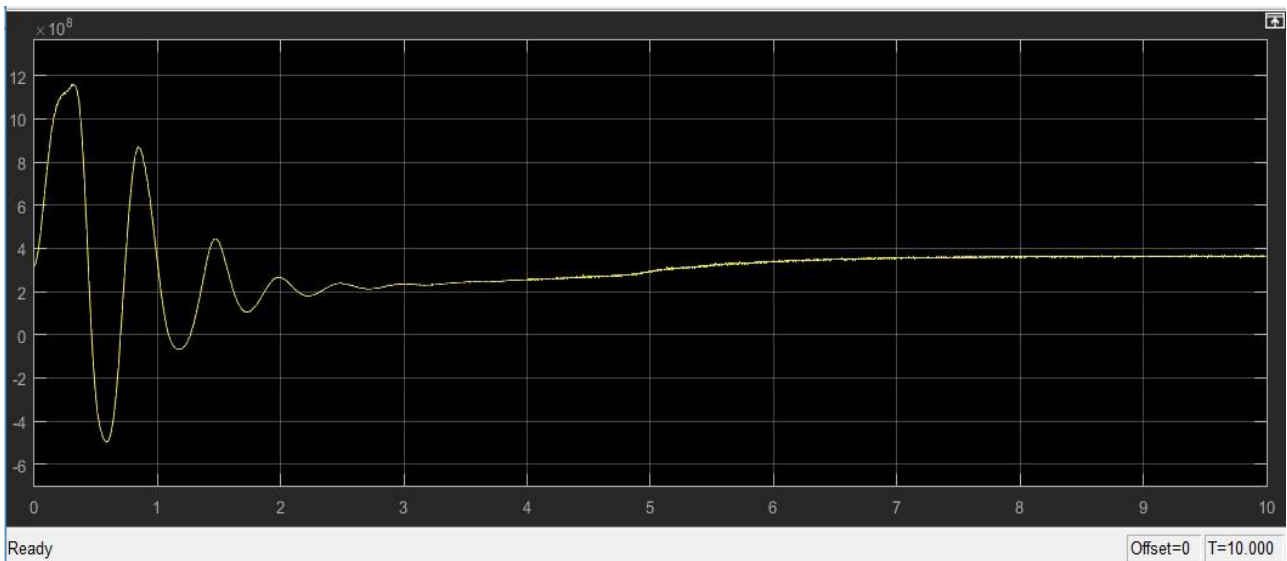


Figure 8.74: Output A. Power of the HPP in Kastraki with active power at 0.8866 pu for each generator with PI-C1

Table 8.35 PI coefficients in Kastraki HPP for 0.9 pu

K_p	K_i
1.497650108	0.23859385

Furthermore the Figure 8.74 shows the same figures for Kastraki HPP when the load of the unit is in the synchronous generator terminals of load of about 79.792 MW(0.8866 pu) which is the maximum at each unit ,in system frequency within the desired limits, the effective terminal voltage is 15.750 kV and the $V_f = 1.4157$ pu. The coefficients of PID for load 0.8866 pu are taken from the ZN method and table 7.1 ($K_p = 1.497650108$, $K_i = 0.23859385$, $K_d = 0$) . It is clear from given graphics that it was loaded with HEPP 79.72 MW load at each generator and 318.88 MW total output active power and came to stable state with minimization of oscillations in voltage and frequency in a short time like 3.1 to 3.2 seconds and the transient time is 6.1 s.

8.9.2 Stratos I HPP in Power Load changes case

I am going to simulate the model of Stratos I HPP for 3 different loads 0.4, 0.6 and 0.8905 pu with PI controller and with PID controller. The simulation time in the models in the simulation test for different values of load is 10 s.

8.9.2.1 PID controller in Stratos I in Power Load changes case

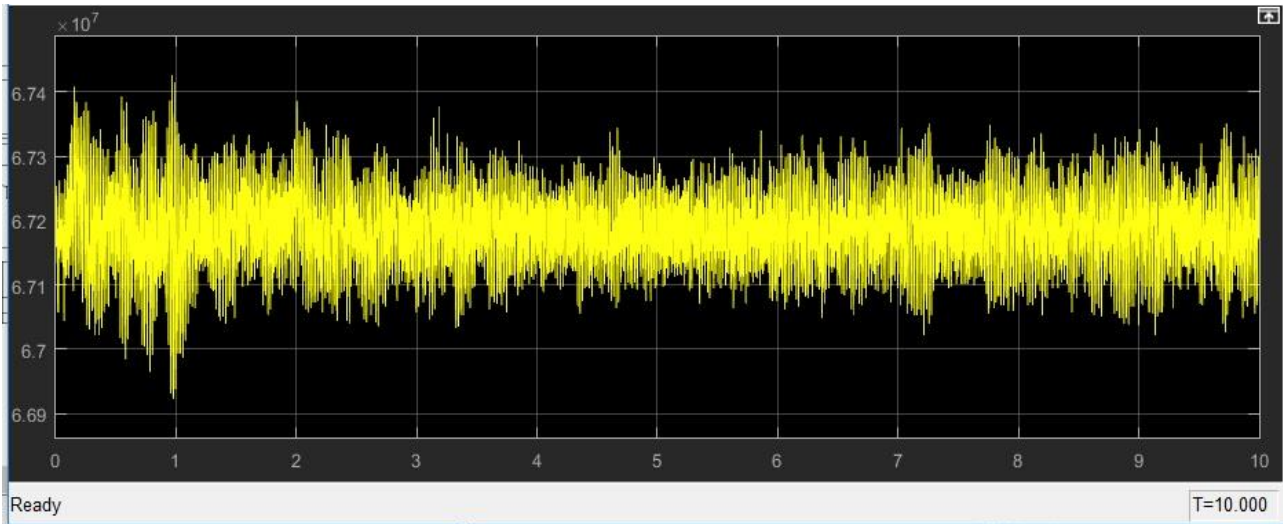


Figure 8.75: Output A. Power of the HPP in Stratos I with active power at 0.4 pu with PID-C1

Table 8.36 PID coefficients in Stratos I HPP for 0.4 pu

K_p	K_i	K_d
0.72541317	0.04513781	-3.10017621

Above in Figure 8.75 I notice the response of the active power with load of about 33.6013 MW(0.4 pu) in each unit and system frequency within the desired limits, the effective terminal voltage is 15.750 kV and the $V_f = 1.0832$ pu. The coefficients of PID for load 0.4 pu are taken from the ZN method ($K_p = 0.72541317$, $K_i = 0.04513781$, $K_d = -3.10017621$). It is clear from given graphics that it was loaded with HEPP 33.6013 MW load at each generator and 67.2026 MW total output active power and came to stable state with minimization of oscillations in voltage and frequency in a time like 5 s but then again starting to have again oscillation in 7 s.

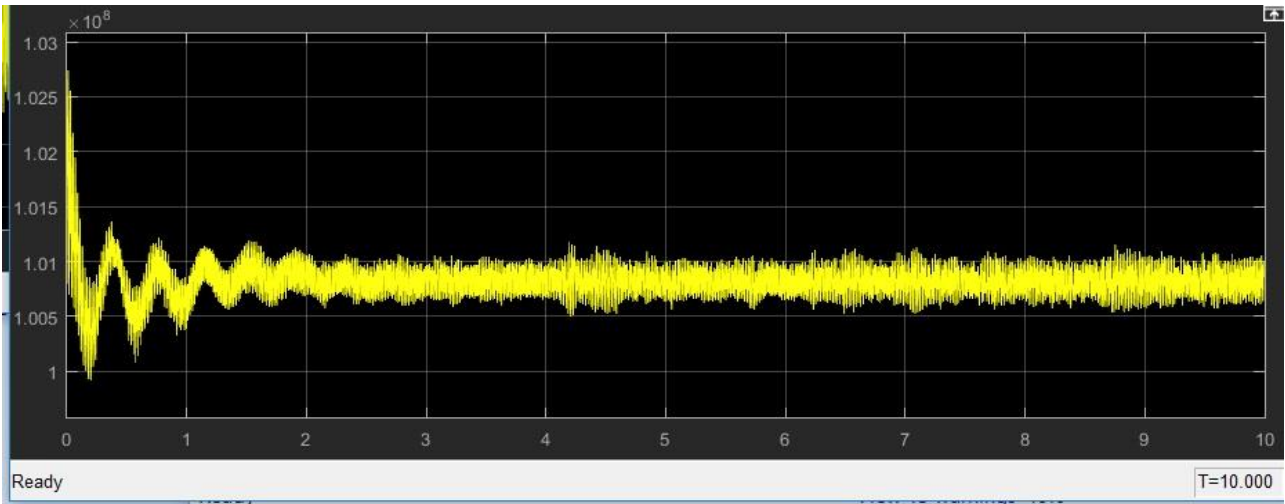


Figure 8.76: Output A. Power of the HPP in Stratos I with active power at 0.6 pu for each generator with PID-C1

Table 8.37 PID coefficients in Stratos I HPP for 0.6 pu

K_p	K_i	K_d
0.876421518	0.068435712	-3.14318167

In the Figure 8.76 indicate which has taken from the synchronous generator terminals of total load of about 50.40202 MW (0.6 pu) in system frequency within the desired limits, the effective terminal voltage is 15.750 kV and the $V_f = 1.1941$ pu. The coefficients of PID for load 0.6 pu are taken from the ZN method ($K_p = 0.876421518$, $K_i = 0.068435712$, $K_d = -3.14318167$). It is clear from given graphics that it was loaded with HEPP 50.40202 MW load at each generator and 100.80 MW total output active power and came to stable state with minimization of oscillations in voltage and frequency in a short time like 2.3 s and the transient time is about at 3 s.

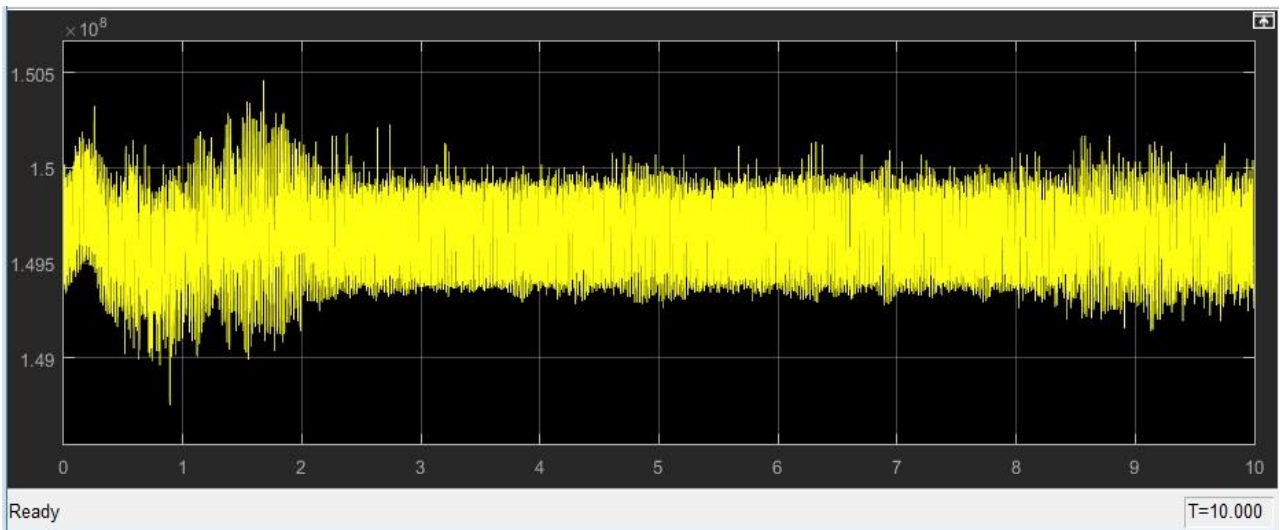


Figure 8.77: Output A. Power of the HPP in Stratos I with active power at 0.8905 pu for each generator with PID-C1

Table 8.38 PID coefficients in Stratos I HPP for 0.9 pu

K_p	K_i	K_d
1.25987312	0.13126167	-0.71356127

Additionally I am recording the figures of Stratos I HPP when the load is about 74.805 MW (0.8905 pu) in system frequency within the desired limits, the effective terminal voltage is 15.750 kV and the $V_f = 1.4118$ pu. The coefficients of PID for load 0.8905 pu are taken from the ZN method ($K_p = 1.25987312$, $K_i = 0.13126167$, $K_d = -0.71356127$). It is obvious from given graphics that it was loaded with HEPP 74.805 MW load at each generator and 149.61 MW total output active power and came to stable state with minimization of oscillations in voltage and frequency in a short time like 2.1 s and the transient time is at 0 to 2.4 s.

8.9.2.2 PI controller in Stratos I HPP in Power Load changes case

I am recording below the same figures of the characteristics of the two generators for the 3 cases of different load but this time with PI controller in Stratos I HPP.

The coefficients of PI controller are calculated for each different load (0.4, 0.6, 0.8866) according to the mathematical combination of the ZN method and the table 7.1.

For 0.4 pu load the coefficients are $K_p = 0.544059877$ $K_i = 0.180551124$

For 0.6 pu load the coefficients are $K_p = 0.657316138$ $K_i = 0.273742848$

For 0.8905 pu load the coefficients are $K_p = 0.94040484$ $K_i = 0.52504668$

Table 8.39 PI coefficients in Stratos I HPP for 0.4 pu

K_p	K_i
0.544049877	0.18055124

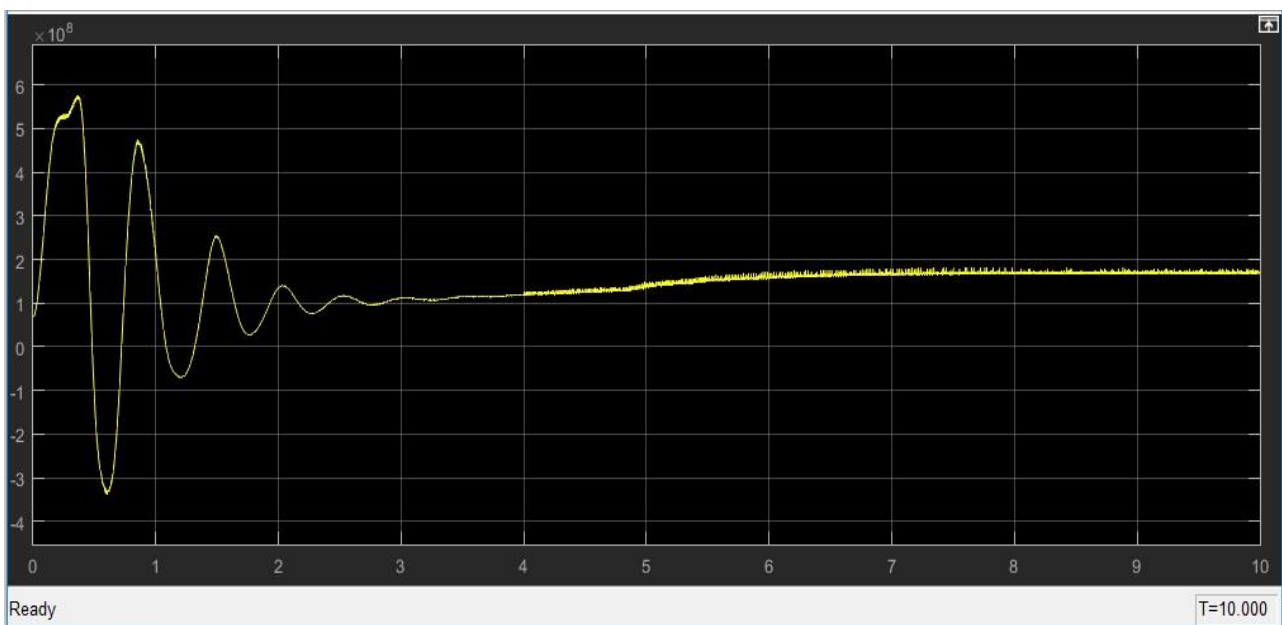


Figure 8.78: Output A. Power of the HPP in Stratos I with active power at 0.4 pu with PI-C1

Above in Figure 8.78 I notice the response of the active power with load of about 33.6013 MW (0.4 pu) in each unit and system frequency within the desired limits, the effective terminal voltage is 15.750 kV and the $V_f = 1.085$ pu. The coefficients of PID for load 0.4 pu are taken from the ZN method & table 7.1 ($K_p = 0.544049877$, $K_i = 0.18055124$, $K_d = 0$). It is clear from given graphics that it was loaded with HEPP 33.6013 MW load at each of the two generators and 67.2026 MW total output active power and came to stable state with minimization of oscillations in voltage and frequency in a short time like 3.2 s and the transient time is about at 6 s.

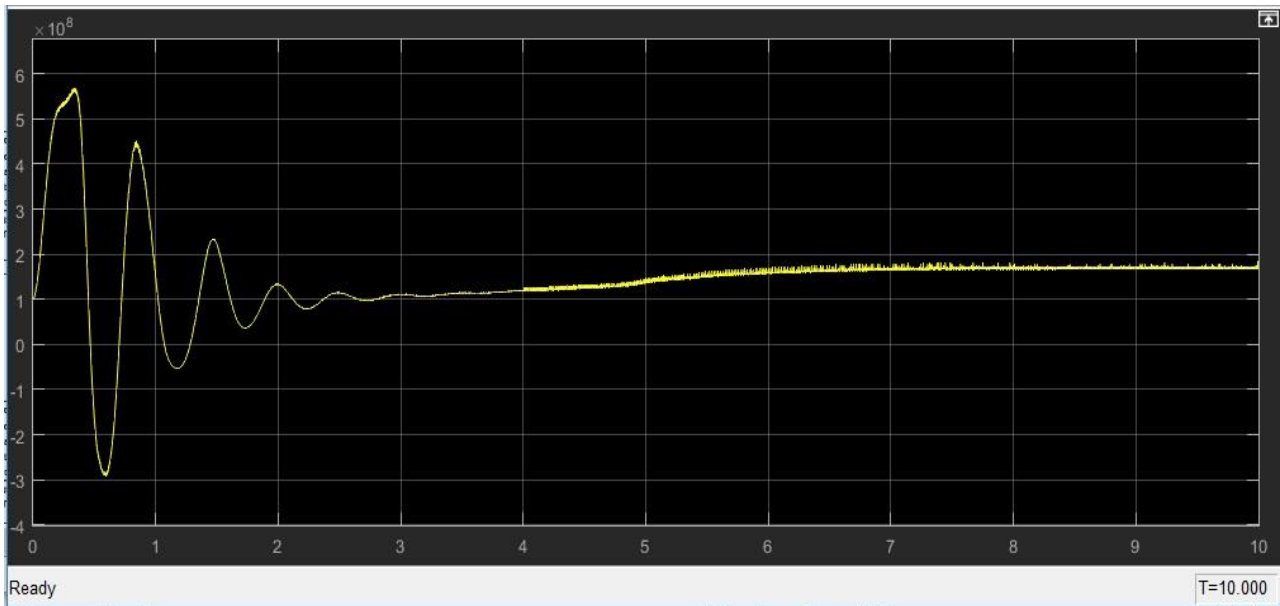


Figure 8.79: Output A. Power of the HPP in Stratos I with active power at 0.6 pu with PI-C1

Table 8.40 PI coefficients in Stratos I HPP for 0.6 pu

K_p	K_i
0.657316138	0.273742848

In the Figure 8.79 indicate which has taken from the synchronous generator terminals of total load of about 50.40202 MW (0.6 pu) in system frequency within the desired limits, the effective terminal voltage is 15.750 kV and the $V_f = 1.1941$ pu. The coefficients of PID for load 0.6 pu are taken from the ZN method and table 7.1 ($K_p = 0.657316138$, $K_i = 0.273742848$, $K_d = 0$). It is clear from given graphics that it was loaded with HEPP 50.40202 MW load at each generator and 100.80 MW total output active power and came to stable state with minimization of oscillations in voltage and frequency in a short time like 3.3 s and the transient time is about at 6 s.

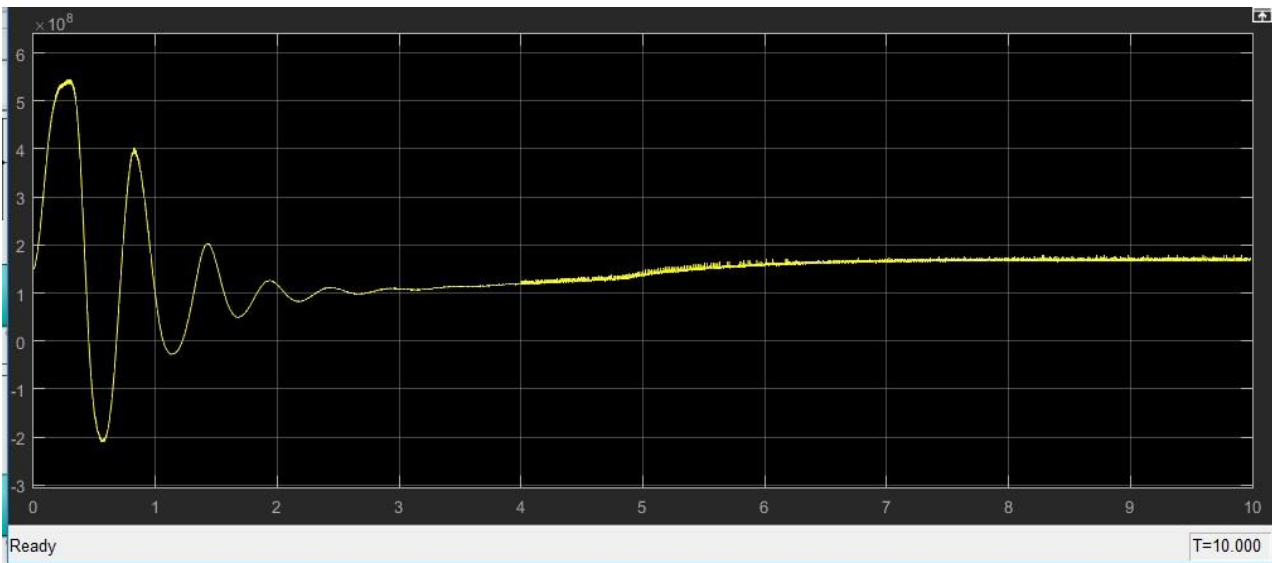


Figure 8.80: Output A. Power of the HPP in Stratos I with active power at 0.8905 pu with PI-C1

Table 8.41 PI coefficients in Stratos I HPP for 0.9 pu

K_p	K_i
0.94040484	0.52504668

Furthermore I am recording the figures of Stratos I HPP when the load is about 74.805 MW (0.8905 pu) in system frequency within the desired limits, the effective terminal voltage is 15.750 kV and the $V_f = 1.4218$ pu. The coefficients of PID for load 0.8905 pu are taken from the ZN method and table 7.1 ($K_p = 0.94040484$, $K_i = 0.52504668$, $K_d = 0$). It is obvious from given graphics that it was loaded with HEPP 74.805 MW load at each generator and 149.61 MW total output active power and came to stable state with minimization of oscillations in voltage and frequency in a short time like 3.5 s and the transient time is at 0 to 6 s.

8.9.3 Conclusions for Power Load Change Simulation Tests

In case of PID controller both in Stratos I and Kastraki HPPs I notice that we have oscillations of lesser amplitude at 0.6 pu but in the 0.9 pu load cases I have a little bigger oscillation but the steady state is obtained more quickly i.e. the transient time is shorter. With PI in both stations I am observing that I don't have almost any oscillations beside the beginning of the simulations but the figures have very long transient times something which is not the optimal for every load change, so I think that that the PID choice would be more safe for this case.

Kastraki HPP Transient Times during Power Load Change Simulation Tests

Table 8.42 C1 Simulation Test for 0.4 pu

0.4 pu	Transient Time
PID	0-7 s
PI	0-6 s

Table 8.43 C1 Simulation Test for 0.6 pu

0.6 pu	Transient Time
PID	0-6.3 s
PI	0-5.3 s

Table 8.44 C1 Simulation Test for 0.8866 pu

0.8866	Transient Time
PID	0-4 s
PI	0-6.1 s

Stratos I HPP Transient Times during Power Load Change Simulation Tests

Table 8.45 C1 Simulation Test for 0.4 pu

0.4 pu	Transient Time
PID	0-7.2 s
PI	0-6 s

Table 8.46 C1 Simulation Test for 0.6 pu

0.6 pu	Transient Time
PID	0-3 s
PI	0-6 s

Table 8.47 C1 Simulation Test for 0.8866 pu

0.8866	Transient Time
PID	0-2.4 s
PI	0-6.1 s

Chapter 9

Conclusion and Future work

9.1 Conclusion

This diploma thesis had as object of study the proposed models for dynamic modeling and simulation of hydro power plant responses under normal conditions and during transient phenomena and provided a proper view of their behavior. Also some of the required equations for the determination of the model parameters and the process needed to obtain them have been presented. I used the non-linear models of the HPP components to understand the structure and the operational characteristics of a HPP. Although the linearized model of the hydraulic turbine allows me to understand mathematically the stability of the HPP and find through Routh's criterion some restriction for the PID-PI coefficients. The stations that I needed to study was Kastraki and Stratos I HPP. The centric idea to construct the models of the two stations was the SMIB system with the parallel units connected to an infinitive bus. Finding a suitable software was a crucial priority. Simscape PowerSystems of Simulink/Matlab gave me opportunity to build fully operational models for the two stations. In order to achieve more accurate PID-PI coefficients I used the ZN for tuning hydro governors which is a classical heuristic method for this purpose. Furthermore, the evaluation of a power system's performance is concerned with the stability of that system: ie. if it remains in an equilibrium after being subjected to a disturbance. In this thesis the most common cases of disturbance (three phase to ground fault in the three phase line, power demand increase/decrease, different power load values in the units presented and I recorded the figures of the responses of a HPP, but many other faults or operating conditions as over load conditions can be applied and examined by this two models.

9.2 Future work

I found as many as possible parameters through the engineering team of PPC S.A. in Kastraki and Stratos I. The values of parameters in hydro turbine and governor models can impact system oscillations so as it is possible a better specification of them lead to better results. In this case, one future work can be the implemetantion of a PID-PI Controller Tuning in Simulink, in order to tune automatically a PID-PI Controller using a block in Simulink so as to reduce the system oscillations during any disturbance. Moreover, there are plenty of other methods and techniques than can be tested in these two models in order to make a comparison between in these two stations Kastraki and Stratos I. The models I constructed may be implemented as a block in other power systems and used for real-time simulation so as to explore models' performance in real time simulation environment or used for other simulation tests. Also It can be tested and recommended that the governor control systems should be improved upon with modern control techniques such as fuzzy logic algorithms and this

should be embedded in future models of hydropower plants because the operation of the turbines for the power potential and power can be optimized more using a FL algorithm.

Obviously for the evaluation of the results were made by me should be noted the error factor is possible as well I dealing with responses with differences of a few seconds, so an automatic way of recording the amplitude and the period of oscillations during transient phenomena could be an excellent improvement and could help for more accurate conclusions.

Bibliography

- [1] Noor Azliza Bt Ibrahim, "Modeling of Micro Hydroelectric System Design." Master Thesis, University Tun Hussein Onn Malaysia, July 2012.
- [2] Thomas Kon.Patsialis, "Mathematical Simulation for the completed design of small hydroelectric /irrigation projects with applications in Greek Area." Doctoral Thesis, AUT, 2014.
- [3] Even Lillefosse Haugen, "Verification of simulation program for high head hydropower plant with air cushion." Master Thesis, NTNU, June 2013.
- [4] Kontini Anna, "Simulation Software of the operation of the Small Hydroelectric Project." Master Thesis, NTUA, 2016.
- [5] Ioannis Argirakis, "The hydroelectric production of PPC. S.A." Technical Chamber of Greece.
- [6] Nikos Mamasis, Dimitris Koutsoyiannis and Andreas Efstratiadis, "Hydroelectric Projects: Economics of Energy." NTUA,2015.
- [7] A. Efstratiadis, A. Tegos, A. Varveris and D. Koutsoyiannis, "Assessment of environmental flows under limited data availability – Case study of Acheloos River, Greece." NTUA,2012.
- [8] Varveris, A., P. Panagopoulos, K. Triantafyllou, A. Tegos, A. Efstratiadis, N. Mamassis, and D. Koutsoyiannis, "Assessment of environmental flows of Acheloos Delta." European Geosciences Union General Assembly 2010 Vienna, Austria, 2-7 May 2010.
- [9] Ioannis Argirakis, "Exploitation Hydroelectric Stations as Projects of multi-Purpose" Technical Chamber of Greece, The Contribution of Hydroelectric Projects in the energy design of the country.
- [10] PPC S.A., "Achelous River: Kastraki Hydroelectric Power Plant."
- [11] PPC S.A., "Achelous River: Stratos Hydroelectric Project."
- [12] A.D.M.I.E., Monthly Reports of Energy,2013-2014,2014-2015,2015-2016
- [13] Nikos Mamasis and Ioannis Stefanakos, "Introduction to Energy Technology: Hydroelectric power energy." NTUA,2010.
- [14] Angeliki Loukatou, "Technologies of Wind Energy Storage with Pumped Storage." NTUA, April 2013.
- [15] D. Bouziotas, "Development to optimize hydroelectric production in Hydronomeas software - Investigation on water system Achelous-Thessaly." Master Thesis, NTUA, October 2012.
- [16] Panagiotis Dimas, "Stochastic simulation for optimum hybrid system design hydroelectric – wind energy: Investigation based on water system Aliakmonas." Master Thesis, NTUA, 2013.
- [17] Anders Karlsson and Thomas Lindberg, "Development of a test bench for dynamic hydroelectric plant control." Master Thesis, Chalmers University of Technology, Göteborg, 2011.
- [18] International Energy Agency (IEA), Implementing agreement for Hydropower Technologies and Programs, "Hydropower and the environment: Present context and guidelines for future action", May 2000
- [19] Mousa Sattouf, "Data Acquisition and control system of Hydroelectric Power Plant using internet techniques." Doctoral Thesis, Brno University of Technology,2015.
- [20] Theodoros Giannopoulos, "Modeling and control of a hybrid system power using fuzzy control." Master Thesis, University of Patras, September 2013.
- [21] Dr. Suad Ibrahim Shahl, "Synchronous Generators."
- [22] Olof Samuelsson, "Synchronous Generators dynamics.", LUND University
- [23] G. Heydt, S. Kalsi and E. Kyriakides, "A Short Course on Synchronous Machines and Synchronous Condensers.", Arizona State University,2003
- [24][https://en.wikipedia.org/wiki/Water_turbine#/media/File:Water_turbine_\(en_2\).svg](https://en.wikipedia.org/wiki/Water_turbine#/media/File:Water_turbine_(en_2).svg), "Kaplan turbine and electrical generator cut-away view."
- [25]https://en.wikipedia.org/wiki/Water_turbine#/media/File:Water_Turbine_Chart.png, "Water turbine application chart."

- [26] Yunus A. Çengel, John M. Cimbala, “Fluid Mechanics: Fundamentals and Applications.”, 1st ed., McGraw-Hill
- [27] John F. Douglas, “Fluid Mechanics.”, 5th ed., Pearson.
- [28] Rachael Haas, Michael Hiebert, Evan Hoatson, “Francis Turbines: Fundamentals and Everything Else You Didn’t Know That You Wanted to Know.” Colorado State University, November 2013.
- [29] Noelle Fillo, Kimberly Fridsma and Callen Hecker, “Francis Turbines Know.”
- [30] Bente Taraldsten Brunnes, “Increasing power output from Francis turbines.” Master Thesis, NTNU, December 2009.
- [31] Dimitris Katsaprakakis “Hydronamic Machines: Characteristic curves Turbines.”, Technical Institute of Crete
- [32] Dimitris Papantonis and Ioannis Anagnostopoulos “Technology and Prospects development of small water turbines.” Laboratory of Hydraulic Machines, NTUA
- [33] Munoz-Hernandez, G. A. and Jones, D. I., “Simulation Studies of a GPC controller for a hydroelectric plant.”,2007
- [34] Nanaware R. A., Sawant S. R. and Jadhav B. T. “Modeling of Hydraulic Turbine and Governor for Dynamic Studies of HPP.”, ICRTITCS – 2012
- [35] Rayes Ahmad Lone and Zahoor Ahmad Ganie “Modeling and Fault Analysis of Canal Type Small Hydro Power Plant.”, International Journal of Computational Engineering Research, Vol, 03, Issue, 6.
- [36]<https://www.mathworks.com/help/phymod/sps/powersys/ref/synchronousmachine.html>
“Synchronous Machine.”
- [37] Wei Li, “Hydro Turbine and Governor Modeling and Scripting for Small-Signal and Transient Stability Analysis of Power Systems.” Master Thesis, KTH Royal Institute of Technology, Sweden, September 2011.
- [38] Naghizadeh, R.A., Jazebi, S. and Vahidi, B., “Modelling Hydro Power Plants and Tuning Hydro Governors as an Educational Guideline.” International Review on Modelling and Simulations (I.R.E.MO. S), Vol. 5, No. 4 ,2012.
- [39] Yüksel Oğuz, Ahmet Kaysal, Selim Köroğlu, “Adıgüzel Hydroelectric Power Plant’s Modelling and Load-Frequency Control by Fuzzy Logic Controller.” ISSN: 2248-9622, Vol. 6, Issue 5, (Part - 5) August 2016, pp.61-66
- [40] Weijia Yang, Jiandong Yang, Wencheng Guo, Wei Zeng, Chao Wang, Linn Saarinen, and Per Norrlund, “A Mathematical Model and Its Application for Hydro Power Units under Different Operating Conditions.” September 2015
- [41] Ola Hoydal Helle, “Electric hydraulic interaction.” Master Thesis, NTNU, July 2011.
- [42] C. Nicolet, J., E. Prenat and F. Avellan, “A new tool for the simulation of Dynamic behavior of Hydroelectric Power Plants.” EPFL – Swiss Federal Institute of Technology of Lausanne, Trondheim, Norway, June,2001.
- [43] Christophe Nicolet, Philippe Allenbach, Jean-Jacques Simond and François Avellan, “Modeling and Numerical Simulation of a Complete Hydroelectric Production Site.”, August 2007.
- [44] Machowski Jan, Bialek Janusz, Bumby James. “Power System Dynamics: Stability and Control, Second Edition, John Wiley & Sons.”,2008
- [45] IEEE Working Group Report. “Hydraulic Turbine and Turbine Control Models for System Dynamic Studies.”, IEEE Trans., Vol. PWRS-7, No.1, pp.167-179, February 1992.
- [46] P. Kundur, “Power System Stability and Control.”, McGraw-Hill, 1993.
- [47] K. Vournas and G. Kontaxis, “Introduction to Power Systems.”
- [48] T. G. Bosona and G. Gebresenbet, “Modeling hydropower plant system to improve its reservoir operation.” Swedish University of Agricultural Sciences, International Journal of Water Resources and Environmental Engineering Vol. 2(4), pp. 87-94, June 2010.
- [49] Jai Dev Sharma, Avneesh Kumar, “Development and Implementation of Non-Linear Hydro Turbine Model with Elastic Effect of Water Column and Surge Tank.” International Journal of

Electrical and Electronics Research ISSN 2348-6988 Vol. 2, Issue 4, pp: (234-243), Month: October - December 2014.

[50] Auwal Abubakar Usman, Rabi'u Aliyu Abdulkadir, "Modelling and simulation of micro Hydro Power plant using Matlab/Simulink." International Journal of Advanced Technology in Engineering and Science Vol. No.3, Issue No. September 2015.

[51] Amevi Acakpovi, Essel Ben Hagan and Francois Xavier Fifatin, "Review of Hydropower Plant Models." International Journal of Computer Applications (0975 – 8887) Volume 108 – No 18, December 2014.

[52] Mousa Sattouf, "Simulation Model of Hydro Power Plant Using Matlab/Simulink." Int. Journal of Engineering Research and Applications ISSN: 2248-9622, Vol. 4, Issue 1(Version 2), January 2014, pp.295-301.

[53] Gbadamosi S. L and Ojo O. Adedayo, "Dynamic Modeling and simulation of Shiroro Hydropower PLANT in Nigeria using Matlab/Simulink." International Journal of Scientific & Engineering Research, Volume 6, Issue 8, August-2015 948 ISSN 2229-5518.

[54] Rayes Ahmad Lone, Zahoor Ahmad Ganie, "Modeling and Fault Analysis of Canal Type Small Hydro Power Plant." International Journal of Computational Engineering Research, Vol, 03, Issue, 6.

[55] Rayes Ahmad Lone, Zahoor Ahmad Ganie, "On-Line Self Tuning of PID Controller for Governor Control Using Successive Approximation Method." International Journal of Power System Analysis (IJPSA) ISSN: 2277 – 257X, Vol: 1, No: 1.

[56] Rajkumar Bansal, A. Patra, Vijay Bhuria, "Design of PID Controller for Plant Control and Comparison with Z-N PID Controller." International Journal of Emerging Technology and Advanced Engineering Website: www.ijetae.com (ISSN 2250-2459, Volume 2, Issue 4, April 2012).

[57] A. Demiroren and H. L. Zeynelgil "Modelling and simulation of synchronous machine transient analysis using SIMULINK." Electrical Engineering Department, Istanbul Technical University, Istanbul, Turkey.

[58] Nanaware R. A., Sawant S. R. and Jadhav B. T. "Modeling of Hydraulic Turbine and Governor for Dynamic Studies of HPP." International Conference in Recent Trends in Information Technology and Computer Science (ICRTITCS - 2012).

[59] J. Culberg, M. Negnevitsky and M. A. Kashem "Hydro-Turbine Governor Control: Theory, Techniques and Limitations." School of Engineering University of Tasmania

[60] Yüksel Oğuz, Ahmet Kaysal and Kübra Kaysal. "Adıgüzel Hydroelectric Power Plant Modeling and Load-Frequency Control." Faculty of Engineering, Department of Electric & Electronic Engineering, Afyon Kocatepe University, Turkey, A. KAYSAL /APJES III-I (2015) 34-41

[61] P Sridhar, K Bhanu Prasad. "Fault Analysis in Hydro Power Plants using MATLAB/SIMULINK." International Journal of Electrical Engineering and Technology, ISSN 0976 – 6545(Print) ISSN 0976 – 6553(Online) Volume 5, Issue 5, May (2014), pp. 89-99.

[62] Dr. Vimalakeerthy Devadoss, Dr.M. Sivakumar, Humaid Abdullah Fadhil Al-Hinai, Hamood Salim Mohamed Al-Bimani. "Design and Simulation of Turbine Design for Improving the Performance of Hydro Electric Power Plant." International Journal of New Technologies in Science and Engineering Vol. 2, Issue. 6, 2015, ISSN 2349-0780.

[63] https://en.wikipedia.org/wiki/List_of_largest_hydroelectric_power_stations, "List of largest hydroelectric power stations."

[64] https://en.wikipedia.org/wiki/Three_Gorges_Dam, "Three Gorges Dam."

[65] I. C. Argirakis, "The Hydroelectric Stations PPC and their contribution to meeting the country's energy needs." Athens 2006

[66] <http://www.ni.com/white-paper/3782/en/>, "PID Theory Explained.", National Instruments

[67] German Ardul Munoz-Hernandez, Sa'ad Petrous Mansoor, Dewi Ieuan Jones "Modelling and Controlling Hydropower Plants.

